Effect of genotype and environment on morphology and processing characteristics of rice and rice starches

Jennifer Minh-Chau Dang

A thesis submitted in fulfillment of the requirement for the degree of
Doctor of Philosophy

Faculty of Agriculture, Food and Natural Resources
University of Sydney
2004

ACKNOWLEDGEMENTS

I would like to express sincere thanks to my supervisor, Professor Les Copeland, for his supervision, guidance and patience throughout the course of this research.

I express my sincere gratitude to the Cooperative Research Centre for Sustainable Rice Production for a scholarship and financial assistance throughout this research. Special thanks to Dr Laurie Lewin, who was always full of encouragement, and was very understanding of a student's needs. Thank you to Tony Blakeney, who was ever so ready with technical support and helpful advice throughout this work, and for encouraging my attendance at many conferences.

To my contacts to the rice industry, Phillip Williams and Michael Bayles, thank you for your readiness to answer all my questions and the prompt supply of samples.

I would like to thank Professor Bob Gilbert for his introduction of the atomic force microscope as a means of examining starch. My sincere thanks to Newport Scientific, in particular Mark Bason and Rodney Booth, for the use of the RVA and for helpful discussions. Thank you also to Mr Shaun Bulcock and Ms Katie McBean (UTS) for their tireless help and guidance in the use of microscopes.

Thank you to Dr Edith Lees for being an understanding postgraduate coordinator. My thanks go to the technical staff of the School: Mr Colin Bailey, Ms Iona György, and Mr Kevin McLauchlan for their assistance throughout my studies. To my student colleagues: Nargis Banu, Roberta Donadini, Lu Feng, Jane Li, Mizan Rahman, Sophie Seligman, Catherine Tabrett, Anita Wang, and Florian Yan for their support, for the many chats to ease the pressures of research, and for the good times throughout the years.

My sincere thanks to my family: Victor, Tania, Loc, Phil, and especially my parents David and Angela, my grandfather Dang Van Tau, and my wonderful partner in life, Rob, for their love and support, patience and understanding.

STATEMENT OF ORIGINALITY

I, Jennifer Minh-Chau Dang, hereby declare that this submission is my own work and that, to the best of my knowledge and belief, it contains no material previously published or written by another person nor material which to a substantial extent has been accepted for the award of any other degree or diploma of the University or other institute of higher learning, except where due acknowledgement is made in the text.

Signed

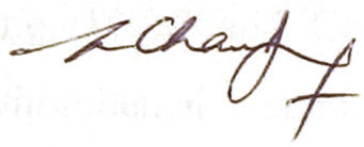

Date

10-02-2004

PUBLICATIONS FROM THIS WORK

The following publications have resulted from this study:

Dang, J.M.C. and Copeland, L. Imaging rice grains using atomic force microscopy. *Journal of Cereal Science* **37** (2003) 165-170.

Dang, J.M.C and Copeland, L. Genotype and environmental influences on pasting properties of rice flour. *Cereal Chemistry*. (in press).

Dang, J.M.C and Copeland, L. Studies of the fracture surface of rice grains using environmental scanning electron microscopy. *Journal of the Science of Food and Agriculture*. (in press).

Dang, J.M.C., Copeland, L. and Bulcock, S. Imaging of starch and starch components using atomic force microscopy. In: *Cereals 2000: Proceedings of the 11th ICC Cereal and Bread Congress and of the 50th Australian Cereal Chemistry Conference* (Wootton, M., Batey, I.L. and Wrigley, C.W. (eds.)), Cereal Chemistry Division, Royal Australian Chemical Institute, North Melbourne, Victoria, Australia (2001) pp. 729-733.

Dang, J.M.C. and Copeland, L. Structural studies of rice grains and starch using atomic force microscopy. In: *Cereals 2001: Proceedings of the 51st Australian Cereal Chemistry Conference* (Wootton, M. Batey, I.L. and Wrigley, C.W. (eds.)), Cereal Chemistry Division, Royal Australian Chemical Institute. North Melbourne, Victoria, Australia. (2002).

Dang, J.M.C. and Copeland, L. Studies of rice grains and starch by microscopy. In: *Cereals 2002: Proceedings of the 52nd Australian Cereal Chemistry Conference* (Black, C.K., Panozzo, J.F., Wrigley, C.W., Batey, I.L. and Larsen, N. (eds.)), Cereal Chemistry Division, Royal Australian Chemical Institute, Royal Australian Chemical Institute, North Melbourne, Victoria, Australia (2002) pp. 65-68.

ABSTRACT

The physicochemical and structural properties of several waxy (long- and medium-grained), low amylose (Langi and Kyeema), and high amylose (Doongara) rice varieties, as well as processed forms (parboiled and quick-cooking) of Doongara rice, were studied by chemical, microscopic and pasting techniques. The effects of genotype and environment on these properties were examined.

Chemical studies on the gross composition of rice showed higher protein content for samples with low amylose content. The high protein content appeared to be offset by low total starch content. There were no significant differences between lipid contents of the samples. Starch and protein contents of processed rice were lower than the unprocessed rice samples. A cooler climate appeared to increase the protein content of rice samples. The amylose content of the same variety was significantly higher in the coolest growing season. For each variety within any particular season, the growth location did not significantly affect the total starch, protein, lipid and amylose content of rice.

Environmental scanning electron microscopy (ESEM), which allows specimens to be imaged at high resolution with minimal preparation, was used to examine the arrangement of starch granules within the rice grain. Images were obtained for milled rice grains that were fractured along natural transverse fracture planes. The images showed two distinct features: a smooth surface, where the fracture plane is suggested to be between endosperm cells, and a rough, more disorganised surface, which is likely to correspond to the fracture plane passing through an endosperm cell. Individual starch granules exposed in the fractured surface ranged in diameter from 3 to 11 μm. The ESEM revealed morphological differences between grains of different varieties. The sizes of endosperm cells varied between varieties, but were not related to the size of starch granules, nor to amylose and amylopectin content of the starch. Parboiled rice showed a glassy fracture surface, in which features of endosperm cells and starch granules were clearly recognisable, but smaller than those of uncooked rice grains. Rice grains that had been heated and puffed showed a complete loss of organisational structure. The ESEM was able to capture the effect of processing treatments on the organisational structure of the grains.

A closer examination of the arrangement of starch within the grain was achieved by atomic force microscopy (AFM). Images obtained from cross sections of grains showed angular starch structures 3 to 8 μm in size that were arranged in layers approximately 400 nm apart. The layers are suggested to represent growth rings of starch granule formation. Cross striations were observed within each layer, and these are suggested to correspond to the blocklets of amorphous and crystalline regions within the starch granule. The blocklets had an average size of 100 nm, and are proposed to comprise approximately 280 amylopectin side chain clusters. Rice grains sectioned with water as a lubricating agent appeared to have lost some of the ordered layered structures, whereas there was a total loss of the ordered structure in cooked grains as a result of gelatinisation.

The AFM was also found to show promise as a technique for studying the structure of starch and starch components in solution. Amylose and amylopectin were imaged using the AFM. Chain length distributions of amylose from potato, and Kyeema and Langi rice were obtained from images at high magnification. Branching was observed on a commercial potato amylopectin used as a standard. AFM shows promise as a tool for studying the structure of rice grains and starch as it allows the examination of grains and starch in their native form, without destructive chemical and physical modification. However, further development of methods of sample preparation are required for imaging starch and its components.

The pasting behaviour of rice flour was determined using the Rapid Visco Analyser (RVA), a heating and cooling viscometer. Genotype, growth season and growth location all affected the pasting behaviour of rice flour. The amylose content of the same variety was significantly higher in the coolest growing season, resulting in RVA traces with lower peak viscosity and higher setback than samples with lower amylose content. When the same variety of rice was grown in different locations in the same season, there were no significant differences in the total starch, protein, lipid and amylose content of the flour, but there were significant differences in the pasting behaviour. This indicates that environmental as well as genetic factors influence the pasting behaviour of rice flour. Flour from processed rice did not paste and had low viscosities compared to unprocessed rice.

Chemical analyses revealed that, apart from the difference in amylose content between non-waxy and waxy rice varieties, there was no significant effect of genotype and

environment on the macro-composition of rice grains and starch. Structural analyses revealed morphological differences between the rice varieties. Although chemical and structural properties of rice were not significantly affected at the macro level by environmental factors, the pasting behaviour of rice flour was significantly affected by both growth season and location. The results suggest a difference in fine structure of amylose and/or amylopectin, which were not identified by the chemical and microscopic analyses used in this study. The combination of chemical, microscopic and pasting analyses allowed a better understanding of the effect of genotype and environment on the structure and behaviour of rice and starch.

TABLE OF CONTENTS

ACKNOWLEDGEMENTS ..... **ii**

STATEMENT OF ORIGINALITY ..... **iii**

PUBLICATIONS FROM THIS WORK ..... **iv**

ABSTRACT ..... **v**

TABLE OF CONTENTS ..... **viii**

ABBREVIATIONS ..... **xii**

LIST OF FIGURES ..... **xiii**

LIST OF TABLES ..... **xv**

CHAPTER 1 ..... **1**

INTRODUCTION 1

1.1 Production and consumption of rice *1*

1.2 Structure and composition of rice *2*

1.2.1 Hull 2

1.2.2 Pericarp, seed coat, nucellus, aleurone, and embryo 3

1.2.3 Subaleurone 4

1.2.4 Starchy endosperm 5

1.3 Starch *6*

1.3.1 Starch composition 6

1.3.2 Starch biosynthesis 10

1.3.3 Organisation of starch granules 11

1.4 Characterisation of starch *18*

1.4.1 Isolation of starch granules 18

1.4.2 Fractionation of starch into its components 19

1.4.2.1 Aqueous leaching 19

1.4.2.2 Complexing 20

1.4.2.3 Separation by size 20

1.4.2.4 Concanavalin A 21

1.4.3 Chemical structure of starch and starch components 21

1.4.3.1 Enzymes used in structural studies 21
1.4.4 Structural studies by microscopy 23
1.4.5 Pasting properties 27
1.5 Variation in starch properties during development 31
1.6 Differences of mature starches among different genotypes 31
1.7 Differences among varieties of the same species and genotype 32
1.8 Relationship between structure and function and the use of starch components 33
1.9 Objectives of the study 35

CHAPTER 2 36

MATERIALS AND METHODS 36
2.1 Samples 36
2.2 Enzymes 36
2.3 Reagents and solutions 36
2.4 Estimation of protein content 39
2.5 Estimation of lipid content 39
2.6 Isolation of starch from rice grains 39
2.7 Preparative fractionation of starch with concanavalin A 42
2.8 Estimation of amylose content of starch 44
2.8.1 Amylose content determination with phenol-sulphuric acid solution 44
2.8.2 Amylose content determination with amylolytic enzymes 45
2.8.3 Amylose content determination by colour with iodine 45
2.9 Reducing end group assay 45
2.10 Average chain length of α-(1→4)(1→6)-D-glucan 46
2.11 Microscopic examinations 46
2.11.1 Rice grain morphology by environmental scanning electron microscopy 46
2.11.2 Rice grain morphology by atomic force microscopy 46
2.11.3 Rice starch morphology by atomic force microscopy 47
2.12 Pasting behaviour of rice flour 48

CHAPTER 3 50

CHEMICAL STUDIES ON RICE AND STARCH 50
3.1 Introduction 50
3.2 Results and Discussion 50
3.2.1 Effect of genotype on total starch, protein and lipid content 50
3.2.2 Effect of environment on total starch, protein and lipid content 52
3.2.3 Amylose content 55

3.2.4 Average chain length....57
3.3 Conclusions....57

CHAPTER 4....**59**

RICE GRAIN MORPHOLOGY BY ENVIRONMENTAL SCANNING ELECTRON MICROSCOPY....59
4.1 Introduction....59
4.2 Results and discussion....59
4.2.1 Fracture surface of unprocessed rice grains by ESEM....59
4.2.2 Effect of genotype on grain surface structure....65
4.2.3 Effect of growth season and location on grain surface structure....77
4.2.4 Effect of processing on grain surface structure....77
4.3 Conclusions....82

CHAPTER 5....**83**

RICE GRAIN AND STARCH MORPHOLOGY BY ATOMIC FORCE MICROSCOPY....83
5.1 Introduction....83
5.2 Results and discussion....83
5.2.1 Rice grain morphology....83
5.2.1.1 Surface structure of rice grains by AFM....84
5.2.1.2 Effect of genotype on grain and starch structure....85
5.2.1.3 Effect of processing and sample preparation on grain and starch structure....89
5.2.1.4 Effect of growth season and location on grain and starch structure....93
5.2.1.5 Images and artefacts....93
5.2.2 Starch and starch components....96
5.2.2.1 Structure of standard amylose and amylopectin....96
5.2.2.2 Structure of rice starch, amylose and amylopectin....104
5.3 Conclusions....105

CHAPTER 6....**112**

PASTING PROPERTIES OF RICE FLOURS....112
6.1 Introduction....112
6.2 Results and discussion....112
6.2.1 Effect of genotype on pasting properties....112
6.2.2 Effect of growth season on pasting properties....115
6.2.3 Effect of growth location on pasting properties....116
6.2.4 Effect of processing....122
6.3 Conclusions....122

CHAPTER 7....**124**

General discussion and conclusions 134

REFERENCES 138

APPENDIX 1 142

ABBREVIATIONS

AACC	American Association of Cereal Chemists
ADPG	Adenosine diphosphoglucose
ADPGPPase	Adenosine diphosphoglucose pyrophosphorylase
AFM	Atomic force microscope/microscopy
AM	Amylose
AP	Amylopectin
SBE	Starch branching enzyme
CIA	Coleambally Irrigation Area
CL	Chain length
con A	Concanavalin A
DBE	Debranching enzyme
D-enzyme	Disproportionating enzyme
DMSO	Dimethyl sulfoxide
DP	Degree of polymerisation
ESEM	Environmental scanning electron microscope/microscopy
GBSS	Granule-bound starch synthase
Glc	Glucose
GOPOD	Glucose oxidase peroxidase
GPC	Gel permeation chromatography
HPLC	High performance liquid chromatography
IBC	Iodine binding capacity
MIA	Murrumbidgee Irrigation Area
MV	Murray Valley
NCAFM	Non-contact AFM
RACI	Royal Australian Chemical Institute
RVA	Rapid Visco Analyser
RVU	Rapid Visco Unit
SEM	scanning electron microscope/microscopy
SS	Starch synthase
TEM	Transmission electron microscope/microscopy

LIST OF FIGURES

Figure 1.1	Structure of the rice grain.....	3
Figure 1.2	Glucose links in amylose and amylopectin.....	9
Figure 1.3	Diagrammatic representation of the proposed structure of amylopectin..	13
Figure 1.4	Arrangement of amylopectin molecules within a growth ring.....	16
Figure 1.5	X-ray diffraction patterns of starch.....	17
Figure 1.6	Action of degradative enzymes on a starch molecule.....	23
Figure 1.7	Typical RVA pasting curve showing commonly measured parameters...	29
Figure 2.1	Methodology for isolation of starch from rice grains.....	41
Figure 2.2	Methodology for fractionation of starch by concanavalin A.....	43
Figure 2.3	RVA profile showing test conditions for pasting studies on rice flour....	49
Figure 3.1	Map of rice growing regions.....	54
Figure 4.1	ESEM of entire fracture surface of rice grains.....	62-64
Figure 4.2	ESEM of entire fracture surface of Langi rice grains.....	68-69
Figure 4.3	ESEM of entire fracture surface of Doongara rice grains.....	71
Figure 4.4	ESEM of entire fracture surface of Kyeema rice grains.....	72
Figure 4.5	ESEM of entire fracture surface of medium-grained waxy rice.....	73
Figure 4.6	ESEM of entire fracture surface of long-grained waxy rice.....	74-75
Figure 4.7	ESEM of entire fracture surface of parboiled Doongara rice grains.....	79-80
Figure 4.8	ESEM of entire fracture surface of quick-cooking Doongara rice grains.	81
Figure 5.1	AFM images of Doongara rice grains.....	87
Figure 5.2	Schematic representation of the proposed arrangement of blocklets in starch granules, based on images from AFM.....	88
Figure 5.3	AFM image of processed rice.....	91
Figure 5.4	Effect of processing and sample preparation on AFM images rice.....	92
Figure 5.5	AFM images of manually fractured rice grains.....	95
Figure 5.6	NCAFM images of potato amylose standard.....	99
Figure 5.7	Contour length distribution for potato amylose molecules observed from NCAFM images.....	100
Figure 5.8	NCAFM images of potato amylopectin standard.....	102
Figure 5.9	Diagrammatic representation of amylopectin branches observed in Fig. 5.8.....	103
Figure 5.10	NCAFM images of Kyeema starch in solution.....	107
Figure 5.11	Contour length distribution of amylose from Kyeema starch.....	108

Figure 5.12 NCAFM images of Langi starch in solution..... 110
Figure 5.13 Contour length distribution of amylose from Langi starch..... 111
Figure 6.1 Effect of genotype on RVA pasting curves of rice flours..... 114
Figure 6.2 Effect of growth season on RVA pasting curves of rice flours..... 119
Figure 6.3 Effect of growth location on RVA pasting curves of rice flours..... 121
Figure 6.4 Effect of processing on RVA pasting curves of Doongara rice flour..... 123

LIST OF TABLES

Table 1.1	Granule size of commercial unmodified starch.....	7
Table 1.2	Properties of amylose and amylopectin.....	8
Table 1.3	Comparison of features of SEM, ESEM and AFM.....	26
Table 2.1	RVA test profile for rice flour.....	48
Table 3.1	Effect of genotype on composition of rice.....	51
Table 3.2	Temperature and yield characteristics of rice growing seasons.....	52
Table 3.3	Effect of growth season on composition of rice.....	53
Table 3.4	Effect of growth location on composition of rice.....	53
Table 3.5	Amylose content of starch from waxy and non-waxy rice.....	55
Table 3.6	Effect of growth season on amylose content of rice starch.....	56
Table 3.7	Effect of growth location on amylose content of rice starch.....	56
Table 3.8	Average chain length of α-(1→4)(α1→6)-D-glucans.....	57
Table 4.1	ESEM measurements of surface features of rice grains.....	76
Table 6.1	Effect of genotype on amylose content and RVA parameters of rice flours.....	113
Table 6.2	Effect of growth season on amylose content and RVA parameters of rice flours.....	118
Table 6.3	Effect of growth location on amylose content and RVA parameters of rice flours.....	120

CHAPTER 1

Introduction

1.1 Production and consumption of rice

Rice (*Oryza sativa* L.) is a member of the grass family. It is a semi aquatic plant that can be grown under a broad range of climatic conditions, from long periods in deep water to dry, hilly slopes (Marshall and Wadsworth, 1994). The two cultivated species are *O. sativa* L. and *O. glaberrima* Steud. Rice is grown in 100 countries on every continent except Antarctica, extending from latitudes of 53° North to 40° South, and from sea level to an altitude of 3000 m. *Oryza glaberrima* is grown only in Africa and only on a limited scale (Marshall and Wadsworth, 1994).

Rice is one of the leading food crops of the world and the staple food for over half the world's population. It is second only to wheat in terms of annual production for food use. Rice accounts for one third to half of the daily caloric intake in many Asian countries, and is also the major source of protein for the masses of Asian people (Marshall and Wadsworth, 1994).

World production of rice is about 579.5 million tonnes per year (FAO, 2002), 90% of which is grown and consumed in tropical Asia (Juliano, 1985). In Australia, this figure is about 1.3 million tonnes (FAO, 2002). In terms of area and production, rice ranked second to wheat in 2001 among the world's cereal crops. In yields, rice is second to maize but higher than wheat (FAO, 2002).

In Australia, rice is grown on irrigated farms in the Riverina area of New South Wales (NSW) and the Murray Valley in Victoria, between the Murray and Murrumbidgee Rivers. Each year, about 150,000 hectares of rice are grown, producing from 1.2 to 1.7 million tonnes of paddy rice (Cooperative Research Centre for Sustainable Rice Production, 2002). Around 2,500 farms in NSW produce rice and a very small number – less than 20 – in Victoria. The Riverina region, located in southeastern Australia, is among the highest yielding rice-growing regions in the world, with average yields of 8 to 10 t/ha. This is due

primarily to high levels of solar radiation and a cooler grain-filling period (Farrell *et al.*, 2001). Rice is sown in October and November, and harvested from early March to May. Australian rice is of high quality and is sought by overseas markets. Up to 85% of Australian rice is exported to more than 40 countries (Rice CRC, 2002).

1.2 Structure and composition of rice

Shape, size and mass are the most readily identifiable characteristics of grains from individual cereal species (Evers and Millar, 2002). However, within species there is considerable variation, and the structure of the grain influences its physical and chemical properties (Juliano and Bechtel, 1985). Morphology can be associated with quality parameters. The ratio of length to breadth of a rice grain is a useful guide to the nature of the endosperm, and more significantly the starch type present. Shorter grains tend to be associated with stickier cooking quality (Evers and Millar, 2002). The structure and development of cereal grains (Evers and Millar, 2002), and in particular rice grains (Juliano and Bechtel, 1985; Hoshikawa, 1993) have been previously described, and will be only briefly discussed in this thesis. The gross structure of a mature rough rice grain is shown in Fig. 1.1. The major parts of the grain are the hull, pericarp, seed coat, nucellus, aleurone layer, subaleurone, embryo and endosperm.

1.2.1 Hull

The mature rice grain is harvested with the hull still intact, and is referred to as rough rice or paddy rice. The hull comprises 18 to 20 per cent by weight of the rough rice (Juliano and Bechtel, 1985), and is the tough covering for the rice caryopsis. The hull provides protection to the rice caryopsis, by serving as a resistance to fungal damage and insect infestation during storage, and resistance to rapid changes in moisture content of the grain due to humidity fluctuations in the external environment (Juliano and Bechtel, 1985; Marshall and Wadsworth, 1994).

The hull consists of the lemma and palea, which cover and protect the ventral and dorsal parts of the grain, respectively. The lemma and palea provide a connection for the rice caryopsis to its parent plant (Hoshikawa, 1993). The hull is low in protein, lipid and starch, but is high in crude fibre, crude ash (mostly silica), and dietary fibre. It contains small quantities of minerals such as calcium, sodium, potassium, magnesium and zinc. The hull

is the only part of the grain that contains appreciable amounts of silica (Marshall and Wadsworth, 1994).

1.2.2 Pericarp, seed coat, nucellus, aleurone, and embryo

Removal of the hull exposes the rice caryopsis, referred to as brown rice. The caryopsis coat consists of four distinct layers of cells and tissues. These are the pericarp, seed coat or testa, nucellus, and aleurone (Fig. 1.1).

Figure 1.1

Structure of the rice grain. Source: Juliano (1985).

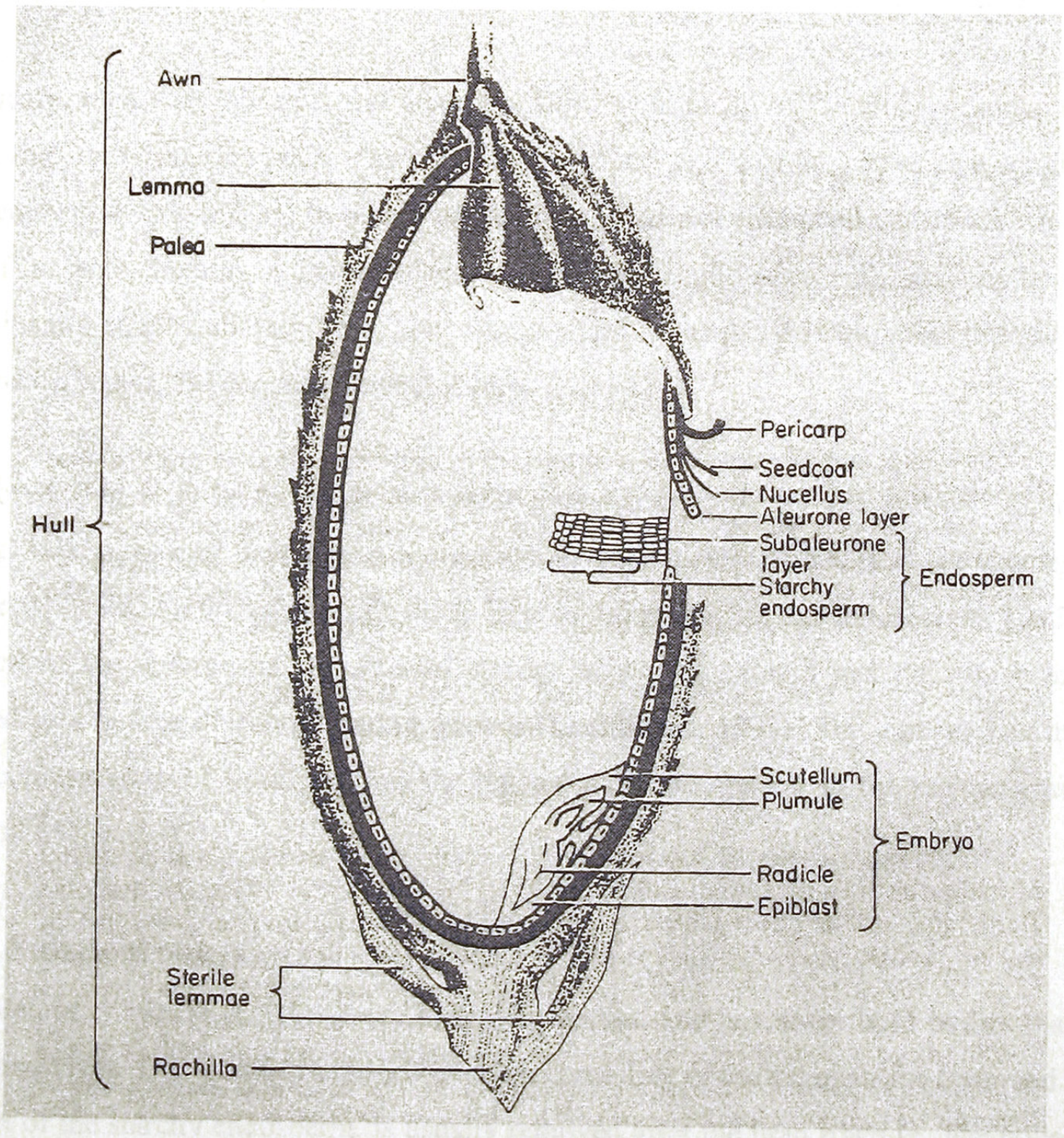

Brown rice is covered by the pericarp, which comprises six or seven layers of spongy tissues formed by half-destroyed parenchymatous cells (Hoshikawa, 1993). During grain growth, nutrients are translocated from the leaves and roots of the parent plant through vascular structures found in the pericarp (Hoshikawa, 1993; Evers and Millar, 2002). The seed coat provides a barrier against water over most of the surface of the grain (Evers and Millar, 2002). The maternal tissue surrounding the aleurone, embryo and endosperm is the nucellar epidermis, which is a compressed epidermis with a thin outer cuticle. The endosperm and embryo develop within the nucellus (Evers and Millar, 2002). Aleurone cells occur in one or more continuous layers surrounding the starchy endosperm, and embryo. These cells have relatively high concentrations of protein, lipid, vitamins and minerals (Juliano and Bechtel, 1985; Evers and Millar, 2002). The majority of aleurone cells within species are uniform in size and shape, and the cell size is not a function of grain size (Evers and Millar, 2002).

The pericarp, seed coat, nucellus and aleurone, along with much of the embryo, make up the bran fraction of the rice grain. The bran accounts for 5 to 8% of the brown rice weight, and is removed during milling to obtain white or polished rice (Marshall and Wadsworth, 1994). The bran contains a good balance of protein, lipids (rice oil), carbohydrates (predominantly starch), dietary fibre, and vitamins and minerals. It is the most nutritious part of the caryopsis (Juliano and Bechtel, 1985).

The embryo (Fig. 1.1) is the most important grain component for the survival of the species as it is capable of developing into a plant (Evers and Millar, 2002). It is extremely small and is located on the ventral side at the base of the grain (Juliano and Bechtel, 1985). Every cell of the embryo has an internal storage of sugars, protein and fat, which are consumed as a source of energy during growth (Hoshikawa, 1993). The embryo has the highest concentration of lipid, and has the highest moisture content in the mature grain (Evers and Millar, 2002).

1.2.3 Subaleurone

The subaleurone layer (Fig. 1.1) is rich in protein bodies, and has fewer lipid bodies than the aleurone layer. The 'polish', a milling fraction consisting of the subaleurone layer and a small part of the starchy endosperm, is usually removed after the bran fraction. The polish

comprises 3 to 4% by weight of brown rice. Compared with the bran fraction, polish contains less protein and lipid, considerably more starch, and is less nutritious because it contains lower levels of vitamins and minerals (Juliano and Bechtel, 1985).

1.2.4 Starchy endosperm

The starchy endosperm (Fig 1.1) is rich in starch granules, containing more starch per unit weight than any other milling fraction (hull, bran, polish). The starchy endosperm contains about 0.5% protein, which includes the enzymes of starch biosynthesis and may contribute to the flavour of starch (Martin and Smith, 1995). The starch and storage proteins, together with cell walls and minor constituents, accumulate as a source of nutrients for the embryo when it begins to germinate. The nutrients are made available as a result of hydrolysis by enzymes produced in the embryo itself or in the aleurone, or both (Evers and Millar, 2002). The starchy endosperm contains almost no lipid bodies. Starchy endosperm comprises an outer endosperm (below the subaleurone layer) and an inner endosperm. Gradients of nutrients occur within the starchy endosperm cells to the centre of the grain. Starch concentration increases with increasing distance from the periphery towards the centre of the grain (Evers and Millar, 2002). The protein content is highest in the outer endosperm, and starch content is highest in the inner endosperm (Marshall and Wadsworth, 1994). Rice that has had the hull, bran and polish removed is referred to as white rice, which is composed almost entirely of starchy endosperm, and is the milling product of greatest commercial importance (Marshall and Wadsworth, 1994; Evers and Millar, 2002).

The white rice grain (hereafter referred to as the rice grain) contains almost 90% starch, 1 to 2% lipid, 2 to 6% protein, and minor components of non-starch polysaccharides, vitamins, minerals and ash (Coultate, 1996). The amount and type of protein and lipid present in the rice grain, and the interaction of these with starch, influence the processing behaviour of the rice. Starch molecules may be trapped in the protein matrix, resulting in an altered behaviour of the starch. Lipids may influence the gelatinisation and retrogradation of starches by inhibiting access for water. As 90% of its dry weight is starch, the processing behaviour of rice therefore largely reflects the behaviour of its starch (Chinnaswamy *et al.*, 1985). Although starch, lipids and proteins are all important components of the rice grain, this study will concentrate mainly on the starch component.

1.3 Starch

1.3.1 Starch composition

Starch is the major carbohydrate reserve of most plants. It is found in greatest abundance in plant tissues such as tubers and the endosperm of seeds. Starch occurs in the form of granules, which usually have an irregular rounded shape, ranging in size from less than 1 μm to greater than 100 μm (Martin and Smith, 1995), depending on the botanical source (Table 1.1). Both the shape and size of granules are characteristic of the species of plant and can be used to identify the origin of a starch or flour (Coultate, 1996). The size of granules also differs between organs, for example starch granules in leaves are generally smaller than those in storage organs (Martin and Smith, 1995).

Native starches can be readily identified according to the shape and size of granules, the brilliance of the interference cross under polarised light, and the form and position – either centric or eccentric – of the hilum (Snyder, 1984). The light microscope provides a rapid and useful means of identifying the various native starches. It has the advantages of colour through selective staining and details of internal structure not observed by scanning electron microscopy (SEM).

Starch is a glucose polymer consisting of a mixture of two fractions: amylose, which is essentially linear, and amylopectin, which has a much higher degree of branching. Most starches contain approximately 25 to 30% amylose, but this proportion may vary considerably with the plant species (from 11 to 35% in a survey of 51 species), variety (from 20 to 36% in a survey of 399 maize varieties), plant organ, developmental age of that organ, and the growth conditions of the plant (Shannon and Garwood, 1984). There are also high amylose starches containing 65 to 70% amylose, and 'waxy' starches that contain little to no amylose at all (Whistler, 1984; Coultate, 1996).

Table 1.1

Granule size of commercial unmodified starches[a]

Starch species	Granule size range (μm)
Waxy rice (Italian)	2-10
High amylose corn	
70 % amylose	-
55 % amylose	5-35
Corn	5-30
Waxy corn	5-25
Wheat	5-35
Potato	10-100
Barley	2-3, 35-40[b]

[a]Source: Snyder (1984)

[b]Sharply bimodal

Amylose consists of long chains of approximately 10^2 to 10^3 D-glucopyranosyl residues in α(1→4) linkages (Fig. 1.2a), and has an average molecular weight of 10^5 (Table 1.2). Amylose usually has a small number of glucose in α(1→6) linkages and is branched at a low level (approximately one branch per 1000 glucose residues) (Ball *et al.*, 1998). Amylose tends to form crystalline structures due to its essentially straight chain structure, and therefore has good film forming properties (Coultate, 1996). Once extracted from plants and in solution, amylose forms inter-chain hydrogen bonds between molecules, resulting in rigid gels (Martin and Smith, 1995).

Amylopectin is a much larger molecule, with molecular weights greater than 10^6 (Table 1.2). The glucose units in amylopectin are joined by α(1→4) glucosidic links, but about 4 to 5% of the glucose units are involved in α(1→6) links, creating branch points as shown in Fig. 1.2b. This proportion of branch points results in an average chain length of 20 to 25 units, but can vary greatly between and within species. Closely packed, highly crystalline structures characteristic of amylopectin from wheat and barley endosperms generally have lower average branch lengths than open structures containing more water commonly found in potato tuber (Martin and Smith, 1995). Chains that are not substituted on the C6 position

are called A chains. These chains are α(1→6) linked to B chains, which are branched at one or several points. The terminal glucose of A and B chains is non-reducing. A single chain per amylopectin molecule, called the C chain, has a free reducing end (Martin and Smith, 1995) (Fig. 1.2c).

Amylopectin, with its many branches, is relatively more soluble in cold water than amylose (Coultate, 1996). After extraction, amylopectin has more limited hydrogen bonding than amylose in solution and is more stable, remaining fluid and giving high viscosity and elasticity to pastes and thickeners (Martin and Smith, 1995).

Table 1.2

Properties of amylose and amylopectin.

Characteristic	**Amylose**	**Amylopectin**
Weight percentage in the granule	15-35	65-85
General structure	Essentially unbranched	Branched
Percentage of α-(1→6) branches	<1	4-6
Molecular weight range	10^4-10^5	10^7-10^8
Degree of polymerisation	10^2-10^3	10^3-10^4
Chain length (glucose units)	3-1000	3-50
β-amylolysis limit (%)	73-95	55-60
IBC (g/100 g)	19.9-21.1	0-2.57
Iodine colouration	Deep blue	Purple/brown
λ_{max} (nm)	620-640	530-540
X-ray diffraction	Crystalline	Amorphous

IBC = iodine binding capacity, λ_{max} = wavelength producing maximum absorbance for iodine-glucan complex. Source: Ball *et al.* (1998).

Figure 1.2

Glucose links in (a) amylose and (b) amylopectin. (c) Diagrammatic representation of an amylopectin molecule showing A, B and C chains. R = reducing end, NR = non-reducing end.

a

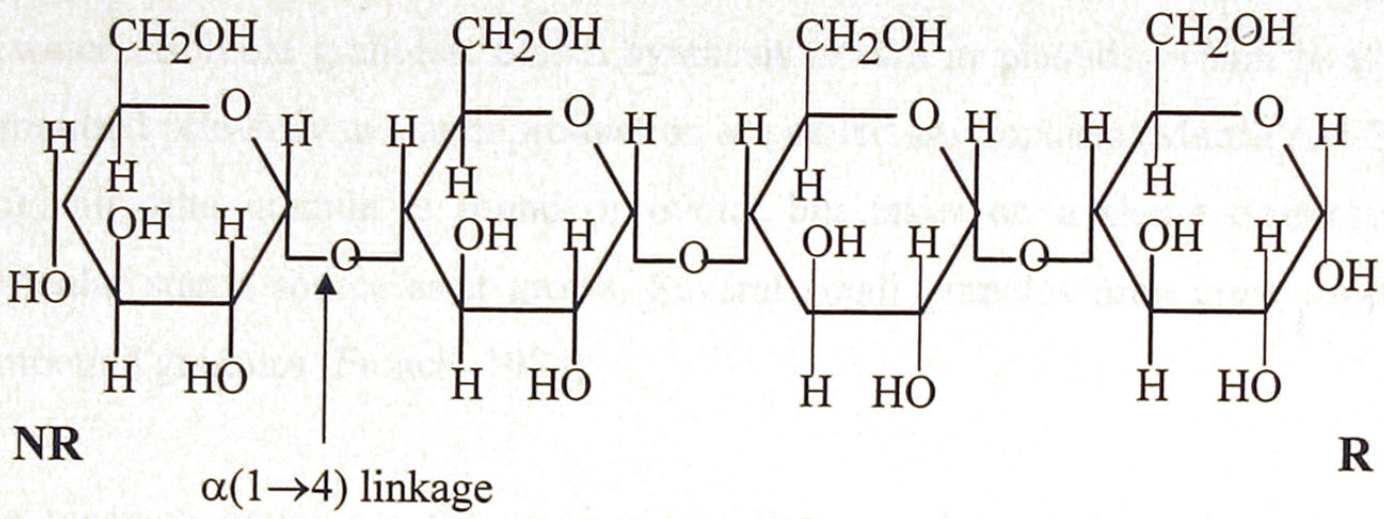

b

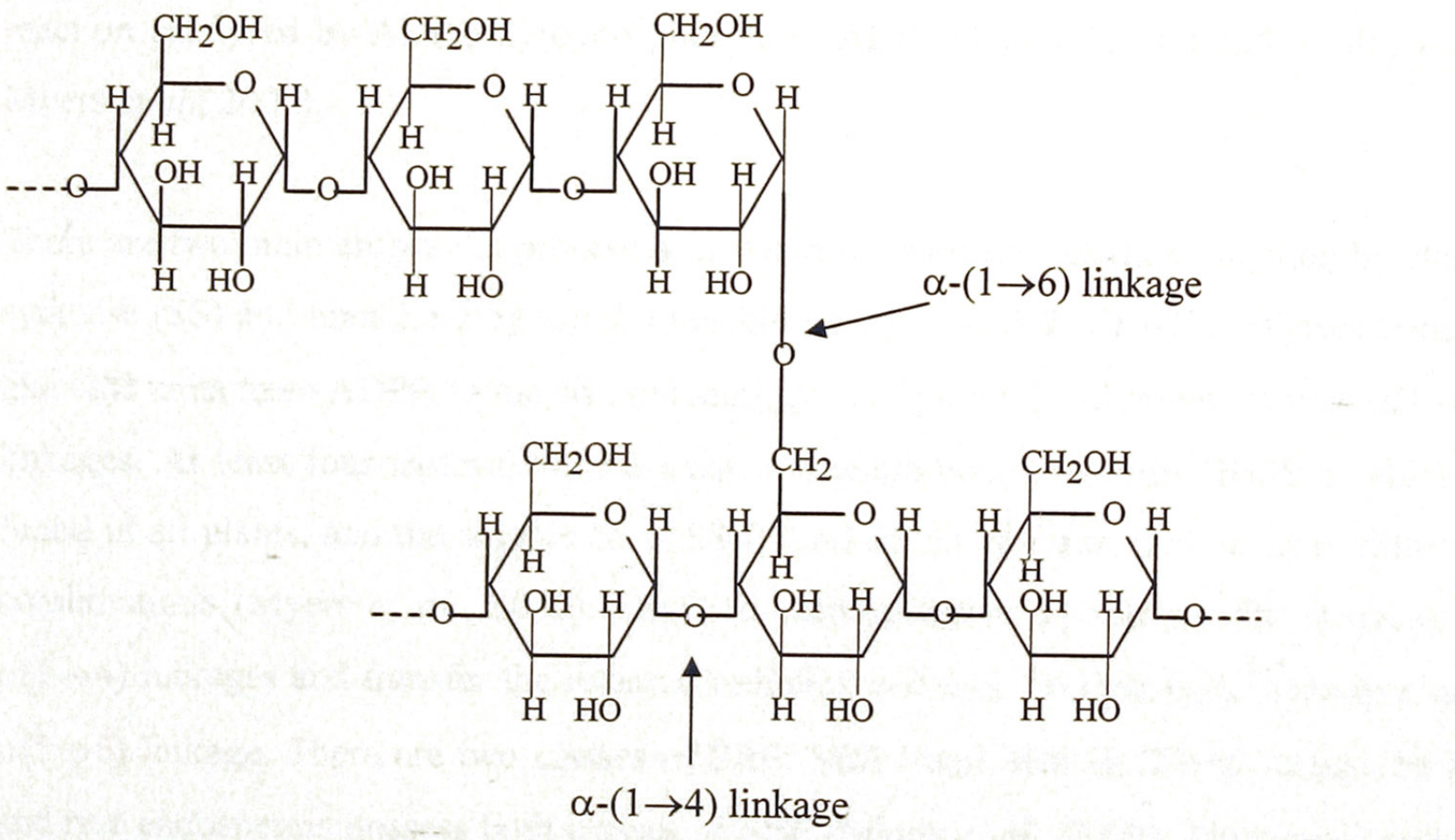

c

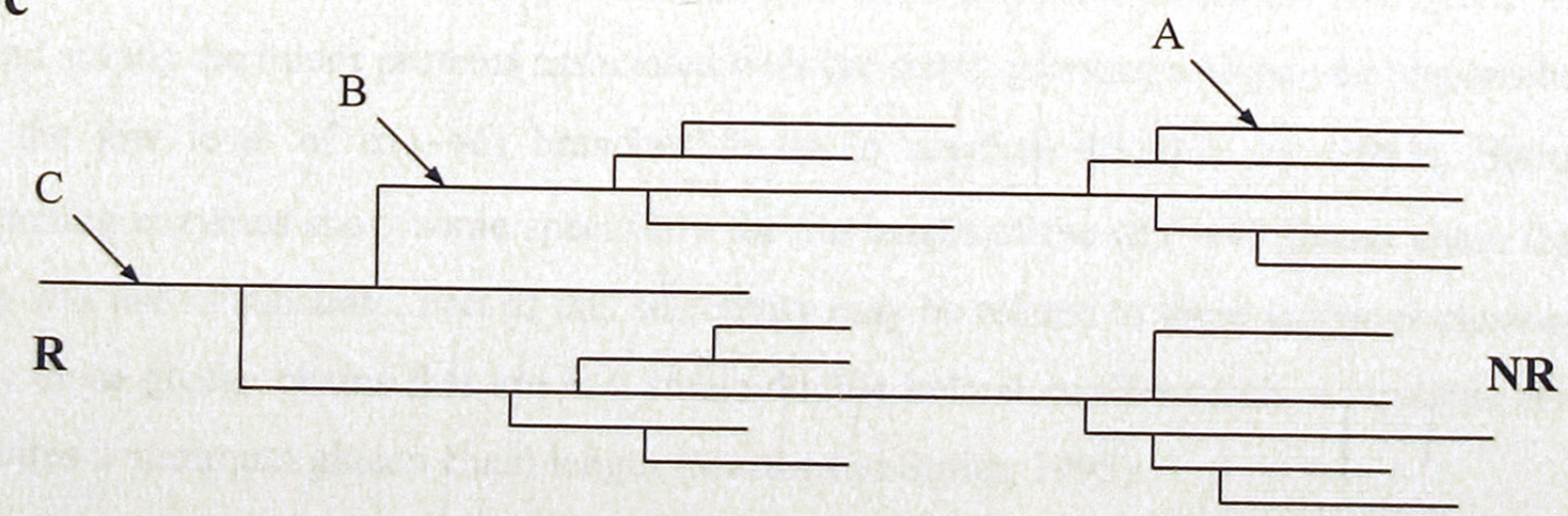

1.3.2 Starch biosynthesis

There is substantial literature on starch biosynthesis, which has been recently reviewed by Martin and Smith (1995), Ball *et al.* (1998) and Myers *et al.* (2000), and will not be discussed in detail here.

Starch shows diurnal synthesis and degradation, and is deposited in semi-crystalline form as water insoluble granules. Starch synthesis occurs in plastids, which in storage organs committed primarily to starch production are called amyloplasts (Martin and Smith, 1995). Originally the granule is round or ovoid, but takes on a shape characteristic of the particular starch source as it grows. Several small granules may grow together to form compound granules (French, 1984).

The glucosyl donor for the synthesis of both amylose and amylopectin is adenosine diphosphoglucose (ADPG), which is synthesised from glucose-1-phosphate and ATP in a reaction catalysed by ADPG pyrophosphorylase (ADPGPPase) (Martin and Smith, 1995; Myers *et al.*, 2000).

There are two main enzymatic processes in starch biosynthesis: chain elongation by starch synthase (SS) and branching by starch branching enzyme (SBE). Starch synthases transfer glucosyl units from ADPG to the non-reducing ends of growing polymers via new $\alpha(1\rightarrow4)$ linkages. At least four isoforms of SS exist: a granule-bound isoform GBSS I, which is found in all plants, and the soluble SS I, SS II, and SS III isoforms that occur in different combinations (Myers *et al.*, 2000). Starch branching enzymes catalyse the cleavage of $\alpha(1\rightarrow4)$ linkages and transfer the released reducing end to a C6 hydroxyl, creating a new $\alpha(1\rightarrow6)$ linkage. There are two classes of SBE: SBE I and SBE II. Wheat, maize, barley and rice endosperms possess both classes of SBE (Myers *et al.*, 2000). The two classes of SBEs have different substrate specificities and form different products. The SBEs are found among the minor proteins associated with the starch granule, and may be responsible for the low level of $\alpha(1\rightarrow6)$ branches found in amylose (Ball *et al.*, 1998). Starch branching enzymes show some specificity for the length of the $\alpha(1\rightarrow4)$ glucan chain that they will use as substrate. Part of this selectivity may be related to these enzymes cleaving only those glucan chains that are in a stable double helical conformation, a structure that requires a minimum glucan chain length (Martin and Smith, 1995).

Two other enzymes, namely starch debranching enzyme (DBE) and disproportionating enzyme (D-enzyme), have recently received attention for their roles in amylopectin biosynthesis. DBEs catalyse the hydrolysis of α(1→6) linkages. There are multiple isoforms of DBEs, referred to as isoamylase-type DBEs and pullulanase-type DBEs. DBE is thought to trim some of the new branches formed during synthesis for more compact packing. Amylopectin does not accumulate to normal levels when an isoamylase-type DBE is mutated, suggesting that this enzyme participates in starch biosynthesis. D-enzymes transfer a segment of one linear chain to another. An internal α(1→4) linkage is cleaved and the released reducing end is attached to a separate chain through a new α(1→4) linkage. Less amylopectin accumulates when D-enzyme is missing, and its structure is altered by a significant increase in the frequency of short A chains. The direct involvement of DBEs and D-enzymes in amylopectin biosynthesis is unclear. They may either modify an amylopectin precursor or participate in a separate pathway indirectly required for normal amylopectin biosynthesis (Myers *et al.*, 2000).

Newly formed starch has been shown to be deposited at or near the granule surface (French, 1984). While mechanisms for chain elongation and branching have been well explored and are widely accepted, there is no firm theory for the side-by-side synthesis of amylose and amylopectin. There is limited understanding of how amylose and amylopectin interact, or whether they are synthesised separately or alongside each other (Ball *et al.*, 1998).

1.3.3 Organisation of starch granules

The structure of starch has been the subject of many investigations. Several models of starch structure have been proposed, and these have been described in detail by Yamaguchi *et al.* (1979); French (1984); Jenkins and Donald (1995); Gallant *et al.* (1997); Ball *et al.* (1998); Myers *et al.* (2000).

Starch granules isolated from different parts of the same plant may be entirely different, suggesting that there are genetic, biological and environmental factors controlling development and regulation of starch formation. The morphology of starch granules is dictated by the particular structure and biochemistry of the starch-synthesising organelle, the chloroplast or amyloplast, as well as by the physiology of the plant (French, 1984).

Amylopectin is essential for granule formation, whereas amylose is not. Amylopectin is the major contributor to both mass and granule structure (Myers *et al.*, 2000). The granule crystallinity is associated with the amylopectin component rather than the linear amylose (Jenkins and Donald, 1995). This is indicated by the observation that waxy starches, which lack amylose, give an X-ray pattern very similar to that of a normal starch (Coultate, 1996). There are no natural starches known that contain only amylose. The discussion of granule structure will therefore concentrate mainly on amylopectin structure.

At the highest level of detail of amylopectin structure, at the 0.1- to 1.0-nm scale, structure within individual chains is described by chain length and branch location (Fig. 1.3a). Enzymatic studies of amylopectin structure show non-random chain length distribution and non-random distances between branch points, indicating that branches are clustered (Myers *et al.*, 2000).

At the 10-nm scale, regions of alternating crystalline and amorphous lamellae are evident (Fig. 1.3b). Each repeating unit of crystalline and amorphous lamellae is about 9 to 10 nm thick, with the amorphous lamellae being about 3 to 4 nm (Gallant *et al.*, 1997; Ball *et al.*, 1998). The 6-nm size of the crystalline lamellae corresponds to a length of 18 glc residues (Ball *et al.*, 1998). The crystalline lamellae are resistant to acid hydrolysis, and are thought to comprise tightly associated double helices containing primarily A chains and unsubstituted spans of B chains (Myers *et al.*, 2000). Manners (1989) estimated that 80 to 90% of the total number of chains in an amylopectin molecule are involved in forming the side chain clusters, while the remaining 10 to 20% of chains form the inter-cluster connections. Crystalline lamellae are thought to be divided into discreet units about 10 nm wide called amylopectin side chain clusters (Gallant *et al.*, 1997). The amorphous lamellae are susceptible to acid hydrolysis, and are thought to contain frequent branch linkages and thus are less densely packed (Myers *et al.*, 2000).

Figure 1.3

Diagrammatic representation of the proposed levels of amylopectin structure (Myers et al., 2000, adapted from Gallant et al., 1997). (a) Glycosidic linkages within the amylopectin molecule. (b) Diagrammatic representation of the cluster model of amylopectin. Solid lines indicate glucan chains, and intersections between them indicate branch linkages. Dotted lines indicate the boundaries of amylopectin side chain clusters in which primarily unbranched chains associate in tightly packed double helices. The amorphous areas that separate amylopectin side chain clusters is represented by 'a'. *(c) Diagrammatic representation of a blocklet, which is made up of alternating crystalline and amorphous lamellae organised into a discreet unit.*

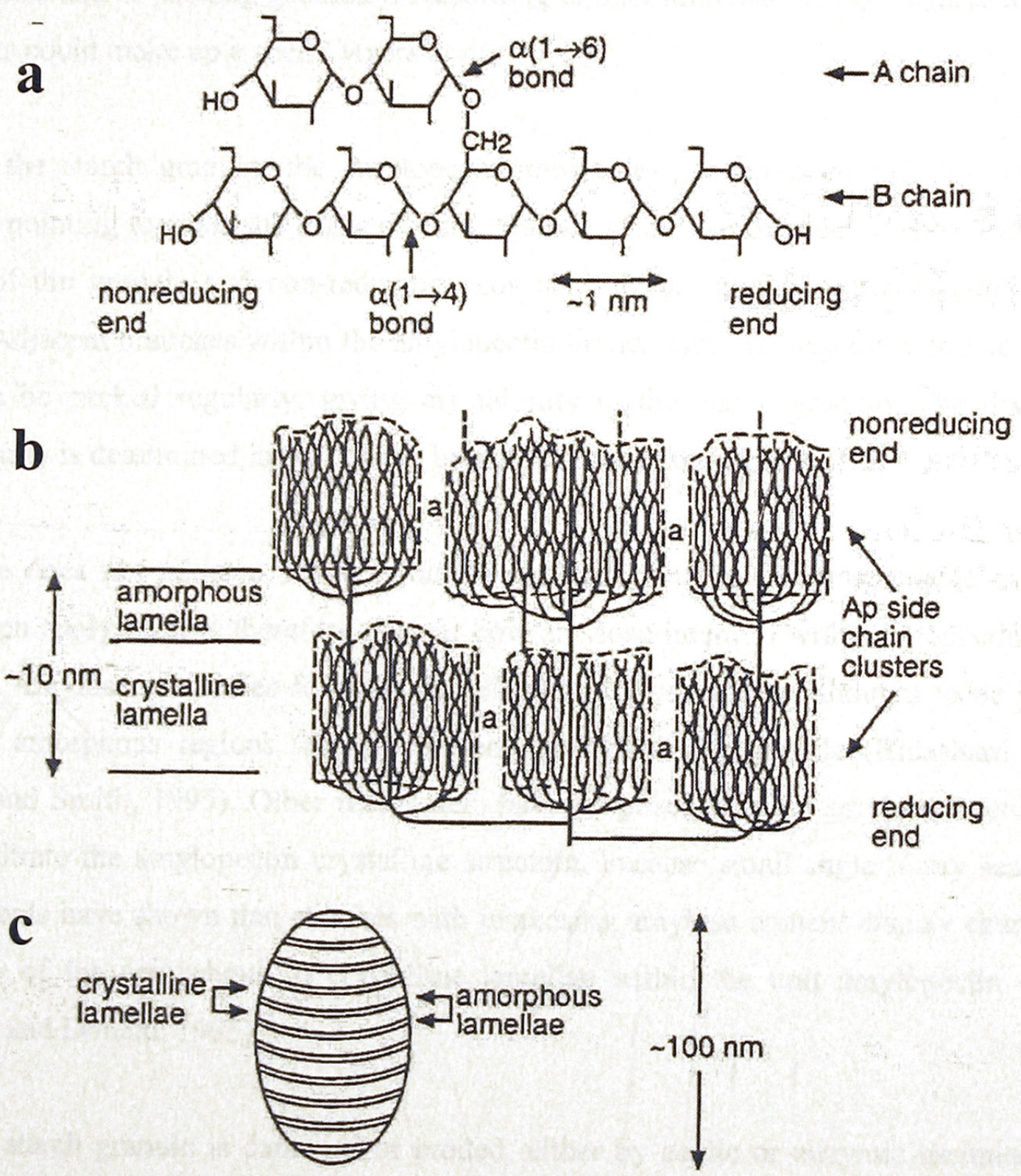

On the 100-nm scale, it is proposed that crystalline and amorphous lamellae are grouped into discreet, elongated structures called blocklets, surrounded by relatively large, non-crystalline regions (Fig. 1.3c) (Gallant *et al.*, 1997). Areas between blocklets are about 10 to 20 nm wide. Blocklets are oblate spheroids with short diameters of 20 to 500 nm, and are believed to be aligned relative to each other in various ways, rather than having a common orientation.

The next level of organisation is made up of alternating semi-crystalline and crystalline shells that are between 120 and 400 nm thick (Yamaguchi *et al.*, 1979, French, 1984). Also known as 'growth rings', the different shells may consist of distinct types of blocklets that vary in size and/or packing geometry. According to their dimensions, two or three layers of blocklets could make up a shell (Myers *et al.*, 2000).

Within the starch granule, the amylopectin molecules are arranged radially, with the glucans pointing towards the surface of the granule (that is, the reducing end towards the center of the granule and non-reducing ends towards the granule surface) (Ball *et al.*, 1998). Adjacent branches within the amylopectin branch clusters may form double helices that can be packed regularly, giving crystallinity to the starch granule. The degree of crystallinity is determined in part by the branch lengths in the amylopectin.

Amylose does not adopt a semi-crystalline structure, thus it is not amenable to X-ray diffraction analysis. It is therefore unclear how amylose interacts with amylopectin in the granule. Amylose molecules form single helical structures and are thought to be packed into the amorphous regions that are present throughout the granule (Blanshard, 1987; Martin and Smith, 1995). Other researchers have proposed that the amylose fraction can also infiltrate the amylopectin crystalline structure, because small-angle X-ray scattering experiments have shown that starches with increasing amylose content display changes in the ratio of the amorphous to crystalline lamellae within the unit amylopectin cluster (Jenkins and Donald, 1995).

When a starch granule is damaged or eroded, either by acidic or enzymic treatment, the starch granules are greatly weakened so that many crack open and expose a pronounced layer structure (Hollinger and Marchessault, 1975; Fuwa *et al.*, 1979). Native starch granules show 'growth rings' when observed by optical microscopy, especially after

chemical treatment. Growth rings are also observed in scanning electron microscopy (SEM) of eroded granules, and transmission electron microscopy (TEM) of thin sections of chemically treated starch granules (French, 1984). The growth rings represent concentric shells of alternating high and low refractive index, density, crystallinity, and resistance or susceptibility to chemical and enzymic attack. The formation of the rings may result from periodic growth and the daily fluctuations in carbohydrate available for starch deposition (French, 1984; Martin and Smith, 1995). Growth rings are readily visible in granules from fresh plant tissue. Examination of amylose-free waxy maize starch by TEM shows that the thickness of a growth ring corresponds to the length of an amylopectin molecule (Fig. 1.4) (Yamaguchi *et al.*, 1979; French, 1984).

As a consequence of their crystallinity, when observed in the polarising microscope starch granules show a 'Maltese Cross' (French, 1984). Using an additional $\lambda/4$ filter, polarised light reveals the positive birefringency of the starch granules which indicates a radial orientation of the principal axis of the crystallites (Gallant *et al.*, 1997).

Dry starch granules are clear and colourless, and have a mean refractive index of 1.5. Large hydrated granules show concentric 'growth rings', which are shells of alternating high and low refractive index. The centre of the granule is the original growing point known as the hilum. The hilum is usually less organised than the rest of the granule, and may contain non-polysaccharide material from the amyloplast. Starch granules that have been dried usually show cracks through the hilum (French, 1984).

Figure 1.4

Schematic representation of the arrangement of amylopectin molecules within a growth ring. Source: French (1984).

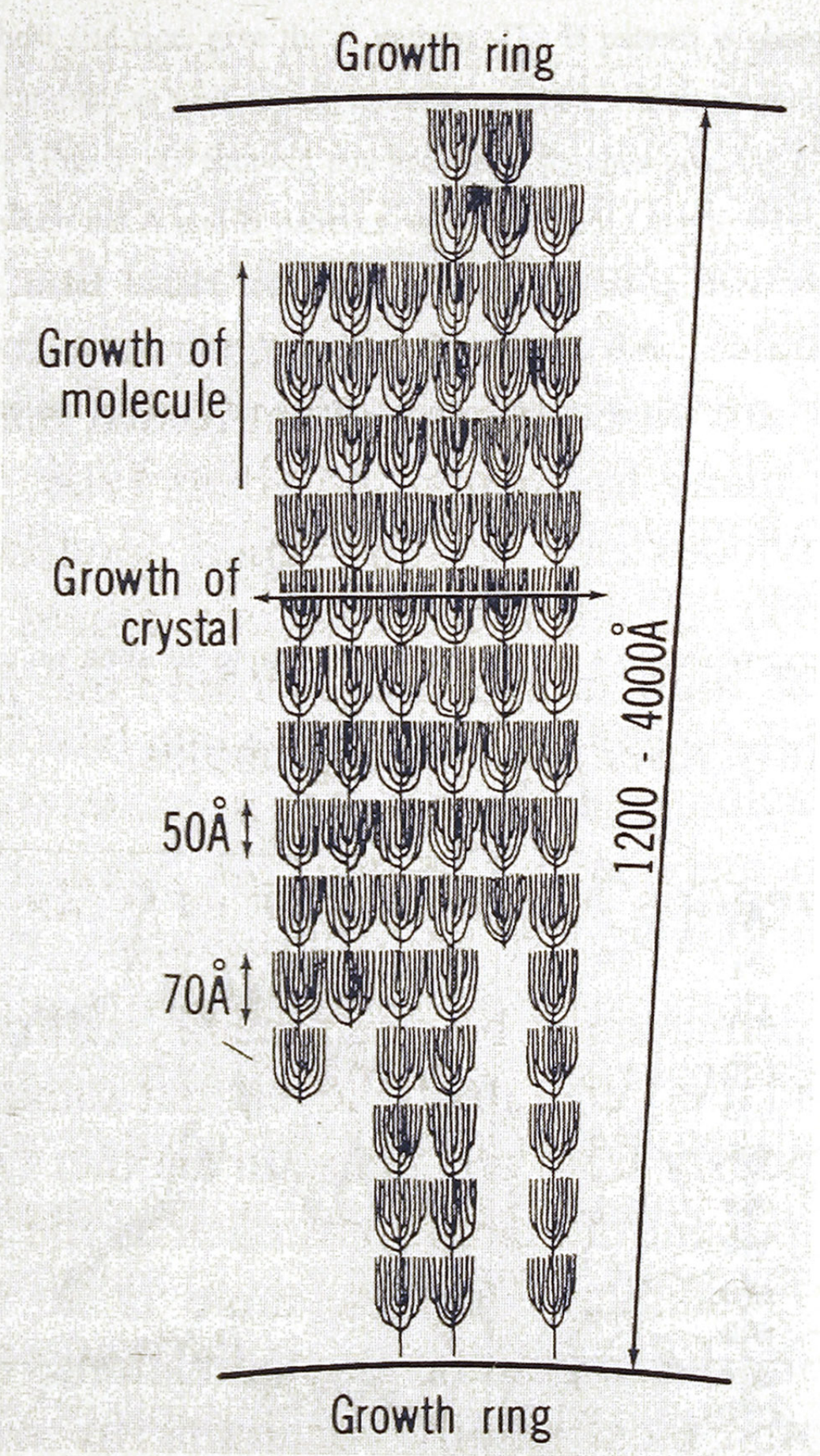

When a crystal is irradiated with X-rays, the X-rays split to form a pattern distinctive to the crystal structure. This technique has been used to study the crystalline nature of starch (Thomas and Atwell, 1999). X-ray diffraction of crystalline shells give three distinctive patterns, classified as A, B, or C (French, 1984; Thomas and Atwell, 1999). Cereal starches such as corn, wheat and rice, give the A pattern. The B pattern is characteristic of tuber, fruit, and stem starches, as well as amylomaize starches, which have an amylose content greater than 60% (Fig. 1.5a). Smooth pea and bean starches give the C pattern, which is intermediate between the A and B patterns, and is probably due to mixtures of A- and B-type crystallites, either within individual granules, or as mixtures of A- and B-type granules. A fourth pattern, the V pattern (Fig. 1.5b), occurs as a result of amylose complexation, and can appear after gelatinisation (Gallant *et al.*, 1997).

Figure 1.5

(a) X-ray diffraction patterns of starch. (b) Simplified V-starch structure (Thomas and Atwell, 1999).

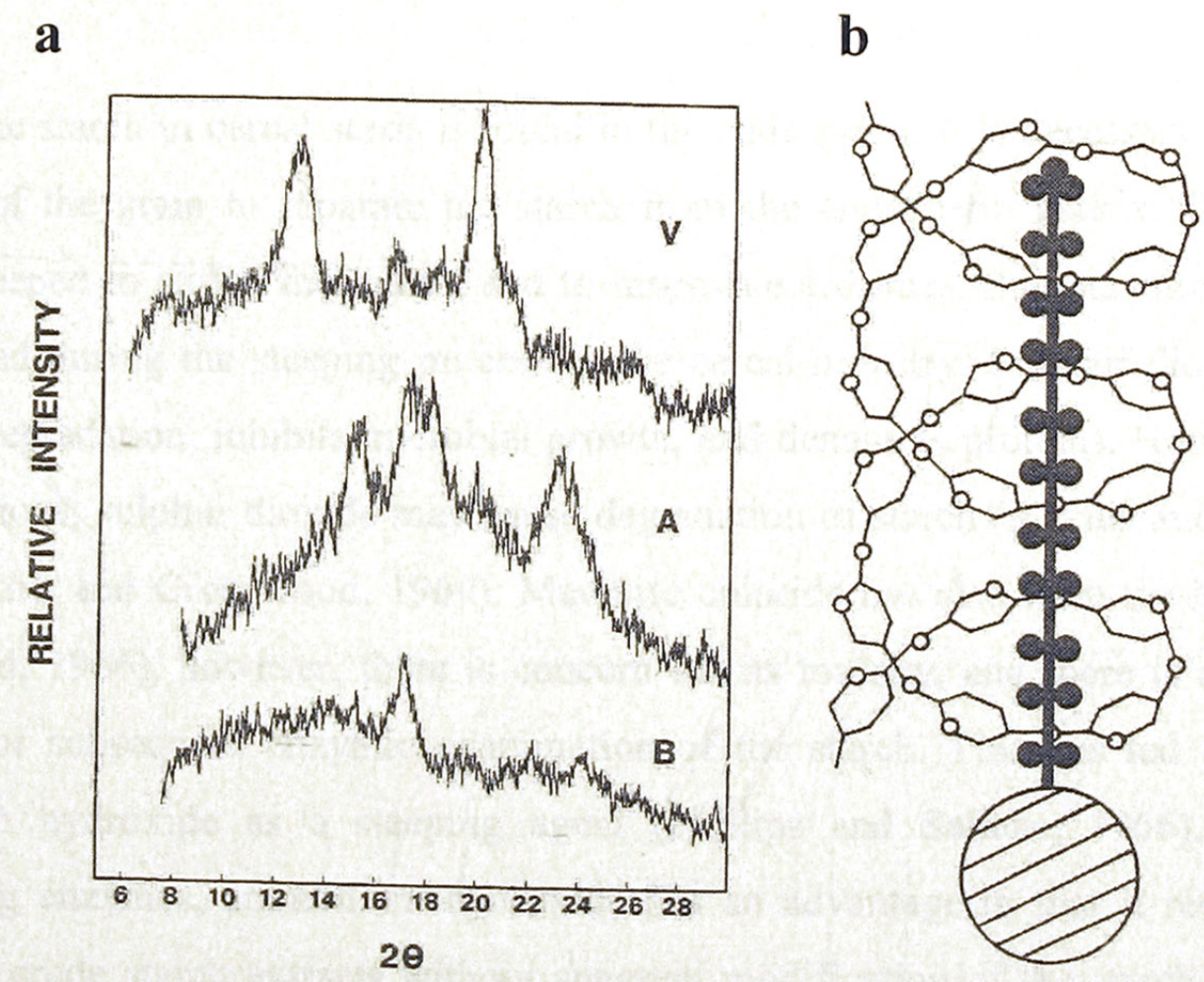

Examination of undamaged and unmodified starch granules by SEM shows that the granule surface is relatively smooth and free from pores, cracks and fissures. Some cereal starches show indentations, thought to be impressions of spherical protein microbodies that have impeded the local growth of the starch granule (French, 1984).

1.4 Characterisation of starch

The structure and composition of starch determine its physical and chemical properties in solution. Knowing the properties of the dispersed starch is important for determining the suitability of a starch for a particular application, understanding the events occurring during processing, and controlling these events to achieve the desired end products (Pomeranz, 1987; Swinkels, 1985).

1.4.1 Isolation of starch granules

For analysis, the starch granules must first be isolated from the grains. The starch should be extracted intact and with as little modification to the granules as possible. The method of extraction used often depends on the botanical source.

Most of the starch in cereal seeds is found in the endosperm. It is necessary to disrupt the structure of the grain to separate the starch from the endosperm matrix. The grains are usually steeped to soften the matrix and to inactivate enzymes. Sulphur dioxide has been widely used during the steeping process in the cereal industry. Sulphur dioxide prevents enzymic degradation, inhibits microbial growth, and denatures proteins. However, at high concentrations, sulphur dioxide may cause degradation of starch (Adkins and Greenwood, 1966; Adkins and Greenwood, 1969). Mercuric chloride has also been used (Adkins and Greenwood, 1966), however, there is concern for its toxicity, and there is a need for its removal for subsequent enzymic examination of the starch. This has led to the use of ammonium hydroxide as a steeping agent (Phillips and Sallans, 1966). As well as inactivating enzymes, ammonium hydroxide has an advantage in that it reduces protein content of crude starch extracts without apparent modification of the starch (Phillips and Sallans, 1966).

Following the steeping process, the softened grains are macerated or milled to separate starch granules from cellular material. The maceration process is carried out in a short

period of time (less than one minute) to minimise physical disruption and release of degrading enzymes from the grains. The macerated grains are filtered to obtain the starch suspension. Proteinaceous material can be removed with repeated extraction with toluene (McDonald and Stark, 1988). For the analysis of polysaccharides, complete dissolution of starch is necessary. Dimethylsulfoxide (DMSO), combined with alkali, ensures good dissolution (Matheson and Welsh, 1988).

1.4.2 Fractionation of starch into its components

Methods have been developed to fractionate starch into its two components: the essentially unbranched amylose, and the highly branched amylopectin molecules. The methods are based on the differences between the two components: the differential ease of dissolution of the two fractions, the capacity to complex and precipitate with small straight-chain compounds (such as *n*-butanol) or lectins (such as concanavalin A), and the difference in the molecular size of the two fractions.

1.4.2.1 Aqueous leaching

Leaching occurs from swelling starch granules in water at temperatures of 57-100°C. Amylose molecules diffuse out of the swollen granules while the granule remains largely intact, whereas most of the amylopectin remains crystallised in the granule residue. The amylose can then be collected in the supernatant by centrifugation, and precipitated from solution by the addition of a suitable alcohol, usually *n*-butanol (Banks and Greenwood, 1975). Successive leaching at higher temperatures releases more amylose, however some of the branched amylopectin molecules may diffuse out to contaminate the amylose fractions (Young, 1984). The different fine structures of amylose and amylopectin may result in incomplete leaching of amylose, and thus the leached amylose may not be representative of the whole.

The insolubility of the amylopectin fraction can be increased relative to that of amylose by pretreating the starch granules with hot aqueous *n*-butanol, or dioxane, before aqueous leaching (Montgomery and Senti, 1958). Pre-treatment of the starch in this way may reduce the length of time needed for leaching and reduce the amount of amylopectin leached (Banks and Greenwood, 1975).

1.4.2.2 Complexing

In 1941, Schoch reported the selective precipitation of amylose from a starch solution by *n*-butanol (Schoch, 1941). Later, defatted corn and potato starches were completely dispersed by autoclaving, and amylose was subsequently precipitated with *n*-butanol or isoamyl alcohol. The amylose was purified by recrystallisation from the same solvent (either isoamyl alcohol or *n*-butanol). Amylopectin was collected from the supernatant, after removal of amylose, by precipitation with ethanol or methanol (Schoch, 1945).

Other reagents have been used that complex with amylose, such as cyclohexanol, thymol, nitroparaffins, and fatty acids in saturated aqueous solution (Bear, 1944; Whistler and Hilbert, 1945; Haworth *et al.*, 1946; Adkins and Greenwood, 1966; Kuge and Takeo, 1968). Starch granules need to be fully dispersed in solution. This is relatively difficult for some cereal starches, where after several hours at 100°C the starch suspensions may still contain amounts of undispersed material. Pre-treatment with liquid ammonia or dimethyl sulfoxide (DMSO) is widely used to destroy the granular structure. The force used in the centrifugation of the *n*-butanol-amylose complex is also critical. At high centrifugal forces, there is a tendency for the amylopectin fraction to precipitate, whereas at low centrifugal forces some amylose complex may be left in solution. The chain length of amylose is also a critical factor. Short-chain amylose does not form an insoluble complex (Muetgeert, 1961).

1.4.2.3 Separation by size

Separation of amylose and amylopectin by gel permeation chromatography (GPC) is a method based on molecular size. The large molecular sized amylopectin elutes first while amylose is retarded in the gel matrix. Quantitative fractionation of wheat starch (Matheson, 1971), maize starch (Ebermann and Schwartz, 1975; Yamada and Taki, 1976), potato starch (Ebermann and Schwartz, 1975) and rice starch (Chinnaswamy and Bhattacharya, 1986) has been carried out on columns of Sepharose 2B (exclusion limit for polysaccharides 20 x 10^6). Sepharose CL-2B (the cross-linked Sepharose 2B) has been used to separate high-amylose pea, tobacco leaf, waxy rice, potato starches (Matheson and Welsh, 1988), alfalfa root starch (Fankhauser *et al.*, 1989), and maize starch (Yeh *et al.*, 1981). Eluents used for chromatography have included water (Ebermann and Schwartz, 1975; Fankhauser *et al.*, 1989), 0.01 M sodium hydroxide solution (Fankhauser *et al.*, 1989), 0.1-0.3% sodium chloride solution (Matheson, 1971; Matheson and Welsh, 1988),

and 0.04% perchloric acid (Yamada and Taki, 1976). Since starch contains a spectrum of structures with various molecular sizes and chain lengths, GPC can lead to mixed fractions. High performance size-exclusion chromatography has been used as a rapid method of fractionating amylose and amylopectin (Kobayashi *et al.*, 1985; Kobayashi *et al.*, 1986).

1.4.2.4 Concanavalin A

Another method of separating amylose from amylopectin involves the use of concanavalin A (con A) in solution (Matheson and Welsh, 1988). Con A is a lectin that binds specifically to the non-reducing terminal α-D-glucopyranosyl or α-D-mannopyranosyl groups of a polysaccharide to form insoluble complexes (Goldstein and So, 1965; Goldstein and Poretz, 1986). The concentration of con A and molecular weight of the polysaccharide are important factors that control the extent of interaction (Doner, 1978). It was observed that quite different glycogen values were obtained for various polysaccharides if the assays were conducted at different con A concentrations. The number of chain ends per unit weight was the major parameter controlling the amount of con A required for fractionation (Doner, 1978). The optimum pH range for the precipitation reaction is between 6.1 and 7.2 (So and Goldstein, 1967).

Amylose and amylopectin from wheat starch have been prepared quantitatively with con A, and subsequent elution profiles by gel chromatography have shown the separated fractions to be pure (Matheson and Welsh, 1988, Matheson, 1990). In this procedure, critical concentrations of branched fractions and con A were examined with potato starch. The reaction between polysaccharide and con A was complete after two hours at room temperature. The con A was removed by addition of a proteinase, thereby releasing the glucan into solution. The glucan was recovered by subsequent centrifugation. The method requires highly pure con A and proteinase.

1.4.3 Chemical structure of starch and starch components

1.4.3.1 Enzymes used in structural studies

Starch-degrading enzymes can be divided into three categories: those that are specific for α(1→4) linkages, those specific for α(1→6) linkages, and those that hydrolyse both α(1→4) and α(1→6) linkages (Guilbot and Mercier, 1985). The actions of these enzymes on starch are summarised in Fig. 1.6.

α-Amylase (EC 3.2.1.1) and β-amylase (EC 3.2.1.2) belong to the first category of enzymes. α-Amylase is an endoenzyme that cleaves internal α(1→4) linkages randomly to produce maltose, maltotriose, and glucose (Robyt and Whelan, 1968a). α-Amylases are able to by-pass interchain linkages, and thus are able to hydrolyse those parts of the chain that lie between branch points. This results in a rapid degradation of the starch, however, the rate of action slows as chain length is reduced (Manners, 1985).

β-Amylase is an exoenzyme that attacks the glucans stepwise from the non-reducing end, producing β-maltose residues. The action of the enzyme is blocked by α-D-(1→6) branch linkages and residues of glucose-6-phosphate, thus a high molecular weight limit dextrin is produced (Robyt and Whelan, 1968b). In the case of amylopectin, the action of β-amylase is confined to the outermost branches. β-Amylase is therefore useful in estimating the average external chain length (Manners, 1985).

Isoamylases (EC 3.2.1.68) and pullulanases (EC 3.2.1.41) belong to the second category of enzymes. The action of these enzymes is specific for α(1→6) linkages. Isoamylase is endo-acting, hydrolysing α(1→6) linkages throughout the glucan molecule, whereas pullulanase is exo-acting, hydrolysing the outermost α(1→6) linkages first.

The third category of enzymes includes amyloglucosidase, which has the ability to hydrolyse both α(1→4) and α(1→6) linkages (Robyt, 1984).

Considerable information on the fine structure of a polysaccharide can be gathered from controlled enzymatic analysis using an enzyme alone or in combination with another enzyme. Yun and Matheson (1993) used a combination of β-amylase, isoamylase and pullulanase to study the structures of rabbit-liver glycogen, phytoglycogen, and the amylopectins from waxy rice starch, and waxy, normal, and amylose extender maize starches. They found that all amylopectin samples had A:B chain ratios of greater than 1, whereas the two glycogens had ratios of less than 1.

Figure 1.6

Diagrammatic representation of the enzymatic digestion of amylose and amylopectin by α-amylase, β-amylase, and debranching enzyme (Thomas and Atwell, 1999).

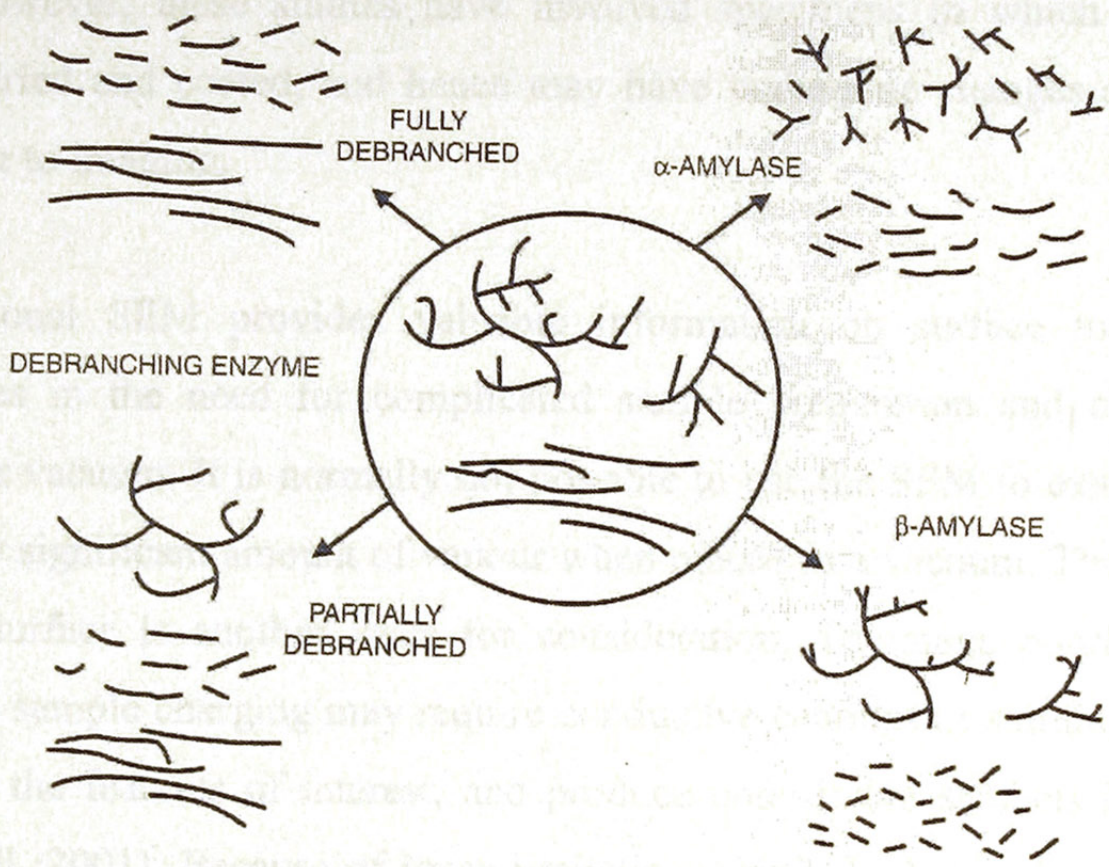

1.4.4 Structural studies by microscopy

An increased understanding of how ingredients change during processing is likely to lead to novel ways to develop improved products. The functional properties of starch are influenced by its chemical and physical structures. The major determinants of functionality are the ratio, structure, and characteristics of the two fractions of starch. There have been many studies on the effect of processing on raw products, but most have involved destructive chemical methods that can bring about significant changes in the material. Chemical analyses of polysaccharides provide good information on the composition but do not provide a picture of the polysaccharide as a whole (Round *et al.*, 1997). Most polysaccharides have complex structures that are difficult to characterise by conventional biophysical methods (Kirby *et al.*, 1996). Knowledge of morphology of cereal grains obtained from light, scanning and transmission electron microscopy has contributed substantially to our understanding of structure-function relationships relevant to processing.

There have been numerous reports describing examinations of the surface structure of fractured raw rice (*Oryza sativa*) grains using scanning electron microscopy (SEM). The effects of heat and chemical treatments on cereal grains and starch, especially from wheat and corn, have also been observed using SEM (Evers and Juliano, 1976; Blakeney, 1980; Zee, 1981). However, these studies have involved specimens in which the fractured surfaces were dried and coated, and hence may have undergone changes due to sample preparation prior to imaging.

While conventional SEM provides valuable information on surface topography, its disadvantage lies in the need for complicated sample preparation and observation of specimens under vacuum. It is normally not possible to use the SEM to examine samples that produce any significant amount of vapour when placed in a vacuum. The conductivity of the sample surface is another issue for consideration. To image poorly conductive surfaces without sample charging may require conductive coatings or staining, which may alter or obscure the features of interest, and produce undesirable artifacts in the images obtained (Russell, 2001). Because of these limitations, biological samples must be dried and metal-coated, and many samples such as grease, adhesives, liquids, foods gels, and other semisolids can not be examined.

The environmental scanning electron microscope (ESEM) was developed to overcome the limitations of the conventional SEM. The ESEM is specifically designed to study wet, oil bearing, or insulating materials. Samples may be examined in water vapour or other gases such as carbon dioxide or nitrogen at near atmospheric pressure due to the unique vacuum system of the ESEM (FEI, 2003).

In order to examine liquid and hydrated samples, an operating pressure of at least 6×10^{-4} atm (4.6 Torr, 612 Pa) is needed. This is the minimum vapour pressure required to maintain water liquid at 0°C. With its multiple pressure limiting apertures and secondary electron detectors, the ESEM is able to offer high resolution imaging at pressures as high as 6.6×10^{-2} atm (50 Torr). The ESEM is equipped with hot and cryogenic stages that permit examination of samples over a wide temperature range of -80°C to 1000°C. The ESEM also has a micro-injection system, which allows the direct application of liquids onto samples while imaging a region of interest. The ESEM is therefore a useful tool for studying dynamic changes in biological tissues and synthetic polymers (FEI, 2003).

ESEM allows specimens to be studied at high resolution, close to their natural states with minimal preparation. Dynamic hydration/dehydration events can be followed by changing the water vapour pressure in the sample chamber (Callow *et al.*, 2003). Samples with high moisture content do not need to be metal-coated as in conventional SEM studies, which makes ESEM a simpler method. The resolution of the ESEM is of the order of 10 nm, and the magnification range is 10- to 10^4-fold (Table 1.3) (Veeco Instruments, 2003). There is little information from ESEM studies of cereal grains and starches, especially on the effects of processing.

The operation of the atomic force microscope (AFM) has been described elsewhere (Hansma and Hoh, 1994; Kirby *et al.*, 1996; Allen *et al.*, 1997; Brant, 1999) and its use in research has been reviewed by Czaikowsky *et al.* (2000). Operation of the AFM will be described only briefly here. The AFM uses a sharp tip attached to a cantilever spring, which is scanned across the surface of the sample. Interaction between the tip and the sample causes the cantilever to deflect. This deflection is monitored and translated into a three dimensional image down to the micrometre-to-nanometre scale (Table 1.3) (Hansma and Hoh, 1994).

There are three imaging modes in using the AFM: 1) contact, 2) non-contact, and 3) tapping modes. In contact mode, the cantilever comes into contact with the sample surface, and the adhesive forces between cantilever and sample are measured. In non-contact mode, the cantilever raster-scans just above the surface of the sample. Van der Waal's forces between the cantilever and sample are measured. As the cantilever does not come in contact with the surface of the sample, non-contact mode reduces the risk of damage to the sample. However, resolution in non-contact mode is lower than that achieved in contact mode. In tapping mode, the cantilever scans in a tapping motion, and thus intermittently comes into contact with the surface of the sample. There is minimal contact between the cantilever and surface of the sample in tapping mode compared to contact mode. Shear forces, which can damage soft samples and reduce image resolution, are therefore greatly reduced in tapping mode (Veeco Instruments, 2003).

Table 1.3

Comparison of features of SEM, ESEM and AFM.

Parameter	**SEM**	**ESEM**	**AFM**
Operating environment	Vacuum	Vacuum	Ambient/liquid/vacuum
Depth of field	Large	Large	Medium
Resolution (*x,y*)	5 nm	10 nm	0.1 – 0.3 nm
Resolution (*z*)	N/A	N/A	0.01 nm
Magnification range	10X – 10^6X	10X – 10^4X	5 x 10^2X – 10^8X
Sample preparation	Freeze drying, coating	Minimal	Minimal

Source: Veeco Instruments (2003).

AFM has been used to study biological membranes, cell surfaces, and the molecular structure of various biological macromolecules, including DNA (Fritzsche *et al.*, 1997), proteins and polysaccharides such as xanthan, acetan, gellan, carrageenan (Kirby *et al.*, 1996; McIntire and Brant, 1997; McIntire and Brant, 1999), and pectin (Round *et al.* 1997). Using the AFM, researchers have been able to obtain information on molecular length, size distribution, and molecular stiffness of polysaccharides such as pectin (Round *et. al.*, 1997), xanthan, acetan (Kirby *et al.*, 1996), and carrageenan (Kirby *et al.*, 1996; McIntire and Brant, 1999). In imaging pectin extracted from unripe tomatoes under butanol with non-contact mode, Round *et al.* (1997) observed branched structures, with branches 30-170 nm long. Kirby *et al.* (1996) imaged bacterial polysaccharides, xanthan and acetan, under a layer of butanol. The high resolution achieved with AFM allowed the observation of the polysaccharide matrices. The mean contour length and apparent height of the plant polysaccharide carrageenan, imaged in air, have been reported by McIntire and Brant (1997, 1999).

AFM has been used to examine the surface of granules of commercial preparations of isolated potato and wheat starch samples (Baldwin *et al.*, 1997). The potato and wheat starch surfaces were rough, with the presence of small raised nodules (approximately 50 to 300 nm in diameter), protruding from a smoother surface consisting of smaller semi-spherical structures (approximately 20 to 50 nm in diameter). The presence of nodules was less frequent in the starch from wheat than in potato starch. The inner surfaces of mechanically disrupted corn, rice, wheat and sweet potato starches have been imaged by

Ohtani *et al.* (2000a, 2000b). Fine particles of approximately 30 nm in diameter were observed inside each granule from these starches. These particles occasionally formed straight chain structures. The authors proposed that these fine particles may correspond to the individual blocklet or single cluster proposed in the cluster model. Baker *et al.* (2001) examined sectioned native corn starch granules using the AFM. The authors observed native granules with blocks 400-500 nm in size that span the growth rings. Lintnerised starch granules showed smaller 'blocklets' within the rings approximately 10-30 nm in size. These observations are in agreement with the blocklet structures that have been proposed in the literature for the clustering of amylopectin helices. However, all of these studies have been performed on starch samples that have been subjected to a degree of disruption. There is no information in the literature on the use of AFM to image starch granules *in situ*.

1.4.5 Pasting properties

Knowledge of pasting properties is often an important indicator of the processing quality of foods and their constituents. For example, such knowledge can enable a processor to optimise conditions (ingredient concentration, temperature/pressure/shear limits) to achieve a desired product. Industrially relevant viscosities of starch pastes and gels range from about 100-10,000 centipoise. The starch source, granule size, molecular weight, amylose-amylopectin ratio, concentration, temperature, shear rate, chemical modification, other components (such as lipids and surfactants), and other factors all affect the apparent viscosity (French, 1984; Bason, 2001).

Pasting properties of starch have traditionally been studied by the Brabender viscoamylograph. However, the method has several disadvantages such as long analysis time (> 1 hour), large sample size (50 g) and high cost of the instrument. The Rapid Visco Analyser (RVA) was developed by the Australian CSIRO Wheat Research Unit (North Ryde, NSW) and Bread Research Institute (North Ryde, NSW) to screen wheat samples for sprout damage (Ross *et al.*, 1987). The RVA is now commonly used to assess the pasting properties of samples where cooked viscosity is important.

The RVA is a heating and cooling viscometer that monitors the resistance of a sample to controlled shear, producing a characteristic pasting curve as shown in Fig. 1.7.

Measurement of viscosity is in centipoise (cP) or Rapid Visco Unit (RVU). One RVU is equivalent to 12 centiPoise (Newport Scientific, 1998).

Since measurement conditions affect viscosity results, identical shear rate and time variables are required to make results comparable. To this end, standard methods have been developed for the RVA (Bason, 2001). RVA tests for rice have been approved as standard methods by the American Association of Cereal Chemists (Method 61-02, AACC, 1995) and the Royal Australian Chemical Institute (Official Method 06-05, RACI, 1995).

The RVA subjects a starch slurry to a heat-hold-cool cycle. When starch granules are heated in water beyond the gelatinisation temperature, the granules absorb water and swell, causing a rapid increase in viscosity. The temperature at the onset of this rise in viscosity is known as the pasting temperature (Fig. 1.7). The pasting temperature provides an indication of the minimum temperature required to cook a given sample (Newport Scientific, 1998). The peak viscosity is the point at which maximum swelling is in equilibrium with rupture of granules (Fig. 1.7). The rate and degree of swelling and breakdown is characteristic of the starch source, and is affected by processing, other components and modification. The peak viscosity is indicative of the water-binding capacity of the starch and the ease with which the starch granules are disintegrated, and is often correlated with final product quality (Thomas and Atwell, 1999; Tran *et al.*, 2001).

The peak is followed by a breakdown in viscosity to a minimum (known as the trough viscosity), as a result of granule rupture and leaching of granular components during exposure to high temperature and shear (Fig. 1.7). The rate of reduction in viscosity is dependent on the nature of the material, the temperature and shear. A cross-linked starch, for example, would resist breakdown and therefore have a smaller breakdown value (that is, higher trough viscosity) compared to its non cross-linked counterpart. High temperature and shear conditions would cause a sample to breakdown more readily due to the extreme stress experienced by the sample. For rice, a higher breakdown is believed to indicate better palatability. Tran *et al.* (2001) compared the physicochemical properties of Vietnamese and Japanese rice cultivars and found that among the Japanese rices, the one with the highest breakdown value was indicated to be the most palatable.

Figure 1.7

A typical RVA pasting curve showing the different parameters used to characterise pasting behaviour of cereal starches and flours.

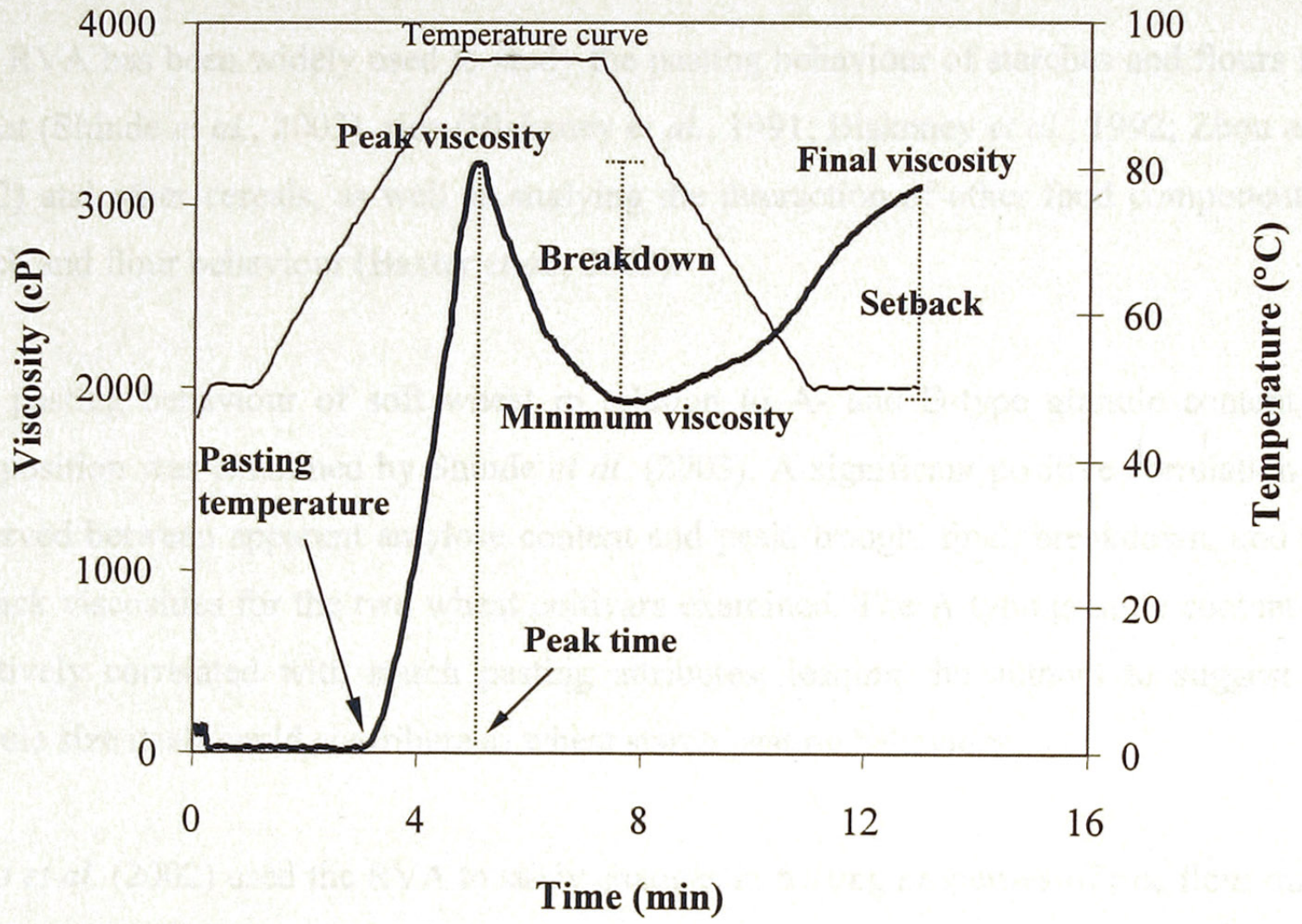

Upon cooling, the decrease in energy of the system allows the formation of hydrogen bonds between starch chains (Hoseney, 1994; Thomas and Atwell, 1999), causing an increase in viscosity at the end of the RVA test (Fig. 1.7). The rise in viscosity may also be contributed by some reassociation of leached molecules undergoing the initial stages of retrogradation. The increase in viscosity from the trough to the final viscosity is commonly termed the setback, and has been correlated with the texture of various end products. High setback is also an indication of the amount of swelling power of the sample, and often this is influenced by the amylose content. The straight chain structure of amylose allows it to readily form hydrogen bonds between molecules, resulting in rigid gels (Martin and Smith, 1995). Amylopectin molecules reassociate more slowly compared to amylose molecules. Tran *et al.* (2001) found a significant and high positive correlation between final viscosity and amylose content in both Vietnamese and Japanese rices ($r = 0.97$ and 0.92, respectively). Shinde *et al.* (2003), in studying the pasting properties of two wheat cultivars in relation to A- and B-type granule content, found that both peak and final viscosities increased with increasing apparent amylose contents.

The final viscosity is the most commonly used parameter to define the quality of a sample, as it indicates the ability of the material to form a viscous paste or gel after cooking and cooling.

The RVA has been widely used to study the pasting behaviour of starches and flours from wheat (Shinde *et al.*, 2003), rice (Blakeney *et al.*, 1991; Blakeney *et al.*, 1992; Zhou *et al.*, 2002) and other cereals, as well as studying the interaction of other food components on starch and flour behaviour (Baxter *et al.*, 2002).

The pasting behaviour of soft wheat in relation to A- and B-type granule content and composition was examined by Shinde *et al.* (2003). A significant positive correlation was observed between apparent amylose content and peak, trough, final, breakdown, and total setback viscosities for the two wheat cultivars examined. The A-type granule content was positively correlated with starch pasting attributes, leading the authors to suggest that granule size itself could contribute to wheat starch pasting behaviour.

Zhou *et al.* (2002) used the RVA to study changes in pasting properties of rice flour during storage at 4 and 37°C. The authors concentrated on the breakdown value. Storage at 37°C had the greatest effect on pasting properties. The breakdown value decreased (that is, higher minimum viscosity) on storage at high temperature, suggesting that the rice grain becomes more organised with time. The decrease in breakdown value indicates that the capacity of the starch granules to rupture after cooking is reduced significantly by aging of the granules.

Baxter *et al.* (2002) studied the variation in pasting due to the protein content of fractions from rice grown under different agronomic conditions (with or without nitrogen fertiliser application, and with or without sodium chloride application). The results indicated that protein content alone may not be a good indicator of the effect of protein on pasting properties, and that changes in the composition of protein fractions may play a role in determining pasting properties of rice. Different rice protein fractions had different effects on RVA profiles, with the albumin and glutelin fractions having greater effect on peak viscosity than globulin and prolamin.

1.5 Variation in starch properties during development

The chemical, structural and physical properties of starch can change significantly during development, as the amylose and amylopectin are synthesised during this time (Juliano, 1985). Briones *et al.* (1968) and Singh and Juliano (1975) studied the properties of several varieties of rice (IR8 and IR28) during development. They found that for the variety IR8, the apparent amylose content increased from 25 to 29% from 4 days to 39 days after flowering, and for the variety IR28, the apparent amylose content increased from 30 to 37% from 3 days after flowering to maturity. Asaoka *et al.* (1985b) found that the amylose percentage of rice starch increased from 9% at 5 days after flowering to 19% in mature grains. The rate of increase in apparent amylose content was affected by temperature during the grain-filling period. A higher temperature (30°C compared to 25°C) caused a decrease in apparent amylose content. The apparent amylose content, measured by iodine affinity, increased from 13 to about 20% in potato tuber starch. There was a direct relation between the percentage of amylose and the granule size (Geddes *et al.*, 1965).

In studying properties of several rice starches during growth, Briones *et al.* (1968) found no significant change in the chain length of amylopectin, as measured by periodate oxidation after fractionation of starch by complexing with *n*-butanol. However, differences were reported in the amylopectin fractions from plants grown at 25°C and 30°C (Asaoka *et al.*, 1984; Asaoka *et al.*, 1985a; Asaoka *et al.*, 1985b). Inouchi *et al.* (2000) studied the effects of environmental temperature during the early development of seeds on the structural characteristics of rice endosperm starch. They found that amylopectin of rice plants grown at 25°C contained increased amounts of short chains and decreased amounts of long chains, compared with amylopectin obtained from rice plants grown at 30°C. The authors confirmed that the environmental temperature between five and ten days after pollination strongly influenced the structure characteristics of the endosperm starch of rice plants.

1.6 Differences of mature starches among different genotypes

The structural characteristics of starch from different plant species vary. There is evidence that starches of a similar genotype from different species can have structural differences and that even within a genotype of a single species differences between varieties of the species can occur (Banks and Greenwood, 1975).

Properties of starches from cereals, legumes, underground storage organs and some seeds and fruits have been examined (Greenwood and Thomson, 1962). The apparent amylose contents varied from 11 to 35% with the average granule size from 5 to 40 μm. A range of gelatinisation temperatures from 53-55°C to greater than 98°C was observed. Williams *et al.* (1970) found that starches from twenty-six different sources varied in amylose content from 10 to 36%.

1.7 Differences among varieties of the same species and genotype

Physicochemical properties of cereal grains and starch can differ among varieties of the same genotype and species (Banks and Greenwood, 1975). The properties of several rice varieties were examined by Reyes *et al.* (1965) and Suzuki and Juliano (1975). It was found that the apparent amylose content varied between 13 and 37%. The properties of the amylose fractions ranged from 80 to 177 ml/g in viscosity, 600 to 13000 glucosyl units in degree of polymerization (DP), and 83 to 90% in β-amylolysis limit. The properties of the amylopectin fractions ranged from 0.4 to 2.7% in iodine binding capacity (IBC), 83 to 168 ml/g in viscosity, 49 to 58% in β-amylolysis limit, and 13 to 18 glucosyl units in external chain length.

Structural characteristics of starch components from other rice varieties (*Indica* and *Japonica*) have been investigated (Takeda *et al.*, 1986; Juliano *et al.*, 1987; Takeda *et al.*, 1989a; Hizukuri *et al.*, 1989; Takeda *et al.*, 1989b). These two sub-species of rice have distinct cooking and processing characteristics. Amyloses fractionated from two *Japonica* and five *Indica* varieties showed slightly differing values for IBC, viscosity, β-amylolysis limit, DP, and distribution of unit chains. The limiting viscosity numbers of the amyloses varied and showed a correlation with the amount of branching in the amylose. Different IBC, viscosity, and DP values were also observed in the amylopectin fractions, however the β-amylolysis limits were similar. Elution profiles by HPLC of amylopectin debranched by isoamylase showed different proportions of long, medium and short unit chains. Fuwa *et al.* (1992) examined fourteen *Indica* rice starches by gel chromatography on Sephadex G-75 after debranching with isoamylase. The amylose content varied between 14 and 27%, with the maximum absorbance of the iodine complex ranging between 580 and 606 nm.

Inouchi *et al.* (2000) studied the effects of genotype and environment on properties of endosperm starch. They concluded that environmental effects on properties of the endosperm starch are, in general, not as pronounced as effects associated with genetic factors such as species and varieties.

1.8 Relationship between structure and function and the use of starch components

Amylose and amylopectin differ in their rheological and viscoelastic properties. Both polymers are hydrophilic, and when heated in a food system readily form a paste with uncombined water (Foster, 1965; Banks and Greenwood, 1975; Whistler, 194).

The rate of amylose gelation depends on time, temperature, pH and concentration of amylose. Gelation rate increases at high concentration. Gel time and temperature are affected by the DP of amylose. Amylose gels are opaque, chalk-white, strong but not stringy, and can be re-solubilised above 124°C (Foster, 1965).

High amylose starches form films readily, and are quick setting to form structurally stable gels. Their ability to bind other materials makes them suitable for improving food products (Coultate, 1996). The behaviour of amylose and high amylose starch is utilised in many industrial areas, particularly its film forming and coating properties. Amylose molecules in solution are not stable on cooling, as these molecules have a high tendency to orient in parallel. In low concentration and at low temperature, amylose readily retrogrades and forms an ordered precipitate that is difficult to redissolve (Foster, 1965).

The branched structure of amylopectin results in the amylopectin having a limited ability to retrograde. Amylopectin solutions are therefore relatively clear and fluid. Gelatinisation of amylopectin, particularly from waxy starch, occurs at low concentrations. Sticky and stringy pastes of amylopectin and waxy starch have a high resistance to syneresis and exhibit an elastic, stringy consistency when cooled. Because of these properties, waxy starch is used as a raw material for food stabilizing (Foster, 1965).

The amylose-amylopectin ratio in rice starch is the major factor involved in cooking and eating quality (Juliano, 1985). The ratio determines many of the properties of boiled rice.

A higher amylose content improves the capacity of the starch granule to absorb water and expand in volume without collapsing, because of the greater capacity of amylose to hydrogen-bond and retrograde. The final gelatinisation temperatures of non-waxy and waxy rice starch granules have a range of 55 to 79°C. Differences in starch gelatinisation temperature may be reflected in the differences in cooking time of milled rice. Rice samples with higher gelatinisation temperatures require longer to cook than do those with low gelatinisation temperatures (Juliano, 1985).

Cooked-rice texture has long been thought to be a result of its amylose extender content. Based on the work of several researchers, the focus of rice texture was changed from amylose to amylopectin (Chinnaswamy and Bhattacharya, 1986; Takeda *et al.*, 1987; Hizukuri *et al.*, 1989; Takeda *et al.*, 1989b; Rhadhika Reddy *et al.*, 1993; Rhadhika Reddy *et al.*, 1994). Ramesh *et al.* (1999) found that the texture of cooked rice was mostly determined by the content of all the long linear chains, free (amylose) or bound (amylopectin), in the starch molecule.

Ramesh *et al.* (1999) studied the structure of rice starch by gel permeation chromatography, and attempted to relate structure to cooked-rice texture. They found that the content of long B chains of the branched molecules, and the calculated amylose content, correlated well with the sensory tenderness of cooked rice. It was also observed that the content of all long linear chains, including amylose if any, govern the texture of cooked rice.

Wang and Wang (2002) studied the structure of four waxy rice starches in relation to thermal, pasting, and textural properties. They observed that the fine structure of amylopectin was different for different waxy rice cultivars, and that the differences in structure determined their different physicochemical properties. The authors suggested that the retrogradation of waxy rice starch might be reduced by the presence of a large amount of A chain and a short external chain length, whereas the increase in hardness of waxy rice starch paste might be favoured by a large amount of A+B1 chains. The large DP of amylopectin was suggested to contribute to a lower water solubility index despite its high swelling power.

1.9 Objectives of the study

The main objective of this study was to examine the influence of genotype and environment on the physicochemical properties of rice, using a combination of chemical, imaging and pasting analyses. The properties of rice studied included 1) the chemical composition of the grains, 2) structural arrangement of starch granules, and 3) pasting behaviour of rice flour. Samples of rice were obtained that were representative of varietal and environmental differences.

Chemical analyses were performed to determine the macro-composition and overall make-up of the rice samples, and provide information on the effect of genotype and environment on chemical composition. Two novel microscopic techniques, namely ESEM and AFM, were explored for examining the structural arrangement of starch within the rice grain. Sample preparation techniques were explored to develop procedures for imaging rice grains and starch components using both microscopic methods. The effect of environment and genotype on the structural arrangement of starch within the rice grain was studied. The pasting behaviour of the samples was studied in an attempt to increase understanding of the effects of differences in chemical and structural properties on processing behaviour.

CHAPTER 2

Materials and Methods

2.1 Samples

Unprocessed and processed rice samples (2 kg) of three varieties (Langi, Doongara and Kyeema) were supplied by SunRice Australia Limited (formerly RiceGrowers Cooperative Limited), Leeton NSW, Australia. Doongara is a long-grained, high amylose variety, with a soft cooked texture; Langi, a long-grained, soft-textured, low amylose variety; and Kyeema, a long-grained, low amylose fragrant rice. Samples were obtained of rice grown in the 1998/1999, 1999/2000, and 2000/2001 seasons and from several locations (Murrumbidgee Irrigation Area – MIA, Coleambally Irrigation Area – CIA, Murray Valley - MV) in the 1998/1999 season. Processed forms (parboiled and quick-cooking) of Doongara rice were also supplied by SunRice Australia Limited. Medium-grained waxy (Shirakiku brand, imported from California, USA) and long-grained waxy (Butterfly brand, imported from Thailand) rices were obtained from a local supermarket. All samples were stored in airtight containers at 4°C until use.

2.2 Enzymes

β-Amylase ((1→4)-α-D-glucan maltohydrolase, E.C. 3.2.1.2, *Bacillus cereus*, cat. no. E-BCBAM), isoamylase (glycogen 6-glucanohydrolase, E.C. 3.2.1.68, *Pseudomonas* sp., cat. no. E-ISAMY) and pullulanase (pullulan 6-glucanohydrolase, E.C. 3.2.1.41, *Klebsiella pneumoniae*, cat. no. E-PULKP) were obtained from Megazyme International Ireland (Bray, Co. Wicklow, Ireland). Amyloglucosidase (E.C. 3.2.1.3, cat. no. 737160), porcine α-amylase (E.C. 3.2.1.1, cat. no. 102814), glucose oxidase (E.C. 1.1.3.4, cat. no. 646431), peroxidase (E.C. 1.11.1.7, cat. no. 413470) and proteinase K (from *Tritirachium album*, cat. no. 745723) were obtained from Roche Diagnostics (Basel, Switzerland).

2.3 Reagents and solutions

Distilled water

Distilled water with conductivity below 0.05 μS/cm was used for all experiments.

Concanavalin A (con A)

Con A (Type V, from *Canavalia ensiformis* (jack bean), cat. no. C7275) was obtained from Sigma.

Amylose and amylopectin

Amylose (from potato, Type III, cat. no. A0512) and amylopectin (from potato starch, cat. no. 10118) were obtained from Sigma.

Buffer A (pH 6.0 or 6.4) for use with concanavalin A

(1 M Na+, 1 mM Ca2+, 1 mM Mg2+, 1 mM Mn2+ as chlorides in 0.5 M acetate buffer)

Anhydrous sodium acetate (41.2 g), sodium chloride (175.5 g), calcium chloride dihydrate (0.5 g), magnesium chloride hexahydrate (0.7 g) and manganese chloride tetrahydrate (0.7 g) were dissolved in distilled water (900 mL). The pH of the solution was adjusted to 6.4 or 6.0 with glacial acetic acid. The volume was made up to 1 L with distilled water. This concentrated solution was stored at 4°C and used within one month of preparation. Stock solution of Buffer A (30 mL) was diluted to 100 mL with distilled water prior to use.

Acetate buffer (0.2 M, pH 5.0)

Anhydrous sodium acetate (16.4 g) was dissolved in distilled water (900 mL). Glacial acetic acid was added to adjust the pH to 5.0, and the volume made up to 1 L. This solution was stored at 4°C.

Con A solution

Buffer A (pH 6.4, 30 mL) was diluted to 100 mL with distilled water. Con A (21 mg) was dissolved in diluted Buffer A (3.5 mL) to make con A solution.

Phenol-sulphuric acid solution

Phenol (May and Baker Pronalys AR, 25 g) was dissolved in 0.2 M sulphuric acid (500 mL).

Amyloglucosidase and α-amylase solution

Amyloglucosidase (250 U) and porcine α-amylase (50 U) were dissolved in 0.2 M acetate buffer (pH 5.0) to a final volume of 15 mL.

Glucose oxidase, peroxidase and 4-aminoantipyrine (GOPOD) reagent

Disodium hydrogen orthophosphate (24.8 g), sodium dihydrogen orthophosphate (16.1 g), benzoic acid (4 g), 4-aminoantipyrine (4-amino phenazone, Sigma A4382, 0.2 g) and 3-hydroxy benzoic acid (Merck, 3 g) were dissolved in distilled water (1800 mL). Glucose oxidase (8000 U, 40 mg) and peroxidase (2500 U, 10 mg) were added and the volume made up to 2 L. The solution was stable for 3 months when stored in the dark at 4°C.

Methyl α-D-mannopyranoside solution

Sodium acetate (1.64 g) was added to 0.05 M calcium chloride (20 mL) and made up to 100 mL with distilled water. Methyl α-D-mannopyranoside (Sigma M3752, 3.2 g) was dissolved in 40 mL of this solution.

Iodine-potassium iodide solution

Iodine (2%)-potassium iodide (20%) solution was made and stored in a brown bottle in the dark. This solution was diluted 1 in 50 in distilled water prior to use.

Sodium arsenite solution (0.1 M sodium arsenite in 0.2 M phosphate buffer)

Sodium arsenite (13 g), disodium hydrogen orthophosphate (3.5 g) and potassium dihydrogen orthophosphate (23.9 g) were dissolved in distilled water (1 L) and sterilised by boiling.

Tris.HCl solution

Tris.HCl solution was prepared by adding trizma base (Sigma T1503, 0.605 g) to 0.05 M calcium chloride (5 mL) and 0.2 M hydrochloric acid (3.35 mL).

Proteinase K solution

Proteinase K (500 U, 25 mg) was dissolved in Tris.HCl solution (10 mL) and made up to 25 mL with distilled water.

Nelson-Somogyi reagents

Reagent A – anhydrous sodium carbonate (25 g), sodium-potassium tartrate (25 g), sodium bicarbonate (20 g) and anhydrous sodium sulphate (200 g) were dissolved in distilled water (1 L) and the solution filtered.

Reagent B – cupric sulphate pentahydrate (30 g) was dissolved in distilled water (200 mL) containing 4 drops of concentrated sulphuric acid.

Copper reagent – Reagent A (25 parts) was mixed with Reagent B (1 part) prior to use.

Reagent C – ammonium molybdate (35 g) was dissolved in distilled water (450 mL) to which concentrated sulphuric acid (21 mL) was added. Sodium arsenate heptahydrate (3g) was dissolved in water (25 g) and added slowly to the ammonium molybdate solution with stirring. The solution was diluted to 500 mL and warmed for 30 min in a water bath at 55°C, or stored overnight at 37°C before use.

2.4 Estimation of protein content

Nitrogen content of rice grains was determined by the Kjeldahl method (AACC 46-12) of the American Association of Cereal Chemists (AACC, 2000). Protein content was calculated from nitrogen content by multiplying Kjeldahl nitrogen by 5.95, which is based on the nitrogen content (16.8%) of the major rice protein, glutelin (Juliano, 1972).

2.5 Estimation of lipid content

Lipid content of rice grains was estimated by solvent extraction. Rice grains (1 g) were crushed and placed in a preweighed Soxlet flask containing a few boiling chips. The crushed grains were extracted with light petroleum using the Soxlet extraction apparatus for 2.5 h. After extraction, the solvent was evaporated and the Soxlet flask was reweighed. A blank determination, containing no rice grains and only light petroleum, was performed. The oil content was the difference in weight of the Soxlet flask before and after extraction, expressed as a percentage dry weight.

2.6 Isolation of starch from rice grains

The method of Matheson and Welsh (1988) was used to isolate starch granules from rice grains as summarised in Fig. 2.1. Briefly, milled rice grains (500 g) were soaked for 48 h in 0.2 M ammonium hydroxide solution (2.5 L). After washing with distilled water at room temperature, the embryos were removed and the endosperms macerated in a blender in 0.1 M sodium chloride with 2 mL toluene. The macerate was filtered through two layers of cheesecloth and the residue was re-treated with sodium chloride and blending until the filtrate was clear. The combined filtrates were centrifuged (600 x g, 15 min, 25°C) and the supernatant discarded. The precipitate was shaken with 0.1 M sodium chloride and toluene

to remove lipid and protein. The mixture was centrifuged, and the process was repeated. The starch was washed with distilled water by centrifugation, followed by washing with ethanol, acetone and ether, and dried in a vacuum desiccator. The starch granules were disrupted using a DMSO treatment (Matheson and Welsh, 1988), as follows. Starch granules were suspended in DMSO (10 mL/g) in a centrifuge tube and shaken for 24 h or until the starch was dissolved. After centrifugation (1000 x g, 10 min, 25°C), the residue was shaken again with DMSO (25 mL) overnight and re-centrifuged. The combined supernatants were added to 3 volumes of ethanol. After centrifugation (600 x g, 15 min, 25°C), the starch precipitate was collected, washed with ethanol, acetone and ether, dried in a desiccator under vacuum and stored at 4°C.

Figure 2.1

Isolation of starch granules from rice grains using the protocol of Matheson and Welsh (1988).

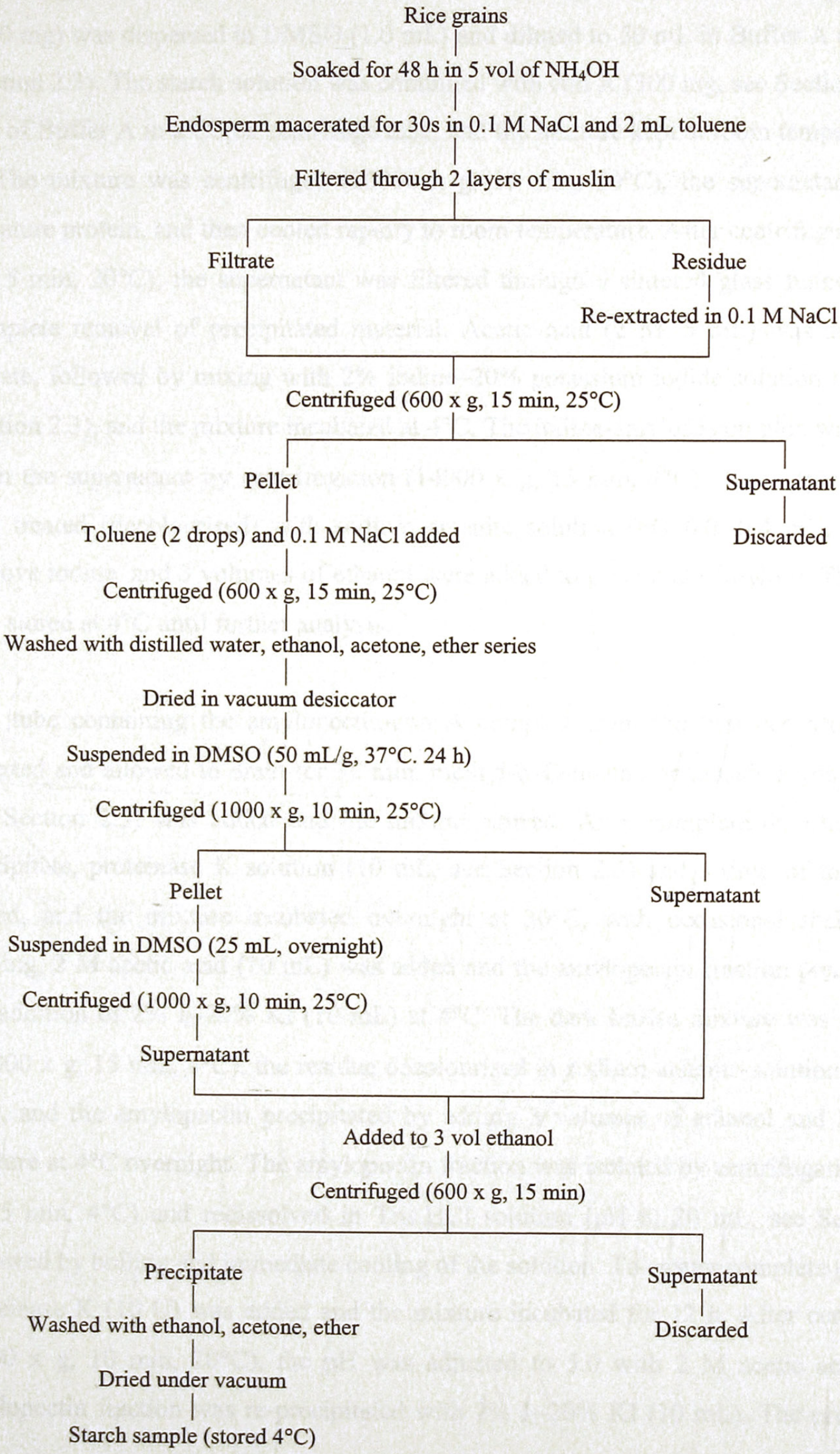

2.7 Preparative fractionation of starch with concanavalin A

Starch was fractionated into amylose and amylopectin by precipitation with con A according to the method of Matheson and Welsh (1988), as summarised in Fig. 2.2. Starch (500 mg) was dispersed in DMSO (1.0 mL) and diluted to 50 mL in Buffer A (pH 6.4, see Section 2.3). The starch solution was combined with con A (300 mg, see Section 2.3) in 50 mL of Buffer A in a Corex centrifuge tube, and the mixture kept at room temperature for 2 h. The mixture was centrifuged (20000 x g, 15 min, 20°C), the supernatant boiled to denature protein, and then cooled rapidly to room temperature. After centrifuging (14000 x g, 15 min, 20°C), the supernatant was filtered through a sintered glass funnel to ensure complete removal of precipitated material. Acetic acid (2 M, 5 mL) was added to the filtrate, followed by mixing with 2% iodine–20% potassium iodide solution (10 mL, see Section 2.3), and the mixture incubated at 4°C. The iodine-amylose complex was separated from the supernatant by centrifugation (14000 x g, 15 min, 4°C). The amylose complex was treated (decolourised) with sodium arsenite solution (pH 6.0, 0.4 mL, see 2.3) to remove iodine, and 3 volumes of ethanol were added to precipitate amylose. This amylose was stored at 4°C until further analysis.

The tube containing the amylopectin-con A complex from the first centrifugation was inverted and allowed to drain for 30 min, methyl-α-D-mannopyranoside solution (40 mL, see Section 2.3) was added and the mixture stirred. After complete dissolution of the precipitate, proteinase K solution (10 mL, see Section 2.3) and a drop of toluene were added, and the mixture incubated overnight at 30°C, with occasional shaking. After cooling, 2 M acetic acid (10 mL) was added and the amylopectin fraction precipitated by the addition of 2% I_2-20% KI (10 mL) at 4°C. The dark brown mixture was centrifuged (14000 x g, 15 min, 4°C), the residue decolourised in sodium arsenite solution (pH 6.0, 1 mL), and the amylopectin precipitated by adding 3 volumes of ethanol and leaving the mixture at 4°C overnight. The amylopectin fraction was isolated by centrifugation (1500 x g, 15 min, 4°C) and redissolved in Tris.HCl solution (pH 8, 20 mL, see Section 2.3), followed by boiling and immediate cooling of the solution. To ensure complete proteolysis, proteinase K (10 U) was added and the mixture incubated for 12 h. After centrifugation (1500 x g, 10 min, 20°C), the pH was adjusted to 5.0 with 2 M acetic acid and the amylopectin fraction was re-precipitated with 2% I_2-20% KI (10 mL). The precipitate of

glucan-iodine complex was decolourised by sodium arsenite solution (1 mL), washed twice with 60% ethanol in a centrifuge tube and stored under ethanol at 4°C.

Figure 2.2

Fractionation of starch by con A using the protocol of Matheson and Welsh (1988).

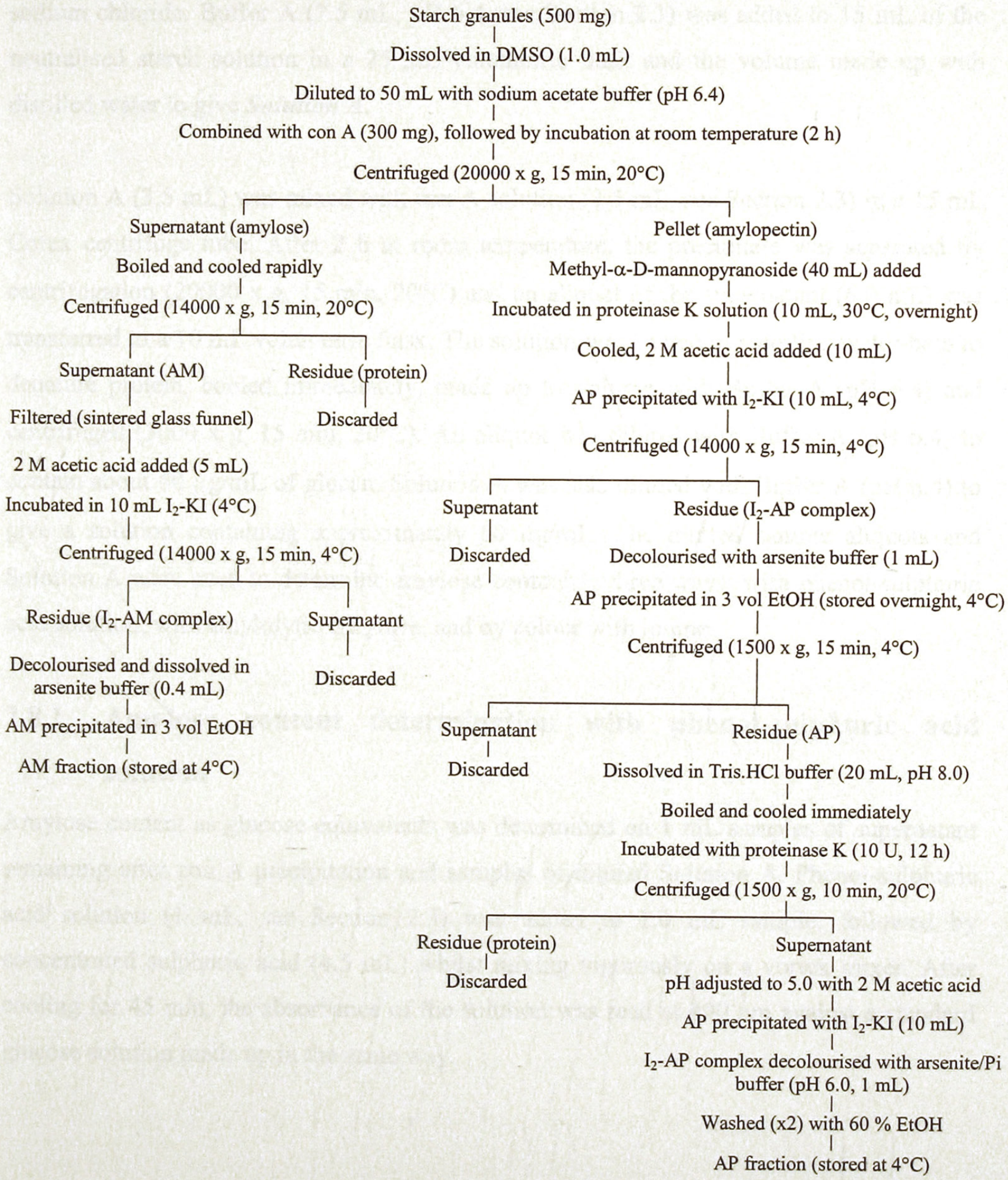

2.8 Estimation of amylose content of starch

The following methods for determining amylose content were adapted from Matheson and Welsh (1988). Starch precipitated from DMSO (25 mg) (Section 2.6) was redissolved with a small amount of DMSO in a 25 mL volumetric flask and incubated at room temperature, with occasional shaking for 18-24 h. Sodium hydroxide (0.1 M, 10 mL) was added and the flask shaken until the starch was in solution. This solution was neutralised with 0.1 M hydrochloric acid, using bromomethyl blue as indicator, and made up to 25 mL with 0.1 M sodium chloride. Buffer A (7.5 mL, pH 6.4, see Section 2.3) was added to 15 mL of the neutralised starch solution in a 25 mL volumetric flask and the volume made up with distilled water to give ***Solution A***.

Solution A (3.5 mL) was mixed with con A solution (3.5 mL, see Section 2.3) in a 15 mL Corex centrifuge tube. After 2 h at room temperature, the precipitate was separated by centrifugation (20000 x g, 15 min, 20°C) and an aliquot of the supernatant (6.0 mL) was transferred to a 10 mL volumetric flask. The solution was heated in a boiling water-bath to denature protein, cooled immediately, made up to volume with Buffer A (pH 6.4) and centrifuged (3000 x g, 15 min, 20°C). An aliquot was diluted with Buffer A (pH 6.4) to contain about 60 μg/mL of glucan. Solution A was also diluted with Buffer A (pH 6.4) to give a solution containing approximately 60 μg/mL. The diluted sample aliquots and Solution A were used to determine amylose content in three ways: with phenol-sulphuric acid solution, with amylolytic enzymes, and by colour with iodine.

2.8.1 Amylose content determination with phenol-sulphuric acid solution

Amylose content as glucose equivalents was determined on 1 mL samples of supernatant remaining after con A precipitation and samples of diluted Solution A. Phenol-sulphuric acid solution (1 mL, see Section 2.3) was added to 1.0 mL sample, followed by concentrated sulphuric acid (4.5 mL) whilst mixing vigorously on a vortex mixer. After cooling for 45 min, the absorbance of the solution was read at 490 nm against a standard glucose solution made up in the same way.

2.8.2 Amylose content determination with amylolytic enzymes

Solution A (3.5 mL) was mixed with con A solution (3.5 mL, see Section 2.3) in a 15 mL Corex centrifuge tube. After 2 h at room temperature, the precipitate was removed by centrifugation (20000 x g, 15 min, 20°C) and an aliquot (6.0 mL) of the supernatant transferred to a 10 mL volumetric flask. Acetic acid (2 M, about 50 μL) was added to reduce the pH to 5.0 and the mixture heated in a boiling water-bath to denature protein. Amyloglucosidase-α-amylase solution (2.0 mL, see Section 2.3) was added to the cooled mixture, and the volume made up with 0.2 M acetate buffer (pH 5.0). The mixture was incubated at 37°C for 2 h and centrifuged (3000 x g, 15 min, 20°C). Aliquots (1 mL) of the supernatant were incubated with GOPOD solution (3 mL, see Section 2.3) at 37°C for 30 min and the absorbance read at 490 nm. To estimate total starch, an aliquot (3 mL) of Solution A was transferred to a 10 mL volumetric flask. A small amount of 2 M acetic acid (about 25 μL) was added to reduce the pH to 5.0. Amyloglucosidase-α-amylase solution (2 mL) was added and the volume made up with 0.2 M acetate buffer. The solution was incubated at 37°C for 2 h and diluted to contain about 60 μg glucan/mL. Aliquots (1 mL) were incubated at 37°C for 30 min with GOPOD solution (3 mL) and the absorbance read at 490 nm.

2.8.3 Amylose content determination by colour with iodine

Solution A (2.0 mL) was mixed with con A solution (2.0 mL, see Section 2.3) in a 15 mL Corex centrifuge tube. After 2 h at room temperature, the precipitate was removed by centrifugation (20000 g, 15 min, 20°C) and an aliquot of the supernatant (3 mL) transferred to a 10 mL volumetric flask. The solution was heated in a steam bath to denature protein, cooled, made up to volume with Buffer A (see Section 2.3) and centrifuged (3000 x g, 15 min, 20°C). Diluted iodine-potassium iodide solution (1.2 mL) was added to duplicate aliquots (2 mL) of the sample and mixed. The absorbance values at 620, 630, and 640 nm were read immediately against a blank prepared from iodine solution (1.2 mL) and Buffer A (2 mL).

2.9 Reducing end group assay

The Nelson-Somogyi method was used for reducing end group assay (Bell, 1955). Copper reagent (1 mL, see Nelson-Somogyi reagents, Section 2.3) was added to hydrolysates (1

mL) from β-amylolysis and to maltose standards (0-120 μg/mL). After heating for 20 min in a boiling water bath, the solutions were cooled rapidly under running tap water for 5 min and Reagent C (1 mL) added. The solutions were mixed on a vortex mixer and the colour allowed to develop for 20 min. The absorbance at 500 nm was measured after appropriate dilution with distilled water.

2.10 Average chain length of α-(1→4)(1→6)-D-glucan

Amylopectin (15 mg) was wetted with a drop of ether and dissolved in pH 5.0 acetate buffer (10 mL, 20 mM). After heating in a steam bath to remove ether, the solution was incubated at 37°C with isoamylase (20 U) for 18 h. The reducing end groups produced were estimated by copper reagent with standards of maltohexaose and blanks of non-debranched amylopectin and enzyme alone. The absorbance due to the reducing ends was measured at 500 nm after dilution with distilled water. Total glucan was estimated by the phenol-sulphuric acid method.

2.11 Microscopic examinations

2.11.1 Rice grain morphology by environmental scanning electron microscopy

Whole milled rice grains were manually snapped in two in the transverse direction. The fractured grain was mounted on an aluminium stub using double-sided adhesive tape, with the broken surface oriented upwards. Images were obtained without further specimen preparation using a Philips XL30 Environmental Electron Microscope (Philips, Denmark) with a GSE detector at a pressure of 1 torr and an accelerating voltage of 15 kV. The working distance was 10 mm. Five grains of each variety of rice were imaged, with five fields of view selected from each grain surface, and different magnifications used within each field of view.

2.11.2 Rice grain morphology by atomic force microscopy

Resin for mounting specimens for examination by atomic force microscopy (AFM) was prepared by mixing 9 g of Epon 812 Substitute (ProSciTech, QLD, Australia), 7.5 g of nadic methyl anhydride (ProSciTech, QLD, Australia), and 0.3 g of benzyldimethylamine (ProSciTech, QLD, Australia). The resin was cured at 60°C overnight in cylindrical molds

(3 cm diameter × 2 cm high). The surface of the solidified resin was polished with sand paper to create a level plane, and five holes, each wide and deep enough to fit an entire rice grain, were drilled into the smoothed surface of the resin. A rice grain was placed in each hole and fresh resin was added to fill in gaps and cover the entire grain, taking care to avoid introducing air bubbles. The rice-filled resin was cured overnight at 60°C. A transverse cut was made through the blocks near the centre of each rice grain, using a diamond saw (Accutom, Struers, Denmark) at 700 rpm and feed rate of 1.5 cm/min. Rice grains were sectioned without lubricant (dry-sectioned samples), or with distilled water supplied to the sectioning blade at a rate of 1 mL/min (wet-sectioned samples). The cut surface was polished lightly using 1200-grade paper on a polishing wheel and imaged immediately. Images were obtained using a Park Scientific Autoprobe CP scanning probe microscope in contact mode, in air at atmospheric pressure and ambient temperature (20-22°C) and humidity. A 2-μm silicon cantilever (Ultralevers, Model number APUL-20-AU-25, Park Scientific Instruments) was used, with a force constant of 13 N/m. The scanner was calibrated in the xy directions using a 1.0 μm grating. Scan areas ranged from 1 to 25 μm^2, and images were analysed using AutoProbe image processing software (Park Scientific Instruments).

2.11.3 Rice starch morphology by atomic force microscopy

Sample preparation techniques were adapted from McIntire and Brant (1999). All samples were dissolved in distilled water to 1.0 mg/mL with stirring at room temperature. The solutions were heated to 90°C for 1 hour, and diluted to 1 μg/ml with distilled water at 90°C. The solutions were cooled to about 40°C and filtered (Millipore 0.45 μm cellulose filters). The sample (2 μl) was deposited onto freshly cleaved mica, and air-dried for 15 min at room temperature in a dust-free environment. Images were obtained using a Park Scientific Autoprobe CP scanning probe microscope (calibrated as above), with a non-contact mode AFM (NCAFM) probe head. A 2-μm silicon cantilever (Ultralevers, Model number APUL-20-AU-25, Park Scientific Instruments) was used, with a force constant of 13 N/m and resonant frequency of 300 kHz. Measurements were performed in air at atmospheric pressure and ambient temperature (20-22°C) and humidity. Scan areas ranged from 1 to 25 μm^2, and images were analysed using AutoProbe image processing software (Park Scientific Instruments).

2.12 Pasting behaviour of rice flour

Rice samples were ground using a hammer mill (Newport Scientific CM6000, Warriewood) to a particle size of 500 μm. The resulting rice flour was brushed through a 500 μm sieve to ensure uniformity of particle size. The moisture content of each sample was determined, in duplicate, using the air-oven method (AACC 44-15A) of the American Association of Cereal Chemists (AACC, 1995). The pasting behaviour of rice flour was tested in duplicate with the Newport Scientific RVA-4, using AACC Method 61-02 (AACC, 1995) (Table 2.1, Fig. 2.3). Sample weights were adjusted to correct for moisture content. Each flour sample (3.50 ± 0.01 g, 12% moisture basis) was added to 25.0 ± 0.1 g of water (adjusted to correct for sample moisture content) in a new test canister. The paddle was stirred vigorously to disperse the sample. The canister and paddle were inserted into the instrument, and the RVA trace recorded over 12.5 minutes. Differences between samples in RVA parameters (see Fig. 1.7), namely peak viscosity, pasting temperature, trough viscosity, final viscosity, breakdown (that is, peak viscosity minus trough viscosity), and setback from trough (that is, final viscosity minus trough viscosity), were assessed by analysis of variance.

Table 2.1

RVA profile for rice flour samples.

Time	Condition	Value
00:00:00	Temperature	50°C
00:00:00	Speed	960 rpm
00:00:10	Speed	160 rpm
00:01:00	Temperature	50°C
00:04:48	Temperature	95°C
00:07:18	Temperature	95°C
00:11:06	Temperature	50°C
00:12:30	End of test	50°C

Figure 2.3

RVA profile showing temperature and speed conditions used in RVA tests.

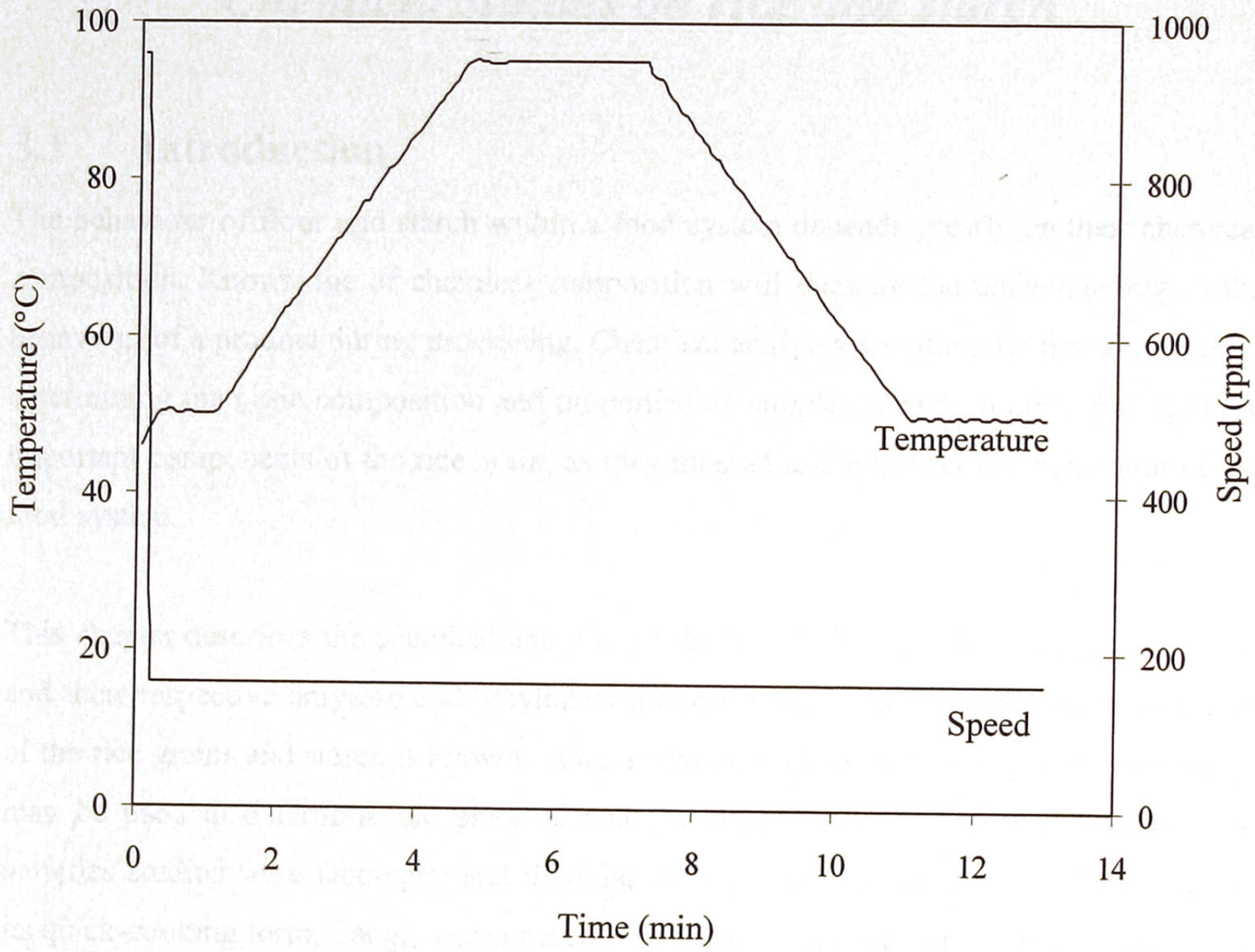

CHAPTER 3

Chemical studies on rice and starch

3.1 Introduction

The behaviour of flour and starch within a food system depends greatly on their chemical composition. Knowledge of chemical composition will increase the understanding of the behaviour of a product during processing. Chemical analyses are often the first approach to determining the basic composition and properties of samples. Starch, protein and lipid are important components of the rice grain, as they interact and influence the behaviour of the food system.

This chapter describes the chemical analyses of the rice grains used in subsequent studies, and their respective amylose and amylopectin components. When the macro-composition of the rice grains and starch is known, other analyses, such as microscopy and viscometry, may be used to determine the physical and processing properties of the samples. The varieties studied were Doongara and its quick-cooking and parboiled forms, Kyeema and its quick-cooking form, Langi, a commercial medium-grained waxy rice, and a commercial long-grained waxy rice.

3.2 Results and Discussion

3.2.1 Effect of genotype on total starch, protein and lipid content

Total starch, protein, and lipid were analysed for each of the ground, polished rice samples as described in the methods (Chapter 2), to determine the effect of genotype and environment on composition.

Subsamples of each polished rice variety (Langi, Doongara, and Kyeema) from all three seasons (1998/1999, 1999/2000, 2000/2001) were mixed to obtain a combined sample that was representative of each variety. The combined sample was then ground to a particle size of 250 μm, and the total starch, protein, and lipid content determined for each variety. The

composition of quick-cooking forms of Doongara and Kyeema, parboiled Doongara, and commercial waxy rices were also determined.

The results show trends of waxy rice samples (low amylose) having slightly lower starch content and higher protein content than non-waxy varieties, however the differences were not statistically significant (Table 3.1). The Doongara variety had the highest starch and lowest protein contents, whereas starch content was similar for Langi and Kyeema, as was protein content of these varieties (Table 3.1). There were no significant differences in lipid content between all samples. The processed rice samples generally had lower starch and protein contents than the unprocessed samples (Table 3.1). This may be an indication of thermal degradation of components. The lipid content did not change significantly as a result of processing.

Table 3.1

Effect of genotype on composition of rice samples.

Sample	Starch (%)	Protein (%)	Lipid (%)
Langi*	84.5 ± 1.7	6.6 ± 0.1	1.5 ± 0.1
Doongara*	85.6 ± 1.2	6.3 ± 0.4	1.6 ± 0.1
Kyeema*	83.3 ± 0.7	6.8 ± 0.6	1.5 ± 0.1
Parboiled Doongara	83.1 ± 1.0	6.1 ± 0.2	1.6 ± 0.3
Quick-cooking Doongara	82.5 ± 0.8	5.9 ± 0.3	1.6 ± 0.1
Quick-cooking Kyeema	84.9 ± 0.5	6.6 ± 0.5	1.5 ± 0.4
Medium-grained waxy	82.2 ± 0.9	7.3 ± 0.4	1.4 ± 0.1
Long-grained waxy	82.3 ± 0.9	6.9 ± 0.1	1.5 ± 0.2

Values are the means ± SD of duplicate determinations. Starch, protein and lipid contents are expressed as a percentage (%) of dry weight. The starch, protein and lipid content of the samples were not significantly different, as determined by analysis of variance.

*Subsamples of each variety from all three seasons were combined as described for total starch, protein, and lipid determinations.

3.2.2 Effect of environment on total starch, protein and lipid content

To determine the effect of growth season on composition, samples were obtained from three different seasons (1998/1999, 1999/2000, 2000/2001) for varieties Langi, Doongara and Kyeema. The season characteristics are summarised in Table 3.2. Rainfall data were not included, as rice is grown under irrigation.

Protein content was generally lower for rice samples from the cooler season (1999/2000) (Table 3.3), which is not consistent with previous observations that protein content tended to be low when high solar radiation occurred during grain development (Gomez and de Datta, 1975; IRRI, 1977). Resurreccion *et al.* (1977) observed that the effect of temperature during grain ripening on protein content varied with the variety, depending on the relative tolerance of the grain to low temperature. As was noted in Section 3.2.1, higher protein content appeared to be associated with lower starch content.

To determine the effect of growth location on composition, samples from the 1998/1999 season were obtained from several locations: Murrumbidgee Irrigation Area (MIA), Coleambally Irrigation Area (CIA) and Murray Valley (MV) (Fig. 3.1). For each of the rice varieties, there were no significant differences in starch, protein and lipid contents between samples from different locations (Table 3.4).

Table 3.2

Temperature and yield characteristics of rice growing seasons.

Season	Ave max temp (°C)	Ave min temp (°C)	Ave yield (tonnes/ha)
1998/1999	28.6	14.2	9.2
1999/2000	28.1	13.9	8.2
2000/2001	29.4	14.6	9.5

Temperature data collected over the rice-growing season from October to April and yield data were provided by the Cooperative Research Centre for Sustainable Rice Production.

Table 3.3

Effect of growth season on composition of rice samples.

Sample	Season	Starch (%)	Protein (%)	Lipid (%)
Langi	1998/1999	84.2 ± 1.0	6.4 ± 0.4	1.4 ± 0.1
	1999/2000	85.3 ± 1.3	6.2 ± 0.2	1.6 ± 0.2
	2000/2001	84.4 ± 0.7	6.9 ± 0.1	1.4 ± 0.1
Doongara	1998/1999	85.5 ± 0.8	6.3 ± 0.1	1.5 ± 0.2
	1999/2000	85.9 ± 1.2	6.0 ± 0.2	1.7 ± 0.1
	2000/2001	85.1 ± 0.9	6.5 ± 0.3	1.5 ± 0.1
Kyeema	1998/1999	83.2 ± 1.1	6.6 ± 0.3	1.6 ± 0.4
	1999/2000	83.6 ± 0.8	6.7 ± 0.3	1.7 ± 0.1
	2000/2001	83.1 ± 0.1	6.9 ± 0.4	1.6 ± 0.2

Values are the means ± SD of duplicate determinations. Starch, protein and lipid contents are expressed as a percentage (%) of dry weight. For each variety, the starch, protein and lipid content of the samples between the seasons were not significantly different, as determined by analysis of variance.

Table 3.4

Effect of growth location on composition of rice samples.

Sample	Location	Starch (%)	Protein (%)	Lipid (%)
Langi	MIA	84.1 ± 1.7	6.4 ± 0.4	1.4 ± 0.1
	CIA	84.8 ± 0.5	6.3 ± 0.1	1.5 ± 0.4
	MV	85.2 ± 2.9	6.4 ± 0.4	1.3 ± 0.1
Doongara	MIA	82.6 ± 1.1	6.2 ± 0.3	1.5 ± 0.1
	CIA	83.9 ± 2.3	6.1 ± 0.2	1.6 ± 0.5
Kyeema	MIA	85.2 ± 1.3	6.6 ± 0.4	1.6 ± 0.4
	CIA	86.5 ± 2.4	6.7 ± 0.3	1.5 ± 0.1

Values are the means ± SD of duplicate determinations. Starch, protein and lipid contents are expressed as a percentage (%) dry weight. For each variety, the starch, protein and lipid content of the samples between the growth locations were not significantly different, as determined by analysis of variance.

Figure 3.1

Map showing rice growing locations.

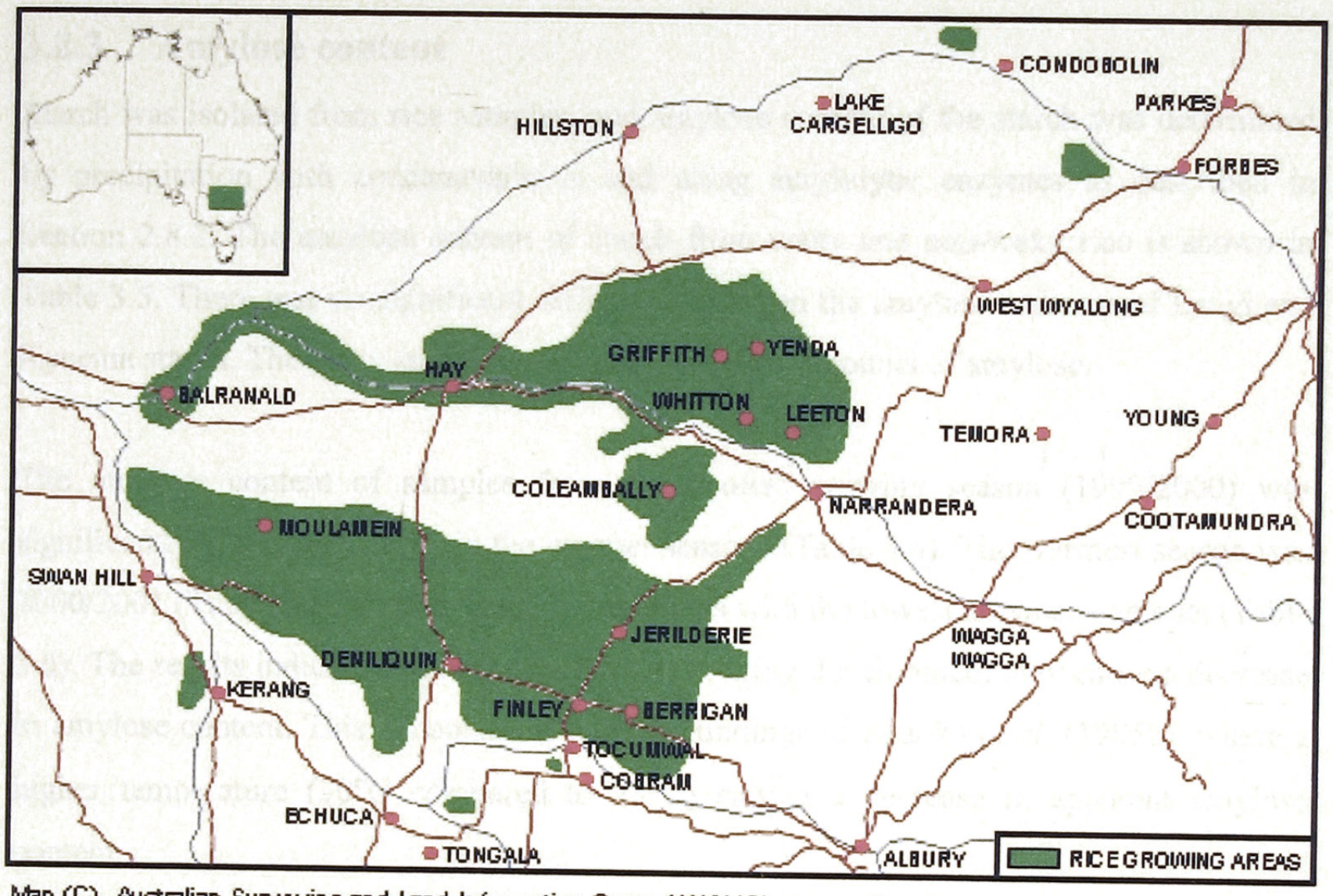

Map (C). Australian Surveying and Land Information Group (AUSLIG) www.auslig.gov.au

For each variety of rice studied, samples were obtained from a large number of growers from each growth location (MIA, CIA and MV). The individual samples from each growth location were combined and thoroughly mixed to be representative of the region. The effect of different cultural practices for each growth location may have been minimised, as the combined sample was a collection of a number of samples. The combined sample would even out differences in cultural practices and variations in soil properties. This may explain the similarity in the macro-composition of samples from the different locations. The MIA, CIA and MV regions are all within 80 km of each other. The regions would experience similar climatic conditions, which would have an influence on the similarity in macro-composition of the samples. In studying the effect of cultural practices on composition, De Datta *et al.* (1972) observed that protein content was higher when wider plant spacing was used, and noted that this was probably because more nitrogen was available per plant. Juliano and Bechtel (1985) reported that management and cultural practices have a major influence on the protein content of rice grains, and that added

nitrogen fertiliser usually increased the protein content of rice, particularly if it were applied during the reproductive stage.

3.2.3 Amylose content

Starch was isolated from rice samples, and amylose content of the starch was determined by precipitation with concanavalin A and using amylolytic enzymes as described in Section 2.8.2. The amylose content of starch from waxy and non-waxy rice is shown in Table 3.5. There was no significant difference between the amylose contents of Langi and Kyeema starch. The waxy starches contained very low amounts of amylose.

The amylose content of samples from the coolest growing season (1999/2000) was significantly higher than those in the warmer seasons (Table 3.6). The warmest season was 2000/2001 (Table 3.2), and produced rice samples with the lowest amylose contents (Table 3.6). The results indicate that high temperatures during development may cause a decrease in amylose content. This is consistent with the findings of Asaoka *et al.* (1985b), where a higher temperature (30°C compared to 25°C) caused a decrease in apparent amylose content.

For each variety studied, there were no significant differences between the amylose content of rice starches from rice grown in different locations within the same season (Table 3.7).

Table 3.5

Amylose content of starch isolated from waxy and non-waxy rice samples.

Sample	Amylose content (%)
Langi*	18.7 ± 0.2
Doongara*	28.7 ± 0.3
Kyeema*	19.3 ± 0.2
Medium-grained waxy	2.0 ± 0.1
Long-grained waxy	1.0 ± 0.4

Amylose content was determined by amylolytic enzymes (Section 2.8.2). Values are the means ± SD of duplicate determinations. Amylose content is expressed as a percentage (%) of total starch.
*Subsamples of each variety from all seasons were combined prior to starch extraction. Amylose content was determined on combined samples.

Table 3.6

Effect of growth season on amylose content of starch isolated from rice samples.

Sample	Season	Amylose content (%)
Langi	1998/1999	18.5 ± 0.4a
	1999/2000	19.1 ± 0.7b
	2000/2001	17.2 ± 0.6c
Doongara	1998/1999	28.1 ± 0.3a
	1999/2000	29.2 ± 0.4b
	2000/2001	27.3 ± 0.4c
Kyeema	1998/1999	19.2 ± 0.4
	1999/2000	19.4 ± 0.5
	2000/2001	18.1 ± 0.2a

Values are the means ± SD of duplicate determinations. Amylose content is expressed as a percentage (%) of total starch. For each variety, different letters after values indicate significant difference between the seasons, as determined by analysis of variance. Within each variety, values in the same column without letters were not significantly different.

Table 3.7

Effect of growth location on amylose content of starch isolated from rice samples.

Sample	Location	Amylose content (%)
Langi	MIA	18.5 ± 0.1
	CIA	18.3 ± 0.4
	MV	18.0 ± 0.2
Doongara	MIA	28.2 ± 0.4
	CIA	28.5 ± 0.5
Kyeema	MIA	19.3 ± 0.4
	CIA	19.5 ± 0.3

Samples are from the 1998/1999 season. Values are the means ± SD of duplicate determinations. Amylose content is expressed as a percentage (%) of total starch. For each variety, the amylose content from different growth locations were not significantly different, as determined by analysis of variance.

3.2.4 Average chain length

The chain length (CL) of amylopectin was estimated by the copper reducing power of the debranched glucan, and the value for each rice variety is shown in Table 3.8. The high-amylose variety Doongara had the longest average CL, while the waxy rices had the shortest. The linear nature of amylose means that it has a longer mean CL than amylopectin (Juliano, 1985). Langi and Kyeema had similar amylose contents, and similar mean CLs.

Table 3.8

Average chain length of α-(1→4)(1→6)-D-glucans.

Sample	Average chain length
Langi	21
Doongara	26
Kyeema	22
Medium-grained waxy	19
Long-grained waxy	18

3.3 Conclusions

There appeared to be a trend for samples with low amylose content to be low in starch content and high in total protein, however the differences were not statistically significant. There were no significant differences between total lipid content of all samples. The lowered starch and protein contents of processed rice samples may be an indication of loss of components during processing.

A review of literature indicates that climate has a large influence on the macro-constituents of rice, mainly the total protein content and CL of amylopectin. However, in this study, the environment did not significantly affect the gross composition of the rice samples. In this study, growth location did not appear to have a significant effect on the macro-composition of rice. The sampling method of combining subsamples of rice from each growth region may have contributed to the apparent similarity in macro-composition. The three main rice-growing regions in Australia are the MIA, CIA, and MV, all of which are within close

proximity. There are therefore only small differences in climatic conditions. This may have also contributed to the similarity in macro-composition.

This study found that environment did not affect macro-constituents, but did influence amylose content (or amylopectin content). The growth season appeared to be mainly responsible for the effect on amylose content.

The basic compositional information provided by chemical analyses is useful in understanding physicochemical properties of a sample. Macro-composition is often the analyses performed on a new sample, as it provides the overall picture of the sample. As samples are made up of different components, its behaviour in processes and food systems is influenced by the behaviour of its components. Further studies on morphological features such as shape and size of starch granules, and rheological properties, will provide a more complete understanding of the behaviour of the sample in food systems.

CHAPTER 4

Rice grain morphology by environmental scanning electron microscopy

4.1 Introduction

Microscopic examination of cereal grains provides information on morphology and composition, which influence processing behaviour of the grains. Most microscopic techniques require extensive sample preparation prior to imaging. While information is gained from imaging these samples, there are issues of artefacts introduced as a result of sample preparation procedures. Microscopic techniques that require minimal sample preparation are of great advantage, allowing samples to be examined in a state as close as possible to the *in situ* state.

Samples for environmental scanning electron microscopy (ESEM) examination require minimal preparation and therefore specimens can be studied in as natural a state as possible. ESEM works on the same principle as SEM but allows samples to be imaged in wet mode such that a metal coating is not required. In this chapter, the use of ESEM to image endosperm cells and starch granules exposed on the surface of fractured rice grains are described. The varieties studied were Langi, Doongara, Kyeema, and two waxy varieties, one a medium-grained and the other long-grained waxy rice. The ESEM was also used to examine the surface structure of parboiled and quick-cooking rice grains, which were prepared in commercial processes.

4.2 Results and discussion

4.2.1 Fracture surface of unprocessed rice grains by ESEM

The fracture surfaces of several varieties of waxy and non-waxy rice grains are shown in Fig. 4.1. The images shown are representative of five grains of each variety of rice, with five fields of view selected from each grain surface, and different magnifications used within each field of view. Two distinct regions were observed on the entire fracture plane of waxy and non-waxy rice grains. One region had a dark, smooth appearance, and the

other gave a brighter image but appeared rougher and more disorganised. The dark, smooth areas are suggested to correspond to regions on the surface where the fracture plane occurs between endosperm cells. The brighter areas appear to correspond to fractures within the endosperm cells, where the starch granules have been exposed and partially disrupted, giving rise to the rough structures seen in the images.

The fracture plane seemed to pass through fewer endosperm cells in the Langi grains (Fig. 4.1a) than in Doongara (Fig. 4.1b). The fracture pattern of Kyeema (Fig. 4.1c) appeared similar to that of Doongara. The proportion of rough and smooth areas in the fracture pattern of the medium-grained waxy rice (Fig. 4.1c) and long-grained waxy rice (Fig. 4.1d) seemed to be intermediate between Langi and Doongara/Kyeema.

Figure 4.1

ESEM images of the entire fracture surface of rice grains. The images shown are of Langi (a), Doongara (b), Kyeema (c), medium-grained waxy rice (d), and long-grained waxy rice (e). Scale bars represent 500 μm. The regions enclosed by the squares and circles, where the fracture planes are proposed to occur between and through endosperm cells, respectively, are shown at higher magnification in Figs. 4.2, 4.3, 4.4, 4.5 and 4.6.

4.1a

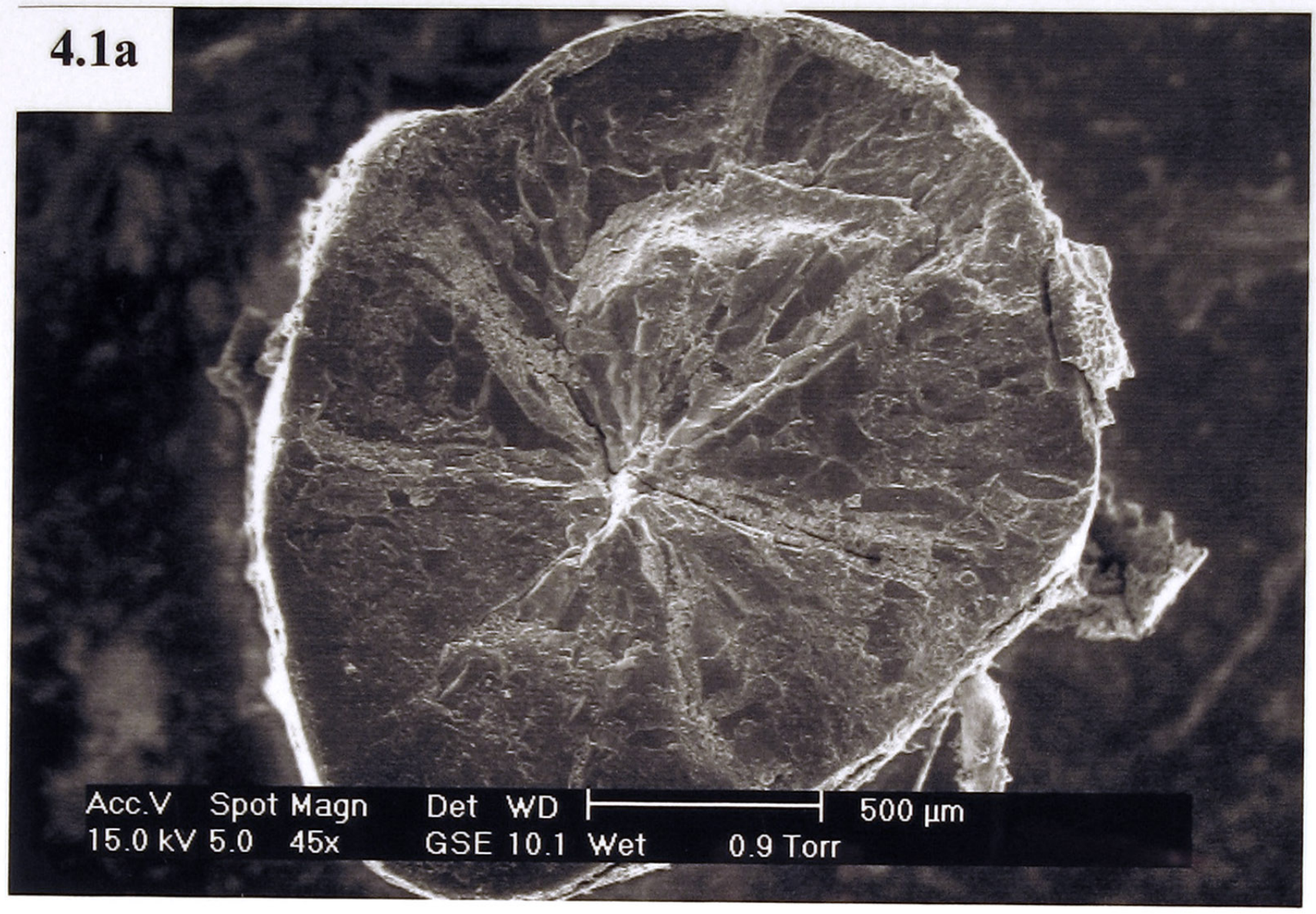
Acc.V Spot Magn Det WD 500 µm
15.0 kV 5.0 45x GSE 10.1 Wet 0.9 Torr

4.1b

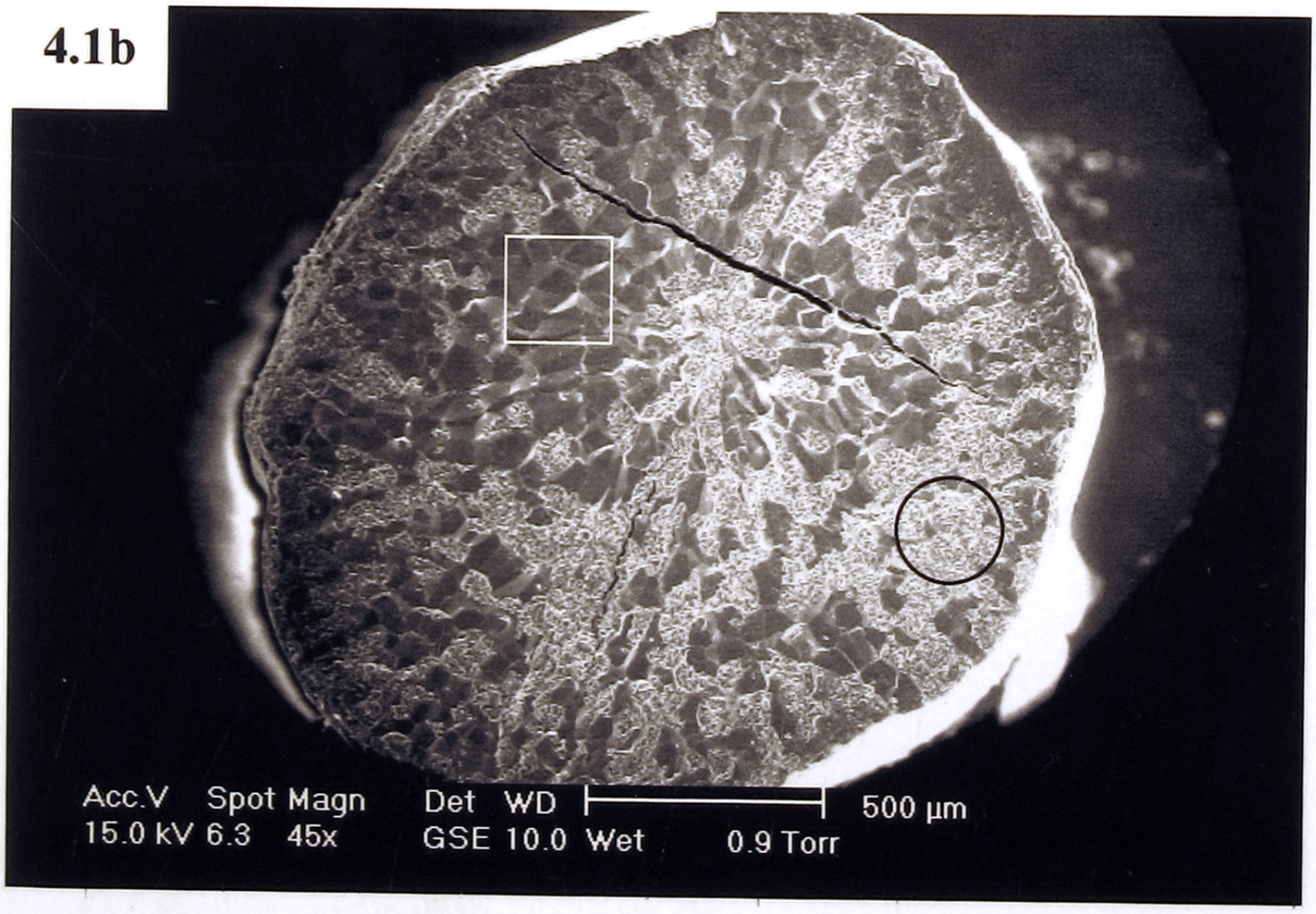
Acc.V Spot Magn Det WD 500 µm
15.0 kV 6.3 45x GSE 10.0 Wet 0.9 Torr

4.1c

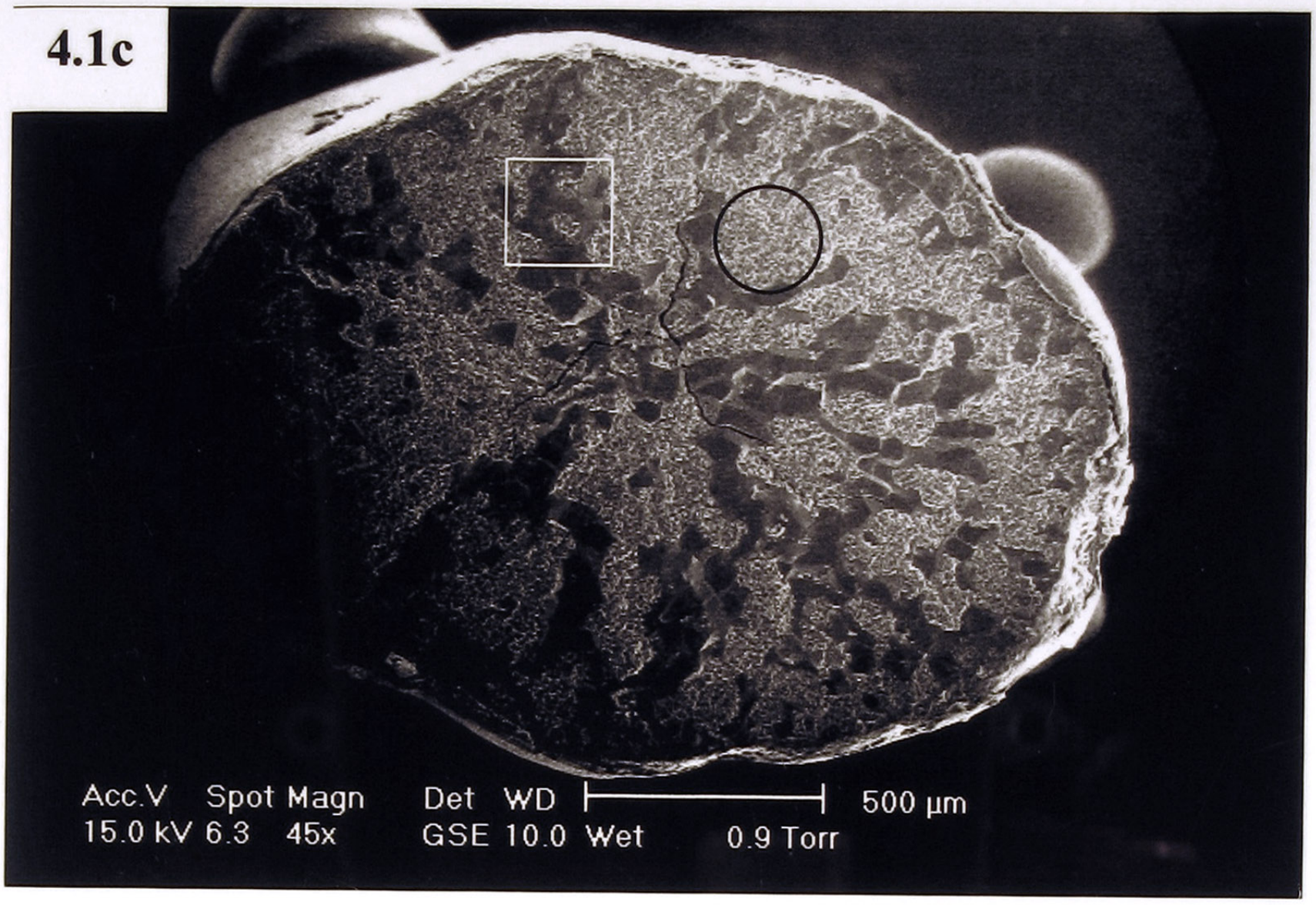
Acc.V Spot Magn Det WD 500 µm
15.0 kV 6.3 45x GSE 10.0 Wet 0.9 Torr

4.1d

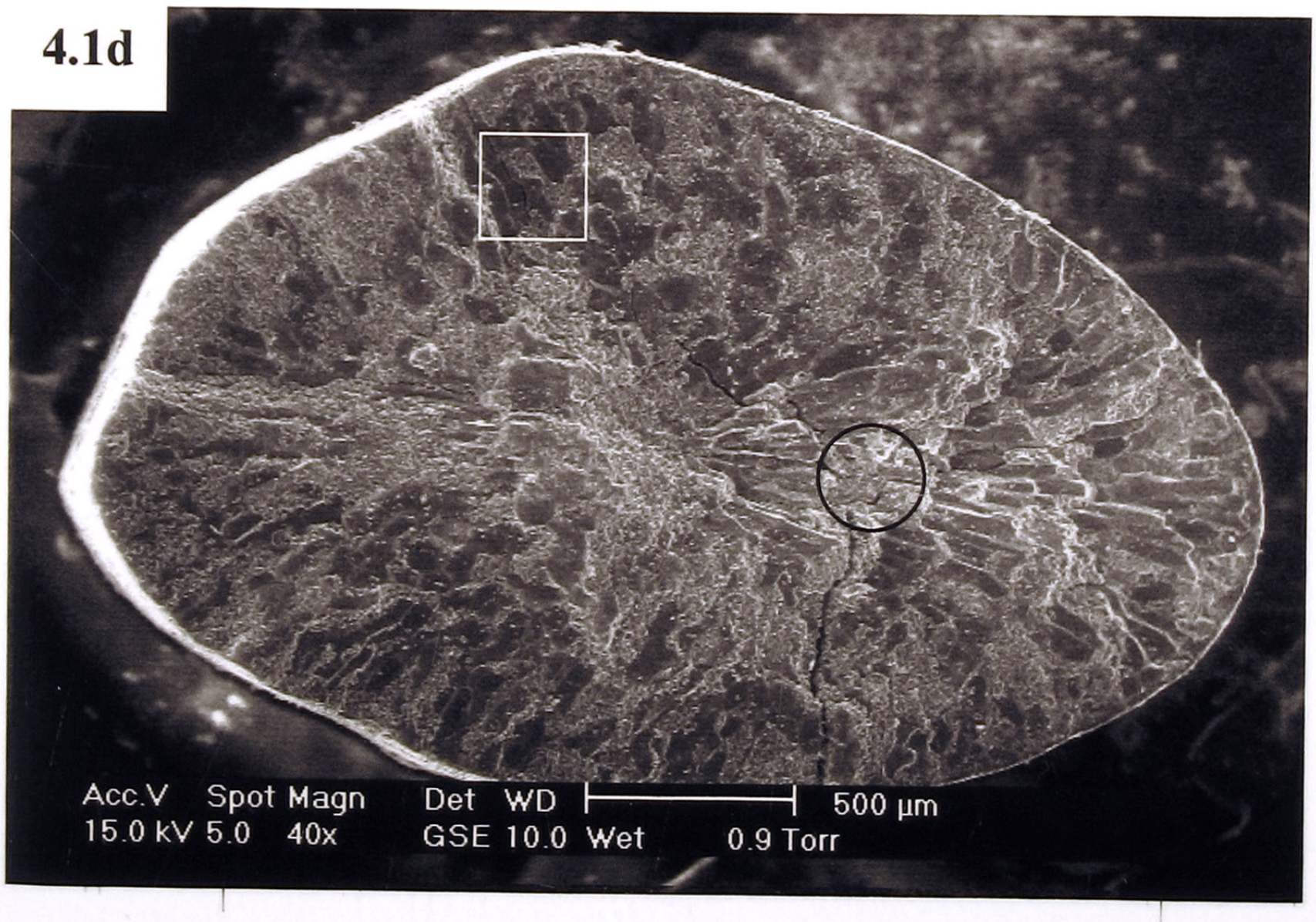
Acc.V Spot Magn Det WD 500 µm
15.0 kV 5.0 40x GSE 10.0 Wet 0.9 Torr

4.1e

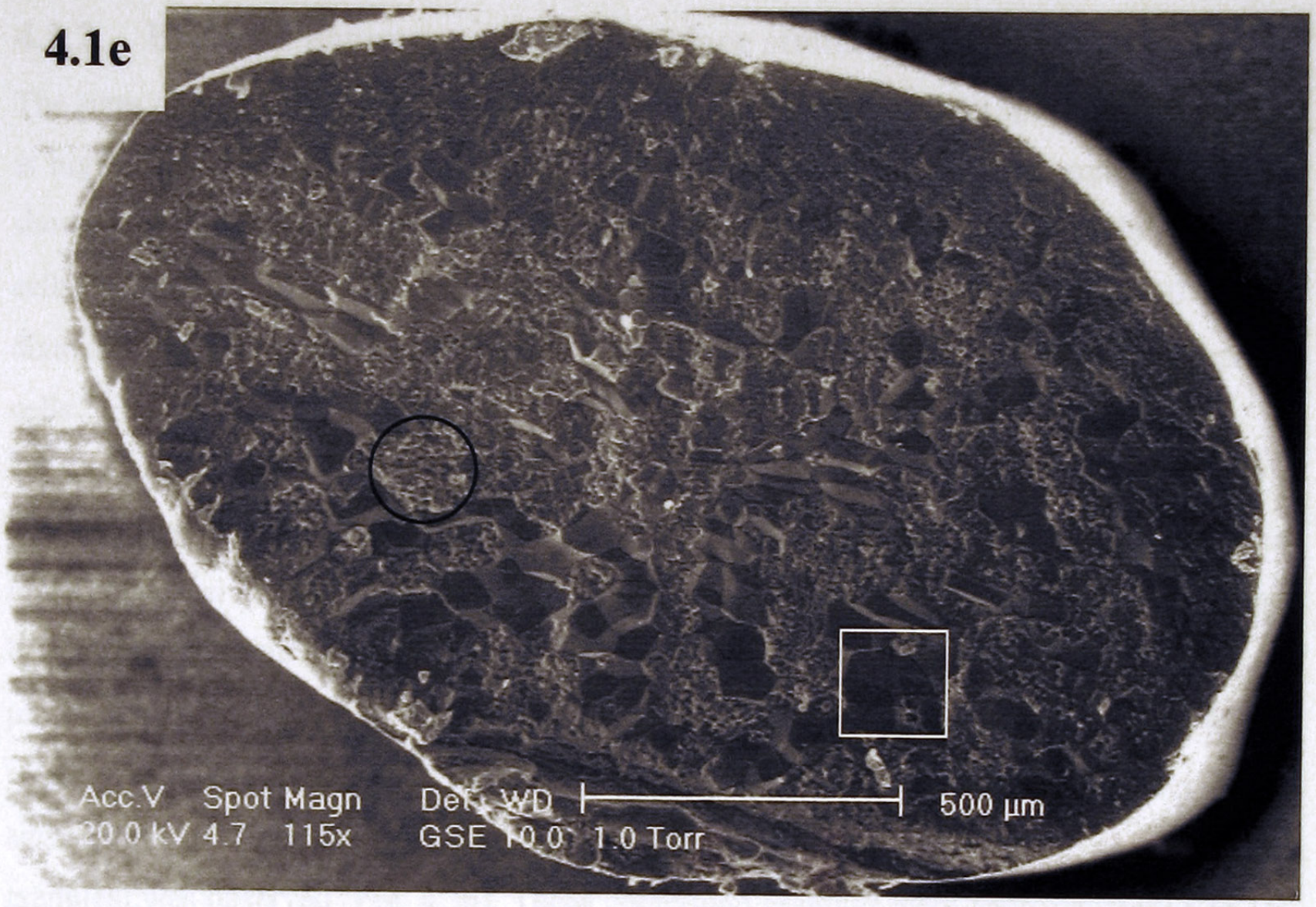

4.2.2 Effect of genotype on grain surface structure

The sizes of endosperm cells and starch granules were estimated from specimens examined at high magnification. Closer views of the fracture surface of Langi rice grains (Fig. 4.2) showed endosperm cells with an average length-to-width ratio of 1.30 (Table 4.1). The cells were observed to contain starch granules that were approximately 3 to 10 μm in diameter. Air spaces were clearly evident between starch granules within intact endosperm cells.

The endosperm cells in the fracture surface of Doongara rice grains (Fig. 4.3) appeared more polygonal than those of Langi rice. Endosperm cells of Doongara rice had an average length-to-width ratio of 1.65 and contained starch granules that were approximately 4 to 10 μm in diameter (Table 4.1). Some pitting was observed on the granule surface (Fig. 4.3a), which may have resulted from the dislodgement of protein bodies from the surface. Some aggregation of individual granules into compound structures (referred to as compound granules) was observed (Fig. 4.3b). These compound granules were approximately 8 to 16 μm in size. As was observed with the Langi samples, granules within intact endosperm cells were more varied in shape, and appeared more rounded than those in disrupted cells.

The fracture surface of Kyeema rice grains showed endosperm cells with an average length-to-width ratio of 1.67 (Fig. 4.4, Table 4.1). The starch granules in Kyeema rice grains were less angular than those found in Langi and Doongara, with sizes 4 to 11 μm in diameter. Fractures seemed to occur to a greater extent within cells than between cells. Some compound granules were observed, which were approximately 10 to 18 μm in diameter (Fig. 4.4a and 4.4b). The starch granules within intact endosperm cells appeared to be packed together more closely than in Langi and Doongara grains.

The fracture surface of the medium-grained waxy rice showed elongated endosperm cells with an average length-to-width ratio of 3.53 (Fig. 4.5a, Table 4.1). The endosperm cells from the waxy rice were more elongated than those from the non-waxy rice varieties imaged in this study, which may reflect the large size of the waxy rice grain. More compound granules were observed in the medium-grained waxy rice (Fig. 4.5b) than in Langi, Doongara and Kyeema varieties. However, individual starch granules in the medium-grained waxy rice (approximately 3 to 7 μm in diameter) were smaller and were

pressed together more closely than those found in Langi, Doongara and Kyeema. There were very few gaps between starch granules of the medium-grained waxy rice.

The average length-to-width ratio of endosperm cells in the long-grained waxy rice was 1.62 (Fig. 4.6a, Table 4.11). Starch granules within these endosperm cells ranged in diameter from 3 μm to 9 μm (Fig. 4.6b, 4.6c, Table 4.1). Many pits were observed on the surface of starch granules (Fig. 4.6c). The endosperm cells observed in the fracture surface of the long-grained waxy rice were not elongated as was observed in the medium-grained waxy rice, which suggests that the size and shape of endosperm cells may be related to the size of the grain rather than to the waxy characteristic. The medium-grained waxy rice (Fig. 4.5) appeared to have elongated endosperm cells rather than an increased number of cells.

Comparison of the length-to-width ratios of endosperm cells of the different varieties indicated that the medium-grained waxy rice had the most elongated cells, and that cells of the Kyeema and Doongara varieties were significantly more elongated than those of Langi (Table 4.1). However, these differences in endosperm cell dimensions are unlikely to be directly attributable to the amylose content of the starch, which was similar for Langi and Kyeema.

Figure 4.2

ESEM images of the fracture plane of Langi rice grains. The images in (a) and (b) show fractures between endosperm cells, (b) is a closer view of the boxed region in (a). The images in (c) and (d) show fractures within endosperm cells. Arrows indicate pitting on the granule surface.

4.2a

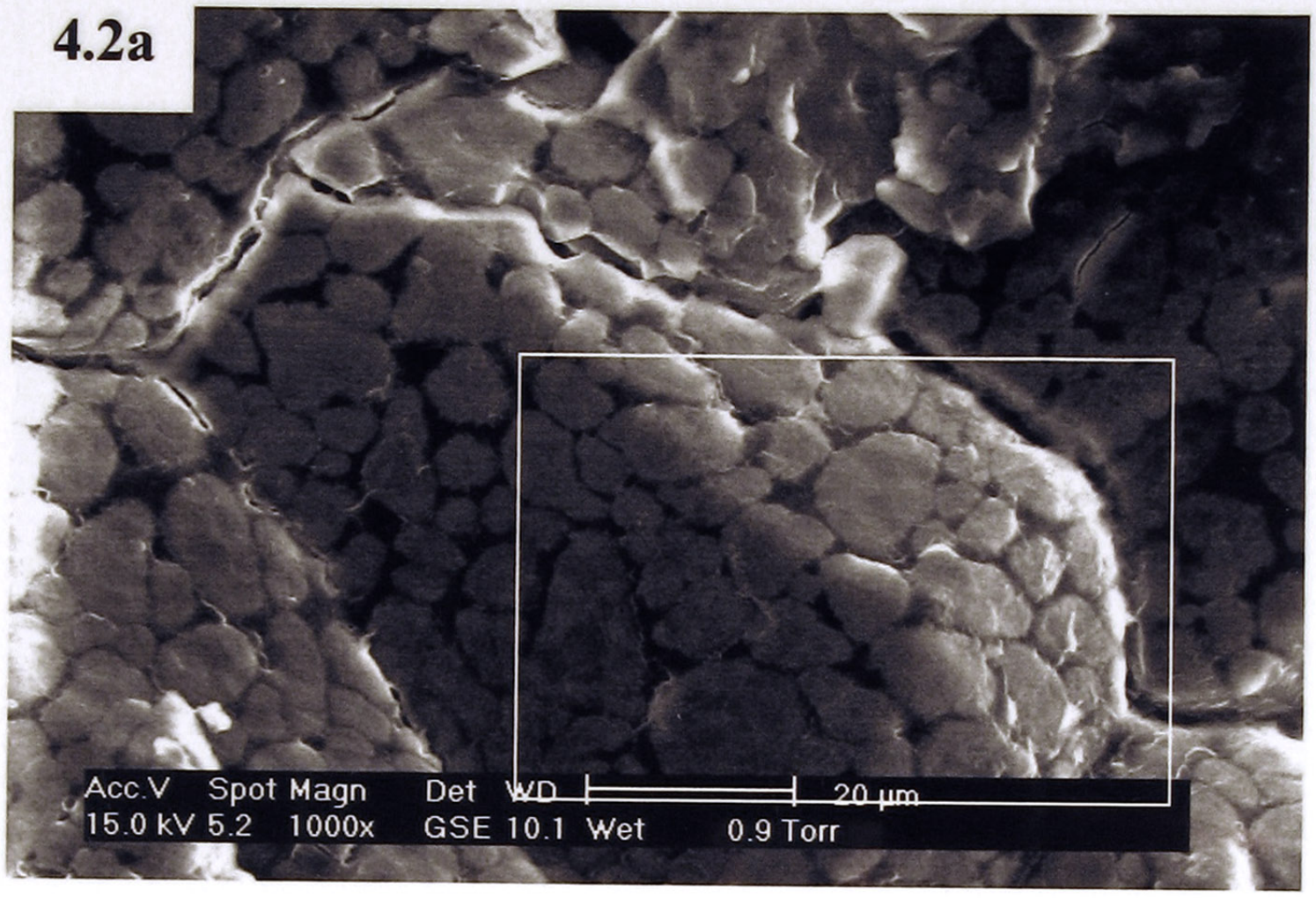
Acc.V Spot Magn Det WD 20 µm
15.0 kV 5.2 1000x GSE 10.1 Wet 0.9 Torr

4.2b

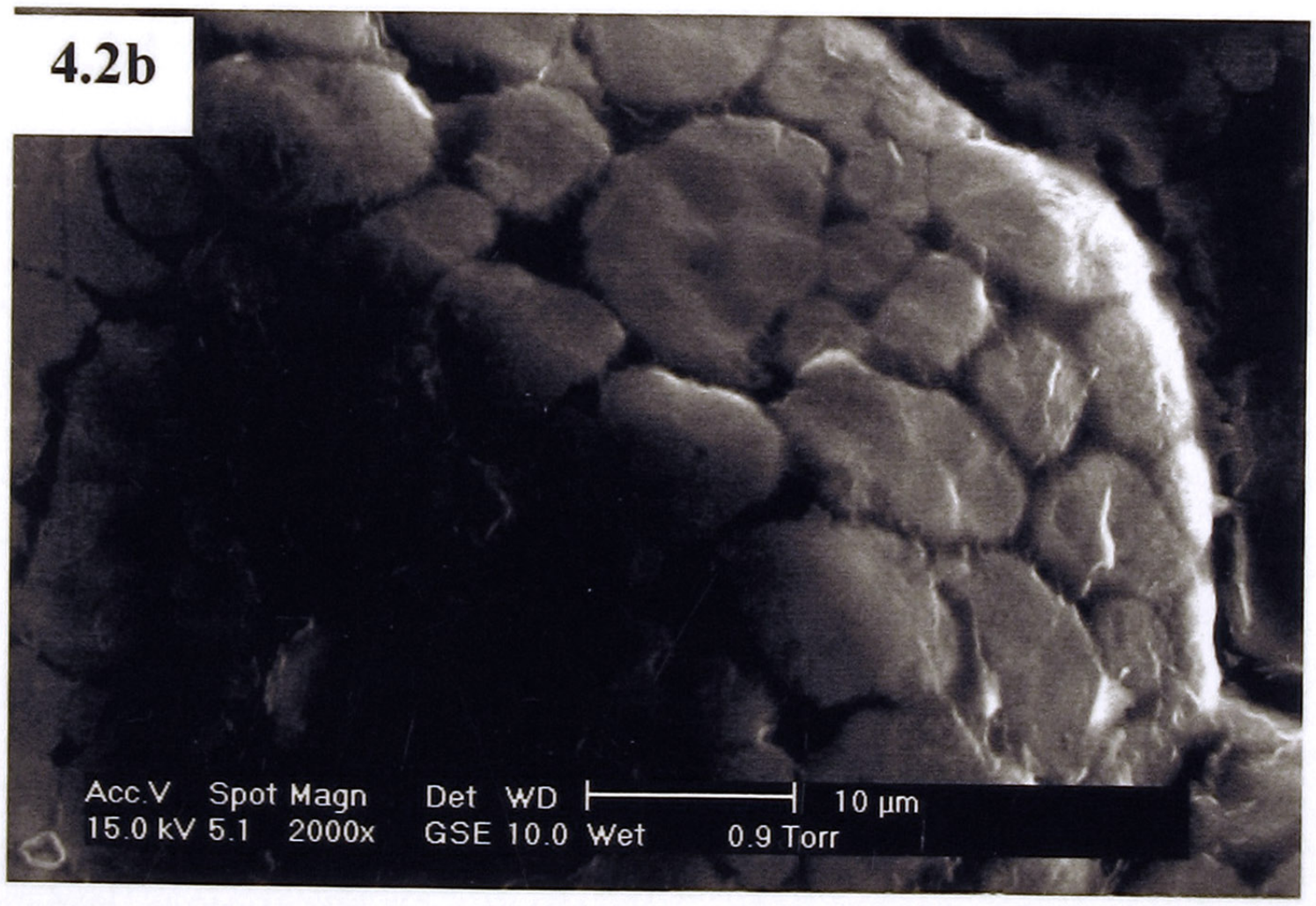
Acc.V Spot Magn Det WD 10 µm
15.0 kV 5.1 2000x GSE 10.0 Wet 0.9 Torr

4.2c

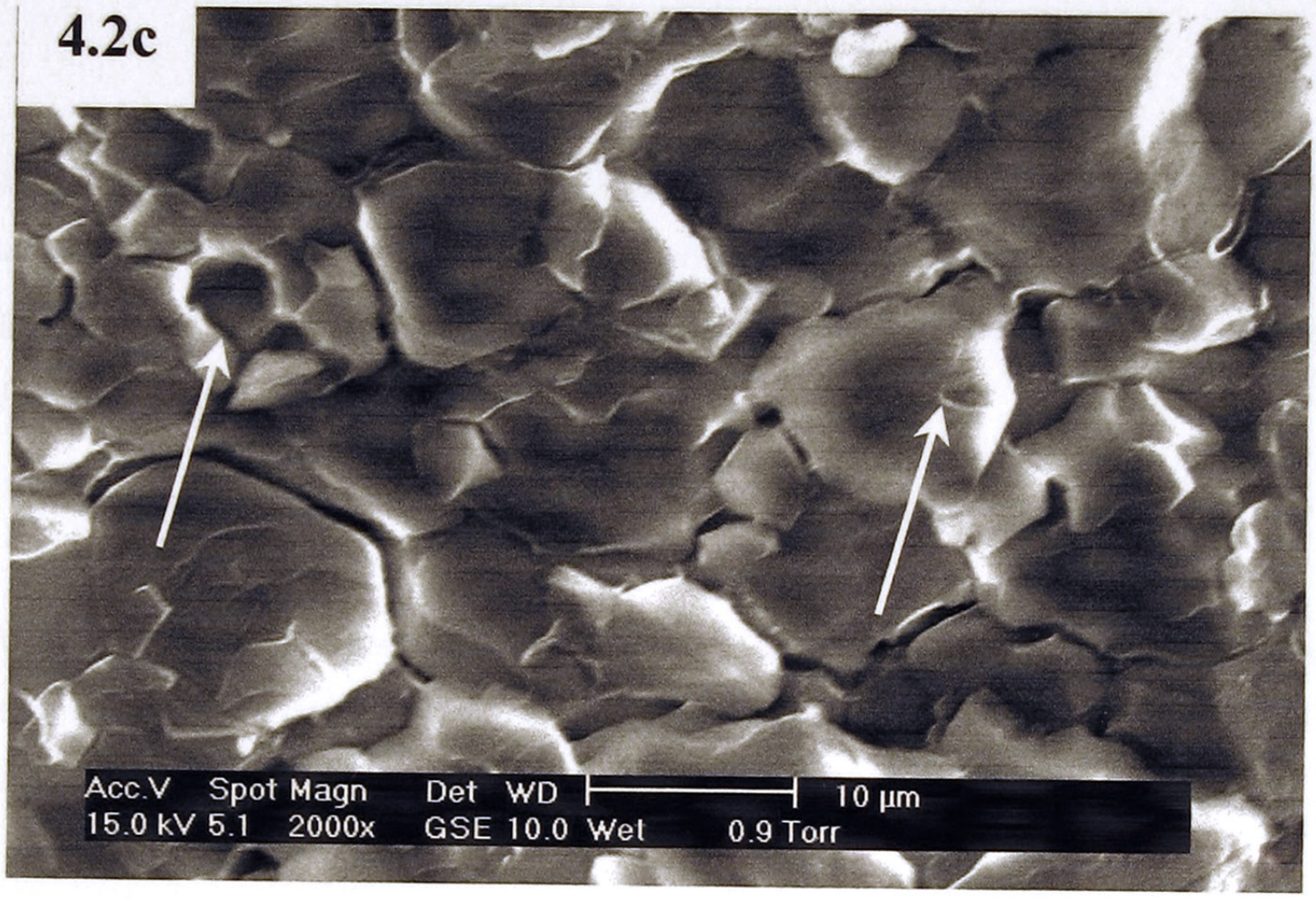
Acc.V Spot Magn Det WD 10 µm
15.0 kV 5.1 2000x GSE 10.0 Wet 0.9 Torr

4.2d

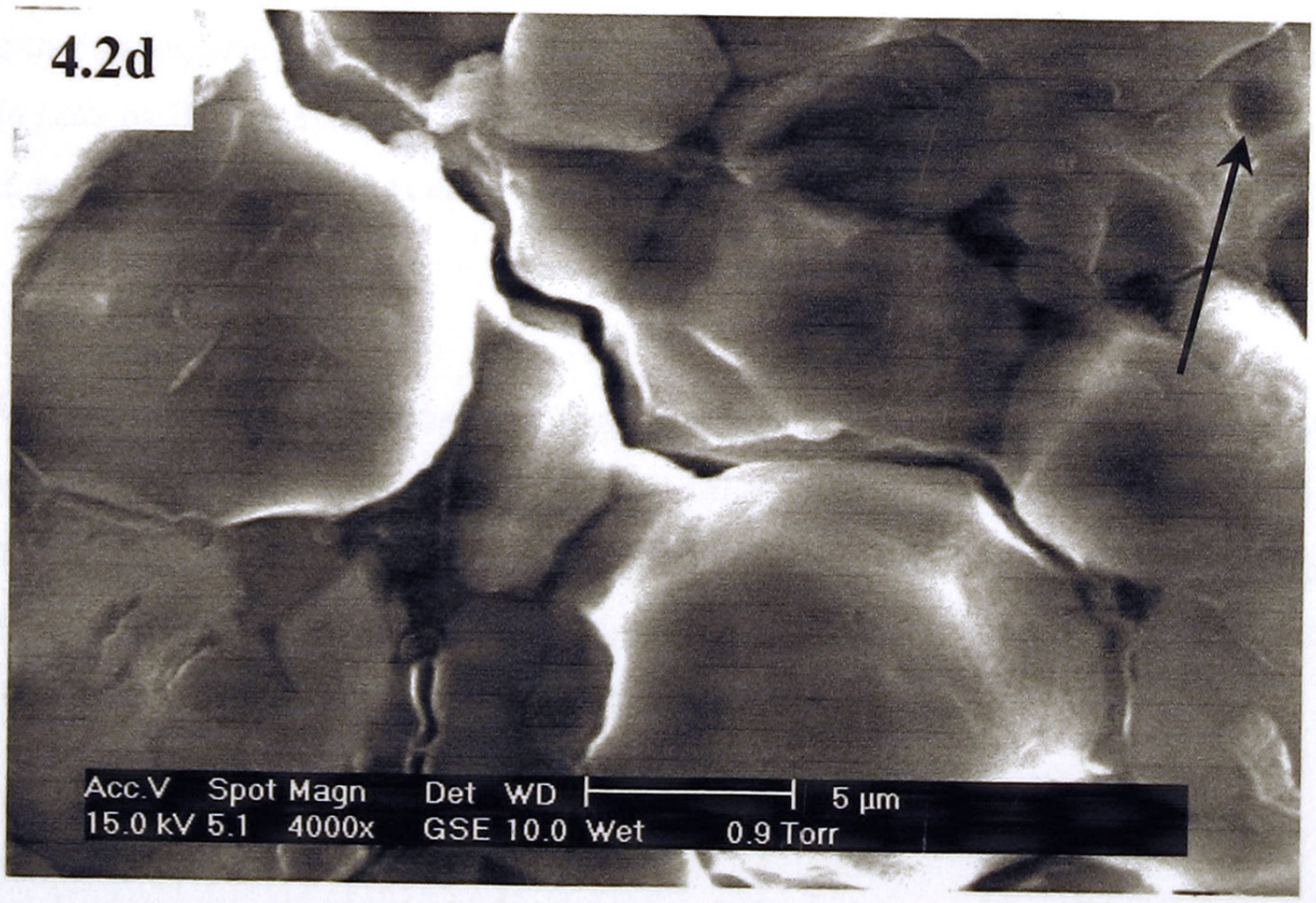
Acc.V Spot Magn Det WD 5 µm
15.0 kV 5.1 4000x GSE 10.0 Wet 0.9 Torr

The figure legends below correspond to figures in the following pages.

Figure 4.3

ESEM images of the fracture plane of Doongara rice grains. The image in (a) shows a fracture occurring within the endosperm cell. Arrows indicate some examples of pitting on the granule surface. The image in (b) shows a fracture between endosperm cells. Compound granules are indicated by CG.

Figure 4.4

ESEM images of the fracture plane of Kyeema rice grains. The images in (a) shows a fracture occurring between endosperm cells. The image in (b) shows a fracture within an endosperm cell. Compound granules are indicated by CG.

Figure 4.5

ESEM images of the fracture plane of medium-grained waxy rice. The image in (a) shows elongated endosperm cells (EC), with fractures between cells indicated by B, and fractures within cells by W. The image in (b) shows a closer view of the between-cell fracture region in (a), with individual (S) and compound starch granules (CG).

Figure 4.6

ESEM images of the fracture planes of long-grained waxy rice. The image in (a) shows the arrangement of endosperm cells on the fracture surface of the grain. The rough feature of a fracture within an endosperm cell is represented by W, and is shown at higher magnification in (b). The smoother feature of a fracture between endosperm cells is represented by B and is shown at higher magnification in (c).

4.3a

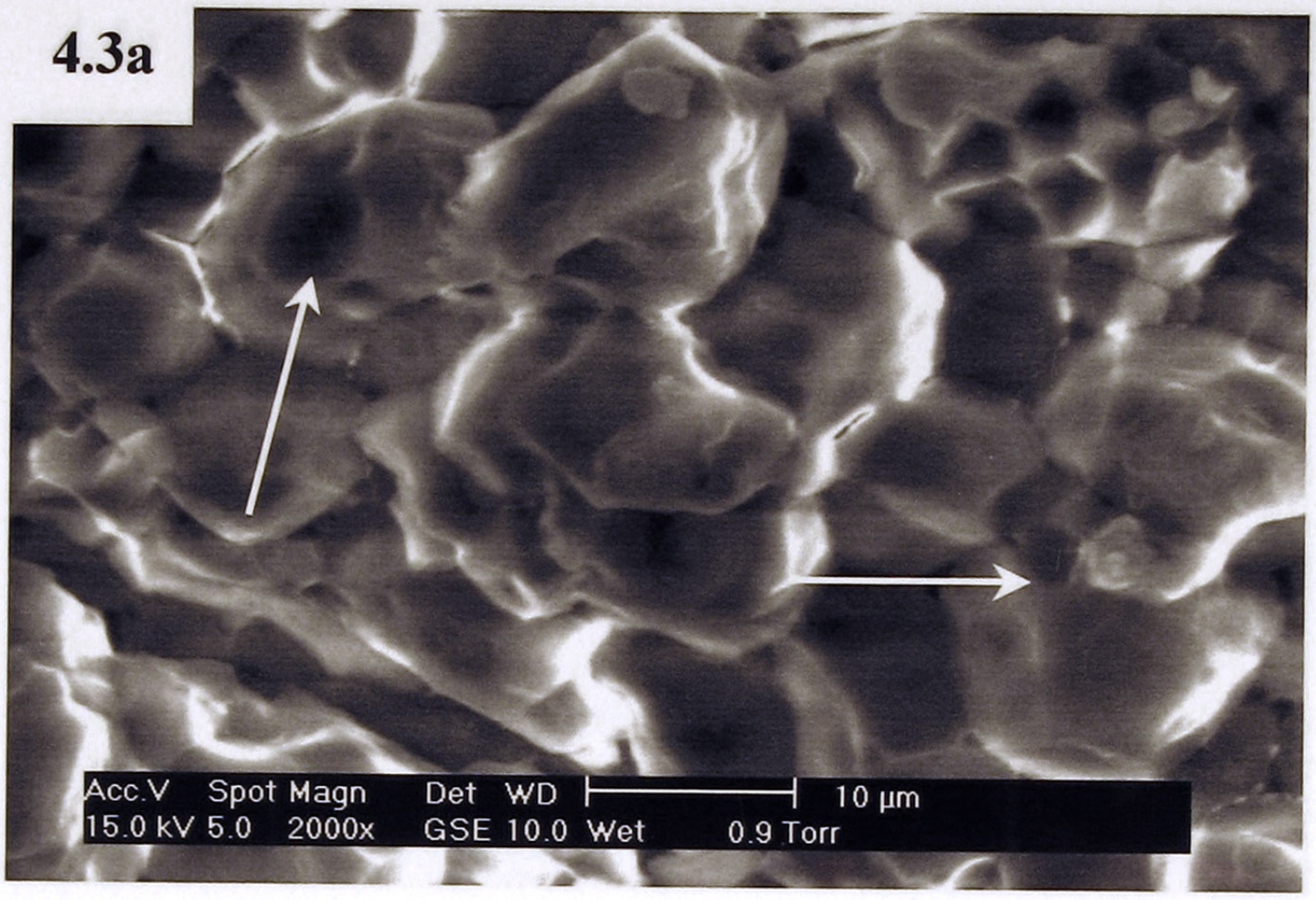
Acc.V Spot Magn Det WD 10 µm
15.0 kV 5.0 2000x GSE 10.0 Wet 0.9 Torr

4.3b

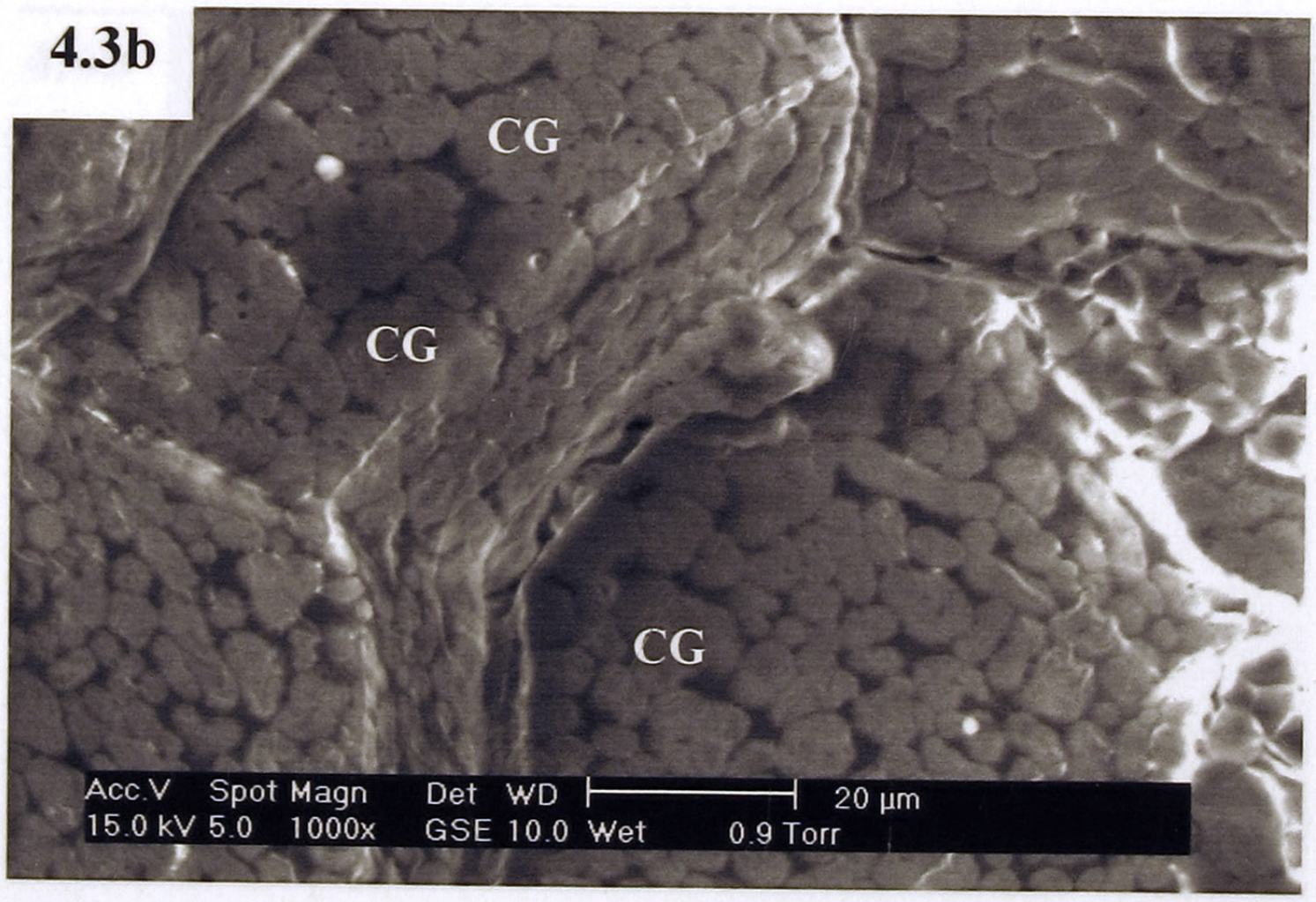
CG
CG
CG
Acc.V Spot Magn Det WD 20 µm
15.0 kV 5.0 1000x GSE 10.0 Wet 0.9 Torr

4.4a

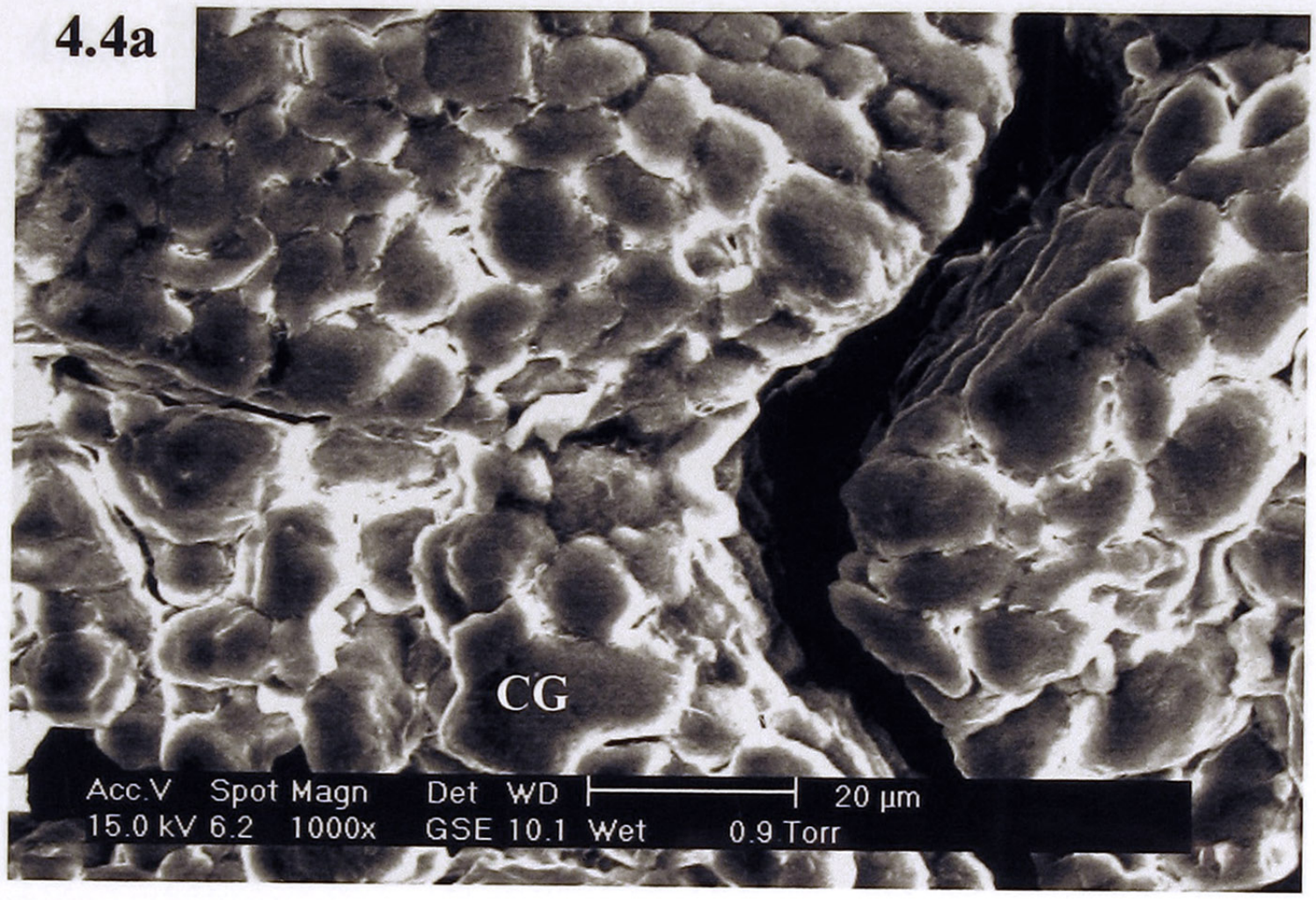
CG
Acc.V Spot Magn Det WD 20 µm
15.0 kV 6.2 1000x GSE 10.1 Wet 0.9 Torr

4.4b

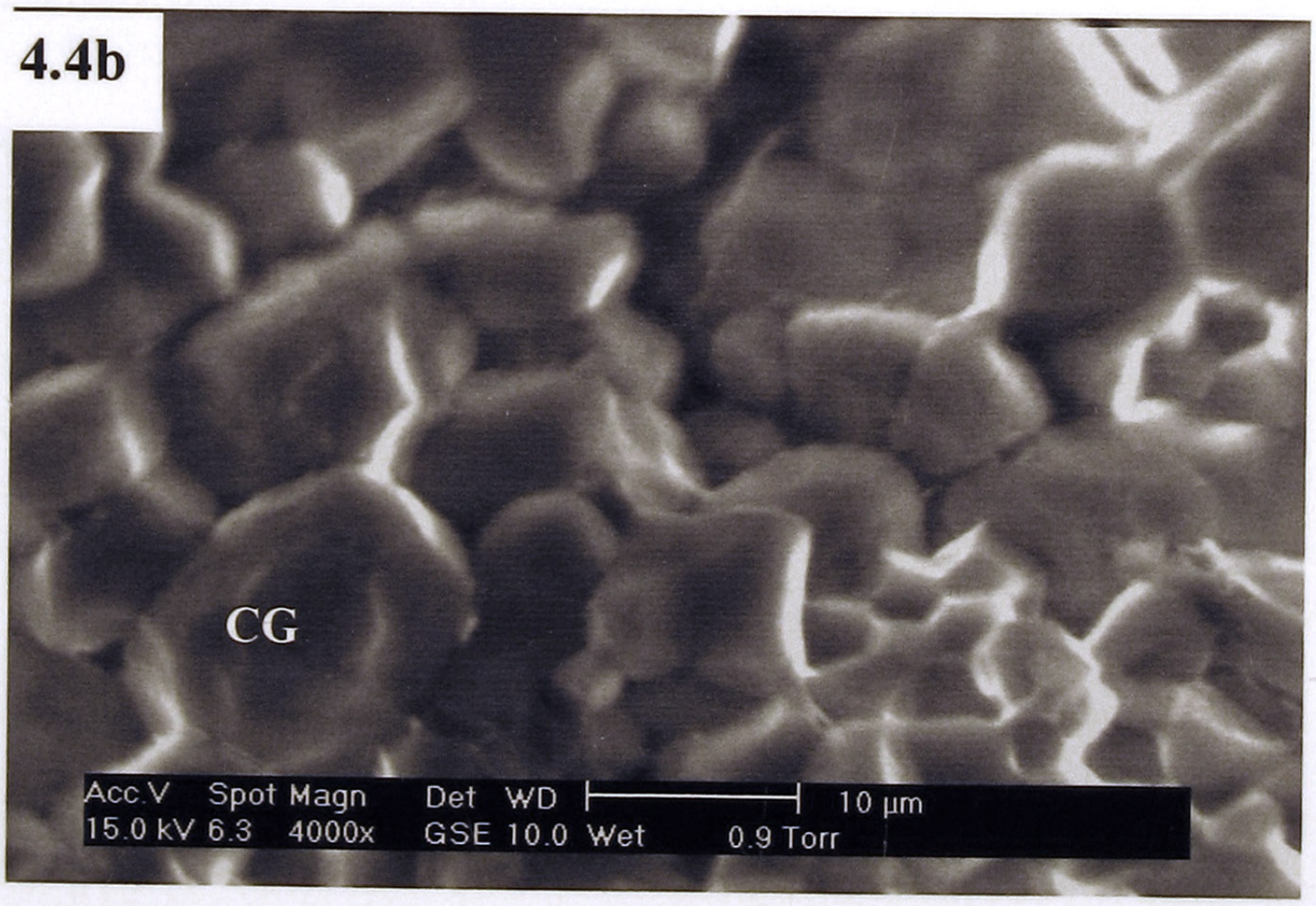
CG
Acc.V Spot Magn Det WD 10 µm
15.0 kV 6.3 4000x GSE 10.0 Wet 0.9 Torr

4.5a

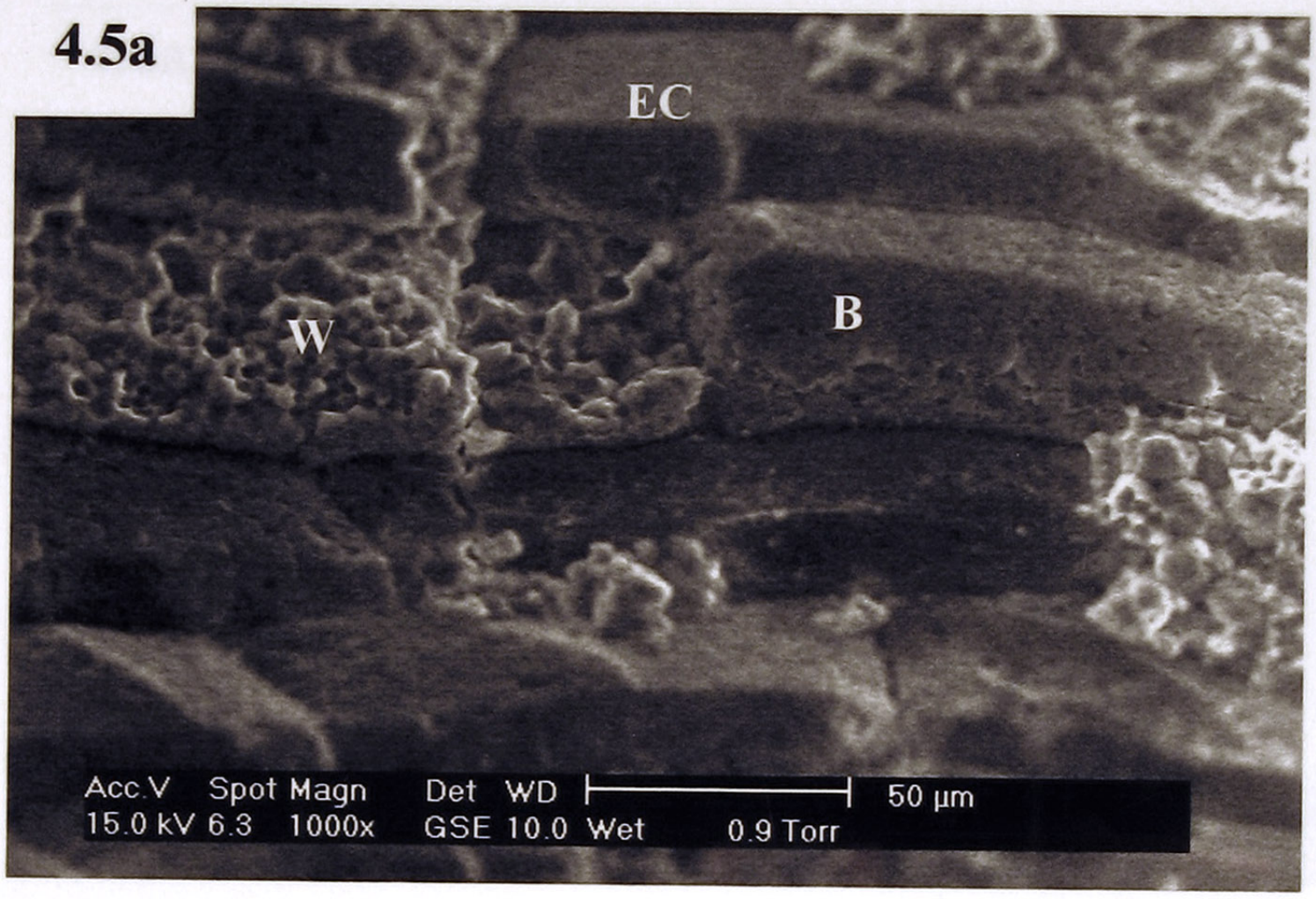
EC
W
B
Acc.V Spot Magn Det WD 50 µm
15.0 kV 6.3 1000x GSE 10.0 Wet 0.9 Torr

4.5b

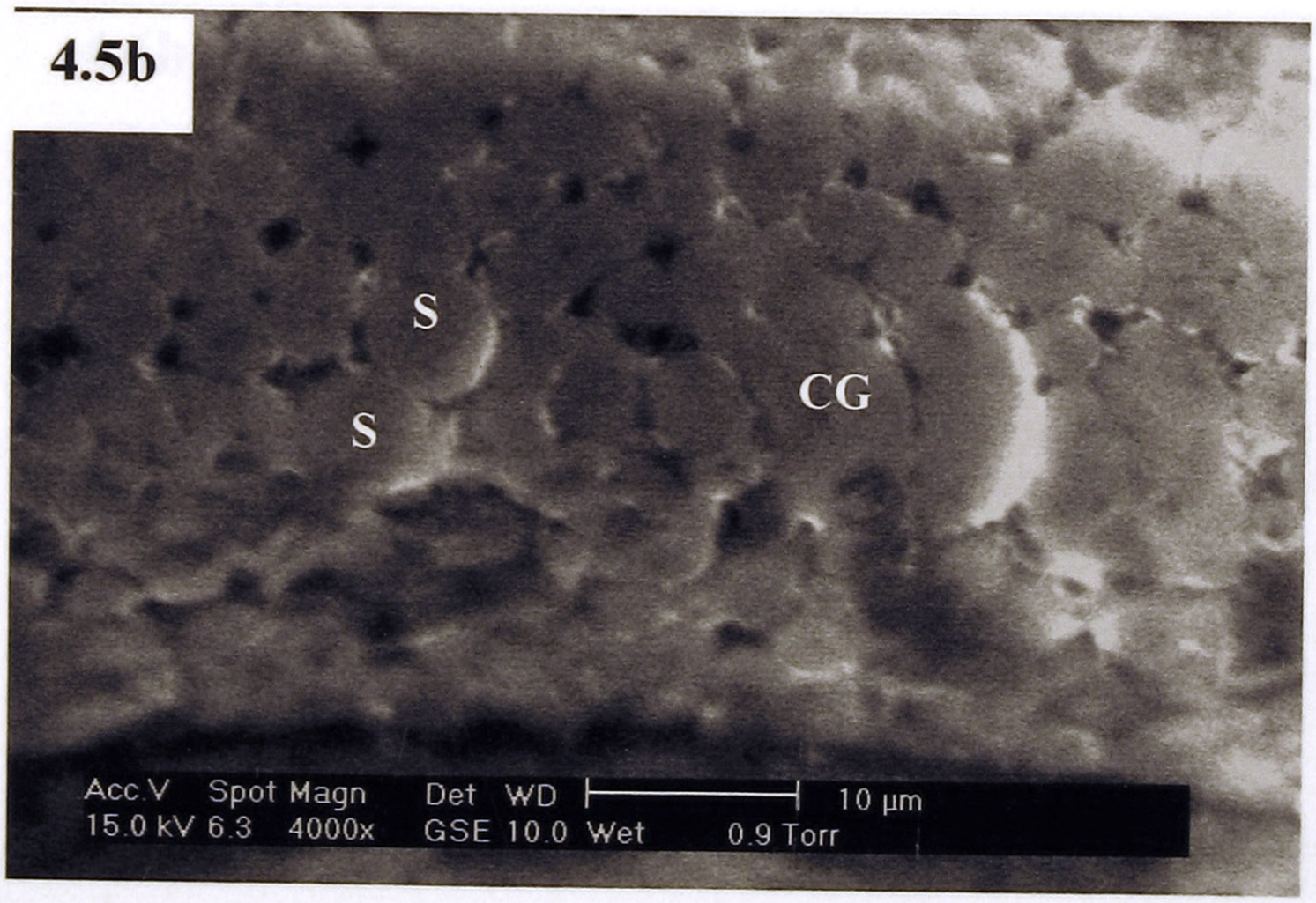
S
CG
S
Acc.V Spot Magn Det WD 10 µm
15.0 kV 6.3 4000x GSE 10.0 Wet 0.9 Torr

4.6a

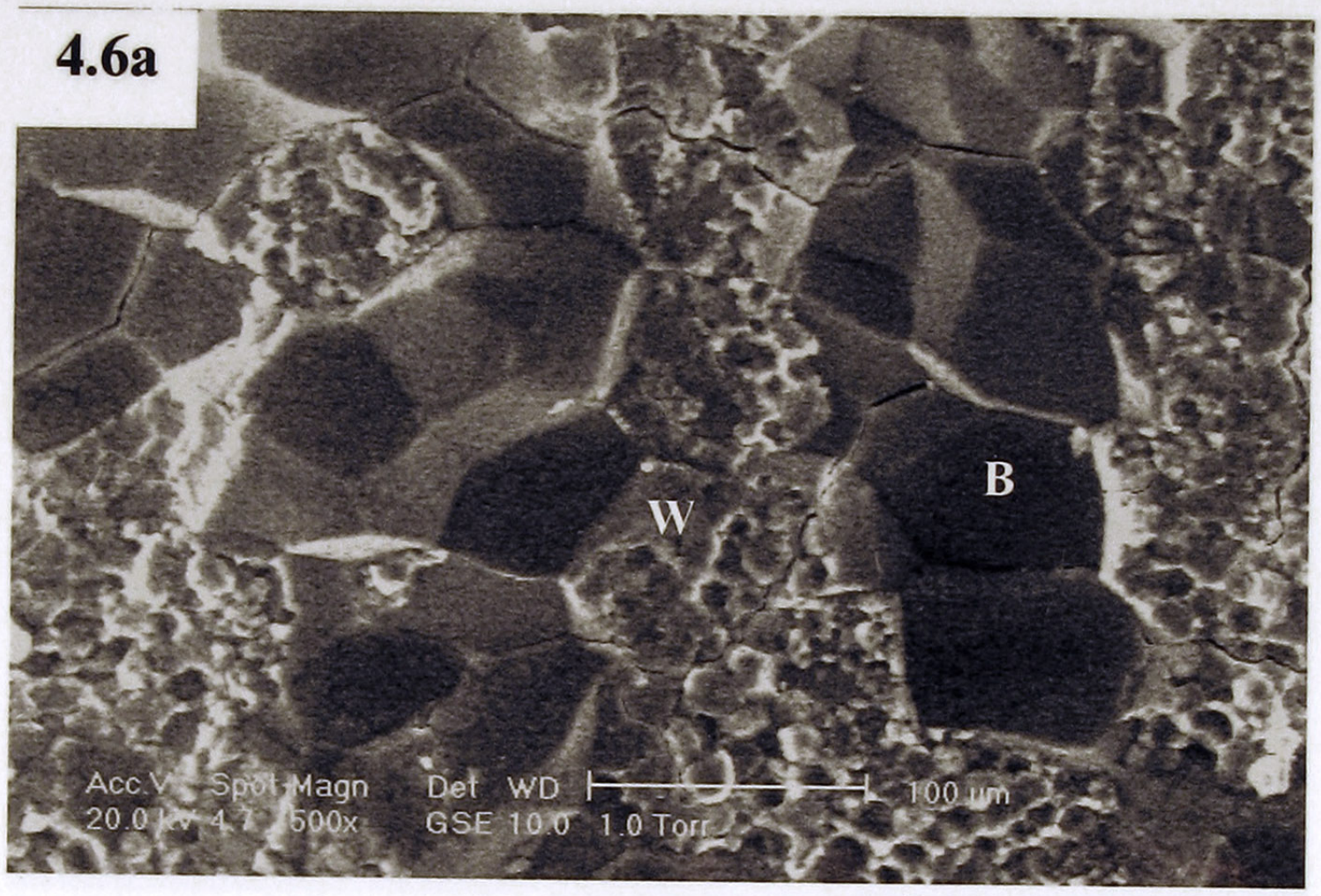
W
B
Acc.V Spot Magn Det WD
20.0 kV 4.7 500x GSE 10.0 1.0 Torr
100 µm

4.6b

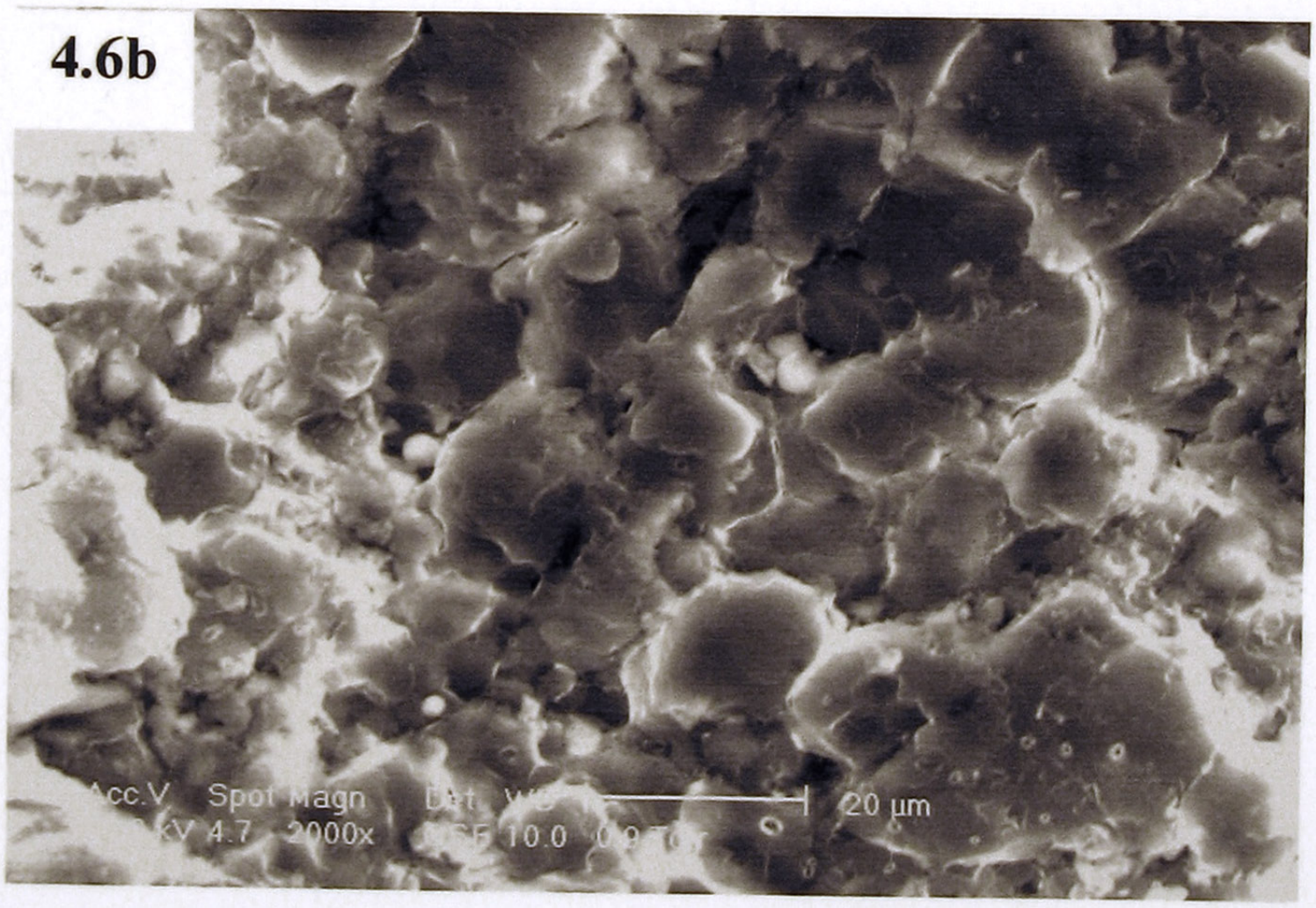
Acc.V Spot Magn
kV 4.7 2000x
20 µm

4.6c

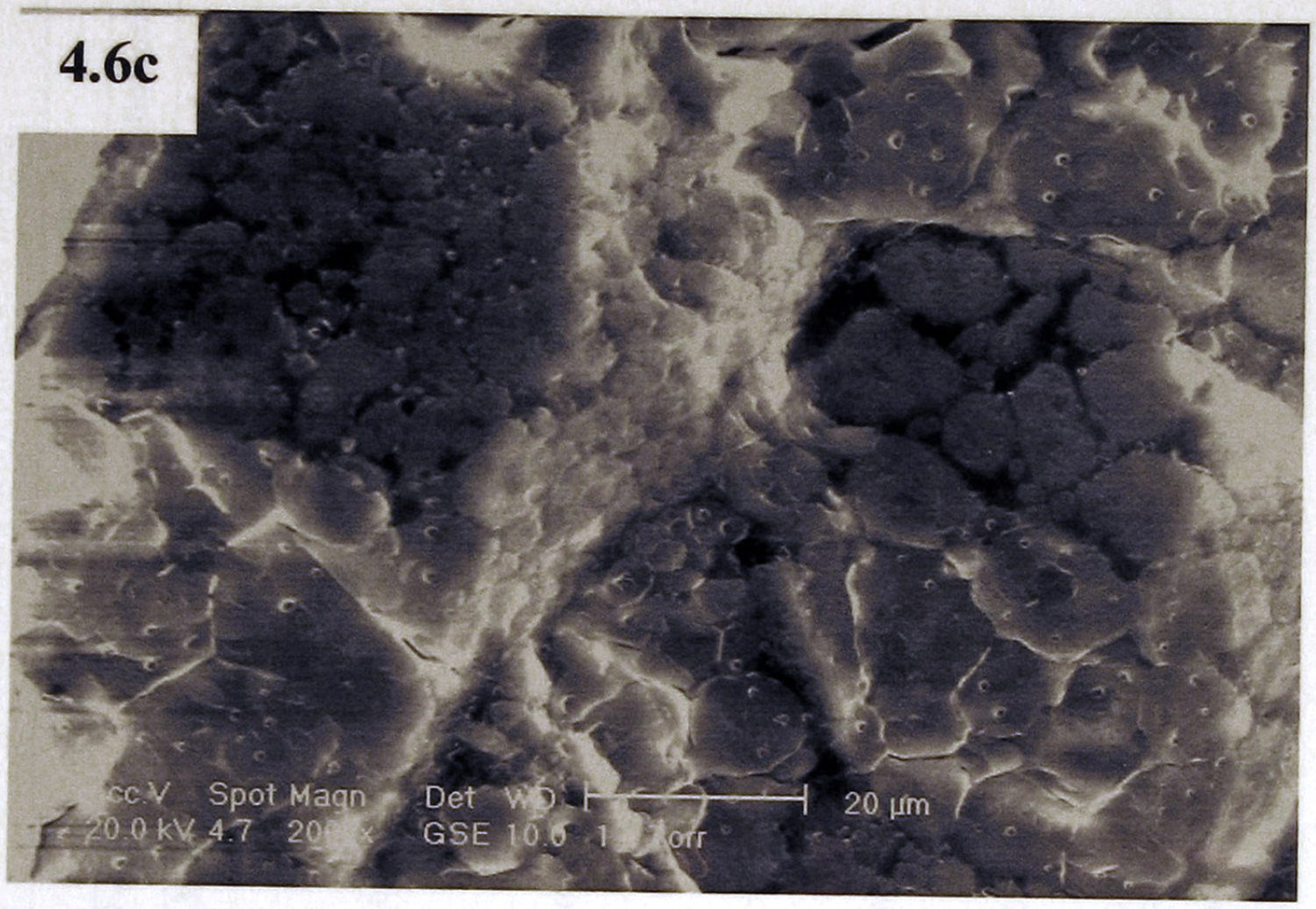

Table 4.1

Characteristics of rice, and dimensions of surface features of the fractured grains as obtained from ESEM images.

Sample	AM (%)	Type (Texture)	Endosperm cells[a]			Starch granules[b]	
			Length (μm)	Width (μm)	L-W ratio[c]	Shortest dimension (μm)	Longest dimension (μm)
Langi	18	Long (Soft)	82 ± 7.6 (70-94)	63 ± 2.4 (60-67)	1.30d	3-7	4-10
Doongara	28	Long (Soft)	91 ± 10.1 (76-109)	55 ± 4.5 (48-61)	1.65e	4-8	5-10
Kyeema	19	Long (Firm)	102 ± 3.9 (97-109)	61 ± 1.2 (60-62)	1.67e	4-9	5-11
Medium-grained waxy	2	Medium (Soft)	134 ± 6.0 (122-141)	38 ± 2.4 (34-41)	3.53f	3-5	4-7
Long-grained waxy	1	Long (Soft)	99 ± 6.4 (86-112)	61 ± 3.3 (54-78)	1.62e	3-8	5-9
Parboiled Doongara	25	Long (Soft)	83 ± 8.2 (69-98)	51 ± 6.8 (46-63)	1.63e	5-7	7-9

[a]Measurements were made on 50 endosperm cells observed from ESEM images. Figures in parentheses give the range of values for the respective dimensions.

[b]Measurements were made on 100 starch granules observed from ESEM images. The data give the range of values for the respective dimensions.

[c]Different letters after values indicate significant difference between ratios as determined by Analysis of Variance.

4.2.3 Effect of growth season and location on grain surface structure

For each genotype, the surface structure of grains showed similar characteristics, in terms of fracture patterns and starch granule dimensions, regardless of growth season or location. Thus, in this study, the growth season and location appeared to have no effect on the arrangement of starch granules or cracking tendencies of rice grains.

4.2.4 Effect of processing on grain surface structure

The parboiled rice used in this study was a commercial product that had been prepared by steeping and draining brown Doongara rice. The drained grains are steamed to gelatinise the starch, and the cooked grains are partially dried, milled and then dried further to a lower moisture content. The grains imaged in this study had a moisture content of 11%. The parboiling process led to a small loss of amylose, from 28% to 25% (Table 4.1). The effects of parboiling produced an amber, glassy rice grain, which was easily fractured to produce a mostly smooth fracture surface (Fig. 4.7a). At a higher magnification of the smooth surface (Fig. 4.7b), the outlines of endosperm cells were visible, however the same level of structural detail of starch granules within cells was not observed as for uncooked rice grains. The smooth glassy surface was typical of all grains of parboiled rice that were imaged. It is likely that during the heating process of parboiling, amylose leached out of starch granules and aggregated to form a semi-crystalline glass-like structure on cooling. Some parts of the fracture surface did not appear glass-like, which suggests that the effects of processing may not be uniform throughout the grain. In less than 2 % of the images observed, there were clearly evident cellular structure on the fractured grain surface. When viewed at higher magnifications, small areas on the parboiled rice surface where structural detail were observed showed the two patterns of between- and within- endosperm cell fractures, as were observed for uncooked grains (Fig. 4.7c). The pitting on the surface (Fig. 4.7c) may be a result of dislodgement of protein bodies from the surface of disrupted endosperm cells. The overall length-to-width ratio of endosperm cells within parboiled Doongara rice was not significantly different to the unprocessed Doongara. Starch granules from the parboiled rice were generally smaller than those of the unprocessed rice, which is likely to be caused by gelatinisation and retrogradation of amylose and amylopectin.

The figure legends below correspond to figures in the following pages.

Figure 4.7

ESEM images of the fracture plane through a parboiled Doongara rice grain. The image in (a) shows the entire fracture surface of the parboiled grain. The boxed area shows the rare occurrence (in less than 2 % of images observed) of clearly evident cellular structure on the fractured grain surface. The smooth, glassy characteristic of the grain surface (outside boxed area) is magnified in (b), where outlines of endosperm cells were observed. A higher magnification of the grain surface within the boxed area is shown in (c), with the arrangement of starch granules within endosperm cells that have been disrupted.

Figure 4.8

ESEM images of the fracture planes of quick-cooking Doongara rice grains. The image in (a) shows the entire fracture surface of the quick-cooking rice grain. The puffing procedure achieved a porous structure containing air pockets, which are represented by A. The shrivelled appearance of the grain structure is shown in (b).

4.7a

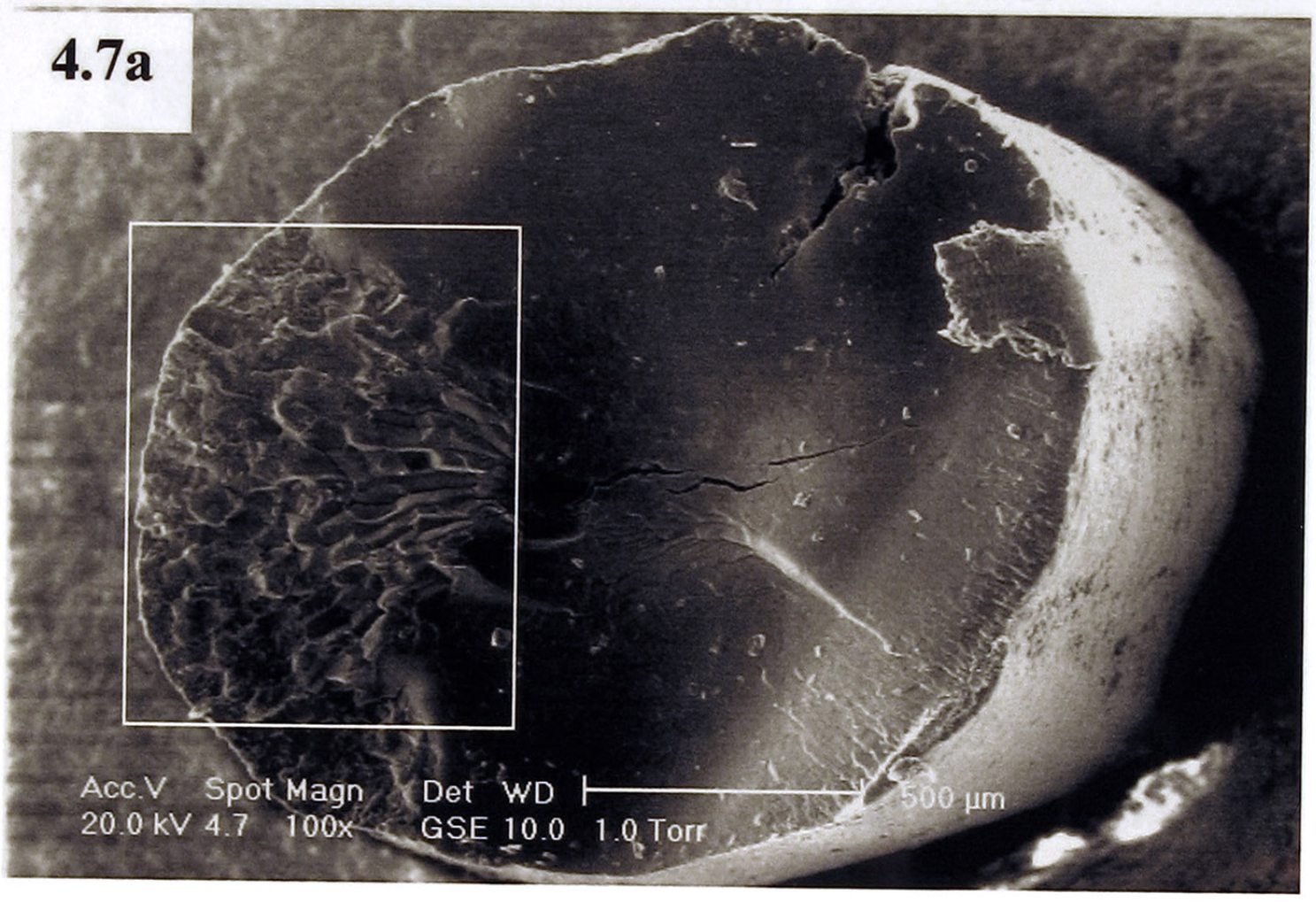
Acc.V Spot Magn Det WD
20.0 kV 4.7 100x GSE 10.0 1.0 Torr
500 µm

4.7b

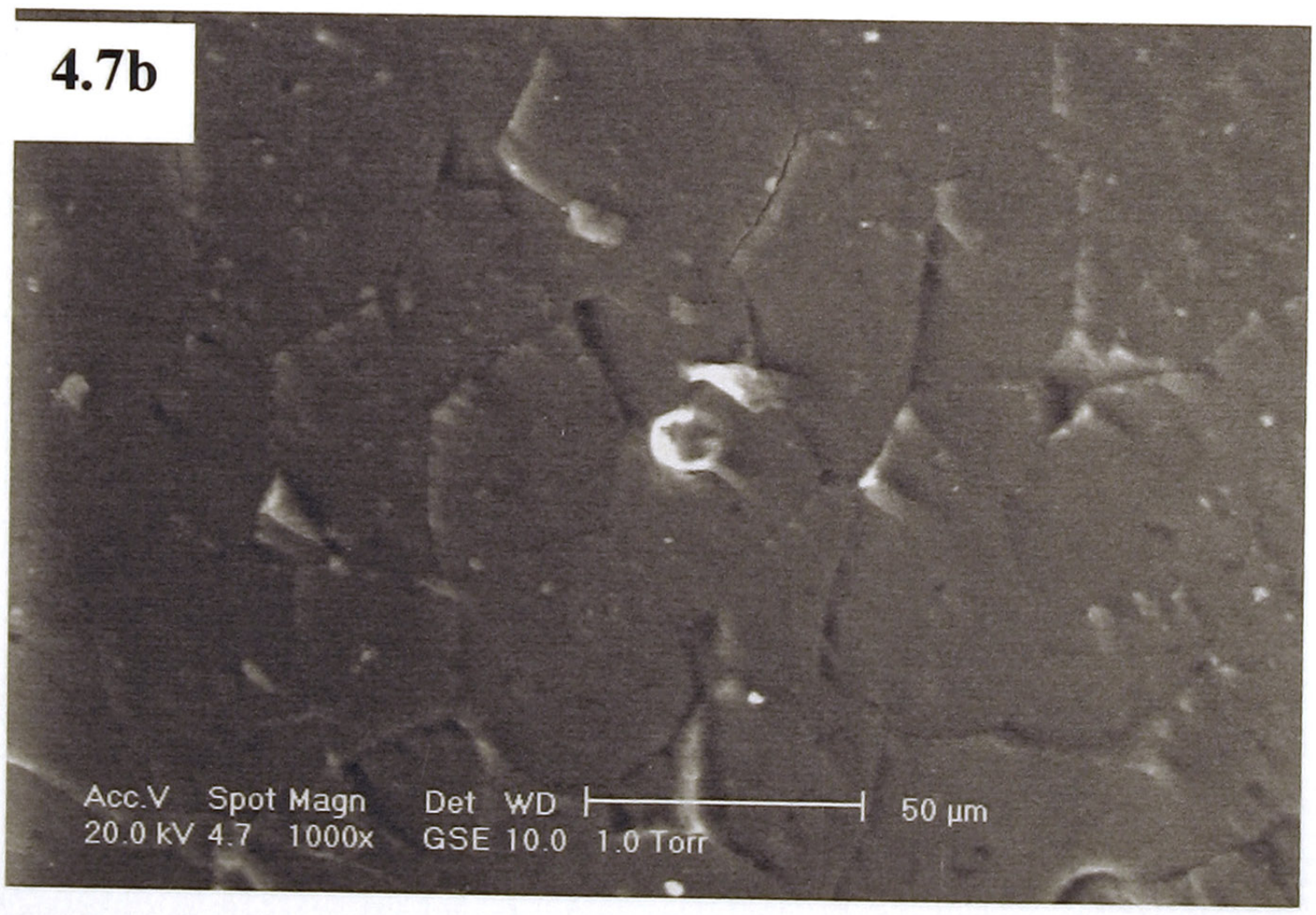
Acc.V Spot Magn Det WD
20.0 kV 4.7 1000x GSE 10.0 1.0 Torr
50 µm

4.7c

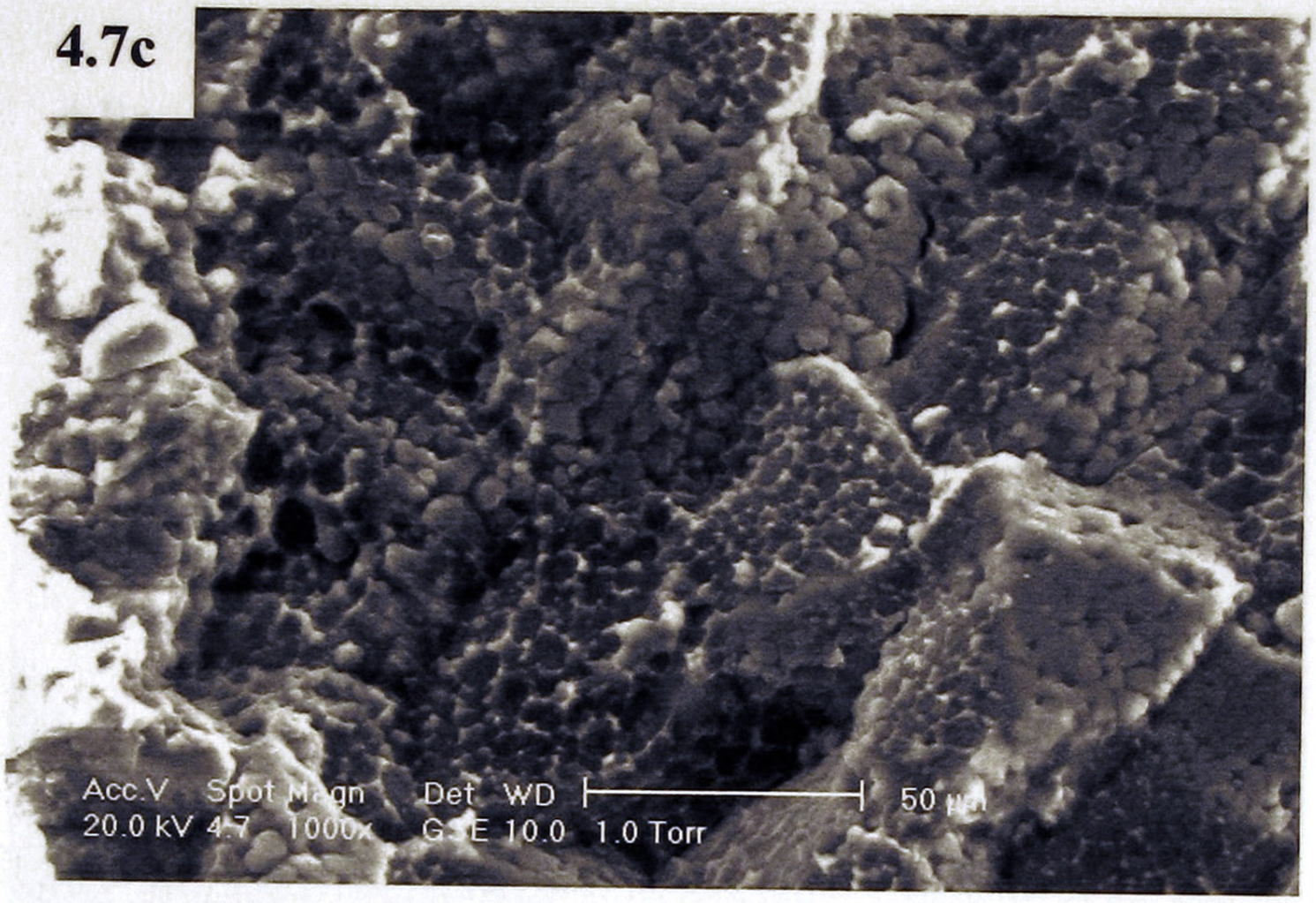

4.8a

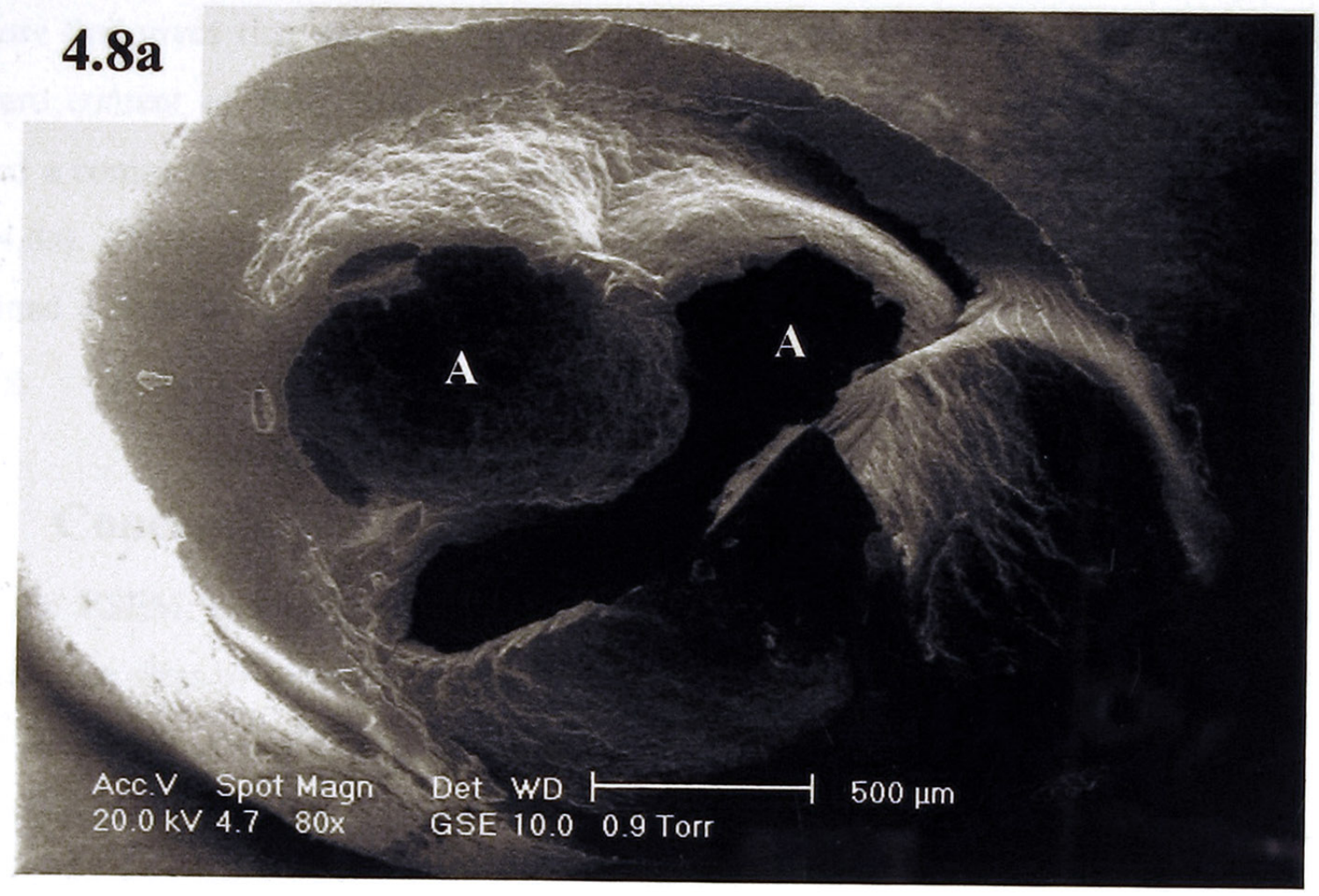
A
A
Acc.V Spot Magn Det WD 500 µm
20.0 kV 4.7 80x GSE 10.0 0.9 Torr

4.8b

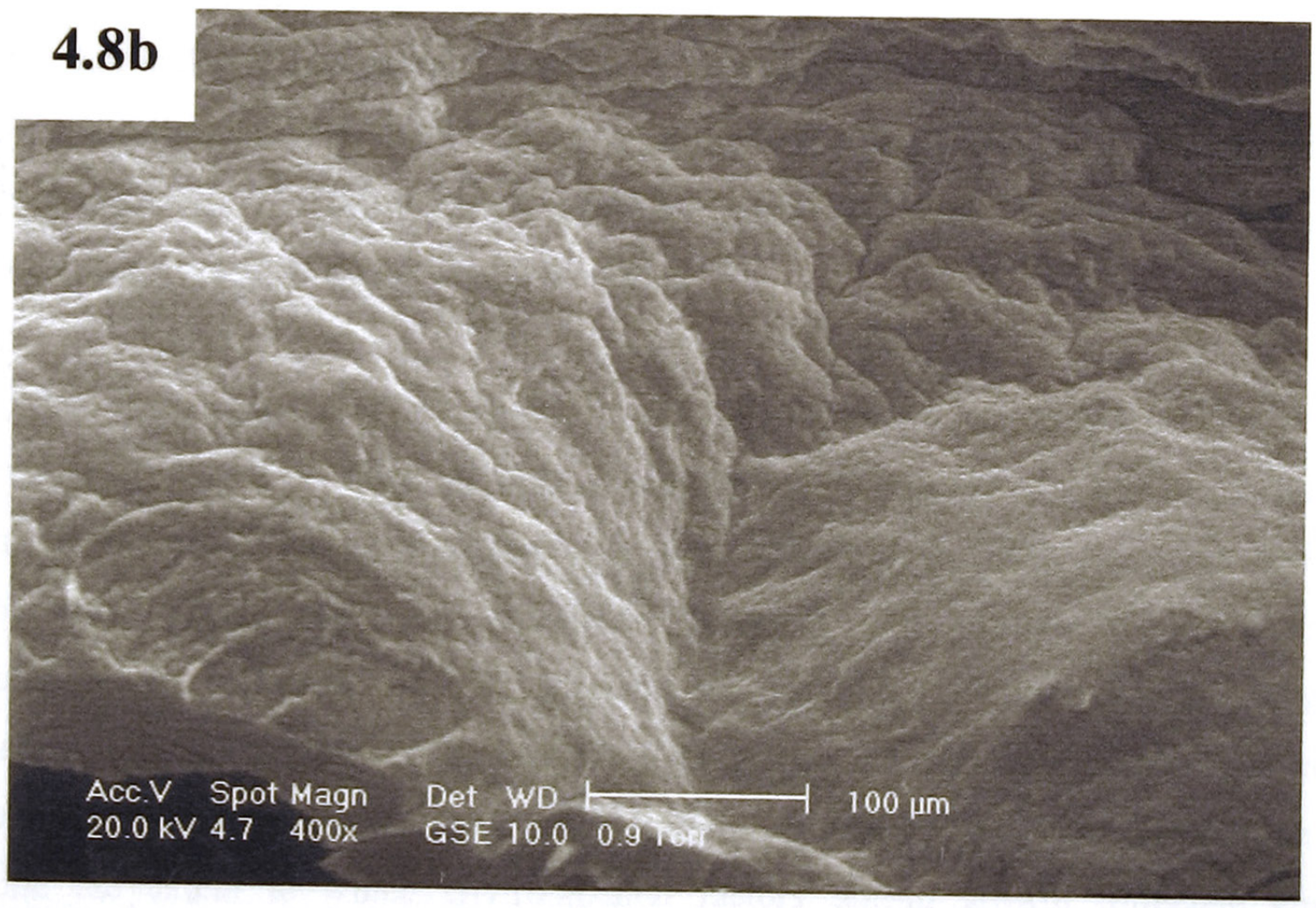
Acc.V Spot Magn Det WD 100 µm
20.0 kV 4.7 400x GSE 10.0 0.9 Torr

Quick-cooking rice is produced in a process similar to parboiled rice, except that after milling, the partially dried rice is puffed by heating at high temperature to achieve a porous structure that gives rise to quick-cooking properties. The grains that were imaged had a moisture content of 10%. The entire fracture surface of the quick-cooking rice grains showed a complete loss of structural organisation, with many air pockets within the grain (Fig. 4.8a). The surface had a shrivelled appearance (Fig. 4.8b), which may be due to the combined effects of gelatinisation of starch, desiccation of the surface upon drying, and puffing.

4.3 Conclusions

Using the ESEM, morphological differences were observed between grains of different varieties. The sizes of endosperm cells varied between varieties, but were not related to the size of starch granules, nor to amylose and amylopectin content of the starch. Differences between varieties were also noted in the fracture patterns of grains. The tendency of rice grains to undergo suncracking and to crack during milling is an important aspect of grain quality that has been related to defects in the grain (Blakeney, 1980). The interface between the cell wall and cytoplasm inside endosperm cells is considered to be an area of weakness that makes grains more susceptible to cracking (Hoshikawa, 1993). It would be interesting to determine if a greater tendency to fracture within rather than between cells, as was observed for Doongara and Kyeema compared to Langi, is associated with an increased susceptibility of rice grains to cracking.

The ESEM images revealed structural details of uncooked rice samples that were consistent with images obtained by SEM. As uncooked rice grains are low in moisture, they can be examined without further drying using conventional SEM. However, ESEM may be more advantageous for examining processed rice. As no further sample manipulation was performed on the processed rice samples prior to imaging, changes observed with the ESEM may be attributed to processing not sample preparation. The ease of specimen preparation would clearly make imaging with the ESEM a useful technique to determine the extent to which environmental factors during growth influence grain morphology.

CHAPTER 5

Rice grain and starch morphology by atomic force microscopy

5.1 Introduction

The composition and arrangement of components of cereal grains influence behaviour in processing operations. Atomic force microscopy (AFM) is a relatively new imaging technique that has been used to study the molecular structure of biological macromolecules (Hansma and Hoh, 1994). Images obtained with the AFM display morphological features at greater resolution than achieved with SEM. Further, AFM allows samples to be examined in their natural state, without the need for metal coatings as are required in SEM, and AFM can provide topographical information that is not obtained with SEM.

The results and discussion in this chapter are divided into two sections: 1) rice grain morphology, and 2) morphology of extracted starch and starch components. Atomic force microscopy was used to first examine the gross structure of rice grains, and the arrangement of starch therein, and then to examine individual amylose and amylopectin molecules within the rice starch in solution.

5.2 Results and discussion

5.2.1 Rice grain morphology

This section describes the use of AFM to image the surface of cut and fractured rice grains, with emphasis on examining the organisation of starch granules within the grain and the structure of the starch granules. The effect of different methods of sample preparation on the images was also examined. The varieties studied (Doongara, Langi, Kyeema, medium-grained waxy rice) were chosen on the basis of different amylose-amylopectin ratios and cooking properties. A quick cooking Kyeema rice that had been subjected to a high heat treatment and a drying process, was also imaged to observe the differences between raw and partially cooked rice samples.

5.2.1.1 Surface structure of rice grains by AFM

The arrangement of starch granules within the grain of several rice varieties was imaged using AFM. Ten grains of each variety of rice were prepared for imaging. Individual rice grains were embedded in a resin and sectioned with a diamond saw, in the presence (wet-sectioned) and absence (dry-sectioned) of water as a lubricant. Approximately ten fields of view were selected from each grain surface, and images were obtained at different magnifications within each field of view. Images of Doongara rice grains that were sectioned dry showed angular starch granules, with sizes in the range 3 to 8 μm (Fig. 5.1a). The angular structures were arranged in layers (Fig. 5.1b), which were observed at higher magnification to contain striated structures (Fig. 5.1c). At even higher magnification, these striations were observed as clusters that seemed to emanate from ridges estimated to be approximately 400 nm apart (Fig. 5.1d). Darker regions in the image appeared to correspond to gaps between the clusters.

The structures observed in this study had similar shapes and sizes (less than 10 μm) to those of starch granules imaged by other microscopic techniques (Moss, 1976; Fitt and Snyder, 1984). However, the fine structure observed with the AFM has provided some fresh insights into the arrangement of amylopectin molecules in starch granules.

Amylopectin is the dominant molecule in most starches and is considered to be the major contributor to the shape and structure of starch granules. Amylopectin chains are proposed to run perpendicular to the growth rings and to the surface of the granule (French, 1984). A diagrammatic representation of Fig. 5.1d is shown in Fig. 5.2, indicating the dimensions that were estimated from AFM images. The layered structures seen clearly in Fig. 5.1b are proposed to be growth rings formed during the deposition of starch, and the clusters seen at low resolution as striations in Fig. 5.1c represent the blocklets comprising groups of amorphous and crystalline lamellae. According to the cluster model, which is currently accepted as the most comprehensive model of starch structure (Myers *et al.*, 2000), crystalline regions consist of amylopectin side chain clusters, which extend approximately 10 nm along the main axis. The crystalline regions are separated by amorphous regions of about 4 nm (Fig. 5.2). Each cluster is estimated to be approximately 10 nm wide (Gallant *et al.*, 1997; Myers *et al.*, 2000). The blocklets observed in this study would therefore consist of approximately 28 repeating units of amorphous and crystalline lamellae in length, and less than 10 side chain clusters in width (Fig. 5.2). According to these

calculations, each blocklet would contain approximately 280 amylopectin side chain clusters. The observations of this study are not directly comparable with those of Ohtani *et al.* (2000b), who examined the internal structure of rice starch that had been disrupted by mechanical blending. The authors observed numerous fine particles with diameter less than 30 nm, which were arranged in aggregated chains, and were suggested to correspond to the clusters predicted in the cluster model.

5.2.1.2 Effect of genotype on grain and starch structure

Images of waxy rice grains, and grains from the Langi and Kyeema varieties showed similar morphological features (results not shown) to those of the Doongara variety. The layered starch structures were seen in many images, with similar dimensions between layers as was observed for Doongara. This indicates that, in this study, the genotype did not appear to affect the arrangement of starch within the rice grain.

Figure 5.1

AFM images of dry-sectioned Doongara rice grains. The areas scanned were 15 × 15 μm (a), 10 x 10 μm (b), 5 × 5 μm (c) and 2 × 2 μm (d). Layered structures are indicated by arrows, and starch granules by S. A closer view of the boxed area in (c) is shown in (d).

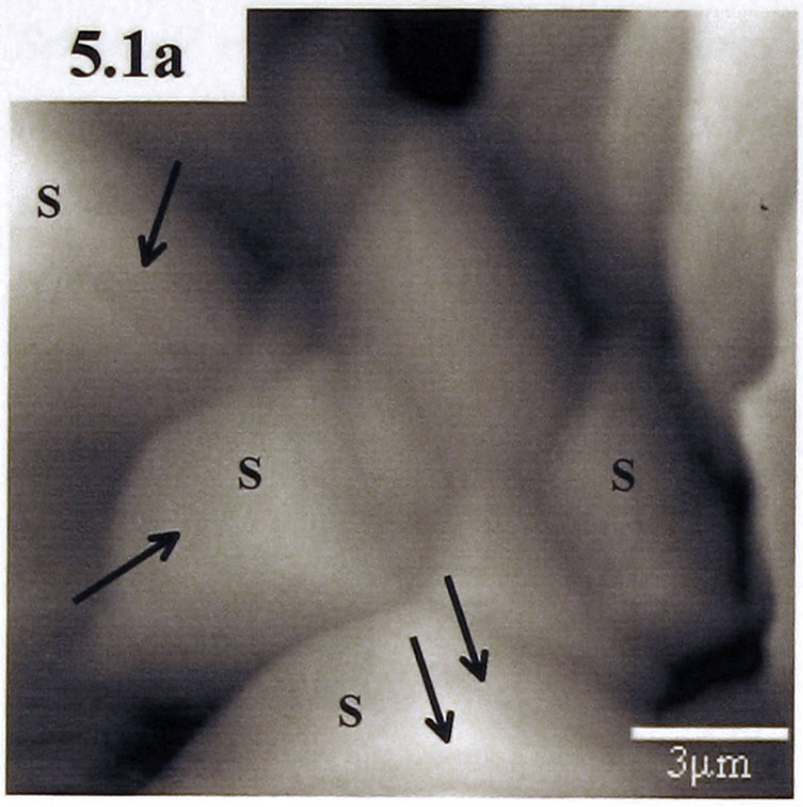
5.1a
S
S
S
S
3µm

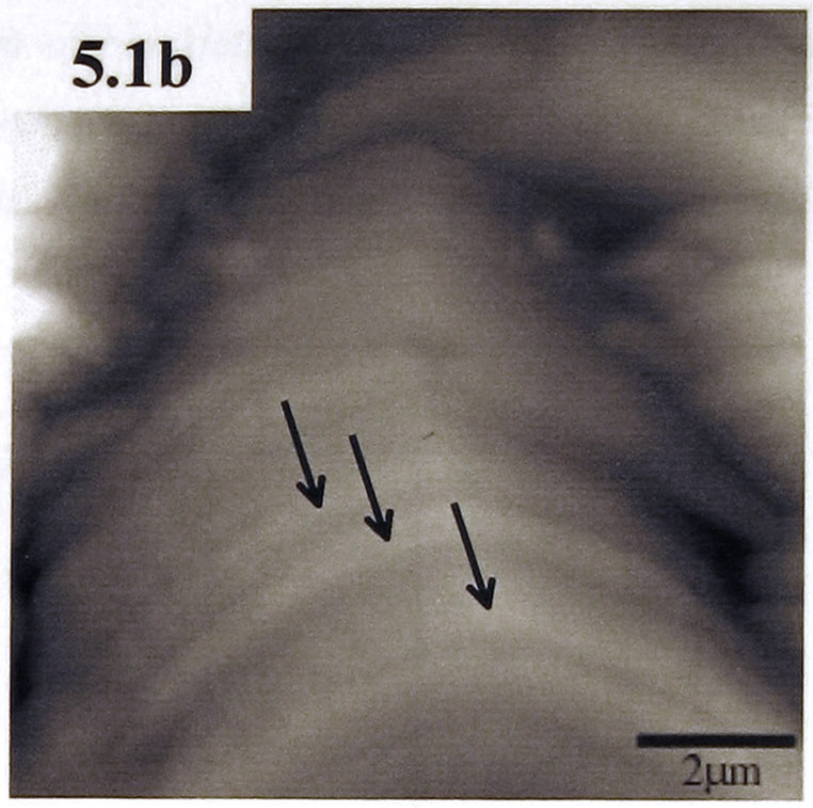
5.1b
2µm

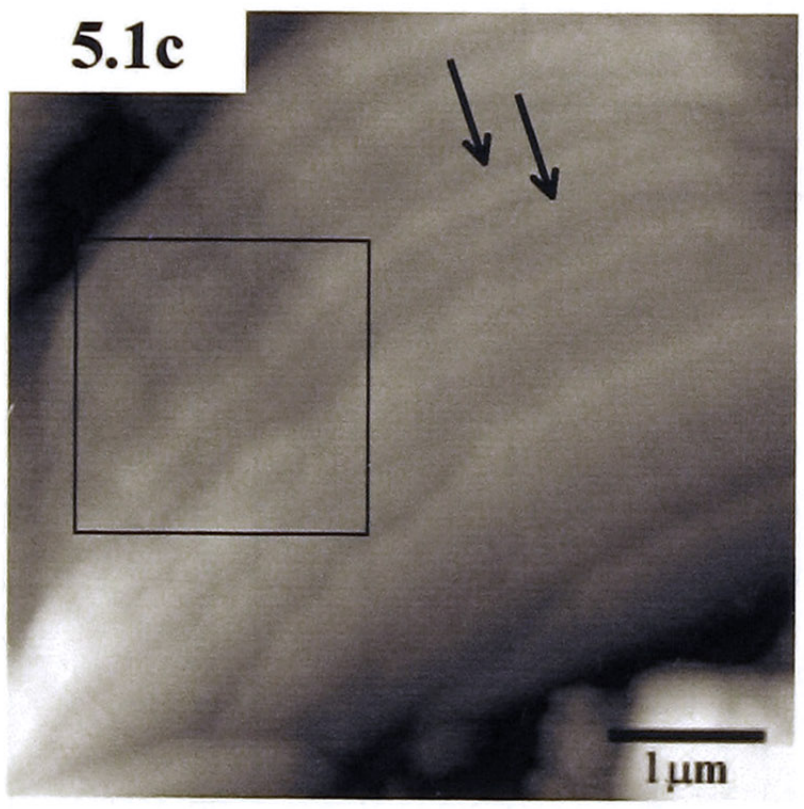
5.1c
1µm

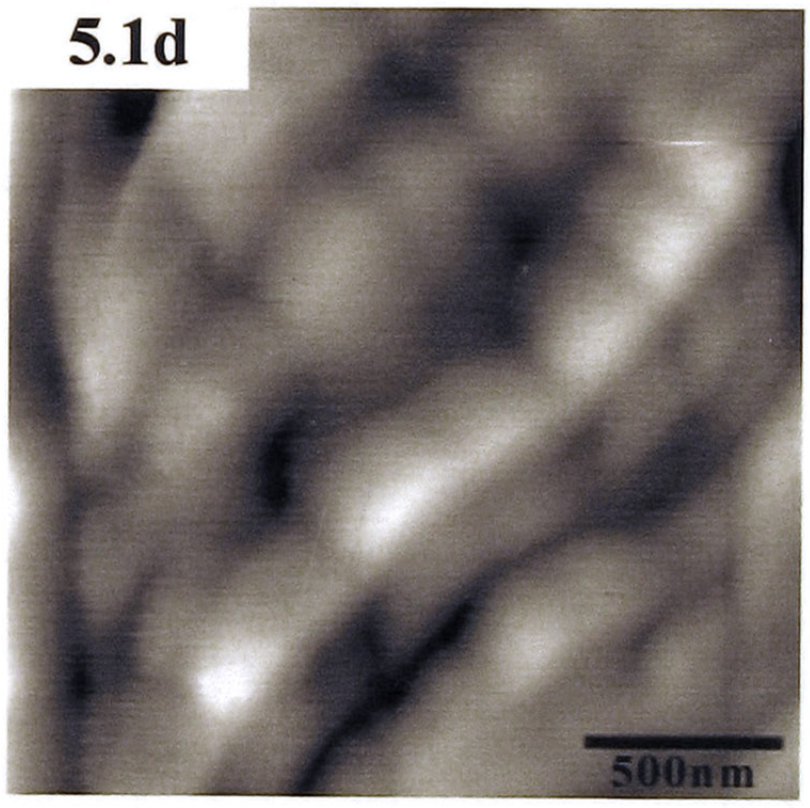
5.1d
500nm

Figure 5.2

Schematic representation of the arrangement of blocklets in starch granules, based on images obtained from AFM. The proposed arrangement of amylopectin side chain clusters within each blocklet is shown. Dashed lines indicate extension of the diagrammatic representation.

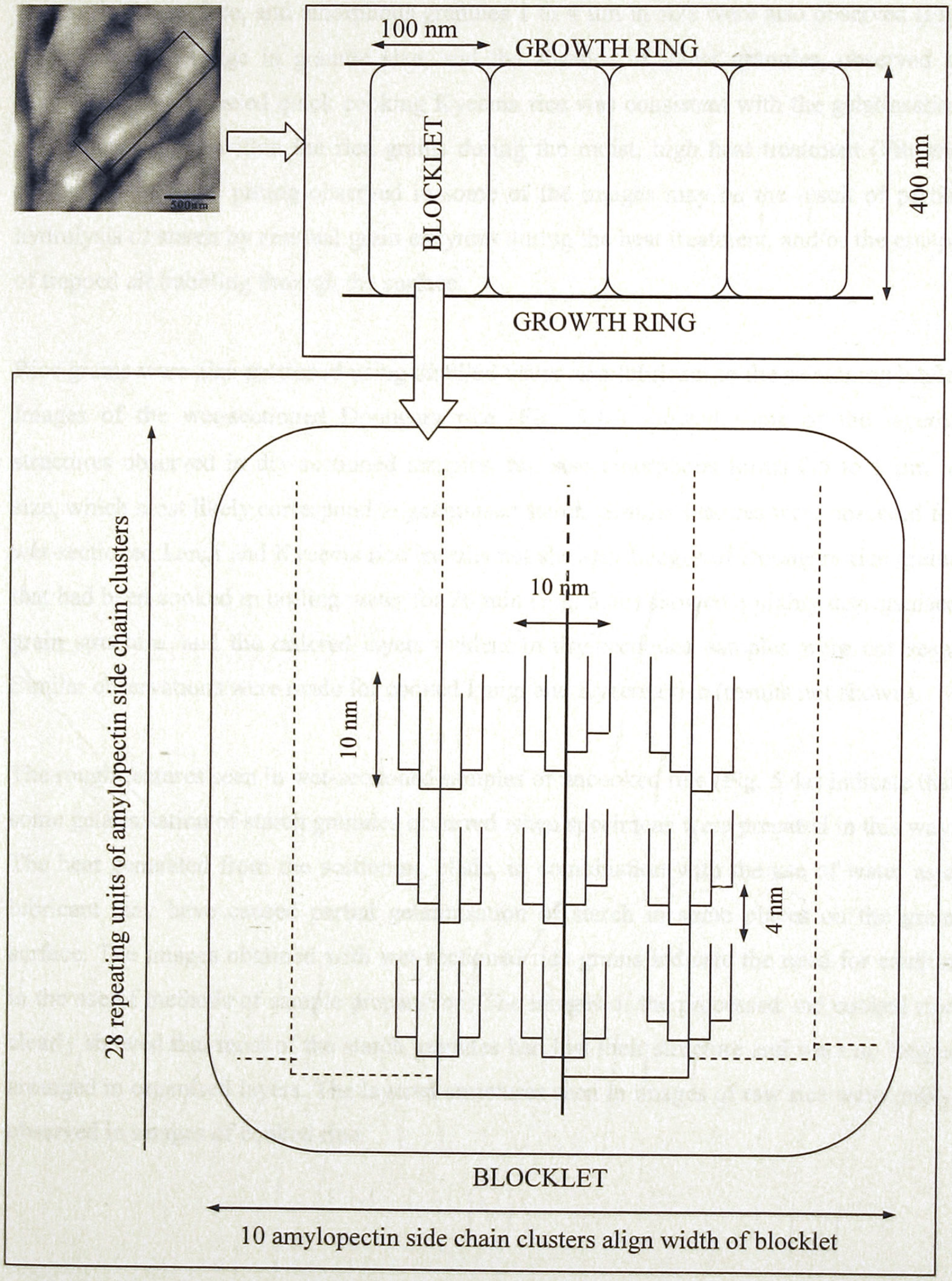

5.2.1.3 Effect of processing and sample preparation on grain and starch structure

Grains of the quick-cooking form of Kyeema, which have gone through a heating and drying process, had lost their granule structure and appeared amorphous (Fig. 5.3). The angular layered starch structures evident in the other rice samples represented by Fig. 5.1 were not seen. Many of the images showed numerous pores about 0.6 μm in diameter to be present in the surface, and amorphous granules 1 to 4 μm in size were also observed (Fig. 5.3). The large range in granule size, and the absence of intact granules, observed in images of the processed quick cooking Kyeema rice was consistent with the gelatinsation of starch granules within the rice grains during the moist, high heat treatment (Fitt and Snyder, 1984). The pitting observed in some of the images may be the result of partial hydrolysis of starch by residual grain enzymes during the heat treatment, and/or the escape of trapped air bubbling through the surface.

Rice grains were also sectioned using distilled water as a lubricant to the sectioning blade. Images of the wet-sectioned Doongara rice (Fig. 5.4a) showed some of the layered structures observed in dry-sectioned samples, but also amorphous forms 0.5 to 1 μm in size, which most likely correspond to gelatinised starch. Similar features were observed for wet-sectioned Langi and Kyeema rice (results not shown). Images of Doongara rice grains that had been cooked in boiling water for 20 min (Fig. 5.4b) showed a highly disorganised grain structure, and the ordered layers evident in dry-sectioned samples were not seen. Similar observations were made for cooked Langi and Kyeema rice (results not shown).

The rough features seen in wet-sectioned samples of uncooked rice (Fig. 5.4a) indicate that some gelatinisation of starch granules occurred when specimens were prepared in this way. The heat generated from the sectioning blade, in combination with the use of water as a lubricant may have caused partial gelatinisation of starch in some places on the grain surface. The images obtained with wet-sectioned rice grains indicate the need for caution in the use of methods of sample preparation. The images of the processed and cooked rice clearly showed that most of the starch granules had lost their structure and were no longer arranged in organised layers. The layered structures seen in images of raw rice were rarely observed in images of cooked rice.

The figure legends below correspond to figures in the following pages.

Figure 5.3

AFM image of dry-sectioned quick-cooking Kyeema rice. Pitting is indicated by black arrows, partially degraded starch granules by white arrows. The area scanned was 15 × 15 μm.

Figure 5.4

AFM images of wet-sectioned (a) and cooked (b) Doongara rice. Areas scanned in both were 10 × 10 μm. The layered structure is indicated by L; rough, gelatinised area by R.

5.3

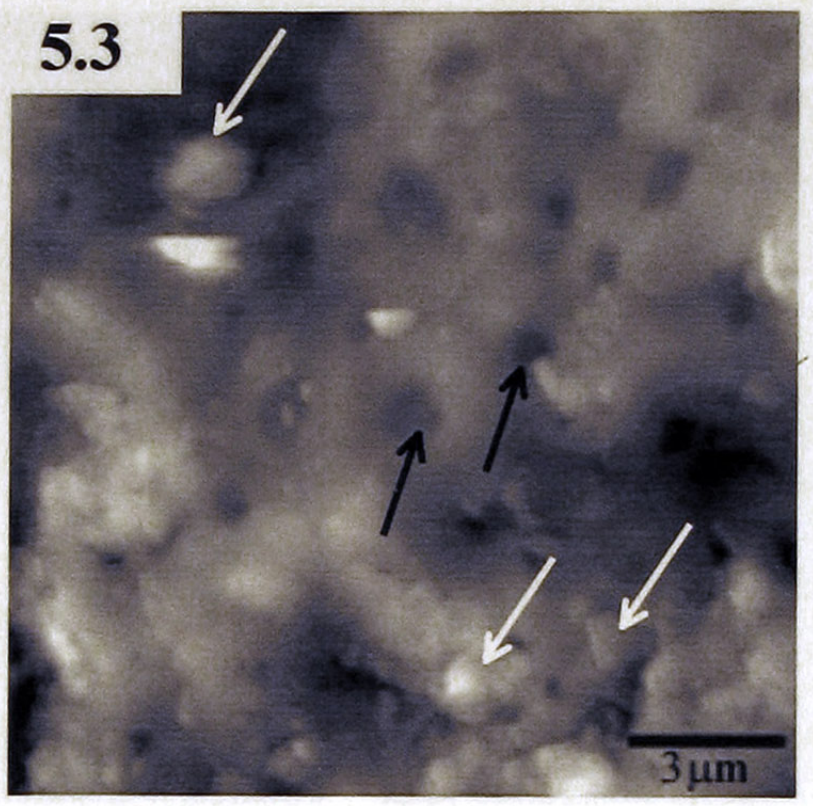

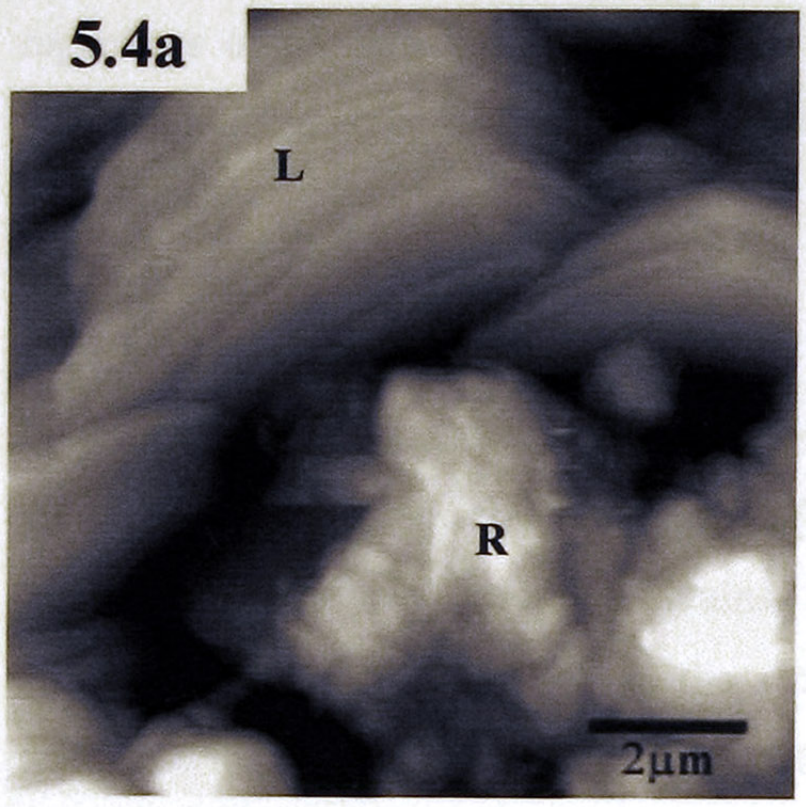
5.4a
L
R
2µm

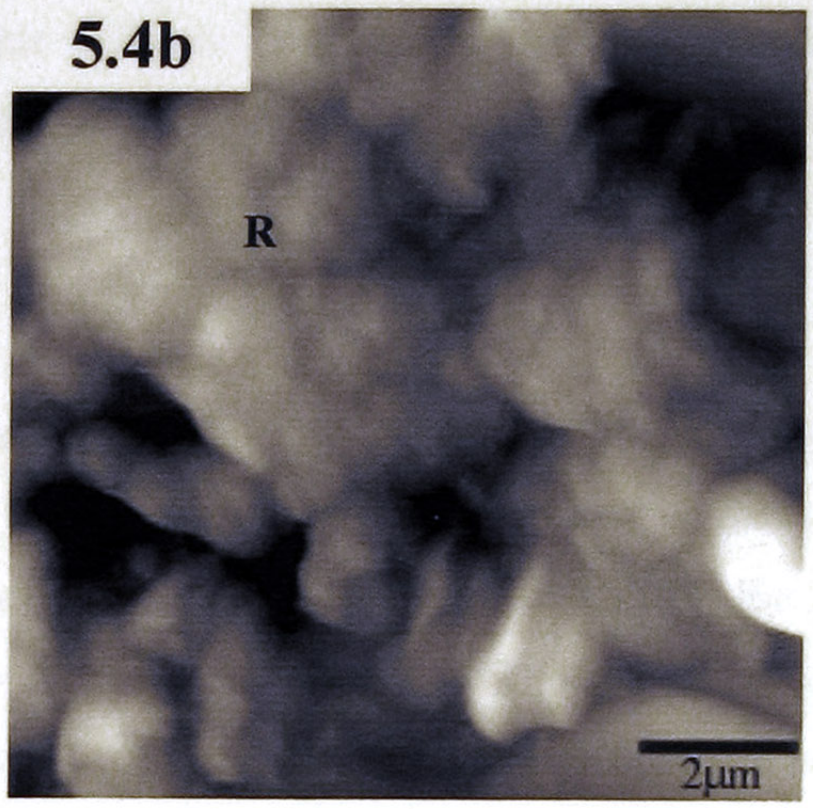
5.4b
R
2µm

5.2.1.4 Effect of growth season and location on grain and starch structure

For each genotype, the dry-sectioned samples showed similar morphological features, regardless of growth season or location. This indicates that, in this study, the growth season and location appeared to have no effect on the arrangement of starch within the rice grain.

5.2.1.5 Images and artefacts

In order to confirm that the striated structures were not an artefact caused by the action of the sectioning blade, different scan angles (at 0°, 45°, and 90° to the *x* direction) were used to image the surface of sectioned grains. For the chosen field of view scanned in the *x* direction, scans at 45° and 90° to the *x* direction did not show a shift in the observed features with the corresponding angles. This is a confirmation that features observed in images are real and not artefacts created by the cantilever. The images obtained from the various scanning angles confirmed that the striated structures were not artefacts.

There were concerns that the sectioning blade and frictional heat may have damaged the grain surface features. To overcome this, the rice grains were manually fractured along the natural fracture planes, and the fractured surface imaged without further preparation. Images obtained from rice grains prepared in this way showed similar features to those that were prepared by dry-sectioning.

The main drawback of imaging manually fractured rice grain surfaces was that reproducibility was poor. The cantilever on the AFM is only able to efficiently register changes in the *z* direction of less than 1 μm. As the manually fractured surface was rough, it was difficult to maintain good contact between the cantilever and sample surface without damaging the cantilever. Therefore, the images were unclear as a result of too much interference between sample and cantilever (Fig. 5.5a). Attempts at imaging manually fractured grain surfaces in non-contact mode produced images that were unclear, making measurements of dimensions difficult (Fig. 5.5b). From this study, the best images were obtained for polished rice grain surfaces that had been sectioned using a diamond saw, without lubricant.

Figure 5.5

Manually fractured unprocessed Doongara rice grain imaged in contact mode (a) and non-contact mode (b), without polishing. Areas scanned in both were 10 × 10 μm.

5.5a

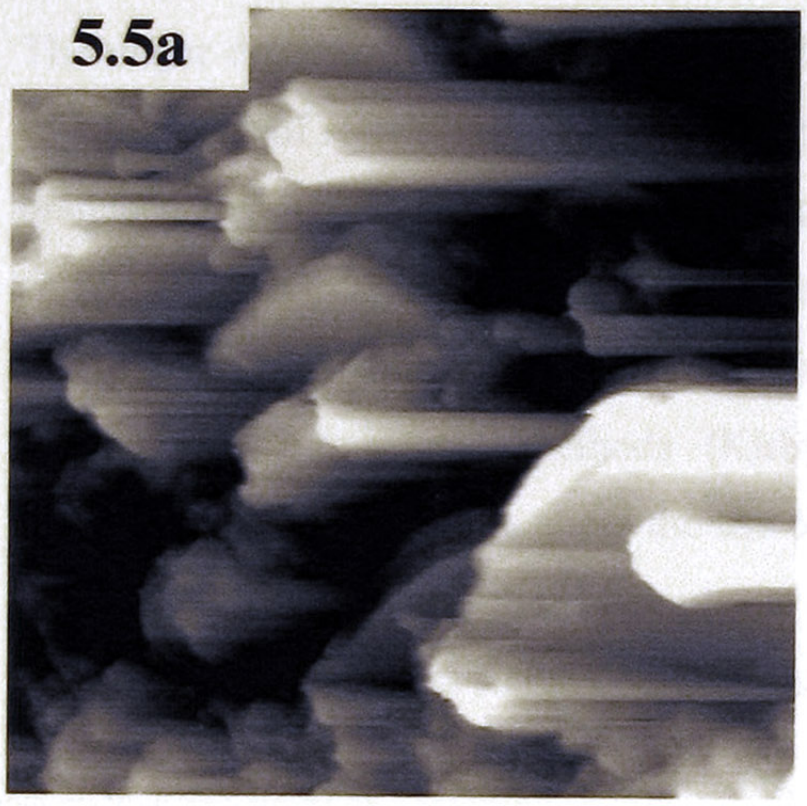

5.5b

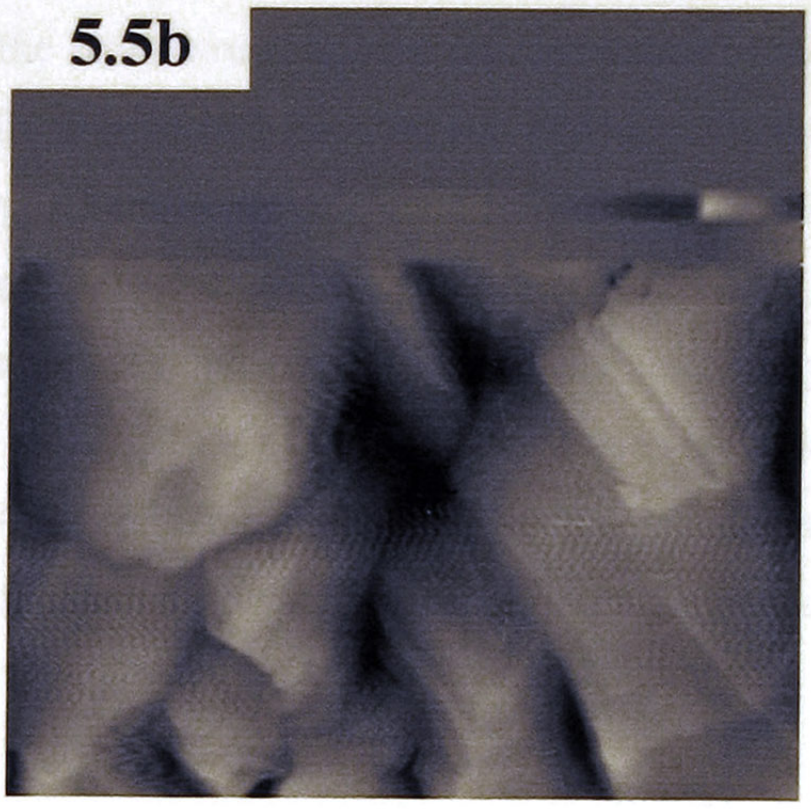

5.2.2 Starch and starch components

The functional properties of starch are influenced by its chemical and physical structures. The major determinants of functionality are the ratio, structure, and characteristics of the two fractions of starch: amylose, the essentially unbranched fraction, and amylopectin, the branched fraction. Chemical analyses of polysaccharides provide good information on the composition but do not provide a picture of the polysaccharide as a whole (Round *et al.*, 1997). Most polysaccharides have complex structures that are difficult to characterise by conventional biophysical methods (Kirby *et al.*, 1996). At present, there is little information in the literature about the use of AFM to image starch and starch components. This section describes the attempts to standardise a procedure for imaging and characterising starch and starch components.

5.2.2.1 Structure of standard amylose and amylopectin

Commercially available potato amylose and amylopectin (Sigma) were used to standardise sample preparation procedures. Potato amylose and amylopectin solutions were prepared and deposited on freshly cleaved mica as described in Section 2.11.3, except that the final concentration was 5 μg/mL. The samples were imaged using non-contact mode in air.

Non-contact atomic force microscope (NCAFM) images of amylose (Fig. 5.6) showed some overlapping of polymer chains, suggesting that the sample solution was too concentrated. Chain ends were difficult to observe where the structures overlapped, a problem similar to that experienced by McIntire and Brant (1997) in trying to image gellan solutions at increasing concentrations. By observing well separated structures in six images, measurements were made of the contour length, which is the length of the observed chain-like structures. From the measurements (n = 36), the contour length distribution and mean contour length of 504 nm for amylose were obtained (Fig. 5.7).

Tuber starches generally give the B-crystalline X-ray pattern. However, the V-pattern may appear after gelatinisation and complexation of amylose, and has also been reported to occur in native starches (Gallant *et al.*, 1997). In this study, the potato amylose and amylopectin fractions were heated to 90°C (Section 2.11.3), well over their gelatinisation temperatures. If it is assumed that the amylose observed in Fig. 5.6 had adopted the V-amylose structure, with six glucose residues per turn corresponding to a period of 2.1 nm

(French, 1984), the mean contour length of 504 nm (Fig. 5.7) for amylose would correspond to a DP of approximately 1440. This value is in reasonable agreement with values of approximately 1000 proposed by other researchers (Ball *et al.*, 1998; McIntire and Brant, 1999).

The width of the structures that were observed ranged from 120 nm to 135 nm. This suggests that the observed amylose chains occurred in aggregates, which may have resulted from retrogradation and desiccation of the crystalline amylose during sample preparation. Assuming the presence of amylose aggregates, and that the thickness of a single stranded amylose is 0.54 nm (McIntire and Brant, 1999), there would be approximately 220 to 250 chains of amylose per aggregate observed in the images.

As expected, amylopectin molecules were much larger than amylose molecules (Fig. 5.8). The images obtained were not of high enough quality to perform contour length measurements. The lack of clarity in the images made it difficult to observe the ends of chains. However, branching of the amylopectin can clearly be seen. A diagrammatic representation of the image observed in Fig. 5.8 is shown in Fig. 5.9. The external branches or A chains of most amylopectins have DPs between 3 and 50 (Yamaguchi *et al.*, 1979; French, 1984; Ball *et al.*, 1998). The branches seen in Fig. 5.8 (blue solid and dotted lines) had contour lengths well over 1 μm, which would correspond to a DP of greater than 1000. It would seem unlikely then that these branches represent A chains. It may be the case that the potato amylopectin had long branches of greater than 1000 glucose units.

The examination of potato amylose and amylopectin produced several images that were suitable for measurement of chain dimensions. The AFM therefore appeared to have promise as a means of studying the fine structure of starch. The structure of amylose and amylopectin that were extracted from rice samples were examined using the same method of sample preparation as for the potato standards.

Figure 5.6

NCAFM images of potato amylose that had been heated up in water (5 μg/mL) to 90 °C and cooled, placed on mica, and imaged in air. The image in (a) shows the arrangement of amylose chains. Image size: 5 μm x 5 μm. A magnification of the boxed area in (a) is shown in (b). Image size: 2 μm x 2 μm.

5.6a

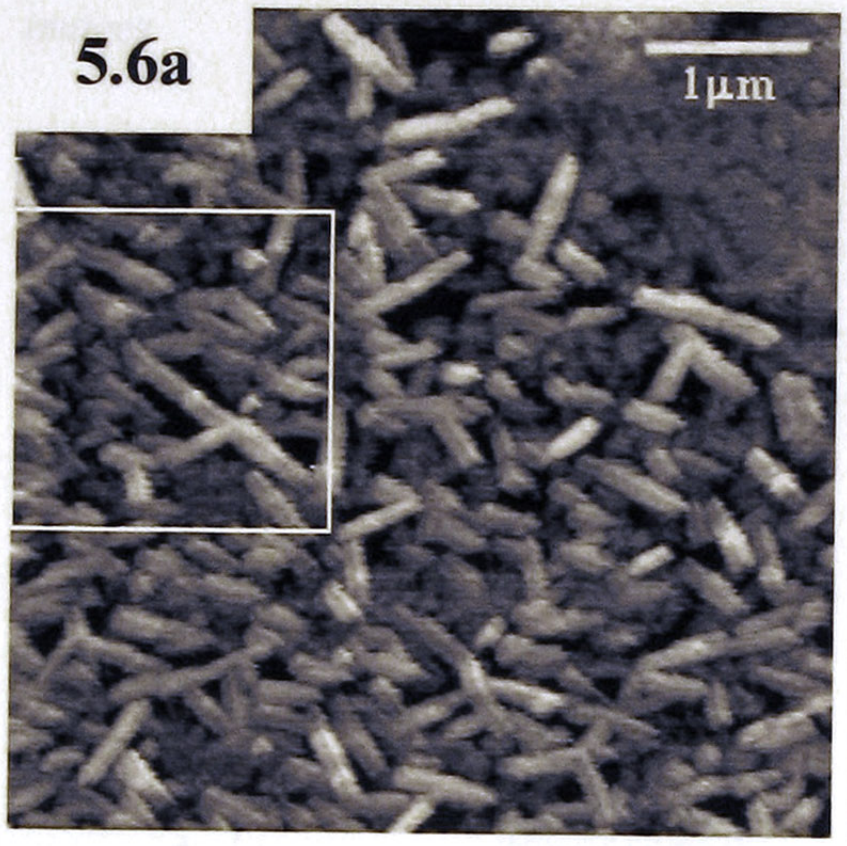

5.6b

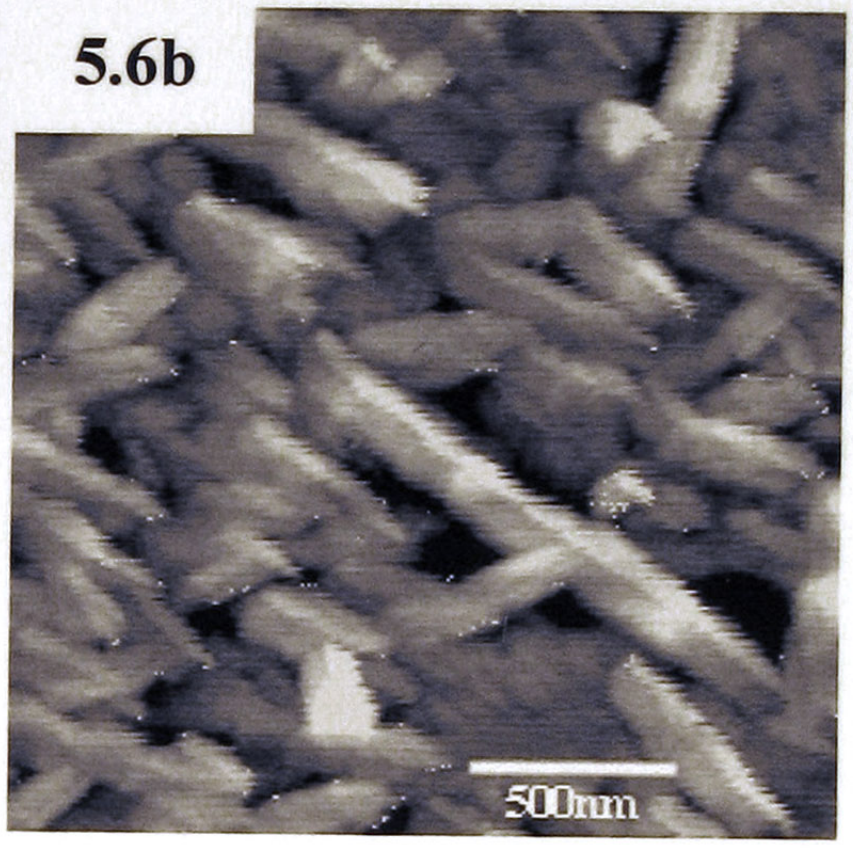

Figure 5.7

Contour length distribution for amylose molecules observed in Fig. 5.6 and other similar images.

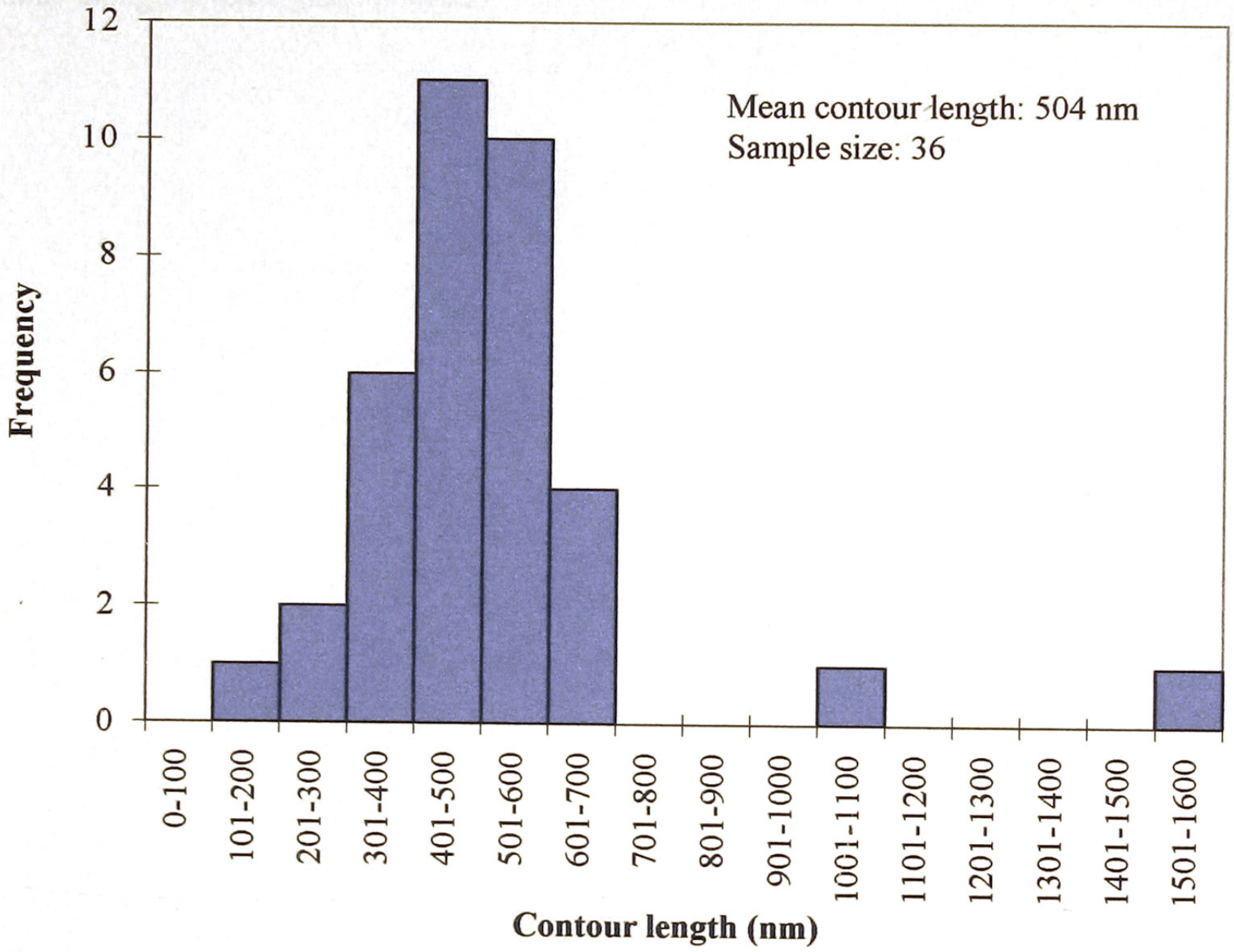

Figure 5.8

NCAFM image of potato amylopectin that had been heated in water (5 μg/mL) to 90 °C and cooled, placed on mica and imaged in air. Image size: 5 μm x 5 μm. The amylopectin molecules appear as white strands over the black background. Arrows point to branch points along the amylopectin chains.

5.8

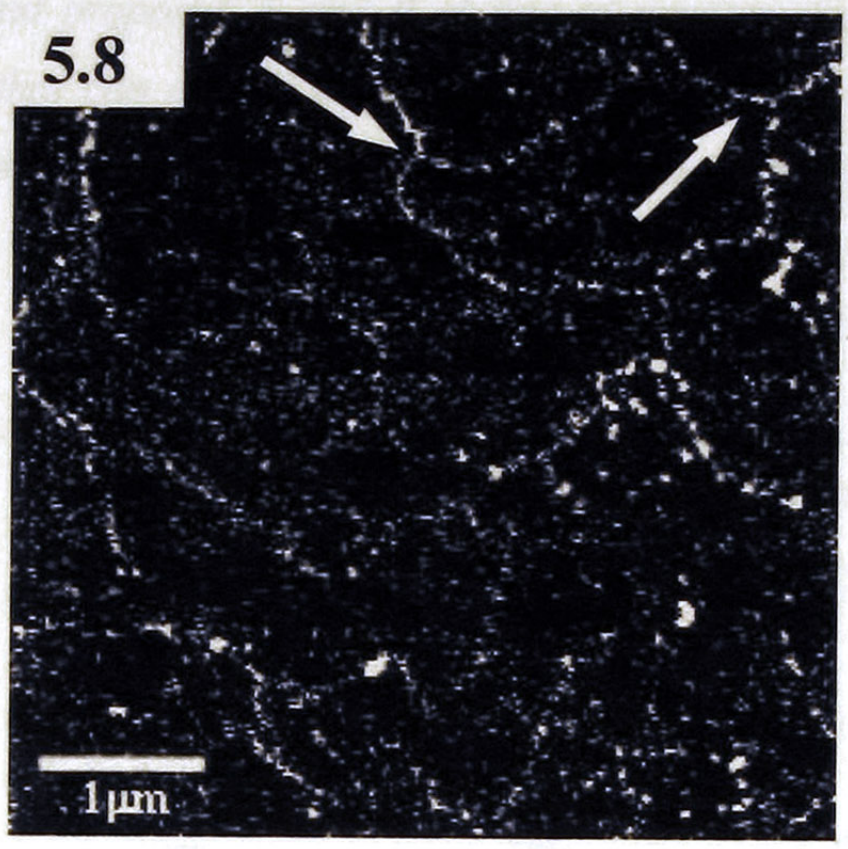

Figure 5.9

A diagrammatic representation of the image observed in Fig. 5.8, showing more clearly the branch points and proposed A and B chains of amylopectin. Solid lines represent amylopectin chains that can clearly be seen from Fig. 5.8, dotted lines represent those sections of the chains that are unclear from the image. Red solid lines are proposed to be either A or B chains.

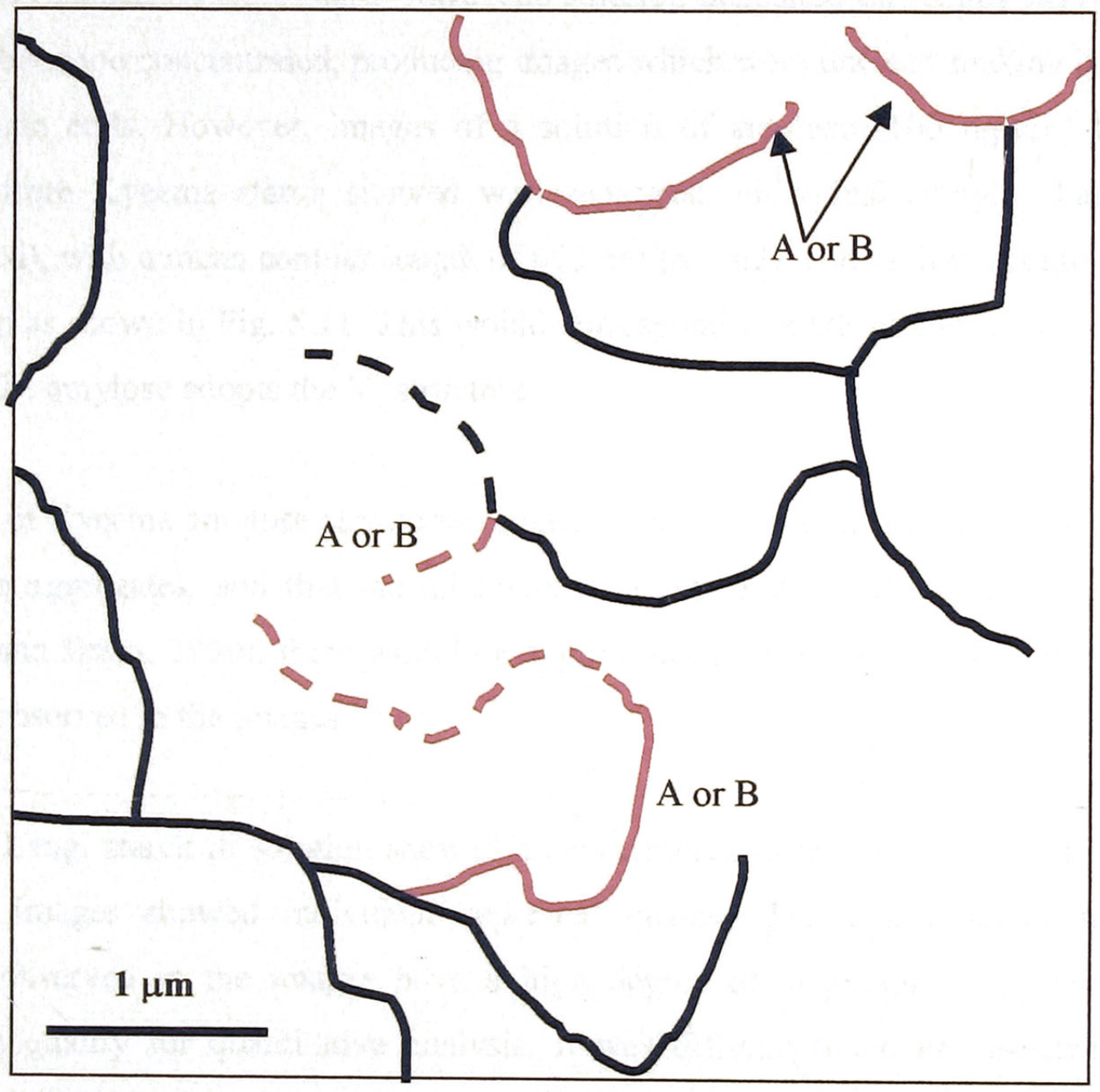

5.2.2.2 Structure of rice starch, amylose and amylopectin

Solutions of starch that were isolated from various rices were prepared for imaging using AFM, as described in Section 2.11.3. The concentration of the sample applied to freshly cleaved mica was reduced to 1 μg/mL to overcome problems of overloading, as experienced with potato amylose and amylopectin (Section 5.2.2.1).

Images of Kyeema starch in solution did not show individual strands where chain ends could clearly be seen (Fig. 5.10a, 5.10b). The solution deposited on freshly cleaved mica may have been too concentrated, producing images which were unclear, making it difficult to find chain ends. However, images of a solution of amylose (100 ng/mL) that was separated from Kyeema starch showed well separated, individual straight chains (Fig. 5.10c, 5.10d), with a mean contour length of 652 nm (n = 42), and giving a contour length distribution as shown in Fig. 5.11. This would correspond to a DP of approximately 1860, assuming the amylose adopts the V- structure.

The width of Kyeema amylose structures ranged from 6 to 19 nm. Assuming the presence of amylose aggregates, and that the thickness of a single stranded amylose is 0.54 nm (McIntire and Brant, 1999), there would be approximately 6 to 19 chains of amylose per aggregate observed in the images.

Images of Langi starch in solution showed a concentrated matrix of strands (Fig. 5.12a). Very few images showed individual separated chains. The measurements made on structures observed in the images have a high degree of uncertainty and were of an insufficient quality for quantitative analysis. It was difficult to obtain repeatable clear images, and to differentiate between amylose and amylopectin strands in Fig. 5.12a and similar images. However, images at higher magnification show mainly strands of straight chain molecules approximately 250 μm in thickness (Fig. 5.12b).

Amylose and amylopectin that were isolated from Langi starch were imaged in solution as described in Chapter 2. Images of Langi amylose showed mainly individual strands approximately 400 nm thick and having an average length of 1198 nm (Fig. 5.12c, 5.12d, 5.13). Assuming that the amylose in Langi starch adopts the V-structure, the mean contour length of 1198 nm for amylose would therefore correspond to a DP of approximately 3420. Similarly to the standard potato amylose, the average width of the chains in Langi starch

was very high at 400 nm. This may also be attributed to aggregation of the crystalline amylose structures as a result of dessication during sample preparation. Lowering the sample concentration to 100 ng/mL did not result in well-separated chains in images. There was no success in obtaining images of Langi amylopectin. Using kerosene instead of water as a dispersant did not improve the quality of chain separation.

The method used in imaging Langi and Kyeema starches was unsuccessful for imaging Doongara starch in solution. This may have been a result of the difference in amylose content between Doongara (highest in amylose content) and Langi/Kyeema.

5.3 Conclusions

The AFM shows promise as a tool for studying the structure of rice grains and starch as it allows the examination of grains and starch in their native form, without destructive chemical and physical modification. Growth rings were estimated to be about 400 nm apart, and blocklets of approximately 100 nm were observed to be aligned within the growth rings. From dimensions obtained in images, and by comparison with current models of the molecular organisation of amylopectin in starch granules, it is proposed that each blocklet contained approximately 280 amylopectin side chain clusters.

There are many issues in sample preparation that need to be explored further to standardise a method for imaging starch and its amylose and amylopectin components, such as sample preparation and concentration, and the dispersant used in imaging. However, several images obtained for amylose and amylopectin from both rice and potato clearly showed structural detail, and were of sufficient quality for quantitative analysis of chain dimensions. Aggregation of chain structures was observed for solutions of amylose extracted from potato, and Langi and Kyeema starch. With further exploration, the AFM appears promising as a means of studying the structure of starch and starch components in solution, which would provide useful information that will add to the understanding of starch and its behaviour during processing.

Figure 5.10

Structure of Kyeema starch and components in solution by AFM. (a) and (b) show NCAFM images at different magnifications of Kyeema starch that had been heated in water (1 μg/mL) to 90 °C and cooled, placed on mica and imaged in air. Image sizes are 2 μm x 2 μm for (a) and 1 μm x 1 μm for (b). Images in (c) and (d) show amylose (separated from Kyeema starch) that had been heated in water (100 ng/mL) to 90 °C and cooled. Both images are 2 x 2 μm. Arrows point to individual strands of amylose, having a mean contour length of 652 nm.

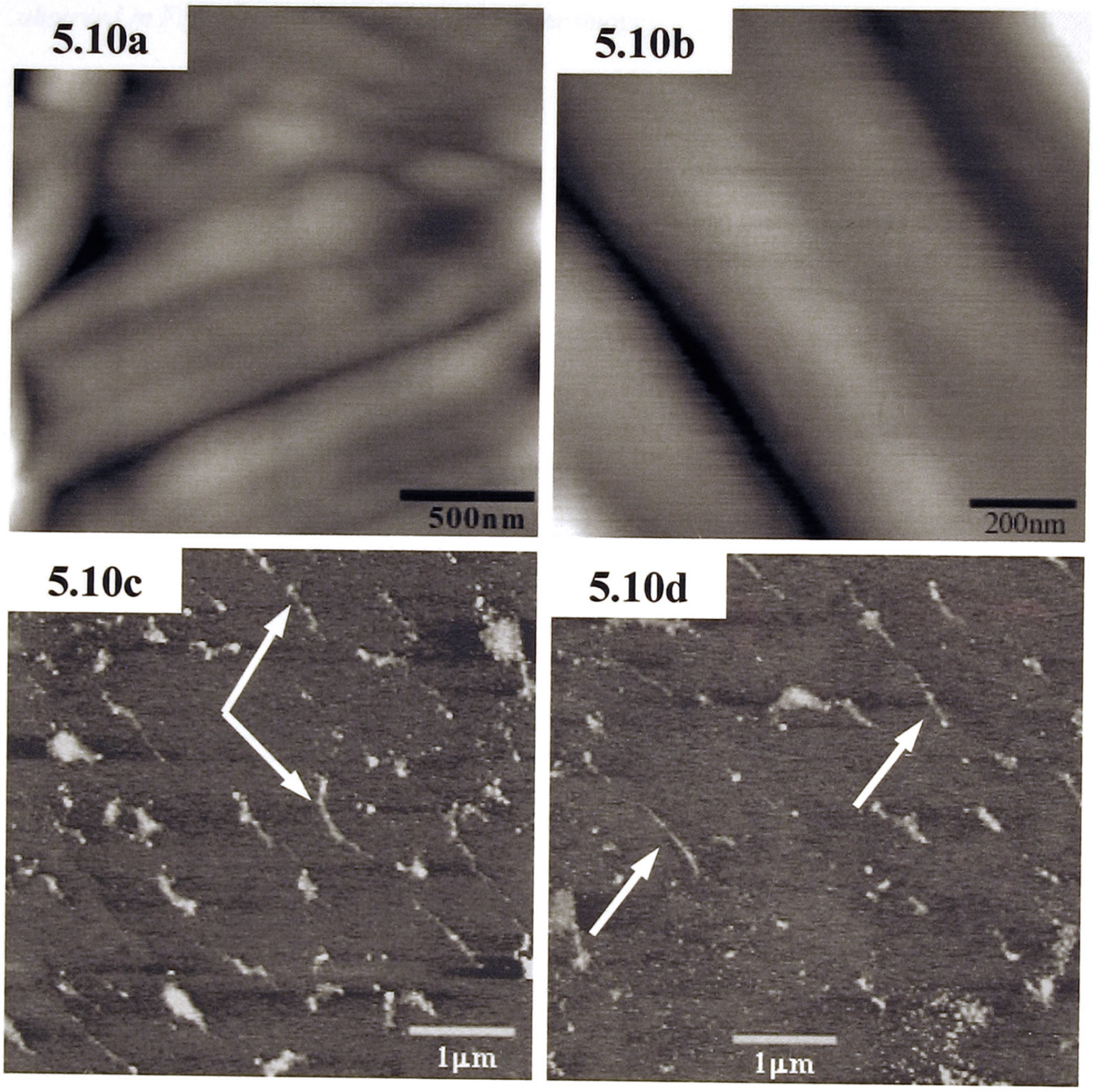
5.10a
500nm
5.10b
200nm
5.10c
1μm
5.10d
1μm

Figure 5.11

Contour length distribution of amylose molecules separated from Kyeema starch as observed in Fig. 5.10c, 5.10d and other similar images.

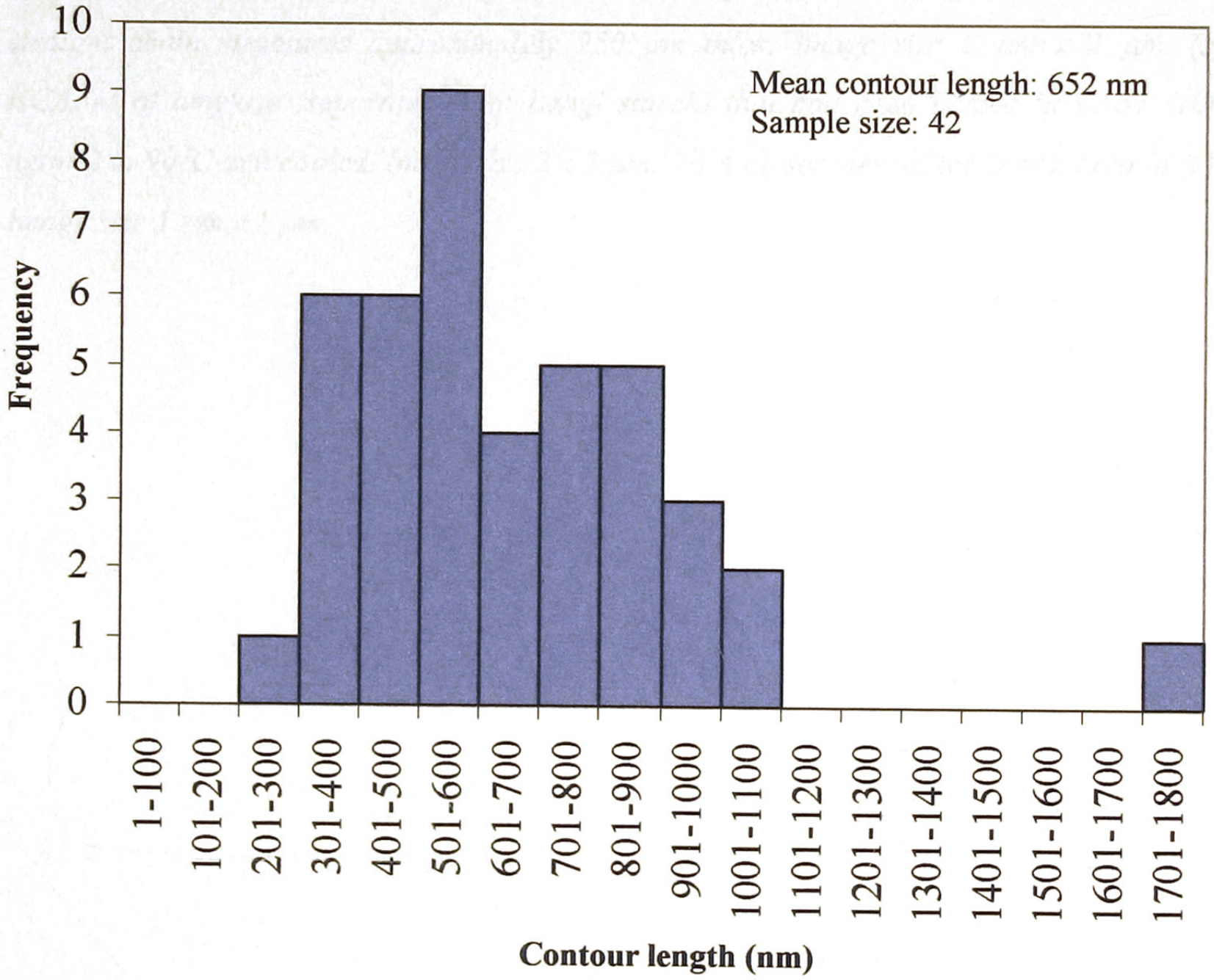

Figure 5.12

Structure of Langi starch and components in solution by AFM. (a) NCAFM image at of Langi starch that had been heated in water (1 μg/mL) to 90 ℃ and cooled, placed on mica, and imaged in air. Image size 5 μm x 5 μ.m. Arrows point to individual strands among a matrix of strands. (b) A higher magnification of Langi starch in solution, showing mainly straight chain structures approximately 250 μm thick. Image size 2 μm x 2 μm. (c) NCAFM of amylose (separated from Langi starch) that had been heated in water (100 ng/mL) to 90 ℃ and cooled. Image size 2 x 2 μm. (d) A closer view of the boxed area in (c). Image size 1 μm x 1 μm.

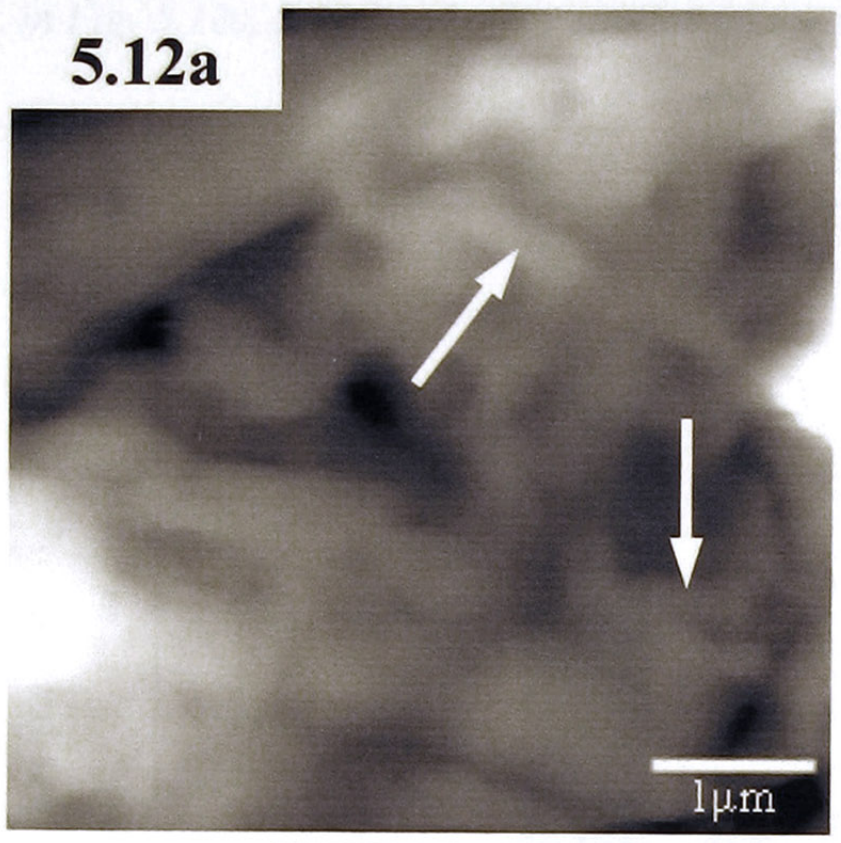
5.12a
1µm

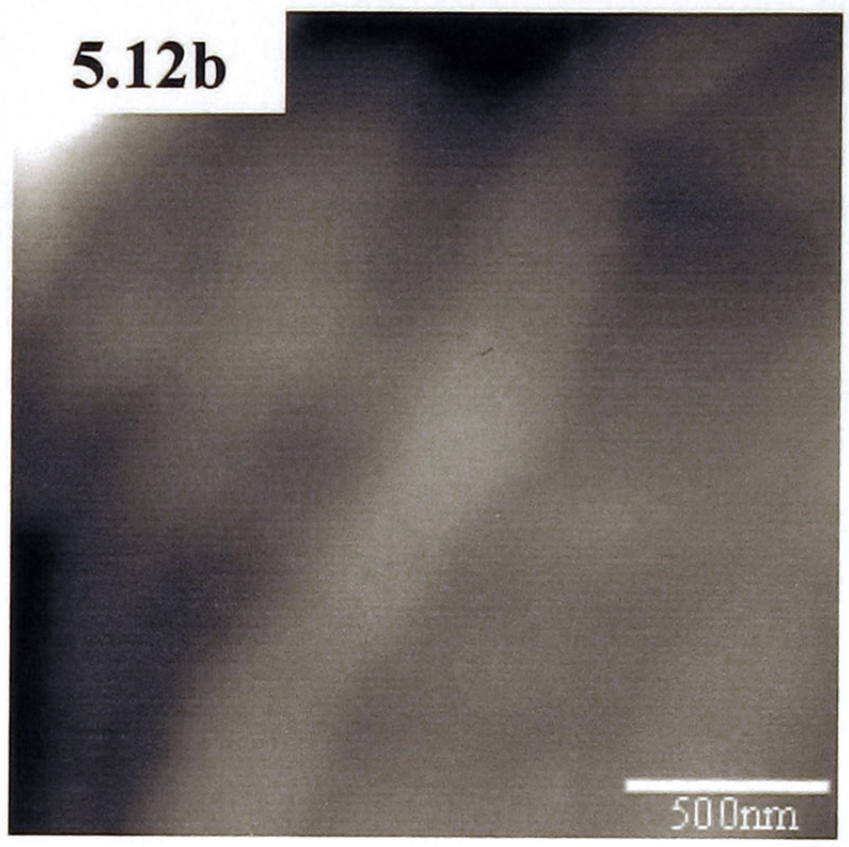
5.12b
500nm

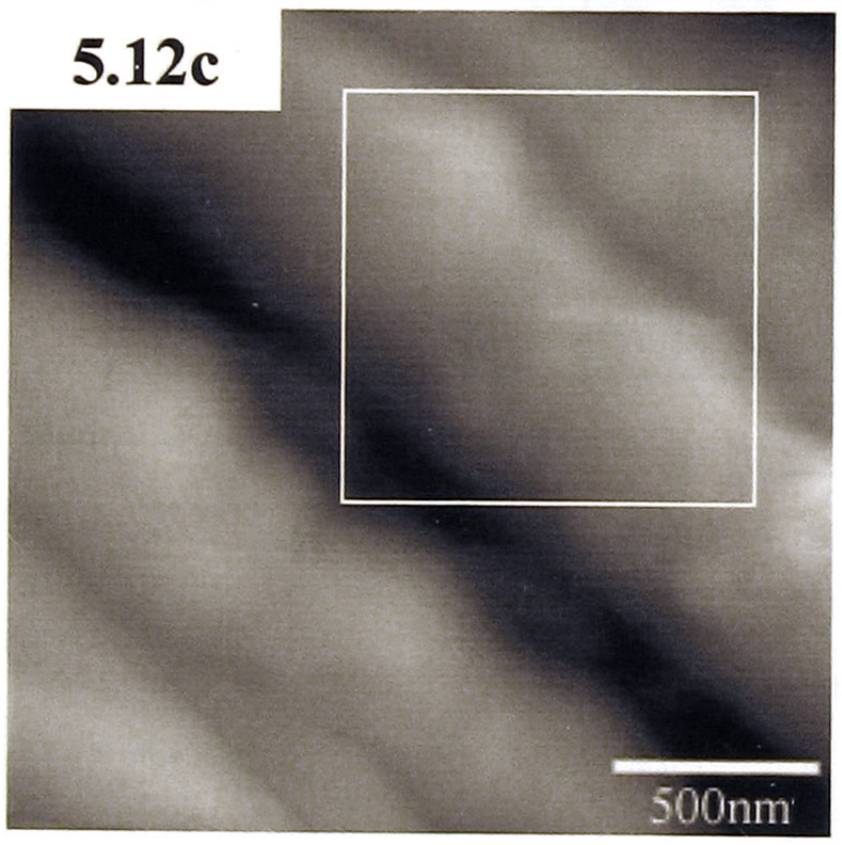
5.12c
500nm

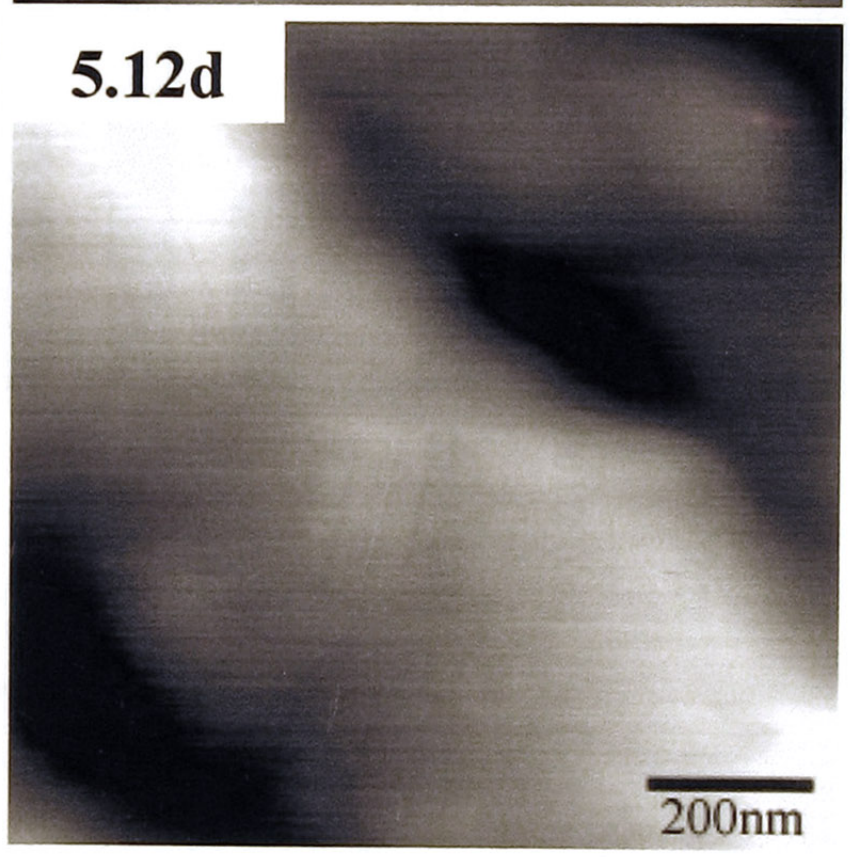
5.12d
200nm

Figure 5.13

Contour length distribution of amylose molecules separated from Langi starch as observed in Fig. 5.12c, 5.12d and other similar images.

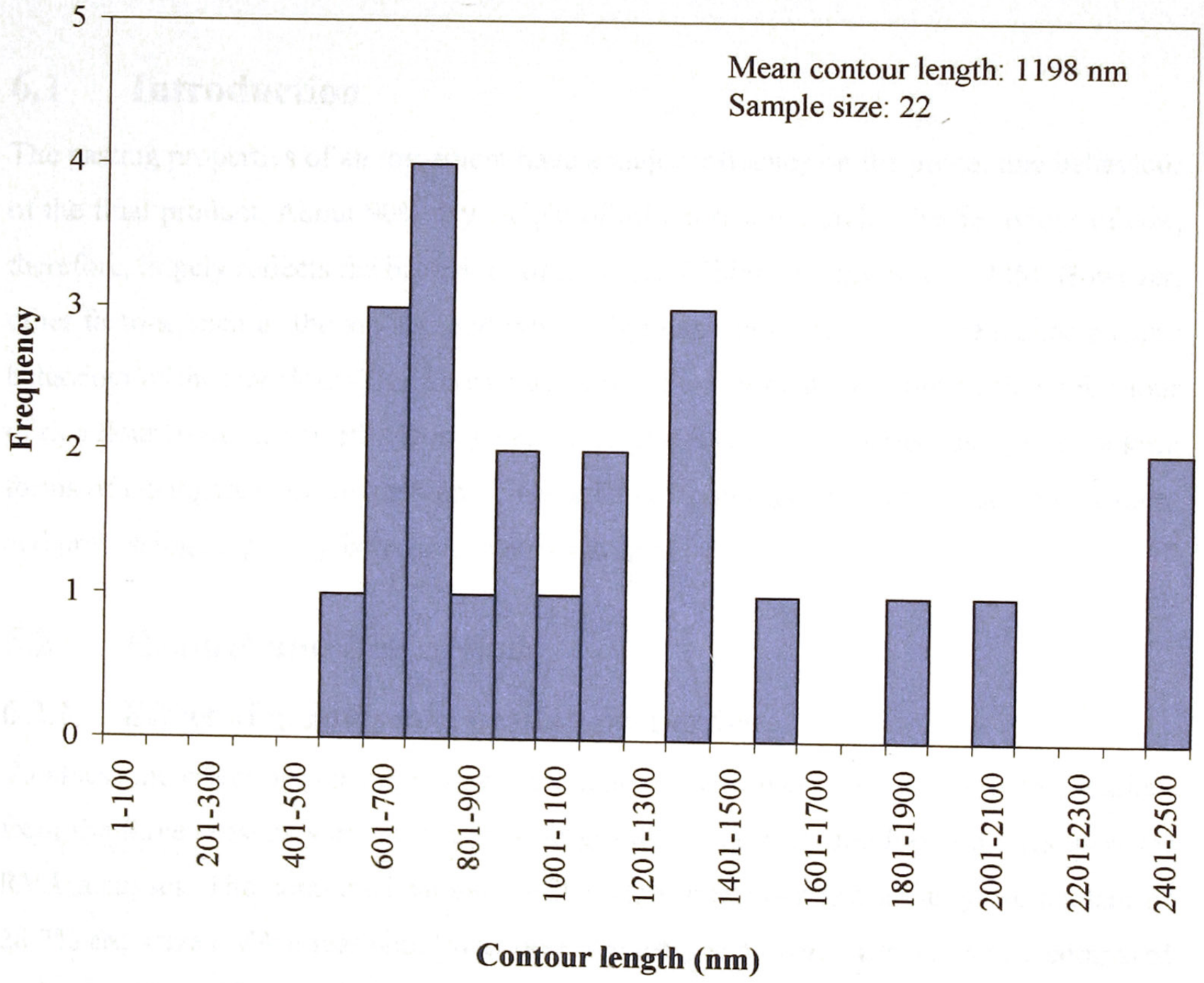

CHAPTER 6

Pasting properties of rice flours

6.1 Introduction

The pasting properties of an ingredient have a major influence on the processing behaviour of the final product. About 90% dry weight of milled rice is starch. The behaviour of rice, therefore, largely reflects the behaviour of its starch (Chinnaswamy *et al.*, 1985). However, other factors, such as the amount and type of lipid and protein, may influence the pasting behaviour of the rice flour. This chapter describes the examination of the pasting behaviour of rice flour from the varieties Doongara, Langi, and Kyeema. Parboiled and quick cooking forms of Doongara were also assessed. The effect of genotype, growth season and location, and processing on pasting behaviour were examined.

6.2 Results and discussion

6.2.1 Effect of genotype on pasting properties

To assess the effect of genotype more thoroughly, subsamples of grains from each variety from the three seasons were mixed prior to grinding, and the combined samples used for RVA analyses. The combined sample of Doongara rice flour had an amylose content of 28.7% and gave RVA traces with lower peak viscosity and higher setback values compared to the combined flour samples of Langi and Kyeema, which had amylose content of 18.7% and 19.3%, respectively. For the combined samples, all RVA parameters for Doongara rice were significantly different from those of Langi and Kyeema, which differed only in peak viscosity and breakdown value (Table 6.1, Fig. 6.1).

Table 6.1

Effect of genotype on amylose content and RVA parameters of rice flour samples.

Sample	AM	Peak	Trough	Breakdown	Final	Setback	PT
Doongara	28.7 ± 0.3a	2720c	1448f	1397h	3280k	1858n	78.3q
Langi	18.7 ± 0.2b	3259d	1701g	1595i	3390m	1688p	82.9r
Kyeema	19.3 ± 0.2b	3543e	1798g	1768j	3460m	1655p	82.4r

Subsamples from all three seasons were mixed to obtain a combined sample. All values are the average of duplicate samples. Viscosities are in centiPoise (cP), pasting temperature (PT) is in °C, and amylose (AM) content is a percentage (%) of total starch. Each RVA parameter was compared between the varieties, by analysis of variance. Within each column, different letters after values indicate significant difference. Doongara differed from Langi and Kyeema in all of the parameters, whereas the values for Langi and Kyeema differed from each other only in peak viscosity and breakdown ($p < 0.01$).

Figure 6.1

Effect of genotype on RVA pasting curves of rice flours.

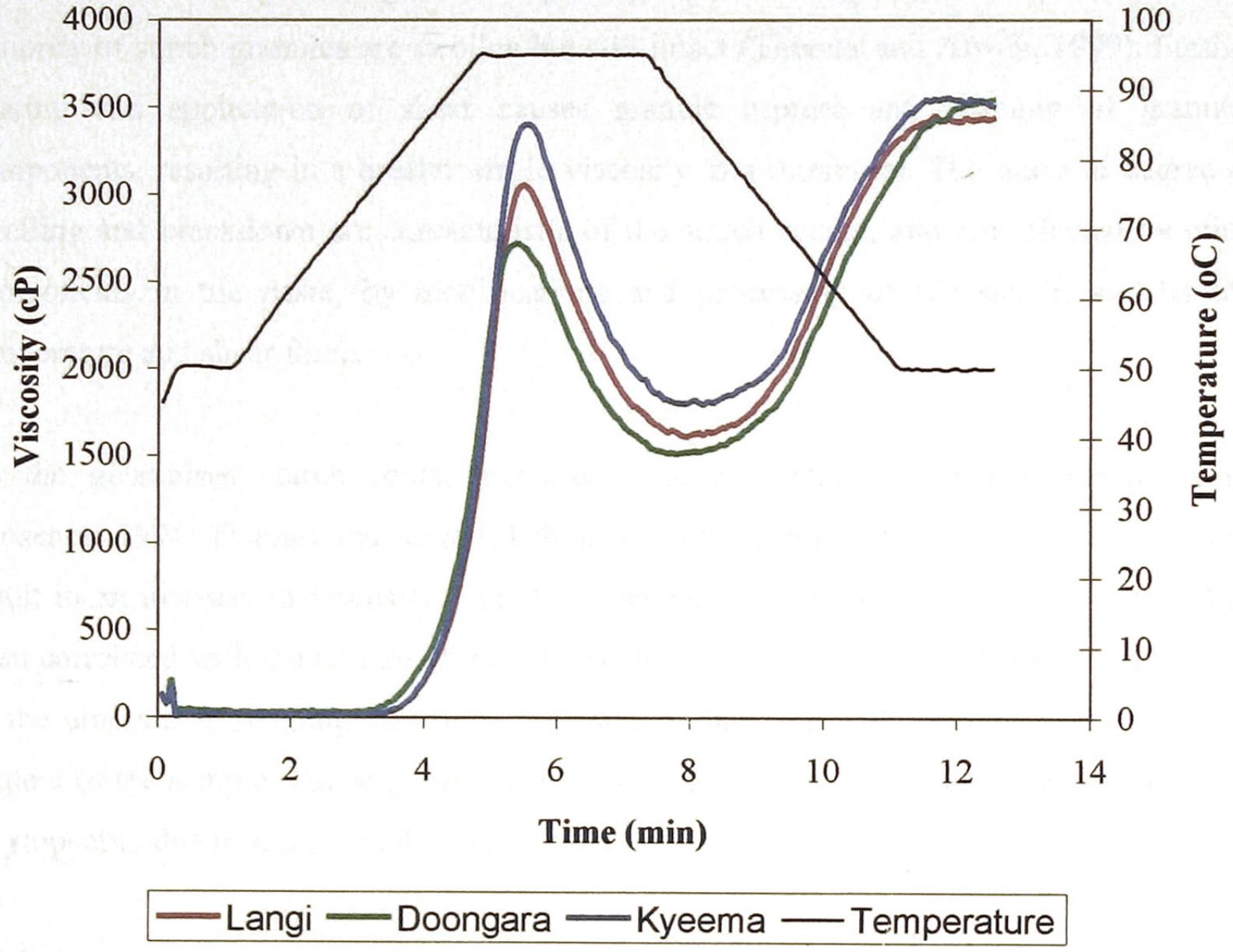

As an aqueous dispersion of starch is heated, the starch granules absorb water and swell, resulting in an increase in viscosity. Glucan polymers with lower molecular weight, particularly amylose molecules, begin to leach from the granules. The viscosity of the paste increases to a peak (Fig. 1.7, Chapter 1), which corresponds to the point when the majority of starch granules are swollen but still intact (Thomas and Atwell, 1999). Further heating and application of shear causes granule rupture and leaching of granular components, resulting in a breakdown in viscosity to a minimum. The rate and degree of swelling and breakdown are characteristic of the starch source, and are affected by other components in the paste, by modifications and processing of the starch, and by the temperature and shear force.

As the gelatinised starch cools, increased hydrogen bonding between starch chains (Hoseney, 1994; Thomas and Atwell, 1999), and some reassociation of leached molecules, result in an increase in viscosity (Fig. 1.7, Chapter 1). This setback from the trough has been correlated with the texture of various end products. High setback is also an indication of the amount of swelling power of the sample, and is usually related to the amylose content of the sample. The amylose component of the starch retrogrades more readily than amylopectin, due to its essentially linear structure.

Of the flours used in this study, Doongara had the highest amylose content, and its RVA trace showed a lower peak viscosity and a lower pasting temperature compared to Langi and Kyeema (Table 6.1). Starch from Doongara, which had a higher amylose content, as expected had a higher setback value than the lower amylose starches of Langi and Kyeema. The pasting temperature and setback were not significantly different for Langi and Kyeema, which have similar amylose content (Table 6.1). Shinde *et al.* (2003), in studying the pasting properties of flour from two wheat cultivars, also found that final viscosity was higher for the flour with higher apparent amylose content

6.2.2 Effect of growth season on pasting properties

Rice samples were obtained from three seasons, 1998/1999, 1999/2000, and 2000/2001, which differed in temperature and yield characteristics (Table 3.2, Chapter 3). Significant differences were observed in the amylose content of Langi and Doongara between all three seasons, whereas for Kyeema, the amylose content in the 2000/2001 season was

significantly lower than in the other two seasons (Table 6.2). The amylose content for all three varieties was highest in the 1999/2000 season (Table 6.2), which was the coolest of the three seasons (Table 3.2, Chapter 3). The RVA traces of Langi, Doongara and Kyeema flours from the different seasons showed the 1999/2000 season samples to have lowest peak viscosities and highest final viscosities and setback values (Table 6.2, Fig. 6.2).

Doongara and Langi rice grown in the cooler 1999/2000 season had significantly higher amylose content than rice grown in the warmer seasons (Table 6.2). The lower peak viscosities (except for Doongara) and higher setback values observed in the RVA traces of the respective samples from the 1999/2000 season indicates the high sensitivity of the pasting properties to subtle changes in the composition of the flour (Table 6.2, Fig. 6.2).

6.2.3 Effect of growth location on pasting properties

Samples of rice were obtained for each of the three varieties grown in the 1998/1999 season in different locations, all of which were in the same climatic region. There were no significant differences between total starch, amylose, protein, and lipid contents for the same variety from different growth locations (Table 6.3). However, pasting curves and RVA parameters were significantly different for the same variety from different regions (Fig. 6.3, Table 6.3).

The peak viscosity and setback values were significantly different for flour of Doongara and Kyeema rice grown in the MIA compared with CIA (Table 6.3). For Langi, flour obtained from rice grown in the MV differed from rice from the MIA and CIA with respect to these properties. The amylose content was not affected by the growth location, indicating that the differences in peak viscosity and setback values were related to other factors. Properties such as total starch, protein and lipid content, and size of starch granules, are unlikely to have caused the differences in RVA traces as these did not vary between growth locations (Table 6.3). Nor were differences in moisture content of samples from the various locations responsible for differences in viscosity values, as the sample and water weights were carefully adjusted to take account of sample moisture content. The difference in viscosities may be a result of differences in fine structure of amylose and/or amylopectin in the samples. Klucinec and Thompson (2002b) found that the development of a starch gel is affected by both the nature of amylopectin and the amylose-amylopectin

ratio of the gel. Localised abiotic and/or biotic factors at the three growth locations may have induced subtle but significant differences in the fine structure of amylose and amylopectin, which affected their water absorbing capacity, and in turn, the viscoelastic properties of starch pastes. Such factors could influence the activity of some of the multitude of enzymes that act in concert in the biosynthesis of starch molecules.

The activities of enzymes of starch synthesis in rice grains are sensitive to temperature during the early stages of grain filling, which can influence the structure of the starch, and in turn, the cooking quality of the rice (Martin and Smith, 1995; Inouchi *et al.*, 2000; Lisle *et al.*, 2000). Amylopectin from rice plants grown at 25°C had increased amounts of short chains and decreased amounts of long chains, compared with amylopectin from plants grown at 30°C, and it was concluded that the temperature between five and ten days after pollination strongly influenced the structural characteristics of endosperm starch of rice plants (Inouchi *et al.*, 2000). Two Australian rice varieties – Amaroo and Illabong – grown at two different day and night temperatures (38/21°C and 26/15°C for day/night) had different pasting profiles on the RVA (Lisle *et al.*, 2000). For both varieties, flour from grains grown at the higher temperatures had significantly larger peak and final viscosities than for the cooler conditions. The availability of nitrogen during plant growth also influences pasting behaviour of rice starch. Fitzgerald *et al.* (2003) found that the setback, and peak and final viscosities decreased as the amount of nitrogen applied during plant growth was increased. Nitrogen nutrition did not affect the amylose content or the amylopectin structure of the rice, but it did affect the viscosity of the flour.

The results suggest that the environment affected the fine structure of amylose and/or amylopectin, which was not identified by chemical analysis of major constituents. Analysing starch, protein, and lipid may be a good means of predicting behaviour. However, subtle differences may not be observed by chemical and microscopic analyses, and may require actual pasting analyses to confirm the behaviour of the rice and starch in food systems.

Table 6.2

Effect of growth season on amylose content and RVA parameters of rice flour samples.

Sample	Season	AM	Peak	Trough	Breakdown	Final	Setback	PT
Doongara	1998/1999	28.1 ± 0.3a	2681d	1418g	1264j	3055m	1638p	79.9s
	1999/2000	29.2 ± 0.4b	2740e	1514h	1226j	3562n	2049q	79.9s
	2000/2001	27.3 ± 0.4c	2870f	1349i	1521k	3167m	1818r	77.9t
Langi	1998/1999	18.5 ± 0.4a	3241d	1720g	1521i	3366m	1646q	83.1s
	1999/2000	19.1 ± 0.7b	3068e	1616h	1453j	3445n	1829r	83.0s
	2000/2001	17.2 ± 0.6c	3429f	1724g	1705k	3264p	1539q	83.1s
Kyeema	1998/1999	19.2 ± 0.4a	3493c	1834e	1659f	3486h	1652k	82.9p
	1999/2000	19.4 ± 0.5a	3406c	1779e	1627f	3517i	1738m	82.6p
	2000/2001	18.1 ± 0.2b	3675d	1752e	1923g	3335j	1583n	82.2p

All values are the average of duplicate samples. Viscosities are in centiPoise (cP), pasting temperature (PT) is in °C, and amylose (AM) content is a percentage (%) of total starch. RVA parameters were compared only within each variety for the three different seasons. For each variety and within each column, different letters after values indicate significant difference between the seasons, as determined by Analysis of Variance.

Figure 6.2

Effect of growth season on RVA pasting curves of Langi (a), Doongara (b), and Kyeema (c) rice flours. Samples from the 1998/1999 season are represented by green curves, 1999/2000 season by red curves, and 2000/2001 season by blue curves.

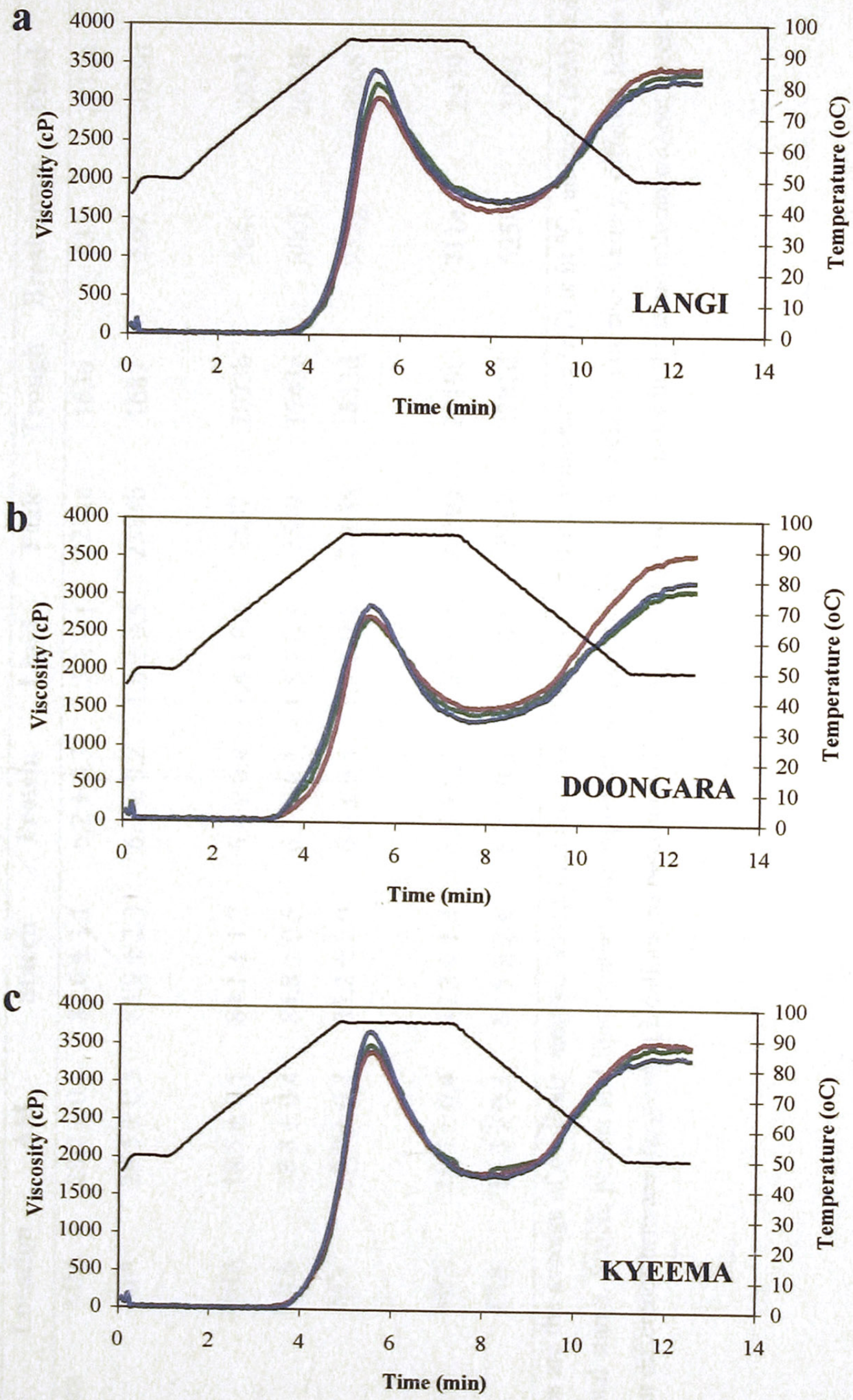

Table 6.3

Effect of growth location on chemical and pasting properties of rice flour samples.

Sample	Location	AM	Starch	Protein	Lipid	Peak	Trough	Breakdown	Final	Setback	PT
Doongara	MIA	28.2 ± 0.4	82.6 ± 1.1	6.2 ± 0.3	1.5 ± 0.1	2271a	1636	635	2812c	1176e	77.4
	CIA	28.5 ± 0.5	83.9 ± 2.3	6.1 ± 0.2	1.6 ± 0.5	2384b	1687	697	3025d	1338f	76.8
Langi	MIA	18.5 ± 0.1	84.1 ± 1.7	6.4 ± 0.4	1.4 ± 0.1	2587	2023b	564e	2927	904	77.5
	CIA	18.3 ± 0.4	84.8 ± 0.5	6.3 ± 0.1	1.5 ± 0.4	2549	1743c	806f	2674h	931	77.5
	MV	18.0 ± 0.2	85.2 ± 2.9	6.4 ± 0.4	1.3 ± 0.1	2765a	1833d	932g	2868	1035i	78.2j
Kyeema	MIA	19.3 ± 0.4	85.2 ± 1.3	6.6 ± 0.4	1.6 ± 0.4	2730a	2019c	711e	2979	960g	78.3j
	CIA	19.5 ± 0.3	86.5 ± 2.4	6.7 ± 0.3	1.5 ± 0.1	2806b	2281d	525f	3048	767h	78.9j

All values are the average of duplicate samples. Viscosities are in centiPoise (cP), pasting temperature (PT) is in °C, amylose (AM) content is a percentage (%) of total starch. Starch, protein and lipid contents are expressed as a percentage (%) dry weight. For each variety, different letters after values indicate significant difference between the growing locations, as determined by Analysis of Variance. Values in the same column without letters were not significantly different.

Figure 6.3

Effect of growth location on RVA pasting curves of Langi (a), Doongara (b), and Kyeema (c) rice flours. Samples from MIA are represented by blue curves, CIA by red curves, and MV by green curves.

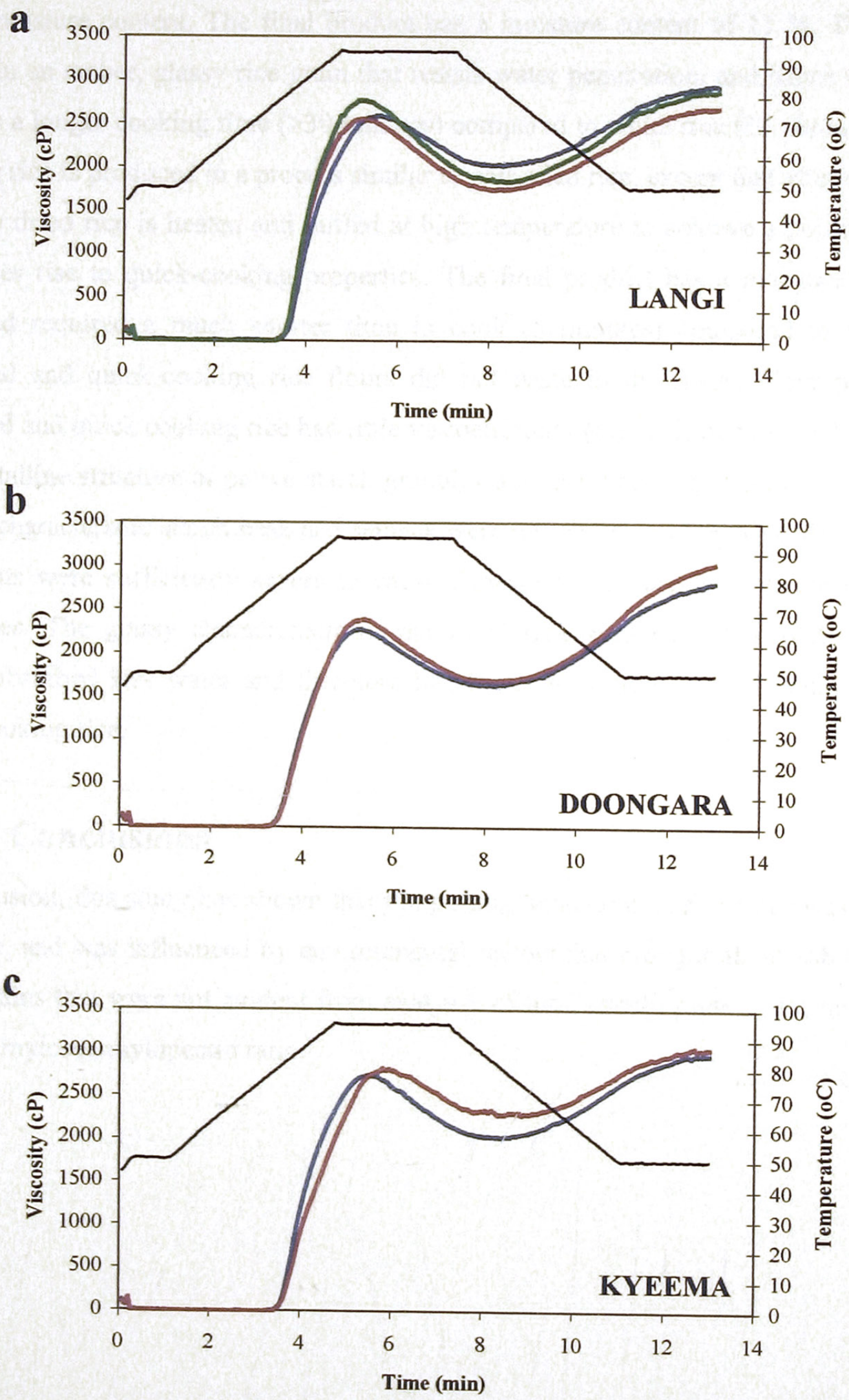

6.2.4 Effect of processing

The parboiled rice used in this study was a commercial product that had been prepared by steeping and draining brown Doongara rice. The drained grains are steamed to gelatinise the starch, and the cooked grains are partially dried, milled and then dried further to a lower moisture content. The final product has a moisture content of 11 %. This process results in an amber, glassy rice grain that resists water penetration, and hence the product requires a longer cooking time (>30 minutes) compared to white rice (20 minutes). Quick-cooking rice is produced in a process similar to parboiled rice, except that after milling, the partially dried rice is heated and puffed at high temperature to achieve a porous structure that gives rise to quick-cooking properties. The final product has a moisture content of 10% and required a much shorter time to cook (5 minutes) compared to white rice. Parboiled and quick-cooking rice flours did not paste in the RVA. Flour pastes from parboiled and quick cooking rice had little viscoelasticity (Fig. 6.4) due to the disruption of the crystalline structure of native starch granules during processing. Viscosities were low, and the characteristic starch peak and setback were not observed (Fig. 6.4). The preprocess treatments were sufficiently severe to cause damage to the starch, lowering the overall viscosities. The glassy characteristic of parboiled Doongara rice, due to its crystalline nature, absorbed less water and therefore had lower viscosities overall compared to the quick-cooking rice.

6.3 Conclusions

In conclusion, this study has shown that the pasting behaviour of rice flour was related to genotype, and was influenced by environmental factors that brought about subtle changes in the grains that were not evident from analyses of total starch, protein and lipid content and the amylose:amylopectin ratio.

Figure 6.4

Effect of processing on RVA pasting curves of Doongara rice flour. The unprocessed Doongara rice is represented by the green curve, quick-cooking Doongara rice by the blue curve, and parboiled Doongara rice by the red curve.

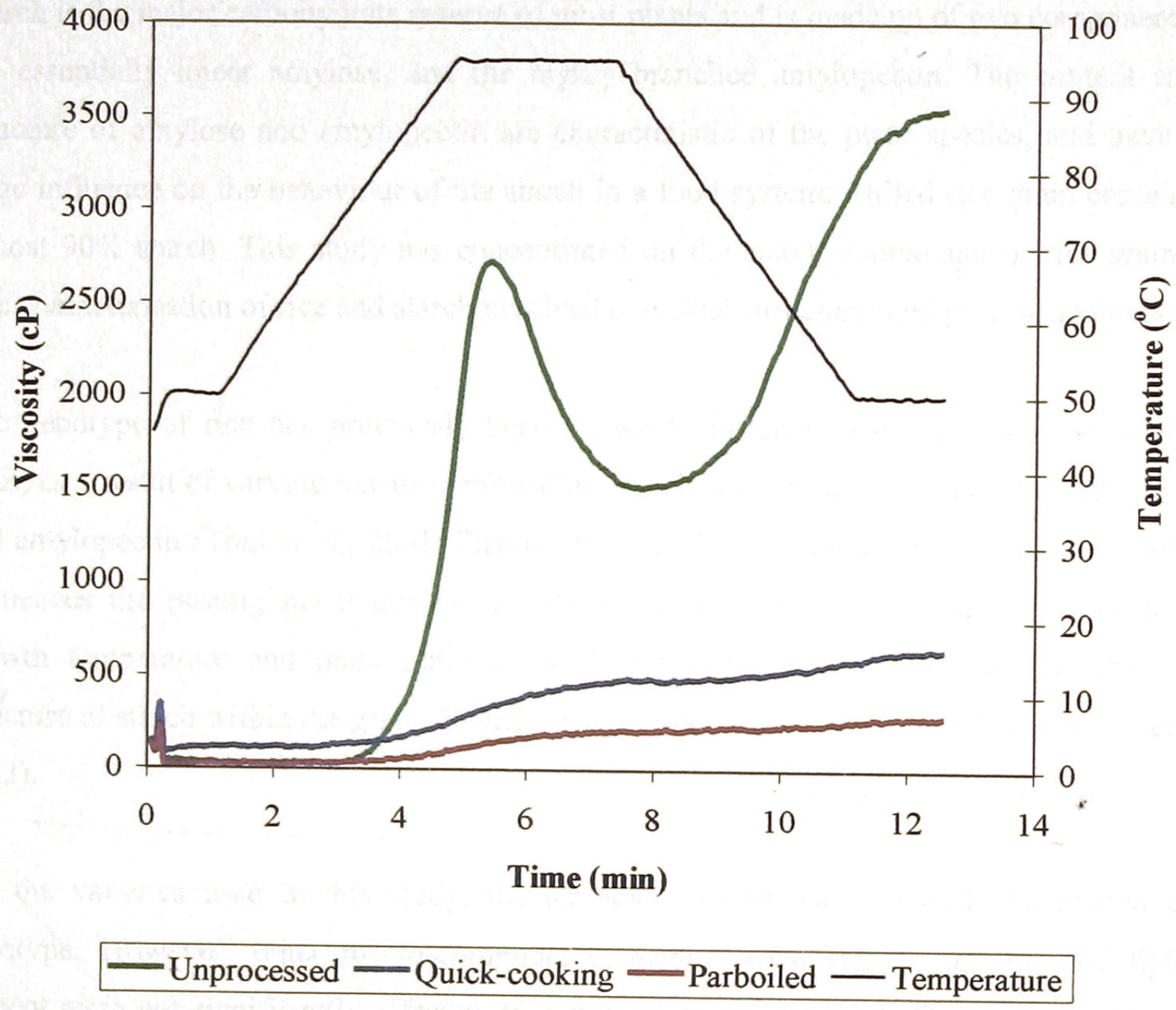

CHAPTER 7

General discussion and conclusions

Starch is the major carbohydrate reserve of most plants and is made up of two components: the essentially linear amylose, and the highly branched amylopectin. The content and structure of amylose and amylopectin are characteristic of the plant species, and have a large influence on the behaviour of the starch in a food system. Milled rice grain contains almost 90% starch. This study has concentrated on the starch component of rice grains. The characterisation of rice and starch involved chemical, structural and pasting analyses.

The genotype of rice has previously been shown to influence pasting properties of the flour, as a result of varying macro-composition, amylose content, and structure of amylose and amylopectin (Tran *et al.*, 2001; Fitzgerald *et al.*, 2003). The environment also greatly influences the pasting behaviour of rice flour, as the growth conditions, in particular growth temperature and plant nutrition, will affect starch synthesis, and in turn the structure of starch within the grain (Inouchi *et al.*, 2000; Lisle *et al.*, 2000; Fitzgerald *et al.*, 2003).

For the varieties used in this study, the amylose content was shown to be related to genotype. However, other macro-components, namely total starch, protein, and lipid content were not significantly affected by genotype or environment. There was a general trend for samples with low amylose content to be high in protein and low in starch content, however the differences were not statistically significant. There were no significant differences between lipid contents of all samples. A cooler season appeared to cause a slight increase in the protein content of rice samples, however this increase was not significant. Growth location did not have a significant effect on the macro-composition or amylose content.

A review of literature suggests that different cultural practices could affect the macro-composition of agricultural crops (Gomez and de Datta, 1975; IRRI, 1977; Resurreccion *et al.*, 1977; Asaoka *et al.*, 1985a; Asaoka *et al.*, 1985b, Inouchi *et al.*, 2000). However, this

study has shown that environment did not have a significant effect on the total starch, protein and lipid content of rice. Amylose content was affected by the growth season. It must be noted that a combined sample of each rice variety was prepared for determination of macro-constituents. For each rice variety, the combined sample consisted of all subsamples from different regions, combined and ground as described. The subsamples were obtained from many farms throughout the rice growing region. The combined sample is likely to have evened out differences in cultural practices and variations in soil properties. Bulking of samples may have contributed to the similarity in macro-composition of rice.

Structural studies in this research concentrated on the arrangement of starch and its amylose and amylopectin components within the rice grain, and how these arrangements are affected by genotype and environment. The structure of rice grains and starch has been extensively examined. However, chemical analyses involved destructive procedures that bring about changes in the material (Round *et al.*, 1997), and microscopic techniques have generally involved the examination of dried and coated samples that were not representative of the starch *in situ* (Zee, 1981). The two microscopic techniques used in this study, ESEM and AFM, were successful in examining rice grains and starch *in situ*. The samples were examined in as close to their natural states as possible, with minimal disruption during sample preparation.

The general arrangement of endosperm cells and starch granules within manually split rice grains was observed using the ESEM. The fracture of rice grains occurred between and within endosperm cells, and was influenced by the variety of rice. The results of this study revealed that the sizes of endosperm cells varied between rice varieties. However, these differences were not related to the size of starch granules, nor to amylose and amylopectin content of the starch. As the interface between the cell wall and cytoplasm inside endosperm cells is considered to be an area of weakness (Hoshikawa, 1993), the tendency for certain varieties to follow a particular fracture pattern may give an indication to its susceptibility to sun-cracking. For Doongara rice, the fractures seemed to occur more often through rather between endosperm cells. This may explain the higher susceptibility of Doongara rice grains (compared to Langi and Kyeema) to suncracking (L. Lewin, pers. comm.).

The environment appeared to have little effect on the structure of grains, as fracture patterns and starch granule dimensions were not significantly different regardless of growth season or location. Processing conditions of parboiling and quick cooking greatly affected the surface structure of rice grains, resulting in little to no granule organisation as observed by ESEM.

The main advantages of the ESEM over conventional SEMs are minimal sample preparation, and the ability to image samples high in moisture. The ESEM was useful in examining processed rice, as no further sample manipulation was performed on the samples prior to imaging. The changes observed in ESEM images can therefore be regarded as changes due to processing and not sample preparation. Samples can therefore be examined *in situ*.

The structure of starch, and of amylose and amylopectin, were examined at high magnification using the AFM. Rice grains were examined in their native form, with little to no sample manipulation. In the examination of rice starch, the AFM revealed growth rings approximately 400 nm apart. Blocklets of 100 nm were observed to be aligned within the growth rings. Comparison of these images with current models of amylopectin structure (Myers *et al.*, 2000) lead to the proposal that each blocklet contained approximately 280 amylopectin side chain clusters.

The AFM images showed similar features and dimensions, regardless of the variety of rice, or the growth season and location. The results from this study therefore indicate that packing of granules was not influenced by genotype and environment.

Rice amylose and amylopectin were dispersed in water and imaged using the AFM. Individual strands of amylose were observed from the images. It was possible to measure the contour length of amylose, and calculate the DP based on an assumed V-amylose structure (French, 1984; Gallant *et al.*, 1997). The calculated DP of rice amylose (1860 and 3420 for Kyeema and Langi, respectively) was within the range documented in the literature (Yamaguchi *et al.*, 1979; French, 1984; Ball *et al.*, 1998). Branching in amylopectin was observed, however the images obtained were insufficiently clear for accurate measurements to be made.

Several AFM images of amylose and amylopectin from rice and potato showed structural detail that has not been achieved by other more conventional microscopic techniques. From the images, the contour length distribution and mean contour length of each sample was obtained by measurement of observable, well-separated chains. Thus, the AFM appears promising as a means of studying the structure of starch and starch components in solution. The widths of amylose structures were greater than predicted values (McIntire and Brant, 1999), indicating aggregation of amylose chains.

Many issues in sample preparation need to be explored to further improve a method for imaging starch and its amylose and amylopectin components. These are 1) the final concentration of the sample, 2) the dispersant used, and 3) the imaging mode used. A suitable concentration of sample is required on the imaging stage to avoid aggregation of polymer chains, so that adequate measurement can be made on well-separated chain structures. In this study, a final sample concentration of 100 ng/mL was deposited onto the imaging stage. At this concentration, aggregation of polymer chains still occurred. However, lowering the concentration further did not achieve clear images with observable chain structures. Thus, high sample concentrations appeared to result in aggregation of chain structures, while low concentrations produced images where chain structures could not be observed. Using the same method of sample preparation, and with the same sample concentration, separated chain structures were observed for Kyeema amylose but not for Langi amylose. This suggests that sample preparation techniques may need to be altered for each sample to achieve suitable images for dimensional analysis.

Chain structures were observed for Kyeema and Langi starch, but not for Doongara starch, despite the same method being used for sample preparation. This may be because water was more effective in dispersing Kyeema and Langi starch than Doongara starch. Further exploration is needed to determine the most suitable dispersant for starch, amylose and amylopectin from different rice varieties. Different dispersants, such as butanol and other short chain alcohols, have been trialed by other researchers (Kirby *et al.*, 1996; McIntire and Brant, 1999).

Although outside the scope of this current study, the above issues should be addressed in further studies on AFM as an advanced microscopic technique for examining starch and starch components.

Despite the need for further work to improve sample preparation, the AFM shows promise as a tool for studying the structure and arrangement of starch within the rice grain, and can be further extended to study other cereal grains. The main advantages of the AFM over other conventional microscopic instruments previously used to study starch, namely SEM and TEM, are its high resolution and minimal sample preparation. The high resolution achieved with the AFM allowed the observation of the fine structure of amylose and amylopectin, where branching of amylopectin was observed. Few studies have been published on the physical observation of the fine structure of amylose and amylopectin by microscopy. Most studies of the fine structure of amylose and amylopectin involve chemical methods, which subject the polymers to degradative sample preparation techniques. The AFM allows the examination of starch either *in situ*, or with minimal sample preparation such that the sample is as close to its natural form as possible.

Used in combination, the ESEM and AFM could provide a more complete picture of the arrangement of starch within the rice grain, as well as amylose and amylopectin within starch granules.

The difference in chemical and structural properties of cereal grains would normally be reflected in their pasting behaviour. The processing behaviour of rice largely reflects the behaviour of its starch (Chinnaswamy *et al.*, 1985). Pasting behaviour of rice flour was studied using the RVA, a heating and cooling viscometer. Genotype had a large effect on the pasting properties of rice flour. Rice with a high amylose content had a lower peak viscosity, lower pasting temperature, and higher setback value than rice with a higher amylose content. These results are in general agreement with those of Lisle *et al.* (1998) and Tran *et al.* (2001) for different rice varieties. The high setback value is due to the ability of amylose to retrograde more readily than amylopectin (Foster, 1965).

Environmental factors also had a significant effect on the pasting properties of rice flours. The cooler season produced flours with lower peak viscosities and higher setback values. This pasting behaviour was mainly influenced by the amylose content of the rice flours. Rice grown in the cooler season had higher amylose content than those grown in the warmer seasons. Although there were no general trends, growth location had a significant effect on the pasting parameters of rice flours.

In this study, apart from the difference in amylose content between non-waxy and waxy rice varieties, chemical analyses did not reveal a significant effect of genotype and environment on the macro-composition of rice grains and starch. Structural analyses revealed morphological differences between the rice varieties. Genotype had a more significant effect on rice morphology than the environment. Chemical and structural properties of rice were not significantly affected by environmental factors, however the pasting behaviour of rice flour was significantly affected by both growth season and location. The results suggest that the environment affected the fine structure of amylose and/or amylopectin, which was not identified by chemical analysis of major constituents. Analysing starch, protein, and lipid may be a good means of predicting behaviour. However, subtle differences may not be observed by chemical analyses and microscopic analyses, and may require actual pasting analyses to confirm the behaviour of the rice and starch in food systems.

Abiotic and/or biotic factors at the different growth locations may have caused some subtle changes to the fine structure of amylose and amylopectin. The changes may have been small but significant, and may have affected the water-absorbing capacity of the molecules, and in turn, the viscoelastic properties of the starch pastes. The change in temperature during the day may affect the activation or inhibition of enzymes involved in starch branching or debranching (Inouchi *et al.*, 2000; Lisle *et al.*, 2000). The reduction in starch debranching enzyme would result in starch with amylopectin behaving more like amylose, which would affect the pasting curve by lowering the peak viscosity and increasing final viscosity. The type of soil used, and the application of nitrogen may have an effect on properties of the rice plant (Lisle *et al.*, 2000). However, in this study, growth conditions did not affect the macro-composition of rice samples.

In conclusion, the combination of chemical, microscopic and pasting analyses allowed a better understanding of the effect of genotype and environment on the structure and behaviour of rice and starch. The chemical, microscopic and pasting methods in combination showed that genotype had a more significant effect on morphology and behaviour than environment. Microscopic techniques used in this study were successful in examining rice grains and starch *in situ*. The AFM has provided new insights into starch structure, with the observation of branching of polymer chains and measurements of dimensions of chain structures. With further exploration, the technique developed has the

potential to study the fine structure of starch, amylose and amylopectin from other rice varieties and other cereal starches. The simplicity and minimal sample preparation requirements of the AFM and ESEM techniques provide a good means of monitoring changes during processing, with the assurance that changes observed are due to processing and not sample manipulation.

REFERENCES

1 Adkins, G.K. and Greenwood, C.T. Studies on starches of high amylose-content: Part VII. Observations on the potentiometric iodine-titration of amylomaize starch. *Carbohydrate Research* **3** (1966) 81-88.

2 Adkins, G.K. and Greenwood, C.T. Physicochemical studies on starches. Part 46: A comparison of laboratory-isolated and commercially-isolated samples of maize starch. *Starch* **21** (1969) 153-155.

3 Allen, S., Davies, M.C., Roberts, C.J., Tendler, S.J.B., and Williams, P.M. Atomic force microscopy in analytical biotechnology. *Trends in Biotechnology* **15** (1997) 101-105.

4 American Association of Cereal Chemists. *Official Methods of Analysis. Method 44-15A: Moisture – Air oven methods, 9th Edition*. American Association of Cereal Chemists Inc, St Paul, MN (1995).

5 American Association of Cereal Chemists. *Official Methods of Analysis. Method 61-02: Using the Rapid Visco Analyser to study the pasting behaviour of rice, 9th Edition*. American Association of Cereal Chemists Inc, St Paul, MN (1995).

6 American Association of Cereal Chemists. *Official Methods of Analysis. Method 30-25: Crude Fat in Wheat, Corn, and Soy Flour, Feeds, and Mixed Feeds, 10th Edition*. American Association of Cereal Chemists Inc, St Paul, MN (2000).

7 American Association of Cereal Chemists. *Official Methods of Analysis. Method 46-12: Crude Protein – Kjeldahl Method, Boric Acid Modification, 10th Edition*. American Association of Cereal Chemists Inc, St Paul, MN (2000).

8 Asaoka, M., Okuno, K., Sugimoto, Y. and Fuwa, H. Effect of environmental temperature at the milky stage on amylose content and fine structure of amylopectin of waxy and nonwaxy endosperm starches of rice (*Oryza sativa* L.). *Agricultural and Biological Chemistry* **49** (1985a) 373-379.

9 Asaoka, M., Okuno, K., Sugimoto, Y. and Fuwa, H. Developmental changes in structure of endosperm starch of rice (*Oryza sativa* L.). *Agricultural and Biological Chemistry* **49** (1985b) 1973-1978.

10 Asaoka, M., Okuno, K., Sugimoto, Y., Kanakami, J. and Fuwa, H. Effect of environmental temperature during development of rice plants on some properties of endosperm starch. *Starch* **36** (1984) 189-193.

11 Baker, A.A., Miles, M.J. and Helbert, W. Internal structure of the starch granule revealed by AFM. *Carbohydrate Research* **330** (2001) 249-256.

12 Baldwin, P.M., Davies, M.C. and Melia, C.D. Starch granule surface imaging using low-voltage scanning electron microscopy and atomic force microscopy. *International Journal of Biological Macromolecules* **21** (1997) 103-107.

13 Ball, S.G., van de Wal, M.H.B.J. and Visser, R.G.F. Progress in understanding the biosynthesis of amylose. *Trends in Plant Science* **3** (1998) 462-467.

14 Banks, W. and Greenwood, C.T. *Starch and its Components*, Edinburgh University Press, Edinburgh (1975) 342p.

15 Bason, M.L. An introduction to the RVA. Presented at the RVA Workshop, 2001 RACI Cereal Chemistry Conference. Sydney, Australia (2001).

16 Baxter, G.A., Blanchard, C.L. and Zhao, J. The effect of changes in rice proteins on pasting properties. In: *Cereals 2002: Proceedings of the 52nd Australian Cereal Chemistry Conference* (Black, C.K., Panozzo, J.F., Wrigley, C.W., Batey, I.L. and Larsen, N. (eds.)), Cereal Chemistry Division, Royal Australian Chemical Institute, Victoria, Australia (2002) pp. 62-64.

17 Bear, R.S. Complex formation between starch and organic molecules. *Journal of the American Chemical Society* **66** (1944) 2122-2123.

18 Bell, D.J. In: *Modern Methods of Plant Analysis, Vol. 2* (Paech, K. and Tracey, M.V. eds.), Springer Verlag, Berlin (1955) pp. 20-21.

19 Blakeney, A.B. *Studies on rice starch. The accumulation and properties of starches in the stem, pollen and grain of some rice varieties grown in Southern New South Wales*. M.S. Agric. Thesis, The University of Sydney, Australia (1980) 140p.

20 Blakeney, A.B., Welsh, L.A. and Bannon, D.R. Rice quality analysis using a computer controlled RVA. In: *Cereals International – Proceedings of the 41st Annual Conference* (Martin, D.J. and Wrigley, C.W. (eds.)), Royal Australian Chemical Institute, Melbourne (1991) pp. 180-182.

21 Blakeney, A.B., Welsh, L.A. and Martin, M. Reproducibility of rice and starch RVA curves. In: *Cereals International – Proceedings of the 42nd Australian Cereal Chemistry Conference* (Humphrey-Taylor, V.J. (ed.)), Royal Australian Chemical Institute, Melbourne (1992) pp. 342-346.

22 Blanshard, J.M.V. Starch granule structure and function. In: *Starch: Properties and Potential (Critical Review of Applied Chemistry Vol. 13)* (Gaillard, T. (ed.), John Wiley and Sons (1987) pp. 16-54.

23 Brant, D.A. (1999). Novel approaches to the analysis of polysaccharide structures. *Current Opinion in Structural Biology* **9** (1999) 556-562.

24 Briones, V.P., Magbanua, L.G. and Juliano, B.O. Changes in physicochemical properties of starch of developing rice grain. *Cereal Chemistry* **45** (1968) 351-357.

25 Callow, J.A., Osborne, M.P., callow, M.E., Bake, F. and Donald, A.M. Use of environmental scanning electron microscopy to image the spore adhesive of the marine alga Enteromorpha in its natural hydrated state. *Colloids and Surfaces B: Biointerfaces* **7** (2003) 315-321.

26 Caton, L., Lampitt, L.H. and Fuller, C.H.F. *Journal of the Science of Food and Agriculture* **6** (1955) 660-664.

27 Chinnaswamy, R. and Bhattacharya, K.R. Characteristics of gel-chromatographic fractions of starch in relation to rice and expanded rice-product qualities. *Starch* **38** (1986) 51-57.

28 Chinnaswamy, R., Unnikrishnan, K.R. and Bhattacharya, K.R. Rheological properties of certain processed rice products. *Starch* **37** (1985) 99-103.

29 Chuang, C-C. and Yeh, A-I. Effects of product temperature and moisture content on viscoelastic properties of glutinous rice extrudates. *Cereal Chemistry* **79** (2002) 36-40.

30 Cooperative Research Centre for Sustainable Rice Production (Rice CRC). *Fact sheet: Rice Growing*. Rice CRC. Yanco NSW (2002). www.ricecrc.org

31 Coultate, T.P. *Food: The Chemistry of its Components, 3rd Edition.* The Royal Society of Chemistry Paperbacks, Cambridge (1996) pp.30-36.

32 Czajkowsky, D.M., Iwamoto, H. and Shao, Z. Atomic force microscopy in structural biology: from the subcellular to the submolecular. *Journal of Electron Microscopy* **49** (2000) 395-406.

33 Decho, A.W. (1999). *Carbohydrate Research* **315** (1999) 330-333.

34 De Datta, S.K.; Obcemea, W.M. and Jana, R.K. Protein content of rice grain as affected by nitrogen fertilizer and some triazines and substituted ureas. *Agronomy Journal* **64** (1972) 785-788.

35 Doner, L.W. Interaction of concanavalin A with high fructose corn syrup glucans and honey components. *Journal of Agricultural and Food Chemistry* **26** (1978) 707-710.

36 Ebermann, R. and Schwartz, R. Fractionation of starch by gel filtration on agarose beads. *Starch* **27** (1975) 361-363.

37 Evers, A.D. and Juliano, B.O. Varietal differences in surface ultrastructure of endosperm cells and starch granules of rice. *Starch* **28** (1976) 160-166.

38 Evers, A.D. and Millar, S. Cereal grain structure and development: some implications for quality. *Journal of Cereal Science* **36** (2002) 261-284.

39 Fankhauser, J.J., Volenee, J.J. and Brown, G.A. Composition and structure of starch from taproots of contrasting genotypes of *Medicago sativa* L. *Plant Physiology* **90** (1989) 1189-1194.

40 FAO, Food and Agriculture Organization of the United Nations. FAO Yearbook: Production. Rome: Food and Agriculture Organization (2002).

41 Farrell, T.C., Williams, R.L. and Fukai, S. The cost of low temperature to the NSW rice industry. In *Proceedings of the 10th Australian Agronomy Conference*, Australian Society of Agronomy, Inc., Hobart (2001).

42 FEI, The Structural Process Management Company. *Applications and Products: ESEM Site* (2003) (from website www.feic.com).

43 Fitt, L.E. and Snyder, E.M. Photomicrographs of starches. In: *Starch – Chemistry and Technology, 2nd Edition* (Whistler R.L., BeMiller J.N. and Paschall E.F. (eds.)). Academic Press Inc, Orlando (1984) pp. 675-689.

44 Fitzgerald, M.A. and Martin, M. The chemistry of rice: Things flow when stirred. In: *Cereals 99. Proceedings of the 49th Royal Australian Cereal Chemistry Conference* (Panozzo, J.F., Ratcliff, M., Wootton, M. and Wrigley, C.W. (eds.)), Royal Australian Chemical Institute, Melbourne (1999) pp. 269-270.

45 Fitzgerald, M.A., Martin, M. and Ward, R.M. Viscosity of rice flour: A rheological and biological study. *Journal of Agricultural and Food Chemistry* **51** (2003) 2295-2299.

46 Foster, J.F. Physical properties of amylose and amylopectin in solution. In: *Starch: Chemistry and Technology Vol. 1, 1st Edition* (Whistler, R.L. and Paschall, E.F. (eds.)), Academic Press Inc., New York (1965) pp. 349-391.

47 French, D. Organization of starch granules. In: *Starch: Chemistry and Technology, 2nd Edition* (Whistler, R.L., BeMiller, J.N. and Paschall, E.F. (eds.)), Academic Press Inc., Orlando (1984) pp. 183-247.

48 Fritzsche, W., Takac, W. and Henderson, E. Application of atomic force microscopy to visualization of DNA, chromatin, and chromosomes. *Critical Reviews in Eukaryotic Gene Expression* **7** (1997) 231-240.

49 Fuwa, H., Sugimota, Y. and Takaya, T. Scanning electron-microscopy of starch granules, with or without amylose attack. *Carbohydrate Research* **70** (1979) 233-238.

50 Fuwa, H., Okuno, K., Asashiba, R. Kikuzaki, H., Asaoka, M. Inouchi, N. and Sugimoto, Y. Characterization of high-amylose type endosperm starches of rice plants cultivated in Asia. *Starch* **44** (1992) 203-205.

51 Gallant, D.J., Bouchet, B. and Baldwin, P.M. Microscopy of starch: evidence of a new level of granule organization. *Carbohydrate Polymers* **32** (1997) 177-191.

52 Geddes, R., Greenwood, C.T. and Mackenzie, S. Studies on the biosynthesis of starch granules: Part III. The properties of the components of starches from the growing potato tuber. *Carbohydrate Research* **1** (1965) 71-82.

53 Goldstein, I.J. and Poretz, R.D. Isolation, physicochemical characterization, and carbohydrate-binding specificity of lectins. In: *Molecular Biology: The Lectins – Properties, functions, and applications in biology and medicine*, (Liener, I.E., Sharon, N. and Goldstein, I.J. (eds.)), Academic Press, Inc., Orlando (1986) pp. 33-247.

54 Goldstein, I.J. and So, L.L. Protein-carbohydrate interaction III. Agar gel-diffusion studies on the interaction of concanavalin A, a lectin isolated from jack bean, with polysaccharides. *Archives of Biochemistry and Biophysics* **111** (1965) 407-414.

55 Gomez, K.A. and De Datta, S.K. Influence of environment on protein content of rice. *Agronomy Journal* **67** (1975) 565-568.

56 Greenwood, C.T. and Thomson, J. Studies on the biosynthesis of starch granules 2. The properties of the components of starches from smooth- and wrinkled-seeded peas during growth. *Biochemical Journal* **82** (1962) 156-164.

57 Guilbot, A. and Mercier, C. Starch. In: *The Polysaccharides, Vol 3* (Aspinall, G.O. (ed.)), Academic Press Inc., Orlando (1985) pp. 209-282.

58 Hansma, H.G. and Hoh, J.H. Biomolecular imaging with the atomic force microscope. *Annual Review of Biophysics and Biomolecular Structure* **23** (1994) 115-139.

59 Haworth, W.N., Peat, S. and Sagrott, P.E. A new method for the separation of the amylose and amylopectin components of starch. *Nature* **157** (1946) 19.

60 Hizukuri, S., Takeda, Y., Maruta, N. and Juliano, B.O. Molecular structures of rice starch. *Carbohydrate Research* **189** (1989) 227-235.

61 Hollinger, G. and Marchessault, R.H. Ultrastructure of acid- and enzyme-modified cross-linked potato starch. *Biopolymers* **14** (1975) 265-276.

62 Hoseney, R.C. *Principles of Cereal Science and Technology, 2nd Edition*, American Association of Cereal Chemists, St. Paul, Minnesota (1994).

63 Hoshikawa, K. Rice seed, germination and seedlings. In: *Science of the Rice Plant, Volume One, Morphology*, (Matsuo, T. and Hoshikawa, K. (eds.)) Ministry of Agriculture, Forestry and Fisheries, Japan (1993) pp. 91-132, 377-412.

64 Inouchi, N., Ando, H. Asaoka, M., Okuno, K. and Fuwa, H. The effect of environmental temperature on distribution of unit chains of rice amylopectin. *Starch* **52** (2000) 8-12.

65 IRRI, International Rice Research Institute. Annual Report for 1976. IRRI, Los Baños, Laguna, Philippines (1977).

66 Jane, J-L. and Chen, J.F. *Cereal Chemistry* **69** (1992) 60-65.

67 Jenkins, P.J. and Donald, A.M. The influence of amylose on starch granule structure. *International Journal of Biological Macromolecules* **17** (1995) 315-321.

68 Juliano, B.O. The rice caryopsis and its composition. In: Rice Chemistry and Technology (Houston, D.F. (ed.)). American Association of Cereal Chemists Inc, St Paul, MN (1972).

69 Juliano, B.O. Polysaccharides, proteins, and lipids of rice. In: *Rice: Chemistry and Technology* (Juliano, B.O. (ed.)). The American Association of Cereal Chemists Inc, St Paul, Minnesota (1985) pp. 59-174.

70 Juliano, B.O. and Bechtel, D.B. The rice grain and its gross composition. In: *Rice: Chemistry and Technology* (Juliano, B.O. (ed.)), American Association of Cereal Chemists, Inc., St. Paul, Minnesota (1985) p. 17.

71 Juliano, B.O., Villareal, R.M., Perez, C.M., Villareal, C.P., Takeda, Y. and Hizukuri, S. Varietal differences in properties among high amylose rice starches. *Starch* **39** (1987) 390-393.

72 Kassenbeck, P. *Starch* **30** (1978) 40.

73 Kirby, A.R., Gunning, A.P., and Morris, V.J. Imaging polysaccharides by atomic force microscopy. *Biopolymers* **38** (1996) 355-366.

74 Klucinec, J.D. and Thompson, D.B. Structure of amylopectins from *ae*-containing maize starches. *Cereal Chemistry* **79** (2002a) 19-23.

75 Klucinec, J.D. and Thompson, D.B. Amylopectin nature and amylose-to-amylopectin ratio as influences on the behaviour of gels of dispersed starch. *Cereal Chemistry* **79** (2002b) 24-35.

76 Kobayashi, S., Schwartz, S.J. and Lineback, D.R. Rapid analysis of starch , amylose and amylopectin by high-performance size-exclusion chromatography. *Journal of Chromatography* **319** (1985) 205-214.

77 Kobayashi, S., Schwartz, S.J. and Lineback, D.R. Comparison of the structures of amylopectins from different wheat varieties. *Cereal Chemistry* **63** (1986) 71-74.

78 Kuge, T. and Takeo, K. Complexes of starchy materials with organic compounds Part III. Complex formation in aqueous solution and formation of starch by *l*-Menthone.*Agricultural and Biological Chemistry* **32** (1968) 1232-1238.

79 Lisle, A.J., Martin, M. and Fitzgerald, M.A. Chalky and translucent rice grains differ in starch composition and structure and cooking properties. *Cereal Chemistry* **77** (2000) 627-632.

80 Lisle, A.J., White, J.M. and Fitzgerald, M.A. The effect of temperature on starch synthesis in Australian rice grains. In: *Cereals 98. Proceedings of the 48th Australian Cereal Chemistry Conference* (O'Brien, L., Blakeney, A.B., Ross, A.S. and Wrigley, C.W. (eds)), Royal Australian Chemical Institute, Melbourne (1998) pp. 283-284.

81 Manners, D.J. *Cereal Foods World*, **30** (1985) 461-467.

82 Manners, D.J. Recent developments in our understanding of amylopectin structure. *Carbohydrate Polymers* **11** (1989) 87-112.

83 Marshall, W.E. and Wadsworth, J.I. Introduction. In: *Rice Science and Technology* (Marshall, W.E. and Wadsworth, J.I. (eds.)), Marcel Dekker Inc., New York (1994) pp. 1-15.

84 Martin, C. and Smith, A.M. Starch Biosynthesis. *The Plant Cell* **7** (1995) 971-985.

85 Matheson, N.K. Amylose changes in the starch of developing wheat grains. *Phytochemistry* **10** (1971) 3213-3219.

86 Matheson, N.K. A comparison of the structures of the fractions of normal and high-amylose pea-seed starches prepared by precipitation with concanavalin A. *Carbohydrate Research* **199** (1990) 195-205.

87 Matheson, N.K. and Welsh, L.A. Estimation and fractionation of the essentially unbranched (amylose) and branched (amylopectin) components of starches with concanavalin A. *Carbohydrate Research* **180** (1988) 301-313.

88 McDonald, A.M.L. and Stark, J.R. A critical examination of the procedures for the isolation of barley starch. *Journal of the Institute of Brewing* **94** (1988) 125-132.

89 McIntire, T.M. and Brant, D.A. Imaging of individual biopolymers and supramolecular assemblies using noncontact atomic force microscopy. *Biopolymers* **42** (1997) 133-146.

90 McIntire, T.M. and Brant, D.A. Imaging of carrageenan macrocycles and amylose using noncontact atomic force microscopy. *International Journal of Biological Macromolecules* **26** (1999) 303-310.

91 Montgomery, E.M. and Senti, F.R. Separation of amylose and amylopectin of starch by an extraction-sedimentation procedure. *Journal of Polymer Science* **28** (1958) 1-9.

92 Morris, V.J., Gunning, A.P., Kirby, A.R., Round, A., Waldron, K., and Ng, A. Atomic force microscopy of plant cell walls, plant cell wall polysaccharides and gels. *International Journal of Biological Macromolecules* **21** (1997) 61-66.

93 Moss, G.E. The microscopy of starch. In: *Examination and Analysis of Starch and Starch Products* (Radley, J.A. (ed.)), Applied Science Publishers Ltd., London (1976) pp. 1-32.

94 Muetgeert, J. the fractionation of starch. *Advances in Carbohydrate Chemistry* **16** (1961) 299-333.

95 Myers, A.M., Morell, M.K., James, M.G. and Ball, S.G. Recent progress toward understanding biosynthesis of the amylopectin crystal. *Plant Physiology* **122** (2000) 989-997.

96 Newport Scientific Pty Ltd. Applications Manual for the Rapid Visco Analyser. Newport Scientific, Warriewood (1998) 123p.

97 Ohtani, T., Yoshino, T., Hagiwara, S. and Maekawa, T. High-resolution imaging of starch granule structure using atomic force microscopy. *Starch* **52** (2000a) 150-153.

98 Ohtani, T., Yoshino, T., Ushiki, T., Hagiwara, S. and Maekawa, T. Structure of rice starch granules in nanometer scale as revealed by atomic microscopy. *Journal of Electron Microscopy* **49** (2000b) 487-489.

99 Phillips, K.L. and Sallans, H.R. Starch and gluten from wheat flour. *Cereal Science Today* **11** (1966) 61-62, 64, 79.

100 Pomeranz, Y. Modern Cereal Science and Technology. VCH Publishers, Inc., New York (1987).

101 Ramesh, M., Ali, S.Z. and Bhattacharya, K.R. Structure of rice starch and its relation to cooked-rice texture. *Carbohydrate Polymers* **38** (1999) 337-347.

102 Resurreccion, A.P.; Hara, T.; Juliano, B.O. and Yoshida, S. Effect of temperature during ripening on grain quality of rice. *Soil Science and Plant Nutrition Tokyo* **23** (1977) 109-112.

103 Reyes, A.C., Albano, E.L., Briones, V.P. and Juliano, B.O. Genetic variation, varietal differences in physicochemical properties of rice starch and its fractions. *Journal of Agricultural and Food Chemistry* **13** (1965) 438-442.

104 Rhadhika Reddy, K., Ali, S.Z. and Bhattacharya, K.R. The fine structure of rice-starch amylopectin and its relation to the texture of cooked rice. *Carbohydrate Polymers* **22** (1993) 267-275.

105 Rhadhika Reddy, K., Subramanian, R., Ali, S.Z. and Bhattacharya, K.R. Viscoelastic properties of rice-flour and their relationship to amylose content and rice quality. *Cereal Chemistry* **71** (1994) 548-552.

106 Robyt, J.F. Enzymes in the hydrolysis and synthesis of starch. In: *Starch: Chemistry and Technology, 2nd Edition* (Whistler, R.L., BeMiller, J.N. and Paschall, E.F. (eds.)), Academic Press Inc., Orlando (1984) pp. 87-123.

107 Robyt, J.F. and Whelan, W.J. The α-amylases. In: *Starch and its Derivatives, 4th Edition* (Radley, J.A. (ed.)), Chapman and Hall ltd., London (1968a) pp. 430-476.

108 Robyt, J.F. and Whelan, W.J. The β-amylases. In: *Starch and its Derivatives, 4th Edition* (Radley, J.A. (ed.)), Chapman and Hall Ltd., London (1968b) pp. 477-497.

109 Ross, A.S., Walker, C.E., Booth, R.I., Orth, R.A. and Wrigley, C.W. The RVA: A new technique for the estimation of sprout damage. *Cereal Foods World* **32** (1987) 827-829.

110 Round, A.N., MacDougall, A.J., Ring, S.G., and Morris, V.J. Unexpected branching in pectin observed by atomic force microscopy. *Carbohydrate Research* **303** (1997) 251-253.

111 Royal Australian Chemical Institute. *RACI Official Method 06-05: Determination of the Pasting Properties of Rice with the Rapid Visco Analyser*. First Approved 1994, Royal Australian Chemical Institute, Melbourne (1995).

112 Russell, P. Complementary techniques for high resolution surface investigations. *Scientific and Laboratory Technology* **12** (2001) 72-76.

113 Schoch, T.J. *Cereal Chemistry* **18** (1941) 121-128.

114 Schoch, T.J. Fractionation of starch by selective precipitation with butanol. *Journal of the American Chemical Society* **64** (1942) 2957-2961.

115 Schoch, T.J. The fractionation of starch. *Advances in Carbohydrate Chemistry* **1** (1945) 247-277.

116 Shannon, J.C. and Garwood, D.L. Genetics and physiology of starch development. In: *Starch: Chemistry and Technology* (Whistler, R.L., BeMiller, J.N. and Paschall, E.F. (eds.)), Academic Press Inc., Orlando (1984) pp. 25-86.

117 Shinde, S.V., Nelson, J.E. and Huber, K.C. Soft wheat starch pasting behavior in relation to A- and B-type granule content and composition. *Cereal Chemistry* **80** (2003) 91-98.

118 Singh, R. and Juliano, B.O. Free sugars in relation to starch accummulation in developing rice grain. *Plant Physiology* **59** (1977) 417-421.

119 Snyder, E.M. Industrial microscopy of starches. In: *Starch: Chemistry and Technology, 2nd Edition* (Whistler, R.L., BeMiller, J.N. and Paschall, E.F. (eds.)), Academic Press Inc., Orlando (1984) pp. 661-673.

120 So, L.L. and Goldstein, I.J. Protein-carbohydrate interaction IV. Application of the quantitative precipitin method to polysaccharide-concanavalin A interaction. *Journal of Biological Chemistry* **242** (1967) 1617-1622.

121 Suzuki, H. and Juliano, B.O. Alkaliviscogram and other properties of starch of tropical rice. *Agricultural and Biological Chemistry* **39** (1975) 811-817.

122 Swinkels, J.J.M. Composition and properties of commercial native starches. *Starch* **37** (1985) 1-5.

123 Takeda, Y., Hizukuri, S. and Juliano, B.O. Purification and structure of amylose from rice starch. *Carbohydrate Research* **148** (1986) 299-308.

124 Takeda, Y., Hizukuri, S. and Juliano, B.O. Structures of rice amylopectins with low and high affinities for iodine. *Carbohydrate Research* **168** (1987) 79-88.

125 Takeda, Y., Hizukuri, S. and Juliano, B.O. Structures and amounts of branched molecules in rice amyloses. *Carbohydrate Research* **186** (1989a) 163-166.

126 Takeda, Y., Maruta, N., Hizukuri, S. and Juliano, B.O. Structures of indica rice starches (IR 48 and IR 64) having intermediate affinities for iodine. *Carbohydrate Research* **187** (1989b) 287-294.

127 Thomas, D.J. and Atwell, W.A. *Eagan Press Handbook Series – Starches*. American Association of Cereal Chemists, St. Paul, Minnesota (1999) 94p.

128 Tran, U.T., Okadome, H., Murata, M., Homma, S. and Ohtsubo, K. Comparison of Vietnamese and Japanese rice cultivars in terms of physicochemical properties. *Food Science and Technology Research* **7** (2001) 323-330.

129 Veeco Instruments. *Product Information: Atomic Force Microscope* (2003) (from website www.veeco.com).

130 Wang, Y-J. and Wang, L. Structures of four waxy rice starches in relation to thermal, pasting, and textural properties. *Cereal Chemistry* **79** (2002) 252-256.

131 Whistler, R.L. History and future expectation of starch use. In: *Starch: Chemistry and Technology, 2nd Edition* (Whistler, R.L., BeMiller, J.N. and Paschall, E.F. (eds.)), Academic Press Inc., Orlando (1984).

132 Whistler, R.L. and Hilbert, G.E. Separation of amylose and amylopectin by certain nitroparaffins. *Journal of the American Chemical Society* **67** (1945) 1161-1165.

133 Williams, P.C., Kuzima, F.D. and Hlynka, I. A rapid colorimetric procedure for estimating the amylose content of starches and flours. *Cereal Chemistry* **47** (1970) 411-420.

134 Yamada, T. and Taki, M. Fractionation of maize starch by gel-chromatography. *Starch* **28** (1976) 374-377.

135 Yamaguchi, M., Kainuma, K. and French, D. Electron microscopic observation of waxy maize starch. *Journal of Ultrastructure Research* **69** (1979) 246-261.

136 Yeh, J.Y., Garwood, D.L. and Shannon, J.C. Characterization of starch from maize endosperm mutants. *Starch* **33** (1981) 222-230.

137 Young, A.H. Fractionation of starch. In: *Starch: Chemistry and Technology, 2nd Edition* (Whistler, R.L., BeMiller, J.N. and Paschall, E.F. (eds.)), Academic Press Inc., Orlando (1984) pp. 249-283.

138 Yun, S. and Matheson, N.K. Structures of the amylopectins of waxy, normal, amylose-extender, and wx:ae genotypes and of the phytoglycogen of maize. *Carbohydrate Research* **243** (1993) 307-321.

139 Zee, S-Y. *Wheat and Rice Plants. A Scanning Electron Microscope Survey*, Cosmos Books Ltd, Hong Kong (1981) 58p.

140 Zhou, Z.K., Robards, K., Blanchard, C. and Helliwell, S. Changes in pasting properties of rice flour following storage. In: *Cereals 2001: Proceedings of the 51st Australian Cereal Chemistry Conference* (Wootton, M., Batey, I.L. and Wrigley, C.W. (eds.)), Cereal Chemistry Division, Royal Australian Chemical Institute, Victoria, Australia (2002) pp. 175-179.

APPENDIX 1

Reprint of paper published in Journal of Cereal Science

Dang, J.M.C. and Copeland, L. Imaging rice grains using atomic force microscopy. *Journal of Cereal Science* **37** (2003) 165-170.

Journal of Cereal Science **37** (2003) 165–170
doi:10.1006/jcrs.2002.0490

Imaging Rice Grains Using Atomic Force Microscopy

J. M. C. Dang† and L. Copeland*‡§

†School of Land, Water and Crop Sciences, ‡Faculty of Agriculture, Food and Natural Resources, §Key Centre for Polymer Colloids, The University of Sydney, Sydney NSW 2006, Australia

Received 18 April 2002

ABSTRACT

Rice (*Oryza sativa*) grains from different varieties were examined using atomic force microscopy. Images obtained from cross sections of grains showed angular starch structures 3–8 μm in size that were arranged in layers approximately 400 nm apart. The layers are suggested to represent growth rings of starch granule formation. Cross striations were observed within each layer, and these are suggested to correspond to the blocklets of amorphous and crystalline regions within the starch granule. The blocklets had an average size of 100 nm, and are proposed to comprise approximately 280 amylopectin side chain clusters. Rice grains sectioned with water as a lubricating agent appeared to have lost some of the ordered layered structures, whereas there was a total loss of the ordered structure in cooked grains as a result of gelatinisation.
© 2003 Elsevier Science Ltd. All rights reserved.

Keywords: atomic force microscopy, starch, rice, *Oryza sativa*.

INTRODUCTION

The composition and arrangement of components of cereal grains influence behaviour in processing operations. Knowledge of morphology gained from microscopic examinations using light and scanning and transmission electron microscopy have contributed substantially to our understanding of the physical and chemical properties of cereal grains. Atomic force microscopy (AFM) is a relatively new imaging technique in which a sharp probing tip is scanned over the surface of a sample. Interactions between the tip and the sample are translated into a three-dimensional image, with resolution in the nanometre to micrometre range[1]. Images can be obtained by having the probe touch the surface of the specimen (contact mode) or by measuring the attractive forces as the probe comes in close proximity to the surface (non-contact mode). In contact mode, the brightness of the images indicates the degree of contact between the probe and the surface. Images obtained with the AFM display morphological features at greater resolution than achieved with scanning electron microscopy (SEM). Further, AFM allows samples to be examined in their natural state, without the need for metal coating as is required in SEM. Moreover, AFM can provide topographical information that is not obtained with SEM.

AFM has been used to study biological membranes, cell surfaces, and the molecular structure of various biological macromolecules, including DNA[2], proteins and polysaccharides such as xanthan, acetan, gellan, carrageenan[3–5], and pectin[6,7]. AFM has been used to examine the surface of granules of commercial potato and wheat starch samples[8], and the surfaces of mechanically disrupted maize, rice, wheat and sweet potato starches have been imaged by Ohtani *et al.*[9,10]. The internal structure of maize

ABBREVIATIONS USED: AFM = atomic force microscope/microscopy; SEM = scanning electron microscope/microscopy.

*Corresponding Author: E-mail: l.Copeland@acss.usyd.edu.au

0733–5210/03/020165 + 06 $35.00/0

© 2003 Elsevier Science Ltd. All rights reserved.

starch has also been examined by AFM[11]. However, there is little information on the use of AFM to image starch granules *in situ*.

In this paper, we describe the use of AFM to image the surface of cut grains of several rice varieties chosen on the basis of different amylose-amylopectin ratios and cooking properties. The rice varieties used were Doongara, a long grain, high amylose variety, with a soft cooked texture; Langi, a long grain, soft-textured, low amylose variety; Kyeema, a long grain, low amylose fragrant rice; and a waxy rice. A quick cooking Kyeema rice that had been subjected to a high heat treatment and a drying process, was also imaged to observe the differences between raw and partially cooked rice samples.

EXPERIMENTAL

Samples

Rice (*Oryza sativa*) varieties Langi, Doongara, Kyeema, and a quick-cooking processed form of Kyeema, were obtained from RiceGrowers Cooperative Limited (Yanco, NSW, Australia). Waxy rice (Shirakiku brand, imported from California, USA, by Jun Pacific Corporation Pty Ltd, Chatswood, Australia) was obtained from a local supermarket.

Estimation of amylose content of starches

The amylose content of starch isolated from milled rice samples was estimated using the concanavalin A method of Matheson and Welsh[12]. The amylose content was 28% for Doongara, 18% for Langi, 19% for Kyeema, and 2% for the waxy rice.

Preparation of samples

Resin for mounting specimens for AFM examination was prepared by mixing 9 g of Epon 812 Substitute (ProSciTech, QLD, Australia), 7·5 g of nadic methyl anhydride (ProSciTech, QLD, Australia), and 0·3 g of benzyldimethylamine (ProSciTech, QLD, Australia). The resin was cured at 60 °C overnight in cylindrical molds (3 cm diameter × 2 cm high). The surface of the solidified resin was polished with sandpaper to create a level plane, and five holes, each wide and deep enough to fit an entire rice grain, were drilled into the smoothed surface of the resin. A rice grain was placed in each hole and fresh resin was added to fill in gaps and cover the entire grain, taking care to avoid introducing air bubbles. The rice-filled resin was cured overnight at 60 °C.

A transverse cut was made through the blocks near the centre of each rice grain, using a diamond saw (Accutom, Struers, Denmark) at 700 rev/min and feed rate of 1·5 cm/min. Rice grains were sectioned without lubricant (dry-sectioned samples), or with distilled water supplied to the sectioning blade at a rate of 1 mL/min (wet-sectioned samples). The cut surface was polished lightly using 1200-grade paper on a polishing wheel and imaged immediately.

Imaging procedures

Images were obtained using a Park Scientific Autoprobe CP scanning probe microscope in contact mode, in air at atmospheric pressure and ambient temperature (20–22 °C) and humidity. A 2-μm silicon cantilever (Ultralevers, Model number APUL-20-AU-25, Park Scientific Instruments) was used, with a force constant of 13 N/m. The scanner was calibrated in the *xy* directions using a 1·0 μm grating. Scan areas ranged from 1 to 25 μm^2, and images were analyzed using AutoProbe image processing software (Park Scientific Instruments).

RESULTS

Ten grains of each variety of rice were prepared for imaging. Approximately ten fields of view were selected from each grain surface, and images were obtained at different magnifications within each field of view. Images of Doongara rice grains that were sectioned dry showed angular starch granules, with sizes in the range 3–8 μm [Fig. 1(a)]. The angular structures were arranged in layers [Fig. 1(b)], which were observed at higher magnification to contain striated structures [Fig. 1(c)]. At even higher magnification, these striations were observed as clusters that seemed to emanate from ridges estimated to be approximately 400 nm apart [Fig. 1(d)]. Darker regions in the image appeared to correspond to gaps between the clusters.

Images of waxy rice grains and grains from the Langi and Kyeema varieties showed similar morphological features (results not shown). However, grains of the quick-cooking form of Kyeema, which have gone through a heating and drying process, had lost their granule structure and appeared amorphous

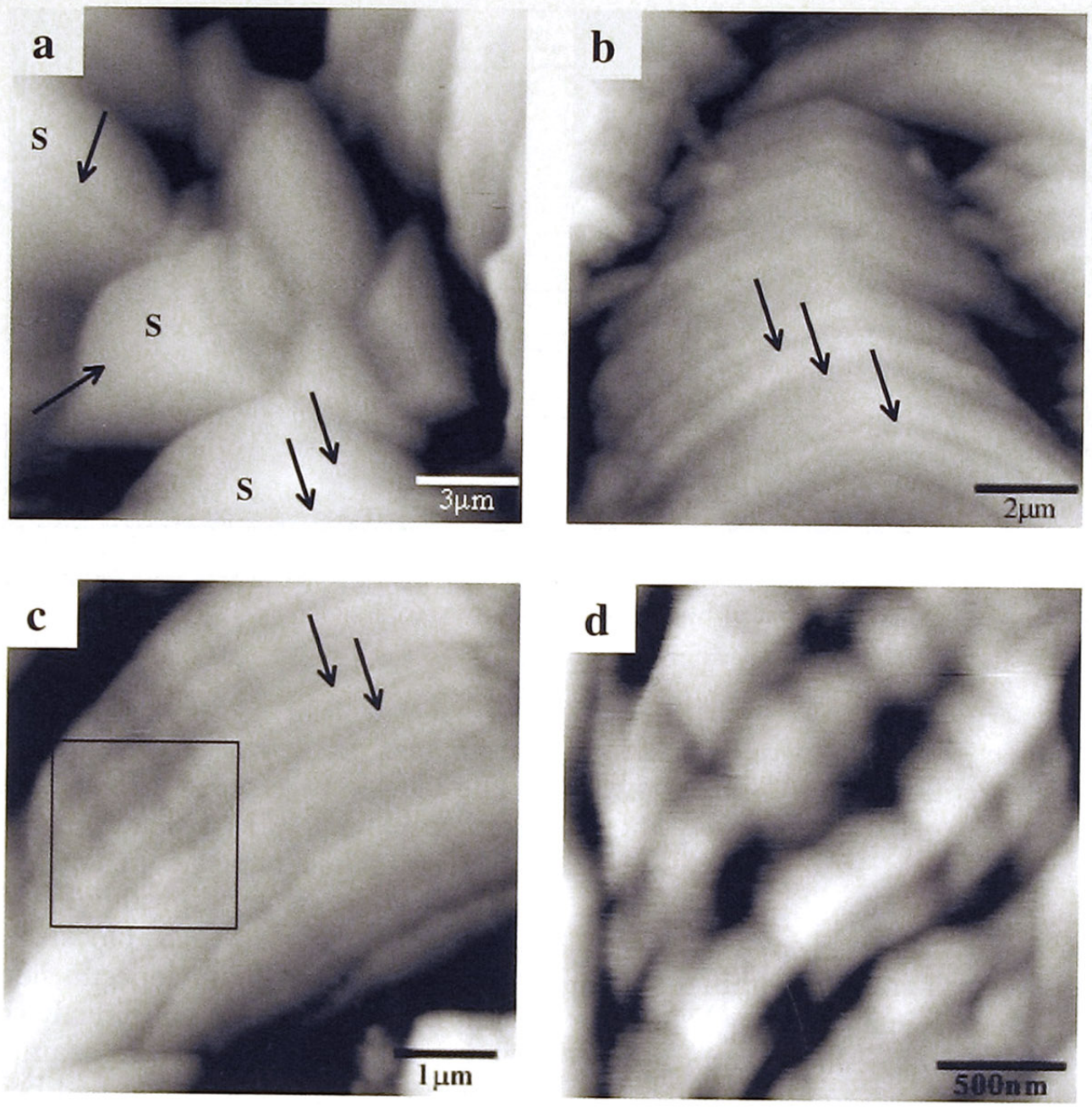

Figure 1 AFM images of dry-sectioned Doongara rice grains. The areas scanned were 15 μm × 15 μm (a, b), 5 μm × 5 μm (c) and 2 μm × 2 μm (d). Layered structures are indicated by arrows, and starch granules by S. A closer view of the boxed area in (c) is shown in (d).

(Fig. 2). The angular layered starch structures evident in the other rice samples represented by Figure 1 were not seen. Many of the images showed numerous pores about 0·6 μm in diameter to be present in the surface, and amorphous granules 1–4 μm in size were also observed (Fig. 2).

Rice grains were also sectioned using distilled water as a lubricant to the sectioning blade. Images of the wet-sectioned Doongara rice [Fig. 3(a)] showed some of the layered structures observed in dry-sectioned samples, but also amorphous forms 0·5–1 μm in size, which most likely correspond to gelatinised starch. Similar features were observed for wet-sectioned Langi and Kyeema rice (results not shown). Images of Doongara rice grains that had been cooked in boiling water for 20 min [Fig. 3(b)] showed a highly disorganised grain structure, and the ordered layers evident in dry-sectioned samples

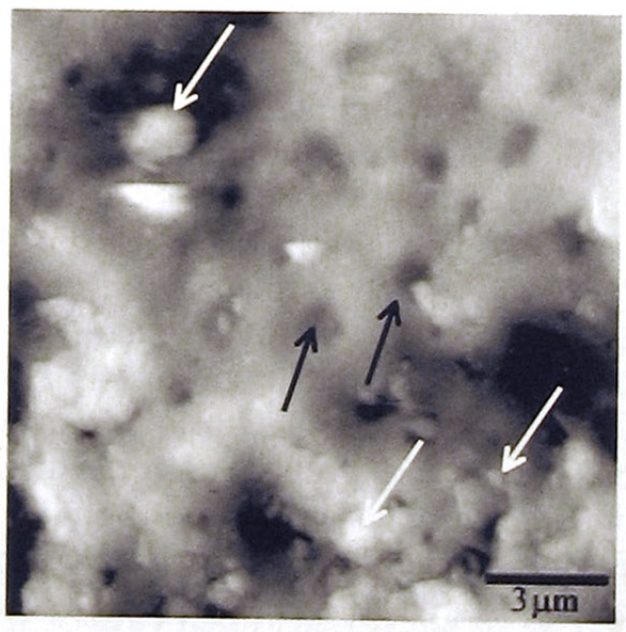

Figure 2 AFM image of dry-sectioned quick-cooking Kyeema rice. Pitting is indicated by black arrows, partially degraded starch granules by white arrows. The area scanned was 15 μm × 15 μm.

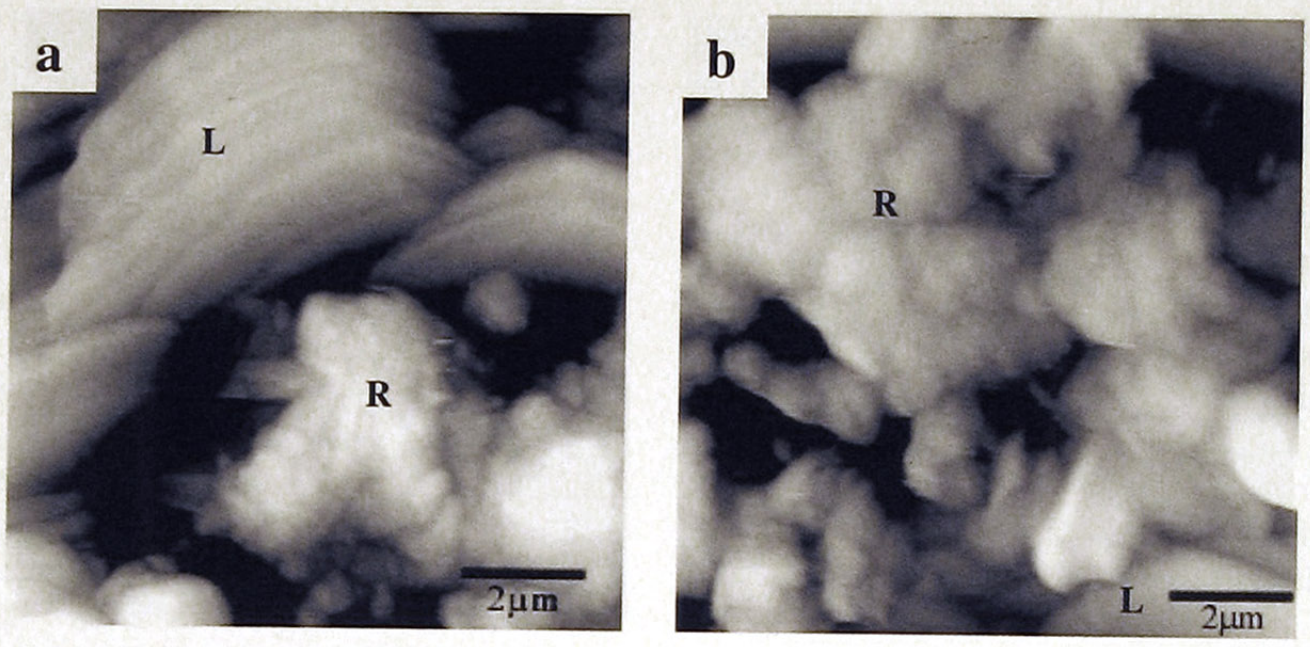

Figure 3 AFM images of wet-sectioned (a) and cooked (b) Doongara rice. Areas scanned in both were 10 μm × 10 μm. The layered structure is indicated by L; rough, gelatinised area by R.

were not seen. Similar observations were made for cooked Langi and Kyeema rice (results not shown).

DISCUSSION

The arrangement of starch granules within the grain of several rice varieties was imaged using AFM. The structures observed had similar shapes and sizes (less than 10 μm) to those of starch granules imaged by other microscopic techniques[13,14]. However, the fine structure observed with the AFM has provided some fresh insights into the arrangement of amylopectin molecules in starch granules.

Amylopectin is the dominant molecule in most starches and is considered to be the major contributor to the shape and structure of starch granules. Amylopectin chains are proposed to run perpendicular to the growth rings and to the surface of the granule[15]. A diagrammatic representation of Figure 1(d) is shown in Figure 4, indicating the dimensions that were estimated from AFM images. We propose that the layered structures seen clearly in Figure 1(b) are growth rings formed during the deposition of starch, and that the clusters seen at low resolution as striations in Figure 1(c) represent the blocklets comprising groups of amorphous and crystalline lamellae. According to the cluster model, which is currently accepted as the most comprehensive model of starch structure[16], crystalline regions consist of amylopectin side chain clusters, which extend approximately 10 nm along the main axis. The crystalline regions are separated by amorphous regions of about 4 nm (Fig. 4). Each cluster is estimated to be approximately 10 nm wide[16,17]. The blocklets we observed would therefore consist of approximately 28 repeating units of amorphous and crystalline lamellae in length, and less than 10 side chain clusters in width (Fig. 4). According to these calculations, each blocklet would contain approximately 280 amylopectin side chain clusters. Our observations are not directly comparable with those of Ohtani *et al.*[10], who examined the internal structure of rice starch that had been disrupted by mechanical blending. The authors observed numerous fine particles with diameter less than 30 nm, which were arranged in aggregated chains, and were suggested to correspond to the clusters predicted in the cluster model.

The large range in granule size, and the absence of intact granules, observed in images of the processed quick cooking Kyeema rice was consistent with the gelatinsation of starch granules within the rice grains during the moist, high heat treatment[14]. The pitting observed in some of the images may be the result of partial hydrolysis of starch by residual grain enzymes during the heat treatment, and/or the escape of trapped air bubbling through the surface.

The rough features seen in wet-sectioned samples of uncooked rice [Fig. 3(a)] indicate that some gelatinisation of starch granules occurred when specimens were prepared in this way. The heat generated from the sectioning blade, in combination with the use of water as a lubricant may have caused partial gelatinisation of starch in some places on the grain surface. The images obtained with wet-sectioned rice grains indicate the need for caution in the use of methods of sample preparation.

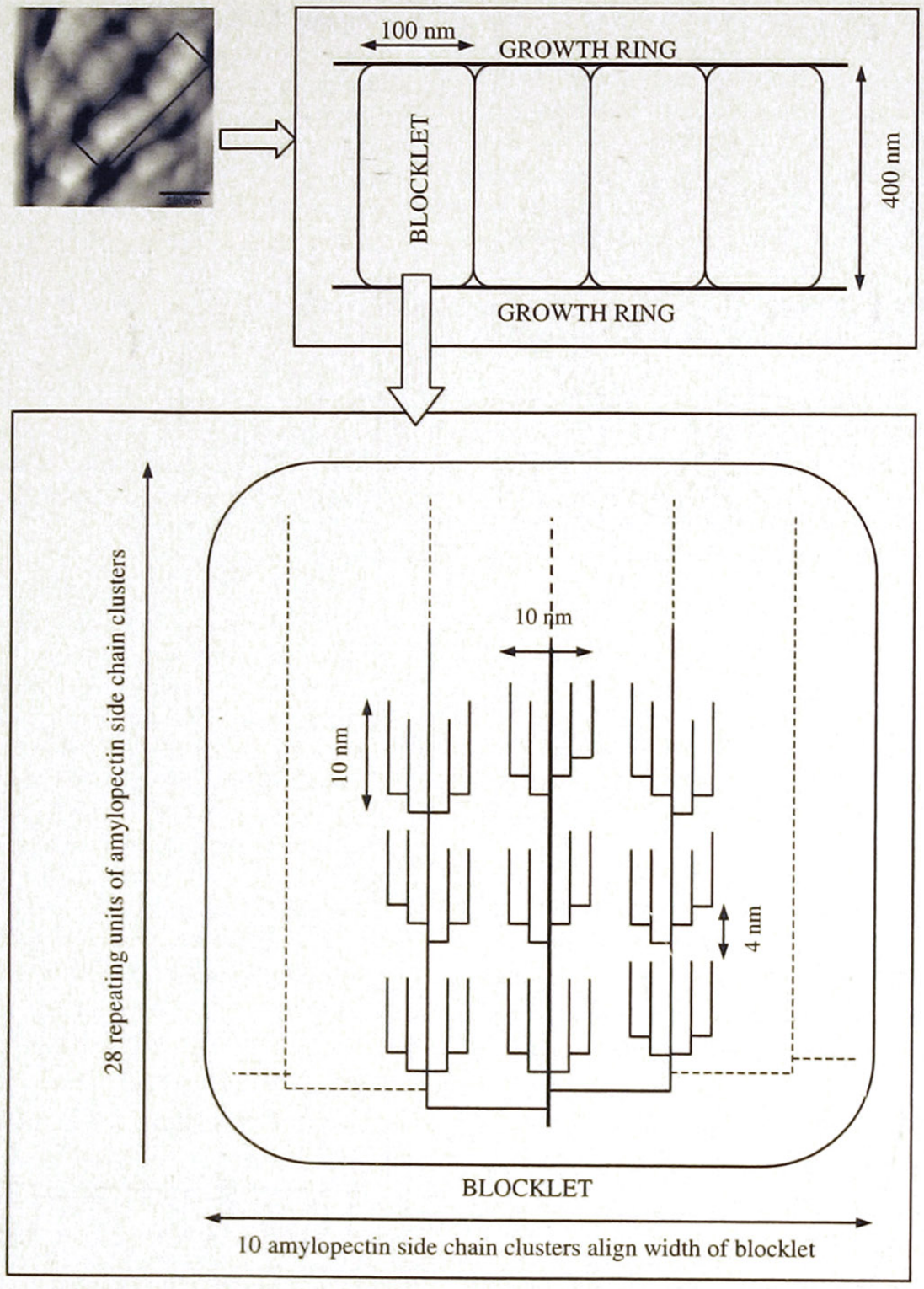

Figure 4 Schematic representation of the arrangement of blocklets in starch granules, based on images obtained from AFM. The proposed arrangement of amylopectin side chain clusters within each blocklet is shown. Dashed lines indicate extension of the diagrammatic representation.

The images of the processed and cooked rice clearly showed that most of the starch granules had lost their structure and were no longer arranged in organised layers. The layered structures seen in images of raw rice were rarely observed in images of cooked rice.

The AFM shows promise as a tool for studying the structure of rice grains and starch as it allows the examination of grains and starch in their native form, without destructive chemical and physical modification. Growth rings were estimated to be about 400 nm apart, and blocklets of approximately 100 nm were observed to be aligned within the growth rings. From dimensions obtained in images, and by comparison with current models of the molecular organisation of amylopectin in starch granules, we propose that each blocklet contained approximately 280 amylopectin side chain clusters.

Acknowledgements

JD is the recipient of a postgraduate research scholarship from the Cooperative Research Centre for Sustainable Rice Production. The authors wish to thank Tony Blakeney for helpful discussion and Shaun Bulcock from the Electron Microscope Unit of the University of Sydney, Australia, for assistance in the use of the AFM.

REFERENCES

1. Hansma, H.G. and Hoh, J.H. Biomolecular imaging with the atomic force microscope. *Annual Review of Biophysics and Biomolecular Structure* **23** (1994) 115–139.
2. Fritzsche, W., Takac, W. and Henderson, E. Application of atomic force microscopy to visualization of DNA, chromatin, and chromosomes. *Critical Reviews in Eukaryotic Gene Expression* **7** (1997) 231–240.
3. Kirby, A.R., Gunning, A.P. and Morris, V.J. Imaging polysaccharides by atomic force microscopy. *Biopolymers* **38** (1996) 355–366.
4. McIntire, T.M. and Brant, D.A. Imaging of individual biopolymers and supramolecular assemblies using noncontact atomic force microscopy. *Biopolymers* **42** (1997) 133–146.
5. McIntire, T.M. and Brant, D.A. Imaging of carrageenan macrocycles and amylose using noncontact atomic force microscopy. *International Journal of Biological Macromolecules* **26** (1999) 303–310.
6. Round, A.N., MacDougall, A.J., Ring, S.G., and Morris, V.J. Unexpected branching in pectin observed by atomic force microscopy. *Carbohydrate Research* **303** (1997) 251–253.
7. Czajkowsky, D.M., Iwamoto, H. and Shao, Z. Atomic force microscopy in structural biology: from the subcellular to the submolecular. *Journal of Electron Microscopy* **49** (2000) 395–406.
8. Baldwin, P.M., Davies, M.C. and Melia, C.D. Starch granule surface imaging using low-voltage scanning electron microscopy and atomic force microscopy. *International Journal of Biological Macromolecules* **21** (1997) 103–107.
9. Ohtani, T., Yoshino, T., Hagiwara, S. and Maekawa, T. High-resolution imaging of starch granule structure using atomic force microscopy. *Starch* **52** (2000) 150–153.
10. Ohtani, T., Yoshino, T., Ushiki, T., Hagiwara, S. and Maekawa, T. Structure of rice starch granules in nanometer scale as revealed by atomic microscopy. *Journal of Electron Microscopy* **49** (2000) 487–489.
11. Baker, A.A., Miles, M.J. and Helbert, W. Internal structure of the starch granule revealed by AFM. *Carbohydrate Research* **330** (2001) 249–256.
12. Matheson, N.K. and Welsh, L.A. Estimation and fractionation of the essentially unbranched (amylose) and branched (amylopectin) components of starches with concanavalin A. *Carbohydrate Research* **180** (1988) 301–313.
13. Moss, G.E. The microscopy of starch. In 'Examination and Analysis of Starch and Starch Products', (J.A. Radley, ed.), Applied Science Publishers Ltd, London (1976) pp 1–32.
14. Fitt, L.E. and Snyder, E.M. Photomicrographs of starches. In 'Starch – Chemistry and Technology', (R.L. Whistler, J.N. BeMiller and E.F. Paschall, eds), 2nd ed., Academic Press, Inc., Orlando (1984) pp 675–689.
15. French, D. Organization of starch granules. In 'Starch – Chemistry and Technology', (R.L. Whistler, J.N. BeMiller and E.F. Paschall, eds), 2nd ed., Academic Press, Inc., Orlando (1984) pp 184–247.
16. Myers, A.M., Morell, M.K., James, M.G. and Ball, S.G. Recent progress toward understanding biosynthesis of the amylopectin crystal. *Plant Physiology* **122** (2000) 989–997.
17. Gallant, D.J., Bouchet, B. and Baldwin, P.M. Microscopy of starch: evidence of a new level of granule organization. *Carbohydrate Polymers* **32** (1997) 177–191.